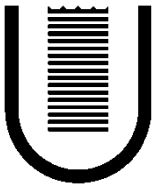

UNIVERSITY OF ROME "TOR VERGATA"

FACULTY OF ENGINEERING
Department of Mechanical Engineering

PH.D
QUANTUM ELECTRONICS AND PLASMA PHYSICS

PH.D COURSE
XXII

Innovative methods and technologies to detect and monitor chemical substances locally or remotely with active optical technologies

Piergiorgio Ventura

INTERNAL SUPERVISOR
Dr. Pasqualino Gaudio
Dr. Eugenio Martinelli

PH.D COORDINATOR
Prof. Carlo Bellecci

2009/2010

Abstract

Considering increasing dangerousness of terrorism and asymmetric war, it is necessary to find equipment, know-how and information that are useful in order to detect and identify dangerous molecules as quickly and far away as possible.
Multiwavelenght Dial, is one of the most powerful optical technologies for remote sensing. For this reason it is needed a "fingerprint" database and a good analysis method able to recognize a substance among many different ones.
A cheap and reliable Lidar which is able to give a warning whenever something strange is found in atmosphere could be useful as well. An early warning followed by recognition using the more complicated Multiwavelength Dial technology seems to be the best solution also compared to existing devices. To recognize the anomaly in atmosphere a multivariate statistical method is proposed.
In this thesis a review of dangerous chemical substances and detecting method is illustrated in chapter one. A project and some experimental activity on a cheap mini Lidar is presented in chapter two. A new system and a new method based on Multiwavelenght Dial is explained in chapter three. IR spectra, made using a CO_2 laser source, of Chemical Weapons, Toxic Industrial Chemicals (TIC) and interfering substances and experimental set up organized are presented in chapter 4. This data will be used to test recognition and discrimination performance of our multivariate statistical analysis and neuronal network based method in chapter 5, where a multipass cell projected to improve system performance is also illustrated. Chapter 6 is devoted to a possible local sensor application of our experimental set up and finally general conclusion will be done.

Keywords: Multiwavelenght Dial, mini Lidar, chemical weapons, fingerprint, CO_2 laser, IR spectroscopy, multivariate statistical analysis, neural network, Multipass cell.

L'aumento del terrorismo e delle guerre asimmetriche inducono a cercare strumentazioni, know how ed informazioni che possano essere utili per rilevare ed identificare le molecole pericolose più rapidamente e lontano possibile.
Il "multiwavelenght DIAL" è una delle tecnologie ottiche più performanti per l'individuazione remota . Per tale obbiettivo è necessario un database dei fingerprint e un buon metodo di analisi che sia in grado di riconoscere una sostanza tra molte differenti che mostrano caratteristiche simili.
Un mini Lidar che sia in grado di dare un allarme precoce tutte le volte che qualcosa di strano si trovi in atmosfera è un altro elemento utile. Un allarme precoce seguito dal riconoscimento usando la più complicata tecnologia Multiwavelenght Dial sembra essere la soluzione migliore anche a confronto con i dispositivi esistenti. Allo scopo di riconoscere l'anomalia in atmosfera una tecnica di analisi multivariata è proposta.
In questa tesi nel capitolo uno vi è una descrizione delle sostanze chimiche pericolose e dei metodi di riconoscimento esistenti. Un progetto ed alcune attività sperimentali su un nuovo mini Lidar viene illustrato nel capitolo due. Un nuovo sistema ed un nuovo metodo basato sul Multiwavelenght Dial è illustrato nel capitolo tre. Spettri nella banda IR, compiuti usando un Laser a CO_2, di armi chimiche, TIC e sostanze interferenti ed il set up sperimentale organizzato sono illustrati nel capitolo quattro. Questi dati sono usati, nel capitolo cinque, per testare il nostro metodo di identificazione basato sull'analisi statistica multivariata e le reti neurali, dove è descritta anche una cella multipasso progettata per aumentare le prestazioni del sistema. Il capitolo sei è dedicato ad un possibile applicazione del nostro set up sperimentale per un sensore locale. Infine le conclusioni dell'intero lavoro saranno date.

Parole chiave: Multiwavelenght Dial, mini Lidar, armi chimiche, fingerprint, laser a CO_2, spettroscopia IR, analisi statistica multivariata, reti neurali, cella multipasso.

Title

Innovative methods and technologies to detect and monitor chemical substances locally or remotely with active optical technologies

Index

SUMMARY

The quick increase of terrorism and asymmetric war is leading to new needs involving defense and security. Nowadays we have to fight several kinds of threats and one of the most dangerous is represented by the use of chemical weapons against civil or military objectives. In chapter 1 we will deal with dangerous compounds, their effects and their classification.
In order to detect and identify dangerous molecules as quickly and far away as possible, it is necessary to find equipment, know-how and information that can prove useful so as to minimize damage they could cause. Among the available devices, there is not a device which is able to identify an unknown substance remotely or at least their performances are really poor. All existing devices, working both locally or remotely, are described in chapter 1.
We need a low cost lidar device to give an alert of something strange in atmosphere which could task a system which is able to identify the substance. A new idea of a mini Lidar project is described in chapter 2. The system was projected and tested but some components were changed during testing. System prototype does not fit expected requirements, but the experience done is useful to develop a working system in the future. Many components in fact, could be used also in a new system.
The main project of this thesis is a new device and, mainly a new method based on Multiwavelenght Dial applications. This is one of the most powerful optical technologies. Multiwavelenght Dial technology uses more than two different wavelengths. It is usually used to perform concentration measure of a single substance with higher precision than Dial because it makes possible to "subtract" the effect of interfering ones. We will use it in order to identify a substance and, after identification, measure concentration profile of an investigated molecule with high precision. For this reason it is needed a "fingerprint" database which consists of an exhaustive collection of absorption coefficients data so as to identify each molecule avoiding confusion with interfering ones. Nowadays there is not such a collection of data in either scientific or technical literature and, moreover, there is not a detailed analysis method able to recognize, jointly to Dial technique, a substance among many different ones that absorb in the same spectral range. For this reason we need to use many wavelengths to have enough pieces of information and a methodology to properly use them to identify substances. The project, considering both hardware and software components of the system, is described in chapter 3.
An important part of the tool, the mentioned database, has been built. Of course it is not an exhaustive collection of data, but it is enough to test methodology. Experimental set up, methodology, data acquired, data filtering and first analysis are described in chapter 4. We used a CO_2 laser source for absorption spectroscopy measurements using a cell filled with the investigated molecules. In this way we can make the proper "fingerprint" database necessary to identify dangerous molecules. The CO_2 laser has been chosen because it is eye safe and, mainly, because it covers a spectral band where there is good absorption for those kinds of molecules.
Discrimination tool is described in chapter 5. We developed a software that could help us discriminating different substances using multivariate statistical analysis where physical data, in our case absorption coefficients, are treated as elements of a multidimensional vector space. In this way it is possible to use all mathematical instruments that allow to maximize useful pieces of information. Each substance becomes a point in this vector space and the performance of a discriminating method is measured through the distance between these points and the probability of reaching the same point in different measures. In this way it is possible to calculate a probability of discrimination. In this thesis IR spectra of common chemical weapons and interfering substances will be presented and used to test recognition and discrimination performance of our method.
The upgrade of the experimental set up needed to increase database performance is also described in chapter 5. One of this upgrades is a multipass cell that allows an optical path longer than 30 m within a cell of one meter. Detailed project of the cell is explained.

Many components developed could be used to build also a local sensor. It will allow to determine the presence of low concentration substances. This local sensor project is described in chapter 6. Performance expected and possible problems are also described. At the end the conclusion and future outline will be done.

Keywords: Multiwavelenght Dial, chemical weapons, fingerprint, CO_2 laser, IR spectroscopy, multivariate statistical analysis

NEEDS TO BE SATISFIED, TECHNOLOGY AND METHOD ALREADY USED AT THE STATE OF ART, AND MULTIWAVELENGHT DIAL ALREADY EMPLOYED OR PROJECTED

1 CHEMICAL AGENTS

1.1 Introduction

Terrorism and asymmetric war are leading towards new threats and one of the most dangerous is the use of chemical weapons against civil or military objectives.
Field sampling and analysis methods are needed for chemical warfare agents (CWAs) that can prove rapid, providing adequate sensitivity and high quality data so that governmental authorities and public health officials may make informed decisions following CWAs exposure or use. Moreover, with the Chemical Weapons Convention (CWC) in force on 29 April 1997, we are expected to develop a fast and sensitive method for detecting chemical warfare agents in the environment during on-site verification.
The methods used to detect and identify CWAs in the field would also preferably allow detection and identification of toxic industrial chemicals and environmental contaminants.
For these reasons we decided to develop know-how and equipment in order to detect and identify dangerous molecules as quickly and far away as possible, so to minimize damage.
A chemical agent is a substance that is intentionally used by military or terrorist forces to seriously harm, incapacitate, or kill people as a result of its damaging physiological effects. Chemical agents affect human organs preventing them from functioning normally. The results are usually disabling or even fatal.
Classical CWAs can be divided into three groups, the most lethal group being represented by the nerve agents (tabun-GA, sarin-GB, soman-GD, and VX); the second group, the blister agents (sulfur mustard-HD, nitrogen mustards-HN, arsenical vesicant Lewisite-L and other solphorated vesicants, e.g., bis [2(2-chloroethyltio)ethyl]ether and sulfide), are used for casualty effects; the third group may involve several kinds of toxicity (systemics toxic compounds), suffocant agents, incapacitating agents, irritants) and cause great discomfort or produce physiological (vomiting) and mental effects on their victims, preventing exposed personnel from performing their military duties.

1.2 Nerve agents

1.2.1 Physical and chemical properties

Among lethal chemical agents, the nerve agents have had an entirely dominant role since World War II and they have been intensively investigated ever since. Particularly, one nerve agent, Sarin (isopropylmethylphosphonofluoridate), was in the news after its use against the population of the Kurdish village of Birjinni in 1993 and after a terrorist attack in the Tokyo underground system on 20 March 1995.
Nerve agents are organic esters of phosphoric acid used as a chemical warfare agents because of their extreme toxicity. They belong to the chemical group of organo-phosphorus compounds as well as many common herbicides and pesticides. Simple chemical techniques can be used to manufacture nerve agents and their precursors are inexpensive, but both Chemical Weapons Convention and the Australia Group Agreement are trying to control them.
Nerve agents affect the transmission of impulses in the nervous system and this is the reason of their name. They react with the enzyme acetylcholinesterase (AChE) in an irreversible reaction in tissue fluid, permitting accumulation of acetylcholine (Ach) and continual stimulation of the nervous system. Ach is a chemical which transmits nerve signals (neurotransmitter), after its release into the nervous system. It plays a vital role in the stimulation of skeletal muscles, nerve endings of the autonomic nervous system concerned with involuntary bodily functions, and many structures within the central nervous system such as the brain, spinal cord, and associated nerves. When AChE

cannot function, ACh accumulates at the synapse (the junctions where nerve impulses pass from one nerve ending to another). This causes the cell to remain in a constant state of stimulation, leading to observed symptoms of nerve agent poisoning.
The body absorbs nerve agents via any of these routes: as a vapor or liquid through the eyes, as a vapor into the lungs, as a liquid through the skin, or as a liquid through ingestion.
The rate of action of nerve agents (the rate at which the body reacts to or is affected by the chemical agent) is very rapid, producing effects within minutes of exposure due to respiratory arrest.
Nerve agents are quite stable, easily dispersed and highly toxic. Their duration is dependent on the type of employment (i.e., explosive dissemination, spray from an aircraft, or release from a cylinder). Weather is a factor affecting the persistency of nerve agents. They are most persistent under low wind, moderate temperatures, and stable air. These weather conditions usually occur at night.
In the following pages general information on each known nerve agent are given. Among the general information useful to understand the dangerousness and the best way to detect these agents there is volatility which is the substance's tendency to vaporize.
Nerve agents in the pure state are colorless liquids with very different volatility. A highly volatile (non-persistent) substance poses a greater respiratory hazard than a less volatile (persistent) one. The physical data linked to volatility is the vapor pressure, the pressure of a vapor which is in equilibrium with its non-vapor phases. It is measured in mmHg and increases by increasing temperature. At a given temperature, substances with higher vapor pressure will vaporize more readily than substances with a lower vapor pressure.

GA - Ethyl N, N-dimethylphosphor-amidocyanidate

GA, also known as tabun, is the first member of the G-series of nerve agents, so designated because three compounds of this series have similar physical and chemical properties and evoke a similar physiological response in man and animals. They were first produced in Germany during World War II. Tabun is the simplest of the nerve agents to produce.
The toxic effects of GA are powerful but relatively short-lived (non-persistent). In vapor or liquid form, GA is extremely toxic. Because the body removes GA slowly, several small doses of GA over a period of several months could ultimately lead to advanced symptoms of nerve agent poisoning and, perhaps, death due to an accumulation of the nerve agent in the body.
The reaction of GA with water (hydrolysis) is fairly slow in an acidic or neutral solution but quite rapid in an alkaline solution. The major hydrolysis products in aqueous 5-percent sodium hydroxide solution are sodium ethyl N,N-dimethylamidophosphate and sodium cyanide.
Although GA is a relatively unstable compound, it can be stored at normal temperatures for several years in corrosion-protected metal containers or munitions.
GA is a low volatility persistent chemical agent; it evaporates 20 times more slowly than water. In fact, heavily splashed liquid GA persists for one to two days under average weather conditions.

GB- Isopropyl methyl phosphonofluoridate

GB, also known as sarin, is a fluorinated organophosporous compound. The toxic effects of GB are powerful but relatively short-lived. In vapor or liquid form, GB is poisonous. If the dose is large enough, GB can kill a person in as few as 2 to 3 minutes.
GB hydrolysis is fairly rapid. Its hydrolysis products are hydrogen fluoride under acidic conditions and isopropyl alcohol and polymers under alkaline conditions. Water-reactive materials may react with GB and produce highly unstable mixtures, heat, and toxic and/or flammable gases. GB is also subject to biodegradation in the soil.
GB is a relatively stable compound. However, GB must be additionally stabilized if long-term storage is planned or if it is stored in metal containers or munitions. A stabilizing effect is obtained by using amines and solvents such as methanol and halogen alkanes.

It is a volatile non-persistent chemical agent and evaporates at the same rate as water or kerosene, so that it is mainly taken up through the respiratory organs.

GD - Pinacolyl methylphosphonofluoridate

GD or Soman is a fluorinated organophosporous compound and is the most toxic of the G-series nerve agents. In either vapor or liquid form, GD is extremely poisonous.
Since the body recovers very slowly from GD poisoning, many small doses of GD over a period of several months could be fatal due to an accumulation of the nerve agent in the body.
The reaction of GD with water (hydrolysis) is fairly rapid. The rate of hydrolysis is pH-dependent. Hydrolysis of GD is complete in five minutes in aqueous five-percent sodium hydroxide (NaOH). Hydrolysis products at high pH are sodium methylphosphonate and sodium fluoride.
It is relatively non-persistent (short-lived) when pure. GD is less stable in storage than GA or GB. For long-term storage, GD must be stabilized, especially if stored in metal containers or munitions. It is a moderately volatile chemical agent and evaporates four times more slowly than water.

VX - O-ethyl S-(2-diisopropylaminoethyl) methylphosphonothiolate

VX belongs to the so-called V-series of OP nerve agents (V for "venom" or "venomous"), several of which were first synthesized in the United Kingdom in the early 1950s. The V-series nerve agents are characterized by their high toxicity, low volatility, and phosphorus-sulfur bond in their molecular structures.
VX is a colorless, odorless liquid with an extremely low vapor pressure and low volatility at room temperature (25°C); hence, it is a persistent liquid that remains in an area (on material, equipment, and soil) for a long time after being disseminate.
Because of its low volatility, an effective vapor cloud is difficult to create without a high munitions expenditure. Therefore, VX is not considered an effective casualty producer by inhalation. However, it is an effective casualty producer in liquid form because of its ability to rapidly penetrate the skin. A dose of liquid VX can cause death within minutes.
Table 1.1 lists the common nerve agents and some of their properties. Water is included in the table as a reference point for the nerve agents.

Property	GA	GB	GD	GF	VX	Water
Molecular weight	162.3	140.1	182.2	180.2	267.4	18
Density, g/cm^3 *	1.073	1.089	1.022	1.120	1.008	1
Boiling-point, °C	240.00	157.78	197.78	238.89	297.78	100
Melting-point, °C	-7.78	-56.11	-42.22	-30.00	< -51	0
Vapour pressure, mm Hg *	0.07	2.9	0.4	0.06	0.0007	23.756
Volatility, mg/m^3 *	610	22,000	3,900	600	10.5	23,010
Solubility in water, % *	10	Miscible with water	2	~2	Slightly	NA

***at 25°C**

Table 1.1: *Physical properties of water and common nerve agents GA, GB, GD, VX.*

1.2.2 Route of entry

Exposure to nerve agents can occur through four portals of entry: the respiratory tract (airway), the eyes, the skin, and the gastrointestinal tract (ingestion).
Inhalation and the skin are the main routes of entry of nerve agents, either as a gas, aerosol, or liquid. Liquids or foods contaminated with nerve agents could also be a sort of poison.

The route of entry also influences the symptoms developed and, to some extent, the sequence of the different symptoms. The fastest poisoning way is the respiratory system because the lungs contain numerous blood vessels and target organs can be reached by the inhaled nerve agent through the blood circulation. Respiratory system itself is one of the most important target organs. If a person is exposed to a high concentration of nerve agent, e.g., 200 mg sarin/m^3, death may occur within a couple of minutes. Nerve agents are somewhat fat-soluble and so they can easily penetrate the outer layers of the skin, but it takes 20 to 30 minutes for the poison to reach the deeper blood vessels. Nevertheless, the poisoning process may be rapid if the total dose of nerve agent is high.

1.2.3 Symptoms

Minor poisoning, caused by a low dose of nerve agent, leads to characteristic muscular symptoms such as increased production of saliva, a runny nose, and a feeling of pressure on the chest. Moreover, the pupil of the eye becomes contracted (miosis), impairing night-vision, and reducing the focal length changing capacity so that short-range vision deteriorates. The victim feels pain when trying to focus on nearby objects. This is accompanied by headache. Other symptoms are tiredness, slurred speech, hallucinations and nausea.

Exposure to a higher dose leads to more dramatic developments and symptoms are more pronounced so that the victim may suffer convulsions and lose consciousness. Difficulty in breathing and coughing are due to bronchoconstriction and secretion of mucus in the respiratory system. Cramping in the gastrointestinal tract, vomiting, involuntary discharge of urine and defecation are present as well. There may be excessive salivating, tearing, and sweating.

On the other hand, if the poisoning is moderate, muscular weakness, local tremors, or convulsions may affect the skeletal muscles.

The poisoning process may be so rapid that symptoms mentioned earlier may never have time to develop when respiratory muscles and respiratory center of the central nervous system are involved inducing a death similar that by suffocation.

1.2.4 Diagnostic

Equipment for the measurement of cholinesterase levels of soldiers in the field is now available. The Test-Mate™ Cholinesterase Test Kit, a self-contained portable cholinesterase test system with a 96-test capacity, can yield results in as little as four minutes. The device has been developed commercially for field use by minimally trained operators and is rugged, simple, portable, and inexpensive. Blood sample requirements are minimal – 10 microlitres drawn from a pricked fingertip. The Test-Mate™ kit utilizes a hemoglobin-normalized red blood cell cholinesterase test method that evaluates declines in cholinesterase activity without the necessity of obtaining a pre-exposure baseline measurement of enzyme activity from each soldier.

Unfortunately, a prophylactic drug to completely prevent the effects of nerve agents exposure has not been discovered, but treatment procedures and antidotes that are highly valuable in saving lives after nerve agents exposure have been developed. The antidotes for nerve agents are atropine and pralidoxime (2-PAM-Cl). At present, these compounds are the best treatment for the adverse effects of nerve agents exposure; however, antidotes should only be administered if nerve agent exposure is certain because the antidotes can cause serious side effects.

This treatment is available to both military personnel and civilian authorities in the form of autoinjectors. Anticonvulsants such as diazepam and pyridostigmine bromide are also crucial in treating nerve agents exposures.

1.3 Blister Agents (Vesicants)

1.3.1 Physical and chemical properties

Vesicant (blistering) warfare agents act locally on the body surface giving symptoms similar to scorches with necrosis of the tissue. They also exert a toxic effect on the whole organism which may lead to death.

There are three major families of blister agents (vesicants): sulfur mustard (HD), nitrogen mustards (HN1, HN2, HN3), and the arsenical vesicants (L). All blister agents are employed in the form of colorless gases and liquids, being persistent.
They damage the respiratory tract (nose, sinuses, and windpipe) when inhaled and cause vomiting and diarrhea when absorbed. The skin or any other part of the body they contact are burned and blistered. The severity of a blister agent burn is directly related to the concentration of the agent and the duration of contact with the skin. Additionally, vesicants poison food and water and make other supplies dangerous to handle.
Although exposure to these agents can be fatal, blister agents are used to produce casualties needing long-term medical care and to degrade combat effectiveness by forcing opposing troops to wear full protective clothing. Thickened blister agents can be used for long-term contamination of terrain, ships, aircraft, vehicles, or equipment since they can penetrate wood, leather, rubber, and paints.
An overview of most used blister agents follows in the next pages, including their physical and chemical properties, their routes of entry, and a description of symptoms.

Mustard gas - [bis(2-chloroethyl)sulfide]
Among necrotic compounds, mustard gas or Yprite is the most important. It was used first during World War I, so its chemical analysis is well developed.
Sulfur mustard produced during World War I typically contained 25 to 30 percent impurities and was referred to as H. The impurities in H give it a yellow to dark brown color and an odor similar to freshly cut hay or rotten onions. Storage problems due to the impurities in H reacting with iron when stored under tropical conditions led to the development of a purified sulfur mustard referred to as HD, or distilled mustard. HD is colorless or light yellow and has an odor similar to garlic or horseradish. During World War II, the United States possessed munitions filled with purified mustard that contained less than 5 percent impurities.
Pure sulfur mustard is a colorless and odorless liquid with a great blistering power. It has very low solubility in water, but once dissolved, it readily hydrolyzes. Its low solubility in water and low vapor pressure contribute to its high persistence in soil and standing water. It reacts violently with oxidants such as chlorine forming nonpoisonous oxidation products and so oxidants are used for the decontamination.
Mustard destruction by hydrolysis or natural weathering in the environment results in the formation of thiodiglycol a non-toxic compound that may be easily handled. However, some munitions grade mustard formulations contain only 50 to 80% mustard with most of the remaining content being other sulfur vesicants that would decompose in other products.
Persistence depends on the amount of liquid contamination, the munitions used, the nature of the terrain and soil, and the weather conditions. Heavily splashed liquid may persist on objects for two or more days in concentrations great enough to cause casualties of military significance. If the temperature is low, mustard may persist several weeks. Mustard on soil retains its vesicant action for about 2 weeks; however, under certain conditions, such as burial in soil, the agent may remain active for years. In running water, sulfur mustard has a short half life; however, in still water it may persist for several months. Mustard persists about twice as long in salt water as in fresh water.
Some HD based mixtures are known being used in artillery shells, and other munitions.
"HT" is a mixture of 60% HD and 40% Sulfur Mustard T – 2(chloroethylthioethyl)ether, a sulfur and chlorine compound similar in structure to HD. Both HD and T are alkylating agents. HT is persisting in soil, sea or standing water even years and its effects would encompass those of both HD and T. HT has a strong blistering effect, has a long duration of effectiveness, is more stable, and has a lower freezing point than HD. Its low volatility makes effective vapor concentrations in the field difficult to obtain.
Moreover, mustard gas has been addictioned with thickening agents in order to enhance its persistence; among the addictioned chemicals, able to modify substantially some physical parameters, chlorinate rub wax and methyl metacrylate were employed. Particularly, the methyl

metacrylate has been employed also for the thickening of some neurotoxical agents, mainly Soman (GD) to obtain the thickened Soman (TGD).

Lewisite - (2-chloroethyl) arsonous dichloride

Pure Lewisite is colorless and odorless liquid. However, small amounts of impurities give it a geranium-like odor and a brownish color. Lewisite is significantly more dense than air. It has low solubility in water but is readily soluble in most organic solvents. Lewisite will slowly penetrate rubber and most impermeable fabrics. Absorption of either vapor or liquid through the skin in adequate dosage may lead to systemic intoxication or death.

Arsenical vesicants are not as common or as stable as the sulfur or nitrogen mustards. Lewisite rapidly hydrolyzes to form less toxic solid arsenic oxides that are non-volatile and non-vesicating. Because of rapid hydrolysis, Lewisite vapor is nonpersistent under humid conditions, so that it is much more dangerous as liquids than as vapors. Under dry conditions, Lewisite is somewhat less persistent than sulfur mustard (HD).

Nitrogen mustards

HN-1 nitrogen mustard - bis(2-chloroethyl)ethylamine is an oily, colorless to pale yellow liquid with a faint, fishy, or musty odor. HN-2 nitrogen mustard - bis(2-chloroethyl)methylamine is a dark liquid with a fruity odor in high concentrations or an odor like soft soap in low concentrations. HN-3 nitrogen mustard - tris (2-chloroethyl) amine is an oily, colorless to pale yellow liquid that has no odor when pure.

The nitrogen mustards are sparingly soluble in water but freely soluble in organic solvents. They hydrolyze less readily than sulfur mustard. The initial two products of hydrolysis are soluble in water and are toxic, and only the final product of hydrolysis is nontoxic. The slow rate of hydrolysis assures that all three toxic substances will be present for a long period of time. After 48 to 72 hours, water contaminated with nitrogen mustard is found to have unreacted nitrogen mustard and the two hydrolysis products in solution. This property is conducive to the poisoning of food and water by these agents.

The nitrogen mustards, unlike the sulfur mustards, are not readily oxidized and require an excess of the reacting chlorine compound to be detoxified during decontamination.

The nitrogen mustards are able to penetrate cell membranes in tissues and also the surfaces of a number of materials. They are persistent in cold and temperate climates. Their persistency can be further increased by dissolving them in non-volatile solvents to create a thickened nitrogen mustard that resists decontamination. At higher temperatures, persistency is less, but higher concentrations of vapor are produced.

HN-1 is more volatile and less persistent than sulfur mustard but only one fifth as vesicant to the skin. HN-2 has the greatest blistering power of the nitrogen mustards in vapor form but is intermediate as a liquid blistering agent. HN-3 is less volatile and more persistent than sulfur mustard with vesicant properties almost equal to those of sulfur mustard. HN-3 is the most stable of the three nitrogen mustards in storage and the one considered to pose the most serious threat as a chemical warfare agent.

The physical properties of the most common blister agents are listed in Table 1.2. Water is included in the table as a reference point for the blister agents.

Property	HD	HN-1	HN-2	HN-3	L	Water
Molecular weight	159.1	170.1	156.1	204.5	207.4	18
Density, g/cm 3	1.27 at 20°C	1.09 at 25°C	1.15 at 20°C	1.24 at 25°C	1.89 at 20°C	1 at 25°C
Boiling-point, °C	216.11	193.89	75 at 15 mm Hg	256.11	190	100
Freezing-point, °C	14.44	-51.78	-65	-32.61	18 to 0	0
Vapor pressure, mm Hg	0.072 at 20°C	0.24 at 25°C	0.29 at 20°C	0.0109 at 25°C	0.394 at 20°C	23.756 at 25°C
Volatility, mg/m3	610 at 20°C	1520 at 20°C	3580 at 25°C	121 at 25°C	4480 at 20°C	23,010 at 25°C
Solubility in water, %	<1%	Sparingly	Sparingly	Insoluble	Insoluble	NA

Table 1.2: *Physical properties of water and common blister agents HD, HN-1, HN-2, HN-3, L.*

1.3.2 Route of entry

Human body readily absorbs most blister agents that are also relatively persistent. Blister agents could also contaminate liquids or foods, which became poisoned. These agents cause inflammation, blisters, and general destruction of tissues. Skin, eyes, lungs, and gastro-intestinal tract are attacked by vesicants both in liquid or gas phase. Also internal organs, mainly blood-generating organs, may be injured as a result of vesicants being taken up through the skin or lungs and transported into the body.

Mustard agents (HD, HN) give no immediate symptoms upon contact. The latent period for the effects from mustards is usually several hours. A delay between two and twenty-four hours may occur before pain is felt and the victim becomes aware of what has happened because (the onset of symptoms from vapors is 4 to 6 hours and the onset of symptoms from skin exposure is 2 to 48 hours). By then, cell damage has already occurred. The delayed effect is a characteristic of mustard agents. There is no latent period for exposure to Lewisite.

1.3.3 Symptoms

Aching eyes with excessive tearing, inflammation of the skin, irritation of the mucous membranes, hoarseness, coughing and sneezing are mild symptoms of vesicants poisoning which normally do not require medical treatment. Eye injuries with loss of sight, the formation of blisters on the skin, nausea, vomiting, and diarrhea together with severe difficulty in breathing are severe injuries that are incapacitating and require medical care. Injury to the bone marrow, spleen, and lymphatic tissue are pronounced effects on inner organs. A drastic reduction in the number of white blood cells 5-10 days after exposure is usually observed, a condition very similar to that after exposure to radiation. This reduction of the immune defense will complicate the already large risk of infection in people with severe skin and lung injuries. Complications after lung injury caused by inhalation of vesicants is the most common cause of death. Most of the chronic and late effects from mustard agent poisoning are also caused by lung injuries.

1.3.4 Diagnostic

There is no specific test for vesicants intoxication. In the absence of agent identification in the environment or reliable intelligence indicating likely enemy use of blistering agent, a diagnosis must be made based on interviews with the victims and the symptoms presented. If victims report that they experienced pain shortly after exposure, the vesicant agent sulfur mustard can be eliminated.

An exposure that is almost immediately painful and results in the development of wheals (welts similar in appearance to bee stings), not blisters, in approximately 30 minutes is likely due to the urticant agent phosgene oxime (CX).

An exposure that is almost immediately painful but does not produce blisters for at least 13 hours is likely due to Lewisite. Lewisite can cause severe damage to the eye membrane if not decontaminated rapidly. Skin contact produces an immediate stinging sensation, followed by reddening of the skin within 30 minutes. After a period of 4 to 13 hours, blisters form and normally cover the entire reddened area.

The typical symptom-free latent phase of nitrogen and sulfur mustards helps to make a differential diagnosis between these agents and the instantly-irritating arsenical vesicants and phosgene oxime.

1.4 The third group

This group is made of five different CWAs type which are not included in the previously described ones thus completing the general description of all CWAs.

Systemics toxic compounds

This class includes blood agents. They are gas (cyanogen chloride-CK, carbon oxide), or highly volatile liquids (hydrogen cyanide-AC) and then they are considered to be non-persistent agents. Symptoms depend upon the dose received. CK irritates the eyes and respiratory tract, even in low concentrations. Acute exposure produces intense irritation of the lungs characterized by coughing and breathing problems, which may quickly lead to a pulmonary edema. Inside the body, cyanogen chloride converts to hydrogen cyanide, which inactivates the enzyme cytochrome oxidase, an enzyme complex in the mitochondrial electron transport chain, preventing the utilization of oxygen by the cells. The cells begin to die, convulsions begin, and cardiac arrest occurs within several minutes. Cyanide can also be ingested through food or drink. Exposure to a high concentration of hydrogen cyanide can lead to death within minutes after heavy, frequent breathing, convulsions, and cardiac arrest. Exposure to a low concentration can lead to headache, anxiety, agitation, respiratory difficulty, nausea, and possibly death if the exposure is sustained.

Suffocant agents

These chemicals include choking agents and tear gases (or lachrymators) which function mainly through eye irritation, but some may affect the respiratory system. The effects of these chemical agents are felt almost instantly and disappear within 15-30 minutes after the exposure ceases. These gases have a very low acute toxicity. Consequently, serious or lethal injuries occur only in instances of highly concentrated exposure.

The most used suffocants are Phosgene (CG) and Chloropicrin (trichloronitromethane-PS). Phosgene is also an important industrial compound used in the preparation and manufacture of many organic chemicals (dyes, pharmaceuticals, herbicides, insecticides, synthetic foams, resins, and polymers). It affects the upper respiratory tract, skin, and eyes and causes severe respiratory damage as well as burns to the skin and eyes.

The symptoms of chloropicrin exposure include eye, lung, and skin irritation. By contacting the body, chloropicrin causes discomfort that disappears at termination of exposure. Pulmonary edema, unconsciousness, and death may occur with high levels of exposure.

Incapacitating agents

These agents are very potent psychoactive chemicals affecting the central nervous system as well as the organs of circulation, digestion, salivation, sweating, and vision. The psychedelic chemical 3-quinuclidinyl benzylate (BZ), also known as "agent buzz", was dropped from the chemical arsenal because its effects on enemy front-line troops would be varied and unpredictable. It is an odorless white crystalline solid and is usually disseminated as an aerosol with the primary route of entry into the body through the respiratory system; the secondary route is through the digestive tract. BZ blocks the action of acetylcholine in both the peripheral and central nervous system. It stimulates the action of noradrenaline (norepinephrine) in the brain, as much as do amphetamines and cocaine.

Irritants

These chemicals include lachrymators, sternites or vomiting agents. These agents are not lethal but by acting on the eyes (lachrymators) and on the respiratory and tract (sternites) they hinder normal functioning. This group of agents includes substances that differ considerably in chemical structure; this is due to, among other things, the large differences in their polarity.

Irritants are used in form of vapor or aerosol dispersed in air and enter the body through inhalation or by direct action on the eyes. The most important are tear gases such as chloroacetophenone (CAP), o-chlorobenzylidenmalononitrile (CS), dibenzo[b,f]-1,4-oxazepine (CR), camite (CA) and sternite adamsite (10-chloro-5,10-dihydrophenarsazine-DM).

Because tear compounds produce only transient casualties, they are widely used for training, riot control, and situations where long-term incapacitation are unacceptable. When released indoors, they can cause serious illness or death. Also DM was not toxic enough for the battlefield, but it proved to be too drastic for use against civilian mobs, so that it was banned for use against civilian populations in the 1930s in the Western nations.

1.5 Toxic Industrial Chemicals (TICs)

The problems connected with the determination of substances classified as potential warfare agents lie also in the non-military sphere of interest. This concerns, for instance, the uncontrolled spread of toxic substances as a result of industrial breakdown or agrotechnical operations, and the generation of poisons, e.g., fluoroacetic acid in plants or phosgene in the troposphere.

Chemicals other than chemical warfare agents that have harmful effects on humans are called TICs, standing for Toxic Industrial Chemicals, often referred to as toxic industrial materials, or TIMs, and are used in a variety of settings such as manufacturing facilities, maintenance areas, and general storage areas. Individual's health after multiple low-level exposures may be severely affected by these compounds even if exposure to some of these chemicals may not be immediately dangerous to life and health (IDLH).

A TIC is defined through its lethal concentration, namely if it has a LCt50 value (lethal concentration for 50% of the population multiplied by exposure time) less than 100,000 mg-min/m^3 in any mammalian species, and through its use, namely if it is produced in quantities exceeding 30 tons per year at one production facility.

The threat deriving from their use is far greater than that deriving from chemical warfare agent since they are quite common, produced in big quantities (multi-ton) and readily available. Thus a terrorist may employ a big amount to obtain even a bigger effect than using nerve agent, although they are not as lethal. It is assumed that a balance is struck between the lethality of a material and the amount of materials produced worldwide, but it is difficult to determine how to rank their potential for use by a terrorist.

Physical and chemical properties for TICs such as ammonia, chlorine, cyanogen chloride, and hydrogen cyanide are presented in Table 1.3. Water is included in the table as a reference point for the TICs. The physical and chemical properties for the remaining TICs identified in this guide can be found in International Task Force 25: Hazard From Industrial Chemicals Final Report, April 1998.

Property	Ammonia	Chlorine	Cyanogen Chloride	Hydrogen Cyanide	Water
Molecular weight	17.03	70.9	61.48	27.02	18
Density, g/cm 3	0.00077 at 25°C	3.214 at 25°C	1.18 at 20°C	0.990 at 20°C	1 at 25°C
Boiling-point, oF	-28	-30	55	78	212
Freezing-point, oF	-108	-150	20	8	32
Vapor pressure, mm Hg at 25°C	7408	5643	1000	742	23.756
Volatility, mg/m3	6,782,064 at 25°C	21,508,124 at 25°C	2,600,000 at 20°C	1,080,000 at 25°C	23,010 at 25°C
Solubility in water, %	89.9	1.5	Slightly	Highly soluble	NA

Table 1.3: *Physical and chemical properties of water and TIMs.*

Three categories were organized to catalog TICs depending on their relative importance and assist in hazard assessment. Table 1.4 lists the TICs with respect to their Hazard Index Ranking (High, Medium, or Low Hazard).

High Hazard indicates a widely produced, stored or transported TIC that has high toxicity and is easily vaporized; Medium Hazard indicates a TIC that may rank high in some categories but lower in others such as number of producers, physical state, or toxicity; a Low Hazard overall ranking indicates that this TIC is not likely to be a hazard unless specific operational factors indicate otherwise.

HIGH	MEDIUM	LOW
Ammonia	Acetone cyanohydrin	Allyl isothiocyanate
Arsine	Acrolein	Arsenic trichloride
Boron trichloride	Acrylonitrile	Bromine
Boron trifluoride	Allyl alcohol	Bromine chloride
Carbon disulfide	Allylamine	Bromine pentafluoride
Chlorine	Allyl chlorocarbonate	Bromine trifluoride
Diborane	Boron tribromide	Carbonyl fluoride
Ethylene oxide	Carbon monoxide	Chlorine pentafluoride
Fluorine	Carbonyl sulfide	Chlorine trifluoride
Formaldehyde	Chloroacetone	Chloroacetaldehyde
Hydrogen bromide	Chloroacetonitrile	Chloroacetyl chloride
Hydrogen chloride	Chlorosulfonic acid	Crotonaldehyde
Hydrogen cyanide	Diketene	Cyanogen chloride
Hydrogen fluoride	1,2-Dimethylhydrazine	Dimethyl sulfate
Hydrogen sulfide	Ethylene dibromide	Diphenylmethane-4,4'-diisocyanate
Nitric acid, fuming	Hydrogen selenide	Ethyl chloroformate
Phosgene	Methanesulfonyl chloride	Ethyl chlorothioformate
Phosphorus trichloride	Methyl bromide	Ethyl phosphonothioic dichloride
Sulfur dioxide	Methyl chloroformate	Ethyl phosphonic dichloride
Sulfuric acid	Methyl chlorosilane	Ethyleneimine
Tungsten hexafluoride	Methyl hydrazine	Hexachlorocyclopentadiene
	Methyl isocyanate	Hydrogen iodide
	Methyl mercaptan	Iron pentacarbonyl
	Nitrogen dioxide	Isobutyl chloroformate
	Phosphine	Isopropyl chloroformate
	Phosphorus oxychloride	Isopropyl isocyanate
	Phosphorus pentafluoride	n-Butyl chloroformate
	Selenium hexafluoride	n-Butyl isocyanate
	Silicon tetrafluoride	Nitric oxide
	Stibine	n-Propyl chloroformate
	Sulfur trioxide	Parathion
	Sulfuryl chloride	Perchloromethyl mercaptan
	Sulfuryl fluoride	sec-Butyl chloroformate
	Tellurium hexafluoride	tert-Butyl isocyanate
	n-Octyl mercaptan	Tetraethyl lead
	Titanium tetrachloride	Tetraethyl pyroposphate
	Trichloroacetyl chloride	Tetramethyl lead
	Trifluoroacetyl chloride	Toluene 2,4-diisocyanate
		Toluene 2,6-diisocyanate

Table 1.4: *TICs listed by hazard index.*

1.6 Volatile Organic Compounds (VOCs)

VOCs are nonpolar and nonreactive organics having boiling points in the range -15 to +120°C. They are an interesting class of chemicals for our purpose because they can be considered as interferents for other substances detection as most of them absorb in the same band of our source. Even if absorption coefficients are usually smaller than that of CWAs and TICs, their volatility is usually much bigger and their use in human activities implies their diffusion in anthropic areas. Sources include industrial and commercial facilities, hazardous waste storage and treatment facilities, etc.., so it is not difficult to find them in concentration high enough to interfere while searching for other compounds.

They are also interesting because many of these are pollutants and many are toxic. Human health impacts as well as environment impacts can be determined knowing concentration of such materials in the ambient atmosphere. Their level of dangerousness is defined by European Commission and was introduced in Italy by law DLs number 152 dated 2006, where concentration limit in atmosphere of several substances belonging to different class are established. For each of these compounds, among which VOCs are included, threshold of dangerousness and emission limit are prescribed.

Traditionally, volatile organic compounds air monitoring methods, described in EPA (Environmental Protection Agency) methods, have relied on carbon adsorption followed by solvent or thermal desorption and GC analysis. Automatic thermal desorption (ATD) is a technique used for the analysis of volatile compounds that have been adsorbed onto an adsorbent bed contained within a tube. Thermal desorption releases these volatile compounds by heating the adsorbent bed in a stream of helium. The volatile compounds are refocused onto a cold-trap and transferred to the GC system for analysis. TD-GC-MS has been demonstrated to be suitable for measurement of volatile organic compounds (VOCs) in the environment. It yields a sensitive, specific analysis procedure. Particularly, ATD is a rapid means of delivering a volatile analyte collected on an air sampling tube to the analytical instrument and shows many advantages over solvent extraction (greater sensitivity, no sample preparation, non interfering solvent peaks, tube can be reused), but has the disadvantage of being a one shot method and once analyzed the sample is not available for re-analysis.

A list of common VOCs is provided in the following table.

Acetone	Chloromethane	Dichlorofluoromethane	Styrene
Acetonitrile	3-Chloro-1-propene	t,cis-1,2-Dichloropropene	1,2,4-Trichlorobenzene
Acrolein	Cyclohexane	1,2-Dichloro-1,1,2,2-tetrafluoroethane	1,1,1-Trichloroethane
Acrylonitrile	Dibromochloromethane	Ethylbenzene	1,1,2-Trichloroethane
Benzene	1,2-Dibromoethane	Heptane	1,1,2,2-Tetrachloroethane
Benzyl chloride	1,2-Dichlorobenzene	Hexachlorobutadiene	Tetrachloroethene
Bromodichloromethane	1,3-Dichlorobenzene	Hexane	Toluene
Bromomethane	1,4-Dichlorobenzene	Methanol	Trichloroethene
1,3-Butadiene	Dichlorodifluoromethane	Methylene chloride	Trichlorofluoromethane
2-Butanone	1,1-Dichloroethane	Methyl methacrylate	1,1,2-Trichloro-1,2,2-trifluoroethane
Carbon tetrachloride	1,2-Dichloroethane	4-Methyl-2-pentanone	1,2,4-Trimethylbenzene
Chlorobenzene	1,1-Dichloroethene	alpha-Methyl styrene	1,3,5-Trimethylbenzene
Chlorodifluoromethane	t, cis-1,2-Dichloroethene	Octane	Vinyl acetate
Chloroethane		n-Pentane	Vinyl chloride
Chloroform	1,2-Dichloropropane	Propylene	Xylenes (o-, m- and p-)

Table 1.5. *VOCs listed by EPA (Environmental Protection Agency) method TO-14.*

2 FIELD DETECTION TECHNOLOGIES AND REAGENTS

2.1 Introduction

In the case of accidents at chemical plants, during transportation of chemicals or during terrorist attacks, hazardous compounds may be released and may harm emergency personnel and population. To prevent this, a simple chemical hazard monitor is required to help locate the dangerous area, its border, and the safe area. Detecting these substances in the field has been the objective of incident detection and measurement device developments. Visual inspection is also an acceptable method of locating leaking agent and is part of the Standard Operating Procedures (SOPs) at stockpile facilities.

CWAs detection is important since there are currently no known pretreatments or prophylaxes to fully protect against them. Therefore, detection systems must be a primary defense against CWAs along with other measures such as intelligence and physical protection. There may be only seconds to employ protective measures, so detection must be simple, rapid, specific and sensitive. Rapid detection and warning of an opponent's use of CWAs are critical in protecting military forces and civilian populations.

In principle, all relevant compounds can be measured at low concentrations by laboratory analysis. However, techniques for task forces in the field are usually limited to simple equipment and are useful for only a limited range of substances. Moreover, there is always the danger of failing to detect important toxic substances if only one sensing technology is used. Making laboratory analytical techniques available to the firefighter is the first successful step in accident analysis.

Several equipments are available to aid in detecting agent vapor or liquid. Measurement techniques use the unique molecular weights, ionization properties, reactions with other chemicals, or select molecular constituents (phosphorus or sulfur, for example) of the CW agents for rapid field characterization. Although these methods are generally considered valid, the sensitivity of the equipment may be too low if trace-level determinations are required. Moreover, some problems could arise if other substances, which have the same kind of response to the instrument, are present. These interferents could be easily found especially in a human modified environment, where many chemicals produced by everyday activities may affect the reliability of the instrument as well as its sensitivity.

So available chemical detectors, while meeting the criteria of being portable and relatively easy to use in the field, offer only limited chemical specificity and sensitivity and are prone to false positive responses. They often are referred to as one-dimensional sensors that can only confirm what is already believed to be present, but cannot provide information about other possible harmful agents. Nowadays big affords are being made to achieve more effective and accurate methods of detection that are less affected by environmental chemicals in operational areas and that could be commercially available at lower costs. For these reasons scientists worldwide are directing enormous efforts to agent-specific detection technologies.

Detector technologies can be divided into two general categories: point and standoff (also called remote). A specific method should be selected based on the conditions of the area (field, work area), the physical state of the agent (liquid or vapor), the desired concentration level, and the necessary alarm response time.

Some of the available equipments for field detection of CWAs and TICs will be presented in the following pages.

2.2 Point detection technologies

Point detectors sample air, soil, or water for the presence of CWAs in the immediate vicinity of the detector. This technology is limited because the device needs to stay in the same place of the chemical agent and usually it is not very fast. Having enough time is possible to map a contaminated area or if detector is fast enough it can be used as source of alarm in a fixed place, even if it may not provide sufficient time to take protective measures. Decontamination site or

collective protection areas could also be monitored to determine the effectiveness of decontamination operations. They can be used also to divide contaminated personnel from no-contaminated so to decontaminate only if necessary, saving resources.
Point detection technologies include ionization (or ion mobility), flame photometry, mass spectrometry, infrared (IR) spectroscopy, electrochemistry, detection kits and tickets that use a variety of chemical reactions.

2.2.1 Ionization/Ion Mobility Spectrometry (IMS)

Many of the point CW agent detectors/alarms in use by military forces worldwide use IMS technology. The basic concept of IMS is to characterize chemical substances through gas-phase ion mobility. The pattern is compared to a sample of clean air; if the pattern is markedly different and unique to certain types of agents, the alarm sounds.
IMS operates by drawing air samples at atmospheric pressure into a reaction chamber where the air and all its constituents (such as chemical agents) are ionized. Ions are then moved through a weak electric field toward a detector plate or receiving electrode where the generated electric charge is recorded respect to travel time. As the ions collide with the detector plate, charge (or current) is registered and an ion mobility spectrum is generated as a series of peaks. The peaks are graphed as time (x axis) versus current (y axis).
The time it takes the species to traverse the distance (the characteristic mobility time) is used to identify the substances because it is proportional to the mass of the ionized chemical species. Matching mobility times for known chemical compounds identifies the unknown chemical agent. While transit time gives information on substances present, the high of peak is proportional to substances concentrations.
Devices need several seconds to a few minutes to analyze. Liquid samples must be volatilized to be analyzed. Nearly all chemical classes can be ionized at atmospheric pressure using different technique such as proton transfer reactions, charge transfer, dissociative charge transfer, or negative ion reactions. However, radioactive Beta emitters are generally used to continuously emit energy (charged particles), which is transferred to the sample molecules, ionizing the sample in most portable detectors. Radioactive sources (such as Ni^{63} or Am^{241}) are preferred since they require no external power, have no electronic components, and do not require service.
An advantage of IMS is that it allows outside air to be drawn directly into the instrument without sample preparation or concentration and yields excellent detection sensitivities. In addition, the actual analysis of the air takes place in a small chamber that is rugged, simple, and relatively inexpensive. A disadvantage of IMS is known as matrix effects whereby the humidity, temperature, and composition of the air that contains the chemical agents of interest may influence the response of the detector. Certain interferents have been found to cause false positive responses in several of the fielded IMS detectors. However, measures have been incorporated to minimize these effects.
The CAM (Chemical Agent Monitor) and ICAM (Improved Chemical Agent Monitor) systems are hand-held, soldier-operated devices designed for monitoring chemical agent contamination on personnel and equipment that use ion-mobility spectrometry technology to detect and discriminate between mustard and nerve agent vapors. The operator must select G or H mode because they cannot detect both types of agent simultaneously. The response time is within one minute.
The CAM is a post-attack monitor and not a detector or alarm. It can only report conditions at the front of the inlet probe (point monitor) and cannot give a realistic assessment of the vapor hazard over an area from one position. The CAM may give false readings when used in enclosed spaces or when sampling near strong vapor sources (such as dense smoke). Aromatic vapors (perfumes, food flavorings, and menthol cigarettes), cleaning compounds (disinfectants), and smokes and fumes may also give false readings. This detector is shown in Figure 1.1.

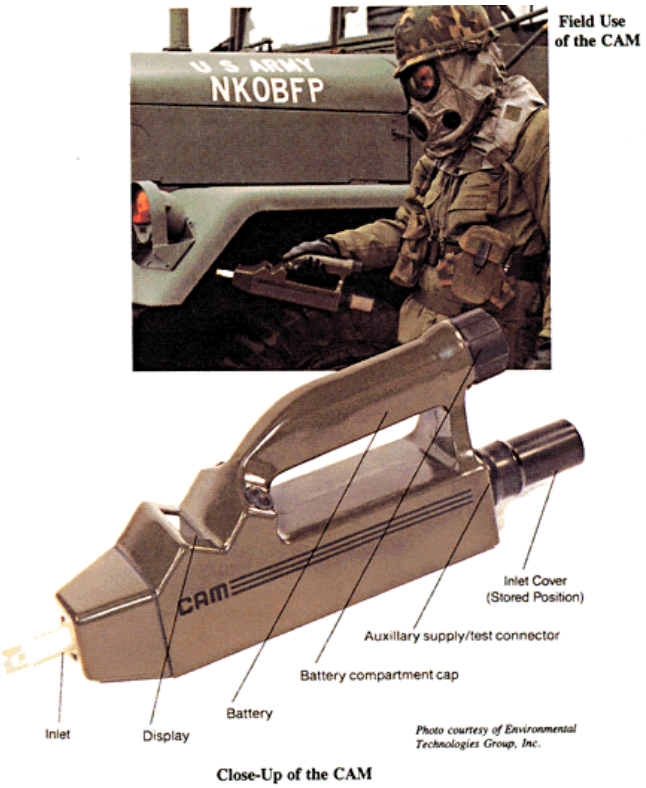

Figure 1.1: *Close-up and field use of the CAM.*

The ICAM was developed to reduce operation and support cost by simplifying the design and improving the reliability of the CAM. It incorporates two major changes to the original CAM: a redesigned molecular sieve that is enlarged and more easily replaced, and an updated electronics board that is less costly to produce. Although these changes are transparent to the user, the ICAM has increased reliability and improved start-up characteristics when compared to the CAM. The units can be held in either hand and operated while wearing chemical protective clothing.

An example of a stand-alone detector based on the same technology, which provides automatic alarm if nerve agent vapors or inhalable aerosols are present, is the M8A1 Automatic Chemical Agent Alarm System. It detects nerve agents and blister agents when the concentration is 0.1 mg/m^3 or greater and alarms within a couple of minutes. The system consists of the M43A1 Detector and M42 Alarm. False alarms will occur to heavy concentrations of rocket propellant smoke, screening smoke, signaling smoke, engine exhausts, and whenever a nuclear blast occurs.

The M43A1 detector is an ionization product diffusion/ion mobility type detector. Air is continuously drawn through the internal sensor past a radioactive source (Am^{241}), and a small percentage are ionized by the beta rays just before the baffle sections of the cell where only heavy ions (different from the ones obtained by standard air components) are able to pass. The current is then much greater if big ions are present and the alarm can be triggered with a critical threshold current.

The M8A1 Alarm System is used primarily to alert stationary units when a cloud of nerve agent vapor has arrived or is about to arrive at their position. When used in a stationary role, unit personnel will position the systems as soon as they arrive at a new location. The detector units are placed upwind and connected to the alarm units with standard communication wire. Once the alarm sounds, the operator must disconnect the power, decontaminate the unit, and go through start-up procedures to reactivate the alarm. M8A1 Alarm System device is shown in Figure 1.2.

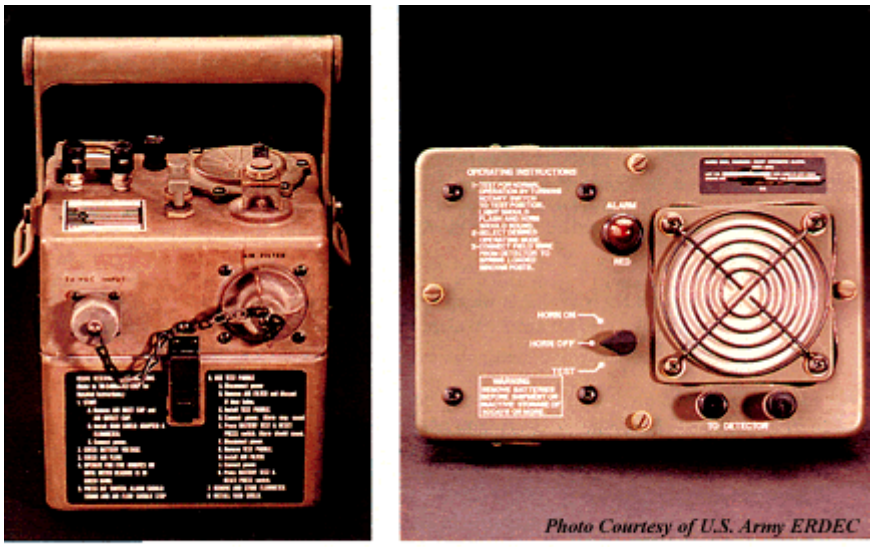

The M8A1 Automatic Chemical Agent Alarm System consists of the M43A1 Detector (left) and M42 Alarm (right)

Figure 1.2: *The M8A1 Automatic Chemical Agent Alarm System.*

The Advanced Portable Detector (APD) 2000 (Figure 1.3), manufactured by Smiths Detection, is another common handheld device that can detect mace and pepper spray as well as nerve agents, blister agents, and hazardous compounds.
The Sabre FR (Figure 1.4) also uses IMS and is manufactured by Smiths Detection. It is in use by first responders because it can use vapor or trace particle samples to detect explosives, drugs such as cocaine and heroin, as well as chemical agents.

Figure 1.3: *APD2000.*

Figure 1.4: *SABRE FR.*

The ChemPro 100 is based on Environics open loop ion mobility spectrometry (IMS) technology and uses an improved Ion Mobility Cell™ that is designed to increase selectivity and sensitivity in detecting CW agents and TICs. It identifies agent class (Nerve, Blister, or Blood), indicates relative concentration (Low, Medium, or High), and indicates whether the concentration is increasing or decreasing. The operator interface is designed to be operated using one hand. The ChemPro 100 stores agent alarm information for retrieval at a later time to provide a historical log of events.

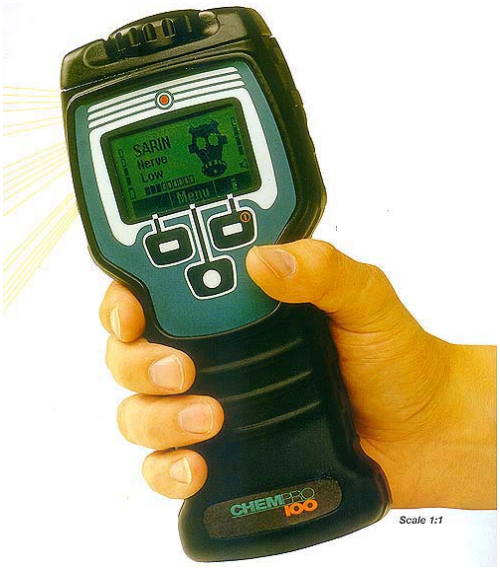

Figure 1.5: *ChemPro 100 Hand-Held Chemical Detector.*

2.2.2 Flame photometry

Several CW agent detectors in use today use the flame photometry technology. In flame photometry, the sampled air is burned in a hydrogen-rich flame. The compounds present, when burned, become exited and will emit light of certain wavelengths in the flame. An optical filter is used to watch the flame and only lets one specific wavelength of light pass through it. A photosensitive detector (photomultiplier tube) senses the light that passes through the selective filter, producing a response signal. Current is thus eventually proportional to concentration.

Flame photometry allows for ambient air samples to be drawn directly into the instrument for analysis. Moreover, this technology is sensitive and selective. However, flame photometry involves elemental analysis, meaning the detector is actually sensing elemental sulfur or phosphorus, and not the larger more complex chemical agent molecules. This fact allows interferences from other compounds containing sulfur and phosphorus, resulting in false positives in some detectors. Sample separation techniques, such as chromatography or a pre-concentrator, can reduce the possibility of common substances interfering with agent detection.

The AP2C handheld detector manufactured by Arrow Tech Inc uses this technology. It can detect sarin at a concentration of 10 mcg/m^3 in 2 seconds. Federal agencies and international agencies use this detector for mass screenings and for confirming decontamination of casualties.

The miniature automatic continuous agent monitoring system (MINICAMS) is a system based on combining gas chromatography with flame photometry. A sample vapor is drawn into the machine and exposed to a heated preconcentrator loop. As each component exudes from the column, it is exposed to flame photometry. This system enables more specific detection. A typical cycle lasts 3-5 minutes, enabling continuous monitoring of the environment.

2.2.3 Mass spectrometry

Mass spectrometry (MS) is one of the most widely used analytical techniques available today. Though primarily a laboratory tool, recent advances in instrumentation have resulted in smaller, more portable MS instruments. Several countries have fielded, or are in the process of fielding, MS instruments specifically for detection of CW agents.

All mass spectrometers consist of a sample inlet system, an ion source, a mass analyzer, a detector, and a signal processing system. A pure chemical sample is introduced into the mass spectrometer detector where they become fragmented by the bombardment of electrons. The fragments (or ions) produced, which range from large to small, are separated by the mass analyzer component. A mass spectrum is produced, which appears as a number of peaks on a graph, each representing a mass-to-

charge ratio for each ion fragment. Individual compounds have a unique spectrum of fragments that are produced by the electron impacts. This spectrum is essentially the same every time the compound is injected into the mass spectrometer and acts like a fingerprint for the molecule.
MS offers some significant advantages for agent detection. It can provide sensitive, reliable, and versatile recognition of chemical agents. Rapid characterization and quantification are possible, and interference is not likely. However, complexity, ruggedness, power, and maintenance requirements of the technology detract from the potential field application for CW detection.
Miniaturization of mass spectrometry (MS) for field measurements has been pursued intensively over the past decade. Efforts to develop small, portable mass analyzers have focused on various types and formats of devices, including time-of-flight MS, electrostatic-magnetic sector MS-MS, cylindrical ion traps, rectilinear ion traps, toroidal ion traps, and halo ion traps.
MS can be used in combination with a gas chromatograph in order to detect and identify unknown chemical compounds present in the same mixture sample. Analytical advantages of high sensitivity, high selectivity, and rapid response time make GC–MS a preferred detection technique for CWAs and TICs as long as it can be packaged for field use in a truly portable, durable, self-supported format that is relatively easy to operate by nonscientific personnel. However, because of relatively high costs only few special-purpose forces use this equipment.
Inficon Hapsite Field Portable System (Figure 1.6) and Spectra TrakTM (Figure 1.7) are two examples of compact, rugged, transportable gas chromatograph/mass spectrometer (GC/MS) designed to provide on-site, laboratory-quality chemical analysis results. They can be used to analyze samples of air, gas, soil, and water. Detection and identification results can be obtained at trace levels. The ability to perform direct MS analyses allows these systems to provide real-time monitoring capabilities. System components include a mass analyzer, vacuum system, gas chromatograph, sampling systems, computer, and transport case. Both detector devices can be transported by vehicle or aircraft to the field site and set up for operational use within minutes.

Figure 1.6: *Inficon Hapsite Field Portable System.*

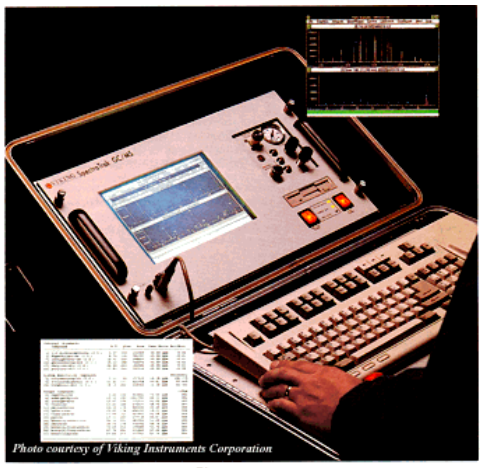

The SpectraTrak™ Transportable GC/MS System

Figure 1.7*: Spectra TrakTM Transportable GC/MS System.*

2.2.4 Infrared spectroscopy

Infrared spectroscopy could be performed both in liquid and gas phase, being essentially a measure of light absorbed by the sample at different wavelengths. Usually mid infrared light (2.5 – 50 μm, 4000 –200 cm^{-1}) is preferred due to the presence of roto-vibrational levels which absorb to get a higher level on this band in numerous compounds. Each molecule has its own spectrum (fingerprint) which could easily give identification if one species at time is present. It is nowadays used for identification of organic and organometallic molecules. Until now photoacoustic infrared pectroscopy (PIRS) and filter based infrared spectroscopy are used.

2.2.4.1 Photoacoustic Infrared Spectroscopy (PIRS)

Photoacoustic effect is based on measuring sound intensity provided by gas expansion and contraction that are due to a change in temperature. This change in temperature is related to the sample absorption of light coming from a proper source, which is modulated to obtain audible frequencies. A specific wavelength of infrared light is pulsated into the sample through an optical filter or grid. A different optical filter is used for each specific type of agent or toxic vapor that is to be detected. The light transmitted by the optical filter or grid (one specific wavelength) is selectively absorbed by the chemical vapor being monitored, so if any of the desired vapors are present the temperature of the gas increases. This temperature increase also causes an equivalent increase in gas pressure since the sample cell is sealed. Because the light entering the cell is pulsating, the pressure in the cell will also fluctuate, creating an acoustic wave in the cell that is directly_proportional to the concentration of the gas in the cell. This is the photo-acoustic effect. Sound intensity is proportional to absorption and thus a sort of absorption spectrum can be obtained. Interferents effect will decrease increasing the number of wavelengths and clear identification needs many wavelengths, as in any spectroscopy. Commercial instruments are available that have been modified to detect most CW agent vapors.

PIRS has the advantage of being selective since a unique optical filter is used for each agent that is to be detected. A disadvantage of this technology is that humidity and temperature affect it. Calibration in the actual detection environment may allow for correcting some of these influences.

Commercial products exist as mobile laboratory equipment. Two examples, made by Innova, are Type 1301 and Type 1312, respectively shown in Figures 1.8 and 1.9.

Figure 1.8: *Innova Type 1301 Multigas Monitor.*

Figure 1.9: *Innova Type 1312 Multigas Monitor.*

2.2.4.2 Filter-based infrared spectrometry

This spectroscopy is based on selecting the component of a broadband light absorbed by the sample, which is crossed by a beam shaped and directed by an optical system, through the use of filters, usually four or more. Response to different wavelength is analyzed in order to calculate absorption and then, if spectrum is recognized, concentration.

Usually concentrations of each component, in each sample, at each station, are used for compiling time weighted average (TWA) reports and trend displays. Further analysis and longer term storage and retrieval can be done with retained data. An example of such device, a portable ambient air Analyzer, the Miran SaphIRe is shown in Figure 1.10.

Figure 1.10: *Miran SaphIRe Portable Ambient Air Analyzer.*

2.2.5 Electrochemistry

Several CW agent detectors operate on the principle of electrochemistry. Fundamentally, electrochemistry is based on a chemical reaction that occurs when the CW agent enters the detection region, producing some change in the electrical potential. A liquid solution is used that reacts with the CW agent. When the reaction occurs, the electrical potential in the solution changes. This change is normally monitored through some type of electrode. A threshold concentration of agent is required, which corresponds to a change in the monitored electrical potential. This principle is used to build electrochemical detectors.

One of the most used electrochemical reactions use the nerve agents property of inhibition of cholinesterase. The air sample is put in contact with a solution containing a known amount of cholinesterase, a percentage of which will be inhibited from the following reaction if nerve agent is present. An electrochemically active product is then produced adding a solution containing a compound that will react with uninhibited cholinesterase. Concentration of nerve agent present in the sampled air is related to the concentration of uninhibited cholinesterase which will change cell potential.

Another kind of electrochemical detector is based on the resistance change of a thin film that increases as the film absorbs chemical agent from the air. The involved electrochemical reaction uses a paint resin in which fine particles of silver are suspended. The paint resin is selectively soluble for the agents of interest. The silver-bearing paint acts as an electrical conductor, which, when attacked by a CW agent, swells and causes a physical separation of the conductive silver flakes. The electrical resistance of the detector grid changes and an alarm condition exists once the threshold resistance is reached.

Many different variations in electrochemical detection exist. These methods are selective, but not as sensitive as some other methods. Their drift related to temperature shift, which change rates of reactions modifying selectivity and sensitivity, and the intrinsic less sensitivity compared to IMS and flame photom etry heavily influence their diffusion. Several of the fielded instruments have experienced problems at environmental extremes.

The ALAD **(**Automatic Liquid Agent Detector System**)** shown in Figure 1.11 is a detector that can be used for point source, local area, and remote detection of nerve and blister agents in liquid or solid form. It uses the principles of electrochemistry technology. ALAD provides a local audible and visible alarm that can warn personnel for ranges of 8 to 15 meters. It can be used as a stand-alone detector or as part of a chemical warning system network for fixed-site applications when hooked to a network or radio link. The sensor is a one-use item that detects small liquid droplets, frozen and thickened forms of blister agents via microprocessor based electronics.

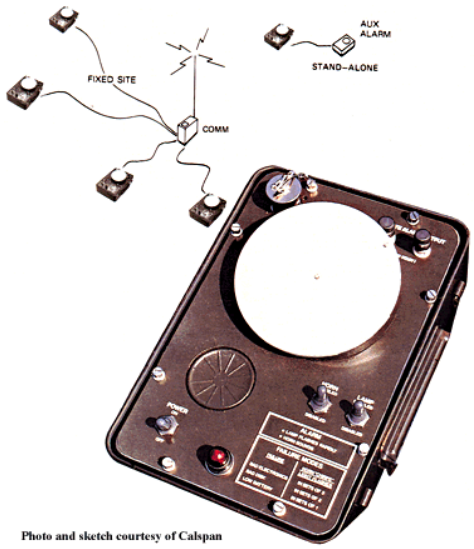

Figure 1.11: *ALAD (Automatic Liquid Agent Detector System).*

The ICAD is a miniature, lightweight, plastic CW agent detector. The unit consists of a sensor module and an electronics module. The sensor module contains two miniature electrochemical sensors and a lithium battery. One sensor detects nerve, blood, and choking agents, while the other detects blister agents. Chemical agent vapors diffuse through membranes on the sensors where they undergo electrochemical reactions. The electronics module continuously monitors the output from the sensor modules. When the threshold concentration of agent is reached, the unit sounds an audible alarm and an LED illuminates. The system is designed to operate continuously for up to four months, at which time the sensor module can be replaced. It is shown in Figure 1.12.

Figure 1.12: *ICAD Miniature Chemical Agent Detector.*

2.2.6 Colorimetric or color change chemistry

Color change due to chemical reactions induced by suspect agent is used to build some kinds of easy use detector kits and tickets. These kits are generally configured for specific purposes, such as CW agent detection in water, or confirmatory detection after an automatic alarm or monitor. The basic technology uses chemical reactions that occur when CW agents interact with the various solutions and substrates. The most common indicator for a positive response is a color change.

To verify gas presence, vapor detection kits or tickets use some form of surface or substrate to which the reagent chemicals are added and exposed to the sampled air. Some kits use a filter paper

surface that is exposed directly or the sampled air is drawn through the paper with an aspirator bulb. Other kits use a glass tube with sensible chemical on his wall which has to be broken on one side and air must be pumped in so to change its color.
M8 chemical agent detection papers, commonly used by the military, identify CAs by changing colors within 30 seconds of exposure: dark green for persistent nerve agents, yellow for nonpersistent nerve agents, and red for blister agents.
The M256A1 chemical agent portable detector kit detects nerve gas, mustard gas, and cyanide and usually is used to define areas of contamination. It contains a package of M8 paper and a vapor sampler (12 enzymatic tickets that contain laboratory filter paper for detecting CA vapors). The vapor sampler uses wet chemistry technology, in which ampules containing different substrates are crushed so that the liquids interact with strips of filter paper, chromatographic media, and glass fiber filter. These substrates then are exposed to the vapor under suspicion. The reaction causes a color change, alerting the user to the presence of a CA. The reactions typically take 15 minutes to occur.
Colorimetric tubes such as those available from Draeger (Figure 1.13) and RAE systems (Figure 1.14) use enzymatic techniques to identify CAs. A hand pump is used to draw a sample into a specific tube, and the concentration of the substance is read from the tube. This is another simple and inexpensive way of detecting and identifying a CA. It is used extensively in civilian response units for this reason, but it has some disadvantages. A tube for each possible CA must be used for thorough detection.

Figure 1.13: *Draeger Tubes.*

Figure 1.14: *Colorimetric gas detection tubes by RAE System.*

2.2.7 Surface Acoustic Wave (SAW)

This kind of detectors uses the change in resonant frequency of the surface acoustic wave on the piezoelectric crystals due to the chemical agent present. This change is induced by the presence of a different mass inside a polymeric film, which has to be chosen for the class of compound looked for, due to the presence of the adsorbed agent. The films, usually two to six, coat the crystals and absorb agent directly from air.
The response pattern generated from the system has then to be analyzed in order to compare them with the ones stored in the database. If the system recognizes the pattern of an agent, the alarm is generated. In order to increase sensitivity pre-concentration tubes may be used. However, false alarm due to the presence of substances different from the agent is possible because selectivity and sensitivity of these detectors depend on the ability of the film to absorb only the suspect chemical agents from the sample air.
Figure 1.15 shows the SAW Minicad II detector based on this technology and manufactured by Microsensor Systems. This portable SAW array detector is lightweight, battery operated and available commercially. It is used remotely to define areas of decontamination but also can be used for active detection.

Figure 1.15: *SAW Minicad II.*

The Joint Chemical Agent Detector (JCAD) ChemSentry also uses SAW technology and is produced by BAE. It is designed to be used by each non specialized department of the armed forces, and is available commercially. It can be used as a personal protection detector to be carried by troops as well as to monitor ships, cargo holds, and wheeled vehicles. It uses a preconcentrator to detect low levels of a specific chemical agent requiring 20 minutes for sample collection but simultaneously monitors ambient air for larger concentrations of most chemical warfare agents.

2.2.8 Photo Ionization Detection (PID)

This detector uses a narrow ultraviolet emission at specific wavelength to ionize the agent. The ions produced are then collected trough an electric field to produce a current or voltage proportional to agent concentration presented in the gas streaming inside the device. Selectivity relies on a narrow emission for chosen wavelengths and the fact that energy transition is not present in other molecules. RAE System produces different devices that use this type of technology.
The MiniRAE Plus (Figure 1.16) is an example of a handheld detector that utilizes the PID technology. The MiniRAE 3000 (Figure 1.17) is an advanced handheld volatile organic compound (VOC) detector. Its photoionization detector's (PID) extended range of 0 to 15,000 ppm makes it an ideal instrument for applications from industrial hygiene, to leak and hazardous materials detection. The rugged MiniRAE 2000 (Figure 1.18) is a small pumped handheld volatile organic compound (VOC) detector employed for environmental site surveying and hazardous materials/homeland security. The MultiRAE Plus (Figure 1.19) combines a PID (Photoionization Detector) with the standard four gases of a confined space monitor (O2, LEL, and two toxic gas sensors) in one compact monitor with sampling pump. Another handheld PID detector is the Photovac 2020 (Figure 1.20) manufactured by Perkin-Elmer.

Figure 1.16: *MiniRAE Plus.*

Figure 1.17: *MiniRAE 3000.*

Figure 1.18: *MiniRAE 2000.*

Figure 1.19: *MiniRAE 2000.*

Figure 1.20: *Photovac 2020 PID Monitor.*

2.2.9 Sensor Array Technology (SAT)

This kind of detector are usually named electronic nose. Using simultaneously several different chemical sensors such as conductive polymer, metal oxide, bulk acoustic wave (BAW) and SAW devices is it possible to make a real time monitoring system. Of course each sensor must be fast and reversible, e.g. it has not to change permanently his properties after being in contact with a chemical agent. A mobile laboratory detector based upon SAT is the EEVeNose 5000 Electronic Nose, shown in Figure 1.21.

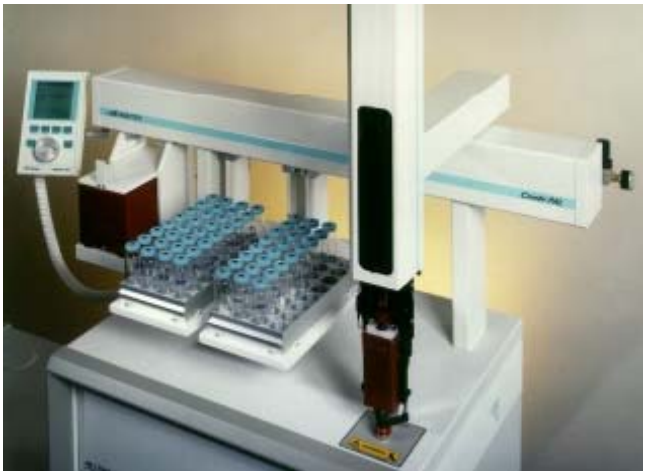

Figure 1.21: *EEV eNose 5000 Electronic Nose.*

2.2.10 Thermal and Electrical Conductivity (TCD)

This kind of detectors makes use of changing in their thermal or electrical conductivity due to the presence of gas adsorbed in their surface. Adsorbing material can be metal oxide surface or metal foil. These changes can be related to the presence of gas. The relative difference of these physical values can be used to identify the substance.

2.2.11 Flame Ionization Detector (FID)

This detector is based on the increased number of ions produced by a burning hydrogenoxygen flame when carbon based compounds are incinerated. It is not able to discriminate different compounds due to its working principle and so it is a general-purpose detector which has to be used linked to other technologies, such as gas chromatograph, if identification is a must.
MicroFID, manufactures by Perkin-Elmer, is a handheld FID for the nonspecific determination of flammable and potentially hazardous compounds in the concentration range of 0.1 to 50,000 ppm. The MicroFID is shown in Figure 1.22.

Figure 1.22: *Perkin-Elmer MicroFID Handheld Detector.*

2.2.12 Neutron based sensors: Portable Isotopic Neutron Spectroscopy (PINS)

This technique employs a nuclear method, neutron interrogation, to obtain a chemical purpose: identification of a chemical composition. A nuclear reaction is determined on the nuclei of investigated molecules by neutron collision using a weak neutron source. The reactions, usually neutron capture or inelastic scattering, produce gamma rays, which when appropriately detected and recorded, produce a gamma-ray spectrum. The gamma-ray spectrum peaks correspond to energies which depend on nuclei involved because specific nuclear de-excitations characteristic of the chemical element is concerned. The ratios of the elements inside the investigated compound can be calculated from the relative heights of the peaks. These energies and ratios are strictly related to substance under investigation, whatever it is. In this way, with a "library" of known fingerprint, it is possible to determine unambiguously the contents of the unknown substance.
This technique is realized using a “portable” nuclear laboratory because a neutron source, a gamma detector able to discriminate different energies, usually cooled with liquid nitrogen, related electronic chain and computer to store and analyze results are needed. It could be an interesting alternative to previously shown method even if problem concerning its real use could rise due to security in using neutron source, e.g. skilled personnel always needed. Example of this systems are ORTEC PINS and miniPINS. The first is showed in the following picture.

Figure 1.23: *ORTEC PINS Detector during real measurements.*

2.3 Standoff detection technologies

This expression generally refers to device able to detect chemical agents that are placed at a distance as great as 5 kilometers.

Our projected device will hold to this kind of device. Standoff detectors working nowadays can detect, if condition are good, chemical agent cloud so to give advance warning. Standoff detectors typically use optical spectroscopy and are generally used by comparing detected spectra with agent-free spectra. They use Optical Remote Sensing (ORS) techniques that are based on infrared (IR) spectral analysis, providing early warning of a threat and allowing contamination avoidance doctrine to be used. Standoff detectors can use active (laser) or passive infrared spectroscopy and generally has to be operated by skilled personnel to both for operating and interpret results. Passive remote sensing systems generally use a Fourier Transform Infrared (FTIR) spectrometer or a spectrally modified Forward Looking Infrared (FLIR) imager while active remote sensing systems use a tunable laser source and Light Detection and Ranging (LIDAR) techniques to illuminate the CW vapor cloud and background.

2.3.1 Passive remote sensing systems

In passive remote sensing systems infrared radiation emitted or adsorbed from the background is used to detect chemical agent or TIC vapors. In remote detection system collected radiation can be analyzed with optical filters, and in this case is called Forward Looking Infrared (FLIR) imager, or analyzed trough an interferometer device, and is called Fourier Transform Infrared spectrometer.

Both passive systems exploit the rich infrared absorption spectrum of CW agents in the 9 to 11 μm region, which is due to the organophosphorus moiety present in the molecular structure of the nerve agents. The 9 to 11 μm region also lies in a spectral transmission area of the atmosphere where atmospheric attenuation due to oxygen, carbon dioxide, and water vapor is low. This lack of interference allows the ORS technology to be effective to five kilometers. Figure 1.23 diagrams the principle of operation of a passive remote infrared chemical sensor.

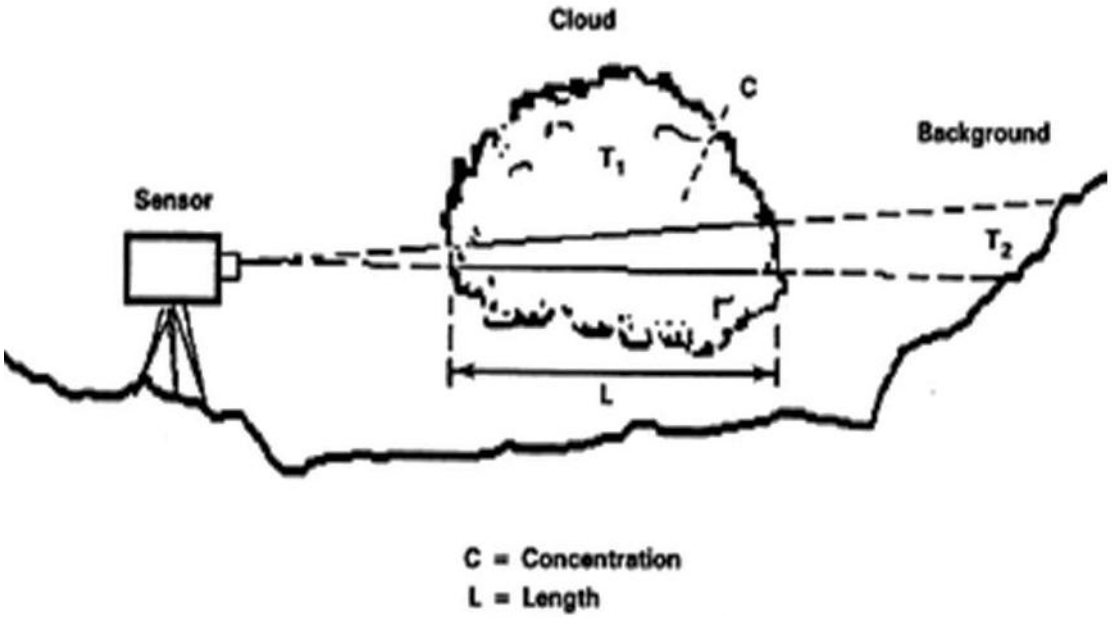

Fig.1.23: *Passive remote infrared chemical sensor working principle.*

The AN/KAS-1 CW Directional Detector, shown in Figure 1.24, is a passive remote detector using FLIR technology. A selectable filter enables the operator to analyze potential threats. By comparing images produced by the filter's three available spectral bands, the operator can distinguish the presence of nerve agent (G and V) vapor accumulations. As a secondary function, the unit provides thermal imaging for night surveillance, navigation, and search and rescue operations.

Armed forces uses the M21 Remote Sensing Chemical Agent Alarm (RSCAAL) based on passive infrared detection. It is the first fielded standoff chemical detection device.

The M21 (see Figure 1.25) is an automatic, scanning sensor which detects nerve and blister agent vapor clouds based on changes in the background's IR spectra caused by the presence of the agent vapor. This system can detect a vapor cloud from 5 km with an 87% detection rate. Response time is 1 minute or less. It automatically scans along a 60° angle, allowing the operator to monitor horizontal movement. It can detect chemical agent vapor clouds and track their movement through its field of view. The sensitivity of the M21 for detecting nerve agents (GA, GB, and GD) is 90 mg/m^3; and for vesicants are 500 mg/m^3 for Lewisite and 2,300 mg/m3 for HD mustard.

The M21 can be set up in 10 minutes and is unaffected by low light conditions. However, it is limited in that it must be stationary and can be obstructed by snow and rain.

This technology is limited by sensitivity, which depends on the temperature difference from background and usually 1000 times lower than active technologies, and is dependent on the background, thus being not useful for portable or platform mounted device, needing calibration depending on the pointing direction where background is generally different[1].

Figure 1.24: *AN/KAS-1 CW Directional Detector.*

Figure: 1.25: *M21 Remote Sensing Chemical Agent Alarm.*

2.3.2 Active remote sensing systems

Active technology makes use of a powerful source, usually a laser, and Light Detection and Ranging (LIDAR)[2] techniques (the laser analog to radar) to illuminate the CW vapor cloud and background. The system collects the scattered or reradiated energy and measures the cloud's wavelength characteristics. Like passive remote systems, active remote systems take advantage of the rich infrared absorption spectrum of CW agents in the 9 to 11 μm region. The absorption properties of CW agents are used for detection and identification.

In our application it uses the small amount of energy retroreflected by molecules found in atmosphere to have a signal; this signal is stronger than that usually provided by atmosphere molecules which have a small cross section because source was properly chosen in one of atmospheric windows. LIDAR is able to found anomalies present in atmosphere and also to determine distance and depth of the vapor cloud, using the times it takes the signal to go and come back from the cloud, but nothing about the substance present in the cloud. If the substance is known, a DIAL[3] (Differential Absorption Lidar), built using a LIDAR able to emit and receive at least two chosen and near wavelengths, may be used to determine concentration calculating effect of atmosphere with a wavelength (λ_{off}) and effect of the substance with another wavelength (λ_{on}). Details of this technology will be explained later in this work. No known system is able to recognize the substance, even if some methods use more than two wavelengths to improve system performance, as will be explained in a following paragraph.

Actually used LIDAR can be employed for tracking a chemical agent cloud once it has been identified with a different method, but cannot be used to identify a chemical agent cloud.

3 LABORATORY ANALYTICAL INSTRUMENTS

3.1 Introduction

Most methods used to perform the identification of unknown toxic substances in the sample frequently reported in literature, are based on laboratory instrumental analysis.

Generally analytical instruments are able to perform analysis starting from sample of few micro liters or milligrams. Unique chemical properties of different molecules are used to distinguish them using sophisticated technology which is able to detect and differentiate trace amounts of chemical agents. Ultra pure reagents and strict protocol are needed to acquire these results, thus precluding

any use outside laboratory and without technical trained personnel. Data has to be interpreted as well because instruments do not give final data. However, as before described, some analytical instruments have been put inside shelter and have been developed for field applications.
Among instrumental analytical methods, chromatographic procedures (gas and liquid) coupled with mass spectrometry play an important role due to their high detect ability, rapidity and the possibility of operation in continuous mode[4]. Particularly chromatographic methods allow the isolation of analytes from complex matrices and their identification and determination even at picogram levels.
The number of publications on the determination of chemical warfare agents by chromatographic systems is considerable, but none of the chromatographic systems is universal, as they do not allow the analysis of all compounds simultaneously and under the same conditions. This is to be expected, as the main property that allows the classification of a substance as a warfare agent is its toxicity and applicability on the battle field. The various CWAs differ considerably in their physico-chemical properties, e.g., polarity and boiling point, which are decisive for chromatographic separations. The problems connected with the selection of chromatographic systems become even more complicated when it is necessary also to take into account the degradation of warfare agents, the starting materials used for their synthesis and contaminants.
Most common laboratory analytical instruments used for chemical agents detection are described in the following pages.

3.2 Mass Spectrometry (MS)

A mass spectrometer is an excellent tool for clearly identifying the structure of a single compound[5]. It takes injected material, ionizes it in a high vacuum, propels and focuses these ions and their fragmentation products through a magnetic mass analyzer, and then collects and measures the amounts of each selected ions in a detector. The mass spectrometer has three basic sections: an ionization chamber, the analyzer, and the ion detector.
In the evacuated ionization chamber the sample is bombarded with electrons or charged molecules to produce ionized sample molecules. These are swept into the high-vacuum analyzer where they are focused electrically and then selected in the quadrupole. The electrically charged poles of the quadrupole create a standing magnetic field in which the ions are aligned. Individual masses are selected from this field by sweeping it with ratio frequency signal. As different frequencies are reached, different mass-charge ratio (m/z) ions are able to escape the analyzer and reach the detector. By sweeping from higher to lower frequency, the available range of m/z ions are released one at a time to the detector, producing a mass spectrum. On entering the detector, the ions are deflected into a cascade plate where the signal is multiplied and then sent to the data system as an ion current versus m/z versus time. The ion current strength for each detected ion fragment plotted over an m/z range produces a mass spectrum.
A mass spectrometer is generally not useful for dealing with mixtures. If a single substance is put into a mass spectrometer, its mass spectrum can be obtained with a variety of ionization methods. Clearly, if a mixture of substances is put into the mass spectrometer the resulting mass spectrum will be a summation of the spectra of all components and it would be impossible to positively identify the various components. So usually, a chromatographic method, which is able to separate the components in the sample, is coupled to the mass spectrometer. MS coupled with gas chromatography (GC) separation technique provides significantly greater capability for identification of compounds in complex mixtures.
Having obtained the spectrum of a single component it is then often possible to make a positive identification of the substances or to confirm its molecular structure. Anyway, determination of the molecular structure of a compound from its molecular weight and fragmentation spectra is a job for a highly trained specialist.

3.3 Gas Chromatography (GC)

Gas chromatography has been used extensively for the separation and identification of the CWAs[6,7]. The gas chromatograph is a temperature-controlled oven designed to hold and heat the chromatographic column which consists of a long, coiled capillary tube of silica with an internal coating of stationary phase either viscous liquid or well-bonded organic material.

Mixtures to be analyzed are injected into an inert gas stream (carrier gas), usually Helium, Nitrogen or Hydrogen, and swept into the GC column where the separation of individual compounds occurs. The injection sample in the carrier gas interacts with the stationary organic phase, and an equilibrium is established between the concentration of each component in the gaseous and solid phases. As fresh carrier gas flushes down the column, each component of the mixture come off the stationary phase at its own rate leading to a different times of transition through the column (retention time); separation increases after many interactions down the length of the column. After volatile components have come out the column they are swept in order through a detector flow cell.

The detected and isolated compounds are recorded as "peaks" (the chromatogram), the area of a peak correlating with the amount of a component and the time taken to pass through the column (the retention time) giving some information on the possible identity of the component.

Gas chromatography suffers from a few weaknesses, such as its requirements for volatile compounds (molecular weight limits), thermal stability and the lack of definitive proof of the nature of the detected compounds as they are separated.

For most GC detectors, identification is based only on the retention time on the column. It is usually done by comparing the retention indices of the substance being analyzed with those of a standard measured in at least two columns filled with stationary phases of different polarity.

The application of a selective detector may facilitate considerably the identification of the substances being analyzed. Many different selective detectors have been used in the analysis of CWAs. They may serve for detecting trace amounts of agents that contain in their molecules elements to which these detectors are particularly sensitive. Such detection methods include electron-capture detection (ECD) for compounds containing halogens, flame photometric detection (FPD) for the detection of compounds containing sulphur and phosphorus, nitrogen-phosphorus specific detection (NPD) for compounds containing nitrogen and phosphorus. Sometimes two detection methods are combined.

Chromatographed CWAs can also be identified by confirming the presence of the compounds being detected with the use of other instrumental methods, e. g., IR, NMR or MS.

The majority of today's GC applications are carried out in combination with mass spectrometry. Such complex devices are capable of separating mixtures into their individual components, identifying and then providing quantitative information.

Because almost all CWAs comply with GC-requirements, due to their sufficiently high vapor pressure and thermal stability, GC-MS is routinely being used by all laboratories involved in the analysis of CWAs and related compounds, as can be derived from the reports on the international laboratory tests organized under the auspices of the CWC (Convention on Chemical Weapon). So far, attempt to apply GC-MS to the analysis of CWAs has failed in only a few instance which concerned chiefly organo arsenic compounds (Lewisite). Because L is thermally labile and its hydrolysis product is essentially non-volatile, chemical derivatisation is used to enable gas chromatography analysis. The derivatisation with dithiols to form stable and volatile cyclic arsodithio compounds in aqueous solution is followed by solvent extraction of the product to introduce it to the GC.

Agilent 6890-5973 GC/MSD, shown in Figure 1.26, uses gas chromatography separation technique coupled with mass spectrometry detector technology.

Figure 1.26: *Agilent 6890-5973 GC/MSD.*

3.4 High Performance Liquid Chromatography (HPLC)

Chromatography can be performed also in liquid phase. Liquid chromatography developed as a means for separating non-volatile polarized and ionized mixtures into their component substances and provided a big step forward in revealing their complexities and analyzing them. It is particularly useful with high weight molecular species and biological agents.

Liquid chromatography as a separation technique with its many modes of operation (reversed phase, normal-phase, ion-exchange, ion-pair and size exclusion) is able to separate essentially all compounds that are soluble in a conventional solvent or solvent mixture, with thermolability, polarity and volatility not playing a major role.

Many CWAs are chemically reactive electrophiles, whose toxicity is mediate by reaction in vivo with key biological nucleophiles. This reactivity with nucleophiles is also a major mechanism for their degradation, e.g., by reaction with water present in the environment. The analysis of environmental and biological residues for products derived from hydrolysis is therefore an important component of CWAs analysis. This technique appears to be an attractive alternative to GC-MS for the analysis of aqueous samples containing the hydrolysis products of chemical agents since the aqueous samples may be analyzed directly with little risk of thermal decomposition and without the need for additional sample handling steps.

However, its major drawback is the lack of detectors matching selectivity and sensitivity of gas chromatography detection systems. This is probably the reason for the many GC applications on CWAs and related compounds even if aqueous sample matrix is involved and laborious and time-consuming sample treatment or derivatisation is required[8]. The above time factor may become unacceptably prolonged, especially if many samples have to be analyzed; besides, derivatisation may lead to the formation of artifacts. LC reduces the sample handling and derivatisation requirements, and therefore increases the sample throughput.

In a simple LC instrument, the emerging components dissolved in the liquid mobile phase are usually measured by passing the liquid stream through either a UV or a refractive index detector. Most CWAs, however, do not show absorption in the UV region or the absorption is very weak, and their conversion to UV-active derivates complicates the analysis.

Other kinds of detectors are possible such as fluorescence spectrometers and electrochemical detectors. A typical fluorescence detector is about 1000 times more sensitive than a UV detector, but it finds very limited application in analysis of CWAs. The applicability of electrochemical detectors in such analysis is even more restricted.

Spectroscopic methods have also been used, e. g., mass spectrometry (MS), Fourier transformation IR (FT-IR) and ion-mobility spectrometry. Good results were obtained by applying nuclear magnetic resonance (NMR).

Hewlett Packard, Perkin-Elmer, Shimadzu, and Varian products are shown in Figures 1.27, 1.28, 1.29, and 1.30 as example of HPLC devices. Currently there is no portable HPLC unit available due to its limitations: need for power requirements (120V house current) and high purity solvents.

Figure 1.27: *Hewlett Packard HP1000 HPLC System.*

Figure 1.28: *Perkin-Elmer Turbo LC Plus.*

Figure 1.29: *Shimadzu LC-10 HPLC System.*

Figure 1.30: *Varian ProStar Analytical HPLC System.*

3.5 The connection between LC and MS: electrospray ionization (ESI)

The widespread use of LC-MS has been hindered by the lack of a robust universal LC-MS interface, problems of sensitivity, and the general cost and availability of the instrumentation. Recent advantages in ionization techniques, and their interfacing to mass spectrometry systems, have overcome most of these disadvantages. Then, in recent years, LC-MS has become one of the most rapidly developing analytical techniques.

Combining LC and mass spectrometry is much more difficult than was the case with GC and mass spectrometry because the solution, which comes from a liquid chromatographic column, cannot be passed straight into the mass spectrometer. In the high vacuum, the rapidly vaporizing solvent would entail a large pressure increase causing the instrument to shut down.

Modern LC-MS is now established routine in many different kinds of laboratories, thanks to the development of different kinds of interface devices, such as the electrospray ionization (ESI)[9].

The principal outcome of the electrospray process is the transfer of analyte species, generally ionized in the condensed phase, into the gas phase as isolated entities. The reason for enormous contribution of electrospray technique to modern MS methodology is that it is unique in providing simultaneously a logical coupling for solution introduction of compounds for analysis and the facility for ionization of highly polar and non-volatile compounds. It represents a liquid inlet system for a mass spectrometer, and at the same time, it is an ionization source.

The essence of the electrospray process can be described with simplicity. A solution of analytes is passed through a capillary which is held at high potential. The effect of the high electric field as the solution emerges is to generate a mist of highly charged droplets which pass down a potential and

pressure gradient towards the analyser portion of the mass spectrometer. During that transition, the droplets reduce in size by evaporation of the solvent or by "Coulomb explosion" (droplet subdivision resulting from the high charge density). Ultimately, fully desolvated ions result from complete evaporation of the solvent or by field desorption from the charged droplets. Nebulization of the solution emerging from the capillary may be facilitated by a sheath flow of nebulizer gas.

3.6 LC-MS vs GC-MS

LC-MS is not used as a substitute for GC-MS in chemical laboratory but as a complementary technique. In terms of sensitivity, and limits of detection in most matrices, GC-MS is superior, so that it has been used extensively for the separation and identification of the CWAs.

However, verification is an important component of monitoring compliance with the Chemical Weapons Convention. This process may involve the analysis of CWAs, their precursors or more persistent degradation products, in samples collected from suspected or storage sites, or from the environment in cases of allegations of use. The analysis of environmental residues for hydrolysis products is therefore an important part of verification analysis.

GC separation, while suitable for the direct analysis of CWAs in organic extracts, is usually not preferred for the direct analysis of aqueous samples or extracts. The analysis of CWAs and their hydrolyzed non-volatile and polar products in aqueous samples or extracts using GC-MS is time consuming, requiring concentration to dryness and derivatisation; the presence of extraneous materials may interfere with derivatisation resulting in low apparent recoveries.

Whereas, LC-MS allows for a more rapid screening of aqueous samples or aqueous extracts with minimal sample pretreatment. LC-MS has the additional advantage that it facilitates the identification of additional components that would be less easily identified in a derivatised extract using GC-MS.

So, even if GC-MS is likely to remain the primary method for the identification of intact CWAs, it is expected that LC-MS will play an increasing role in the analysis of environmental samples for the hydrolysis products of CWAs. Several procedures employing these techniques for analysis of CWAs and their degradation products are described in literature.

Water sample containing CWAs have been analyzed by GC-MS following solid-phase microextraction[10], by capillary electrophoresis and by microcolumn LC with flame photometric detection.

Increasingly, researchers have developed LC-MS analytical methods to deal with the analysis of aqueous samples containing these non-volatile compounds[11].

Several screening procedures for the detection and identification of CWAs using LC-MS with APCI, where a corona discharge is used as a modification of electrospray in order to enhance the yield of ions, and the application of ESI to the analysis of phosphonic acid degradation products of nerve agents have been developed[12]. Moreover, U.S. Army Materiel Command's Treaty Verification Laboratory used liquid ion chromatography in the analysis of several chemical nerve agents and their degradation products.

The described procedures have been used successfully in proficiency tests organized by the Organization for the Prohibition of Chemical Weapons.

4 MONITORING PROCEDURES: DEVICES ALREADY USED AT STOCKPILE DISPOSAL FACILITIES

A problem related with CWAs detection technologies is monitor at chemical agent disposal facilities. In the USA a committee (Committee on Monitoring at Chemical Agent Disposal Facilities)[13] was appointed to review the instrumentation systems and practices for monitoring airborne chemical agent levels associated with chemical weapons demilitarization and stockpile storage facilities and whether new applicable monitoring technologies were available and could be effectively incorporated into airborne chemical agent monitoring strategies.

Current monitoring systems used at stockpile disposal facilities to detect the presence of chemical agent in the ambient air and measure its concentration, use an approach that involves air sampling. The most used is gas chromatography, but also the use of optical spectroscopy, with the variant of Raman spectroscopy and fluorescence spectroscopy, mass spectrometry and chemical sensing are increasing. Most of these techniques are point monitoring. Optical spectroscopy could be performed also in an open path, passing a light beam directly through the air in the ambient monitored. This kind of measures give the average concentration in the light path, whereas the other techniques give the concentration of the agent averaged over the duration of the time that air is passed through the system. Many of the systems used at stockpile disposal facilities nowadays rely on univariate determination, that means only one analyte is measured by the particular sensor. Multivariate determination can be carried out by Open Path Fourier Transform Infrared Spectroscopy (OP/FT-IR) which is able to distinguish among several chemical agents or interferents. Whereas is quite difficult to minimize false positive in univariate systems, it is possible to reduce false alarms in a multivariate system obtaining or preparing a set of calibration data in which all possible interferences are represented. This is one of the larger challenges of multivariate methods of analysis such as OP/FT-IR spectroscopy. The new method presented in this work is also of this kind. Differences will be explained in the next paragraph. Also the Limit Of Detection (LOD) and Limit Of Quantification (LOQ) are important for this kind of application. Time necessary to exploit measure depends on technique; open path techniques are usually faster, but they become slower if the same LOD of other technique is mandatory.

5 NEW POSSIBLE DEVICE

DIAL could be considered as a spectroscopic analyzer which works using just two wavelengths. Using more than two wavelengths is then a natural extension that could improve DIAL performance. Nevertheless, multiple wavelength has not been employed until recently, with the exception of tunable CO_2 laser using topographic targets.

Multiwavelenght Dial is a formidable tool because it can detect and identify chemical agents, and chemical weapons present in atmosphere. It presents considerable advantages compared to other detection methods based on “in situ” chemical analysis performed by electronic nose or quick spectroscopic scan, currently used or projected. Due to its very high sensitivity and spatial resolution, this active detection technique enables efficient location of chemical weapons during night and day and over a considerable range.

It may also improve knowledge of aerosol optical properties, which would improve the accuracy of aerosol corrections.

The few experience and paper in this sector are described in the following pages.

Simultaneous measurements of methane, ethane and propane were discussed by Weibring and others[14]. They selected a set of seven wavelengths in the mid IR in order to use the Swedish mobile LIDAR van upgraded for this purpose, described by Fredriksson[15].

Wang and others[16] built a method that provide ozone measurements much less sensitive to aerosol effects and also nearly immune to interference from SO_2 and NO_2. The system, called dual DIAL, used two pairs of lines and just with three lines (one in common for the two couple) was able to provide expected results.

Dual DIAL was analyzed by Kovalev and Bristol[17] which explain the technique as a compensational one, leading to a three wavelength version which does not need correction for aerosol differential extinction and backscattering. They demonstrated in which way a proper choice of wavelength could decrease interfering species errors.

Rambaldi and others[18] instead use a five wavelengths system to find SO_2 concentration and then use it to subtract its contribution to O_3 concentration measurement. They were able to measure 15 ppbv of O_3 while SO_2 concentration was as high as 1 ppmv.

A theoretical analysis of a new device, reported by Jones[19], was performed by Strong and Jones[20]. The system is not a real Multiwavelenght DIAL because employed a broadband pulsed source, a

spectrometer and a CCD camera so to generate range resolved spectra. The different wavelengths are determined from the spectrometer instead of the source. They estimated the errors in simultaneous profile of O_3, SO_2 and NO_2 using formal retrieval theory. Their calculation showed it is possible to obtain vertical profiles of all three gasses simultaneously with 30% uncertainty in 20 minutes over 15 Km with a resolution of three Km.
A real improvement in SO_2 concentration measurement accuracy, reaching 1ppbv level at 300 m resolution, was obtained by Fukuki and others[21]. They ipotize to use Multiwavelenght Dial on dual DIAL version using three or four lines, and to minimize both aerosol effects and interference from ozone. The predicted accuracy was actually achieved by Fujii and others[22]. Moreover they were able to measure SO_2 and O_3 simultaneously with conventional DIAL technique and so evaluate experimentally the effect of background and the ability to reduce it.
The same researchers later developed a curve-fitting technique to perform five wavelengths measures and calculate SO_2 and O_3 with higher precision so improving dual DIAL technique. The problem was that measurement time was 25 minutes.
A completely different method is going to be presented in this thesis based on the principle of complex data analysis method, such as multivariate statistical analysis and neural network analysis, applied to data coming from a multiwavelenght DIAL with the purpose of identification and concentration measurements.

6 CONCLUSION: WHY CHOOSE ACTIVE OPTICAL TECHNOLOGY

Active optical technology has to be chosen for the simple reason that it is the only one which is able to perform remote sensing night and day and pointing wherever is needed. Until now the real obstacles in the use of this technology is the absence of a proper database and the difficulty in determining and apply a method to discriminate among different substances. We are now trying to fill the gap in order to transform DIAL, through its Multiwavelenght version, from "the next big thing in science and technology", as it is usually presented during scientific conference, to the "present big thing in science and technology".
Difficulties are still scaring but the challenge has to be taken.

6 REFERENCES

[1] A. Beil, R. Daum, R. Harig, and G. Matz, Remote sensing of atmospheric pollution by passive FTIR spectrometry, Proc. SPIE Vol. 3493, 32–43, Spectroscopic Environmental Monitoring Techniques (1998)

[2] Fiocco G. and L. D. Smullin, Detection of Scattering Layers in the Upper Atmosphere (60 – 140 Km) by Optical Radar, Nature, 199, 1275 – 1276. (1963).

[3] C. Bellecci, G. Caputi, F. De Donato, P. Gaudio, M. Valentini, CO_2 Dial for monitoring atmospheric pollutants at the University of Calabria, Il Nuovo Cimento, **18**, 5, 463-472 (1995).

[4] Ch. E. Kientz. Chromatography and mass spectrometry of chemical warfare agents, toxins and related compounds: state of the art and future prospects, Journal of Chromatography A, 814, 1-23 (1998).

[5] P. D'Agostino and L. R. Provost, Mass spectrometric identification of products formed during degradation of ethyldimethylphosphoramidocyanidate (tabun), Journal of Chromatography, 598, 89-95 (1992).

[6] D. K. Rourbaugh, Yu-Chu Yang and J.R. Ward, Identification of degradation products of 2-chloroethylethyl sulfide by gas chromatography-mass spectrometry, Journal of Chromatography, 447, 165-169 (1988).

[7] Z. Witkiewicz, M. Mazurek and J. Szulc, Chromatographic analysis of chemical warfare agents, Journal of Chromatography, 503, 293-357 (1990).

[8] P. D'Agostino and L. R. Provost, Determination of chemical warfare agents, their hydrolysis products and related compounds in soil, Journal of Chromatography, 589, 287-294 (1992).

[9] P. A. D'Agostino, J. R. Hancock, L. R. Provost, Determination of sarin, soman and their hydrolysis products in soil by packed capillary liquid chromatography-electrospray mass spectrometry, Journal of Chromatography A, 912, 291-299 (2001).

[10] B.Szostek, J. H. Aldstadt, Determination of organoarsenicals in the environment by solid-phase micro extraction-gas chromatography-mass spectrometry, Journal of Chromatography A, 807, 253-263 (1998).

[11] R. M. Black and R. W. Read, Application of liquid chromatography-atmospheric pressure chemical ionization mass spectrometry, and tandem mass spectrometry, to the analysis and identification of degradation products of chemical warfare agents, Journal of Chromatography A, 759 79-92 (1997)

[12] R. M. Black and R. W. Read, Analysis of degradation product of organophosphorus chemical warfare agents and related compounds by liquid chromatography-mass spectrometry using electrospray and atmospheric pressure chemical ionization, Journal of Chromatography A, 794 233-244 (1998)

[13] Committee on monitoring at chemical agent disposal facilities, Monitoring at chemical agent disposal facilities, National academy of sciences - USA (online: http://www.nap.edu/catalog /11431.html), 2005.

[14] Petter Weibring, Hans Edner, and Sune Svanberg, Versatile mobile lidar system for environmental monitoring, Applied Optics vol. 42 n° 18 (20 June 2003).

[15] Kent A. Frediksson, DIAL technique for pollution monitoring: improvements and complementary systems, Applied Optics Vol 24 n° 19 (1 October 1985).

[16] Z. Wang, S. Zhou, H. Hu et al. Appl. Phys. B 62, 143 (1996).

[17] Vladimir A. Kovalev and Michael P. Bristow, Compensational three-wavelenght differential-absorption lidar technique for reducing the influence of differential scattering on ozone-concentration measurements, Applied Optics vol. 35 n° 24 (20 August 1996).

[18] P. Rambaldi, M. Douard, J. Wolf, Appl. Phys. B 61, 117 (1995).

[19] R. L. Jones, Proc. SPIE 1715, 393 (1992).

[20] K. Strong and R.L. Jones, Remote measurement of vertical profiles of atmospheric constituents with a UV-visible ranging spectrometer, Applied Optics vol. 34 n° 27 (20 September 1995).

[21] Tetsuo Fukuchi, Takashi Fujii, Naohiko Goto, Koshichi Nemoto, Evaluation of differential absorption lidar (DIAL) measurement error by simultaneous DIAL and null profiling, Opt. Eng. 40(3) 392-397 (March 2001).

[22] Takashi Fujii, Tetsuo Fukuchi, Nianwen Cao, Koshichi Nemoto and Nobuo Takeuchi, Trace atmospheric SO_2 measurement by multiwavelenght curve-fitting and wavelength-optimized dual differential absorption lidar, Applied Optics, vol. 43 n°3 (20 January 2002) .

2. A LOW COST DEVICE ABLE TO PERFORM EYE SAFE SHORT RANGE LIDAR MEASUREMENT AT 1550 NM

1. INTRODUCTION

In the previous chapter it was pointed out that there is a lack of instrumentation able to recognize substances remotely. But this could be not enough. You can't have enough devices able to recognize substances to scan everywhere for many reasons, first of all price and skilled personnel to use it. If there is another device which gives some advice whenever there is a change in atmosphere optical characteristic, you can just look towards the area indicated. A cheap and reliable detector which is able to quickly scan a big area signalling any change in atmosphere due to change in optical properties, even at one wavelength, could be also important.

We need a system that is able to give an advice whenever there is a variation in atmosphere or in the characteristic of the place where it is used remotely. There is not a cheap and reliable system on the market nowadays, as stated on chapter 1. The price must be low enough so that many of them could be deployed whenever a check is needed. Also reliability and simplicity are leading point of our system as well.

When something strange is found, another system able to discriminate the substance, as the one suggested in the following chapters, could be used. For this reasons a system based on LIDAR technology could be the best solution. COTS (Commercial Off The Shelf) components were chosen to get the price as low as possible. Also eye safety and response of atmosphere to wavelength were considered. This led to use a laser diode of 1550 nm as source. The most sensitive and quick receiver at these wavelength (commercially available) are avalanche photodiode. We need also transmission optics and receiving one, projected as explained in the following paragraph.

2. PROJECT OF THE SYSTEM AND CHOICE OF COMPONENTS

A lidar device needs the following components:

a) Laser source;

b) Detector;

c) Transmission optics;

d) Receiving optics;

e) ADC and computer;

f) Temperature, pressure and other detectors to improve system performance;

g) Other utilities (GPS, Data transmission, etc...).

Only components from a) to d) are essential to test a system. We thus realize a working test LIDAR choosing components and performing measures. A picture taken with our laboratory test system is showed in the following picture when transmitting and receiving optics are clearly visible. Each element will be described in the following subparagraph. IR camera used to see source emission is also visible in the picture.

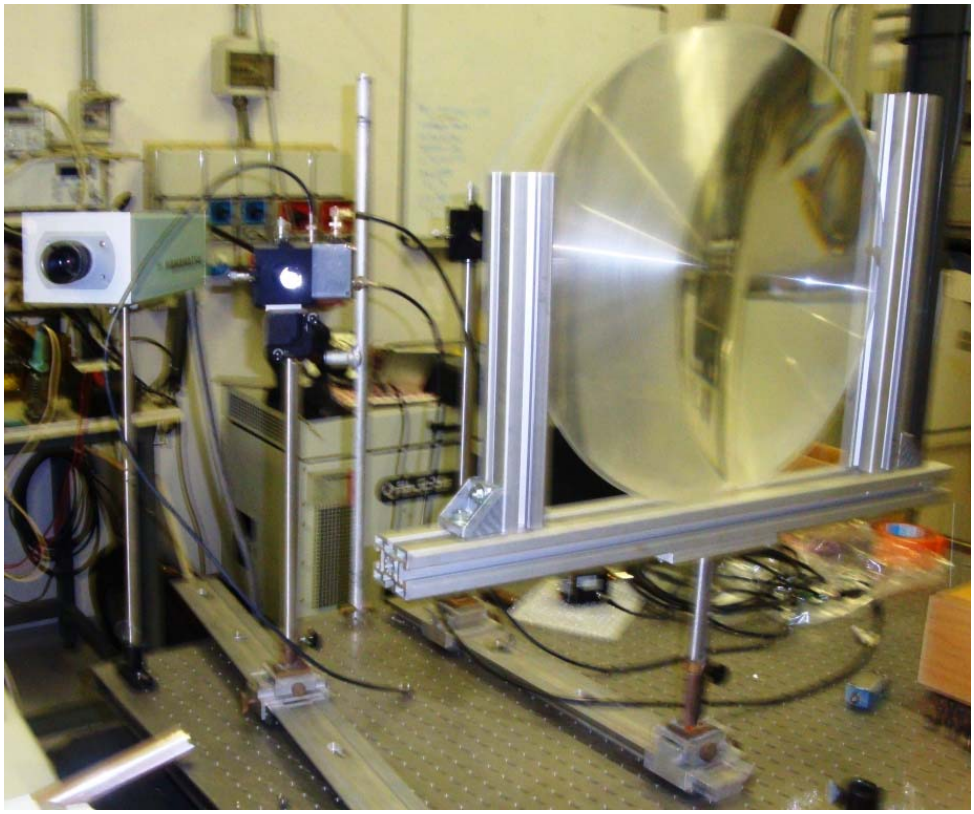

Figure 1: *A picture where source box and transmitting optics are visible on the left while receiving optics is visible on the right, both mounted on a guide to change relative position of subsystems.*

2.1 Laser source

The source was chosen among those present in the market. First of all the wavelength was chosen because it is the third transparency windows inside modern optical fibre and because it is eye safe; moreover there is almost no absorption in clear atmosphere. For these reasons there are many sources in the market. We choose the powerful laser diode which also have pulse duration short enough for LIDAR applications.

Name	brand	Band – λ (nm)	Power (mW)	Div. (°)	Price (€)
1550 HPPLD**	Roithner	1550 (±30)	30000	20x40	570

Table 2.1: *characteristic of the source chosen for our LIDAR. See text for details.*

The driver was not so easy to be found, since there were any suggested by the diode seller and it is not easy to found a commercial one. Fortunately one produced by DEI inc., named PCO 7810 with a price of 650 € met requirements needed. We also need a high voltage power supply, able to give 500 mA at 500 V, as, for example, Hamamatsu C4840 with a price of 1770 €, a low voltage power supply and a pulse generator. Device already present in laboratory were used but it is quite simple to find low cost commercial one.

Source was then assembled using the provided component.

Voltage and current requirements for our source was calculated after the driver was bought using its manual. In particular we know that nominal voltage for our source is 495 V.

The minimal value of current had to be calculated via the following formula:

$I=(C_{fet}+C_{pfn}+C_{stray})*V*f=(4080+150+600)*10^{-12}*495*2000=4{,}782$ mA

Where V is potential applied, f is working frequency, C_{fet} , C_{pfn} e C_{stray} are capacity due to FET, pulse and STRAY.

An aluminium box was then chosen so to fit driver, source head and link to the other components. So there are BNC connection to pulse generator, low voltage supply (±15 V), high voltage supply with the minimal characteristics described above. Outside the box but firmly connected there is transmission optics. Critical points are position and distance of head to the first lens, as it will be explained in the following paragraph. For this reason an optical mechanical component, namely THORLAB ST1XY-S, was fixed to the box so to easily get the optical axis of the source. Distance of first and second lens was then varied through another mechanical component, namely THORLAB SM1V05. The aluminium box was then modified making the necessary holes to fix driver and mechanical component, to let laser head be connected to the optics and to connect driver to other devices with BNC cable. Laser head was then connected to the driver soldering pins and wire with a pins-wire connecting them. An aluminium box is the common end for all neutral cable.

After some preliminary tests, source started to work properly.

2.2 Transmission optics

Even if there are many commercial beam expanders that can be used with laser diode, none of them is suitable for our source. The main reason is that radiation emitting area (370x200 μm) is bigger than usually employed laser diode. Moreover there are less beam expanders among which to choose the suitable one for 1550 nm radiation.
For these reasons transmission optics, i.e. a beam expander with divergence less than 10 mRad, was projected and Built. The value of 10 mRad as upper limit was chosen in function of calculated Field Of View (FOV) of the receiving system, as it will be explained later.
The choice of component lets us determine also the price of the system, which has to be as low as possible to be faithful to low cost device philosophy.
Some preliminary work was projecting an "ideal" beam expander for our purpose using the software ZEMAX[1] in order to optimize component characteristics of a two lenses system. All parameters, such as focal length, diameter and distance of components, glass material and radius of curvature were chosen to optimize the system and commercial components were not considered in this step. Later commercial components found in ZEMAX database were chosen so to minimize the difference with the already found ideal components. Components were chosen mainly for their focal length and so to be transparent for radiation at 1550 nm. Remaining parameters, such as lenses distance, were then optimized to minimize energy loss and beam divergence and they are better explained later on. After many changes of configuration, the components described in the following table were chosen.

Model	Manufacturer	Material	Dep.(mm)	NA	F.l.(mm)	Diam. (mm)
45551 drum	Edmund Optics	BK7	5	0.37	3,67	4
08016	Edmund Optics	F_silica	5.66	0.37	50	25.4

Table 2.2: *characteristics of optical transmission components.*

The first lens is a drum type (a sphere with north and south pole cut off) with very short focal length to collect the initial radiation, which has a huge divergence (20°x40°, see source characteristics for details). This lens diameter is only 4 mm and a mechanical dedicated support has to be fabricated so as to fit the Thorlabs standard 25,4 lens mount and to be coupled to the second one.

The second lens is a short focal biconvex lens, chosen to collect all radiation from the first lens minimizing beam divergence at the same time. Both lenses are mounted on Thorlabs XY translating lens mount where it is possible to change finely the distance between lenses.

Source was simulated in ZEMAX using a tool which is dedicated to simulate a diode laser, so it is particularly fitted to our needs.

The real task is, of course, to reduce long distance beam divergence to the lowest possible value. The energy received at a fixed distance was used to optimize the system set up. In particular, the distance between lenses was fixed to the value of 37.29 mm which was found maximizing energy received in a small circle at the distance of 100 m. Finally, the system is theoretically able to send 90% of energy in a spot of 743 mm, as clearly visible in the figure 2.3, which represents the fractional amount of energy enclosed inside a circle, whose radius value is represented in x axis and centred in optical axis, at the distance of 100 m.

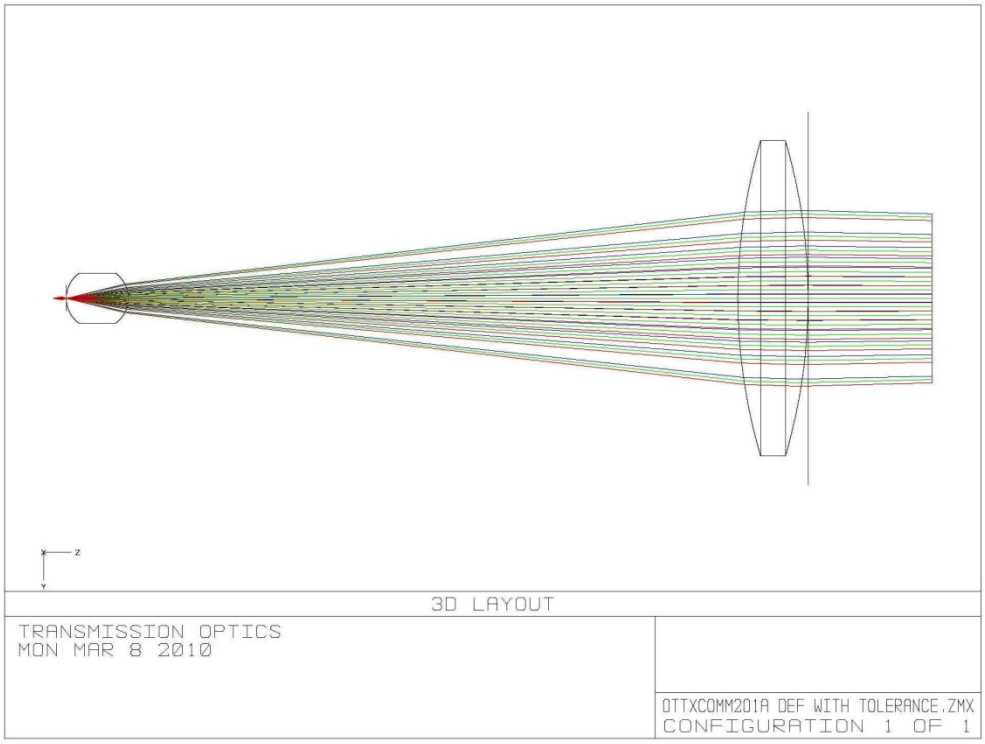

Figure 4.2: *Optical transmission system layout. See text for details.*

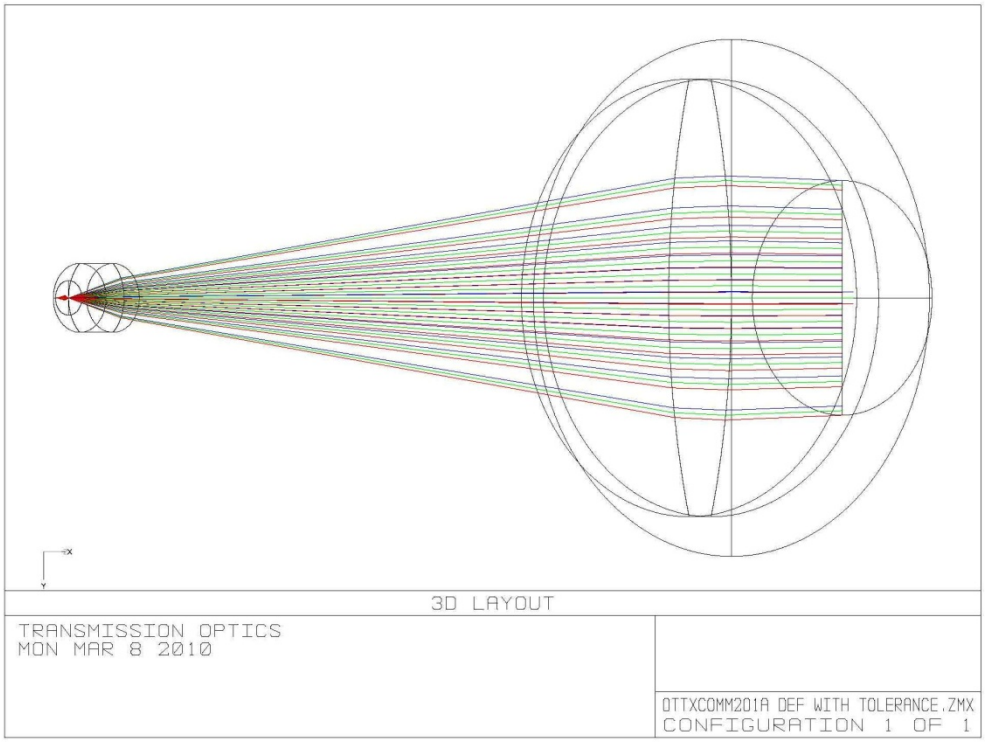

Figure 4.3: *Optical transmission system layout, 3d view. See text for details.*

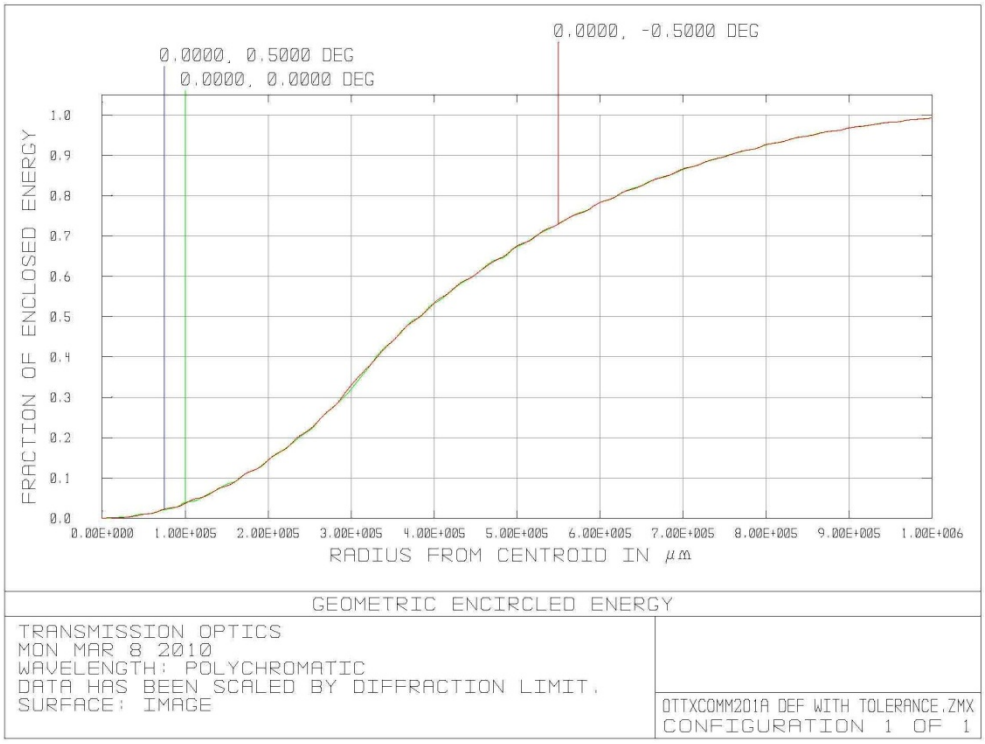

Figure 2.4: *Fraction of energy enclosed in a circle at a distance of 100 m. See text for details.*

Another critical point which is vignetting, determined by collision of rays against optical system wall or generally by unwanted reflection and other optical deviation and cause energy loss as well. Vignetting is generally absent, even if it could become a critical point in some cases, as better explained later on.

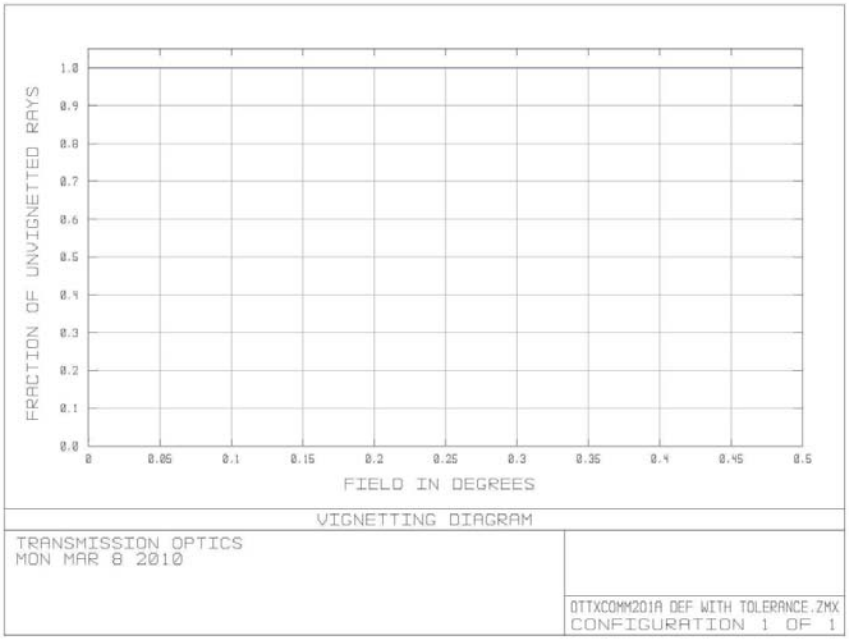

Figure 2.5: *Fraction of unvignetted rays in function of source inclination respect to optical axis.*

Beam shape could also be interesting in some cases. At a distance of 100 m the shape is determined by source difference in the two axis divergence, as visible in the next picture.

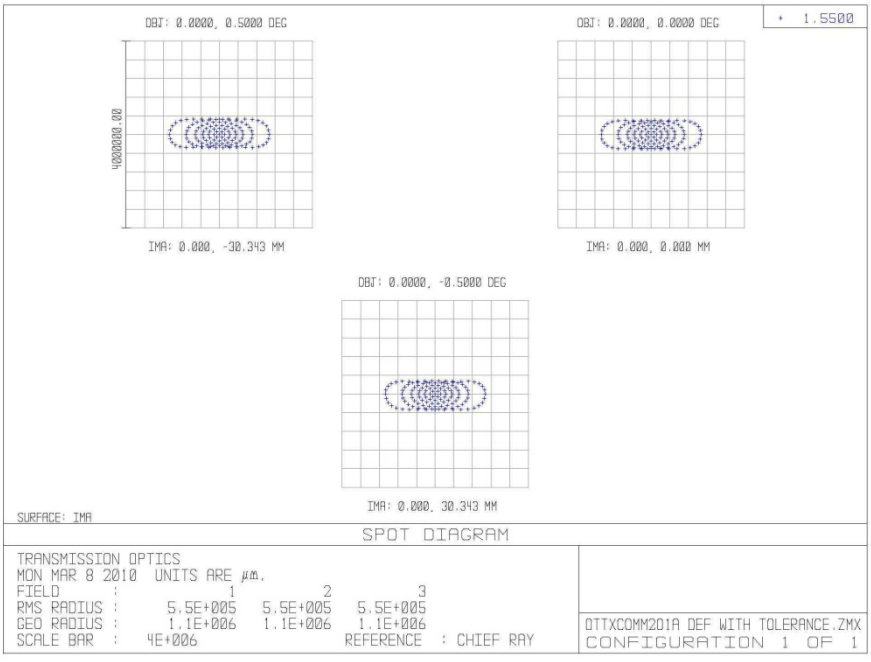

Figure 2.6: *Shape of source at a distance of 100 m from the source itself. See text for details.*

The ability of the system to work properly even if mounting is not perfect, i.e. study of tolerance, was also performed in order to avoid a good but unrealistic optical system. So we suppose a maximum difference in position from optical axis of 0.5 mm for the first lens and 1 mm for the second lens. A maximum tilt of 5° was also supposed for both lenses. Tilts and distance from optical axis refer to both axis of a reference system on a plane orthogonal to optical axis and with origin on optical axis.
Results obtained are really good because RMS of spot size at a distance of 100 m change from the original value of 743 mm to 799 mm in the worst case. Misalignment is not a major cause of fault inside reasonable value.
A major fault is determined instead by changing the distance of the source from the first lens. The necessity to verify this value arises from experimental activity described in the following paragraph. Both the divergence and the power lost inside the system due to vignetting are strongly influenced by this value. Its value may change from 0 to 0.5 mm, otherwise the system will not work properly. A value of 2 mm is enough to increase divergence up to 90 mRad. Some correction in distance between lenses could help reducing this catastrophic results, but the distance between source and first lens is the most critical point of transmitting optics.

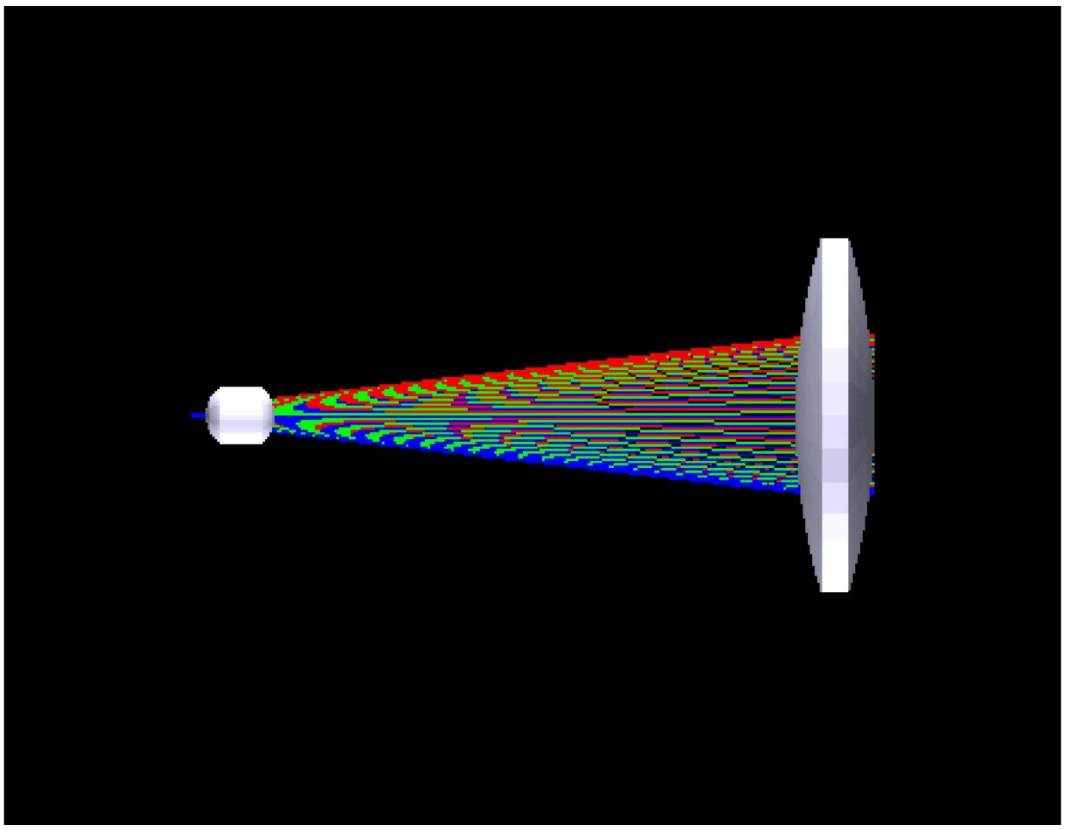

Figure 2.7: *A 3D reconstruction of transmission optics.*

2.3 Test of source and transmission optics

After having chosen the component, the next step was to mount components one at a time and test system performance step by step comparing measured values to expected ones. The first lens of transmission optics was mounted on a handmade support so as to be aligned to the optical axis of source using a lens mounting kit able to change position on two axis (THORLABS ST1XY-S). This system was fixed as close as possible to the output of our source using four screws which link the mounting kit to the aluminum box of the source.

In figure 2.7 the aluminum box containing driver and the optical support with the source pins visible are showed, while in figure 8 transmitting optics and source box as it was tested are visible.

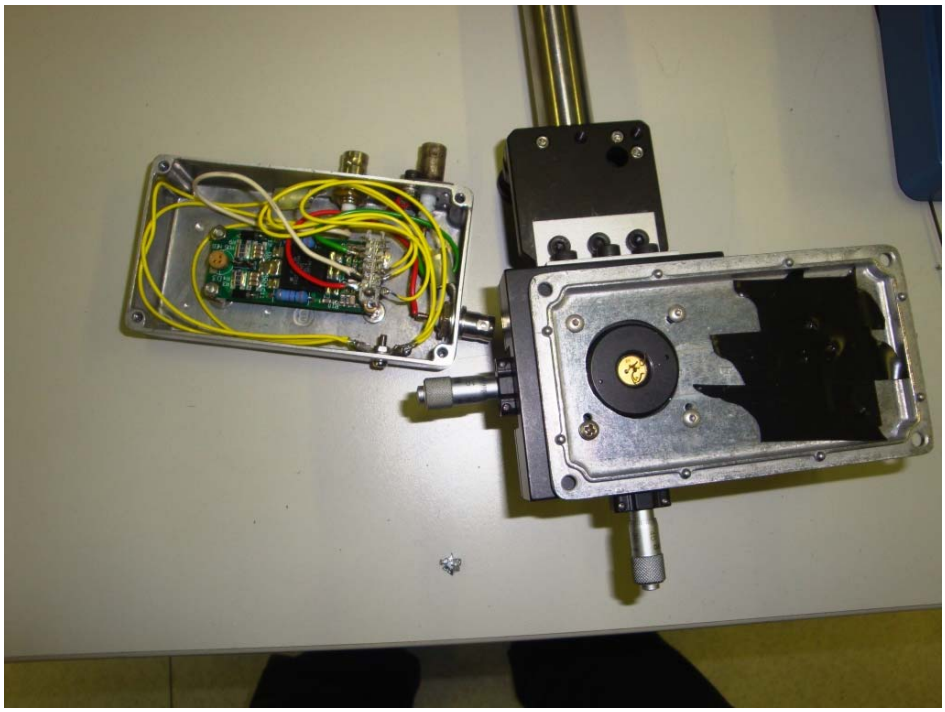

Figure 2.8: *Shot of source box and the backside of source which is closely linked to first lens support.*

Figure 2.9: *Shot of source box and transmitting optics mounted as used during tests.*

An avalanche photodiode, namely Hamamatsu APD310 was mounted in front of the described set up, at a distance of 100 mm and on a support able to move the system in both axes, so to check if beam shape and power measured were compatible to expected ones. A filter was needed to avoid detector destruction and laser emitting power was limited using a voltage of 395 V instead of the maximum value (495 V).

The following pictures show the signal collected along horizontal axis and vertical axis in front of the source.

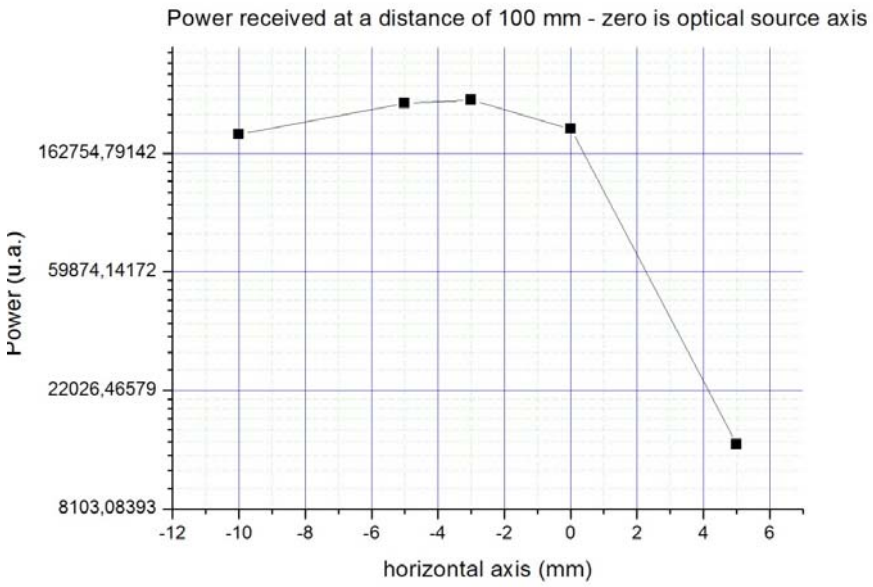

Figure 2.10: *Spatial distribution of power in front of the source at a distance of 100 mm along horizontal axis. See text for details.*

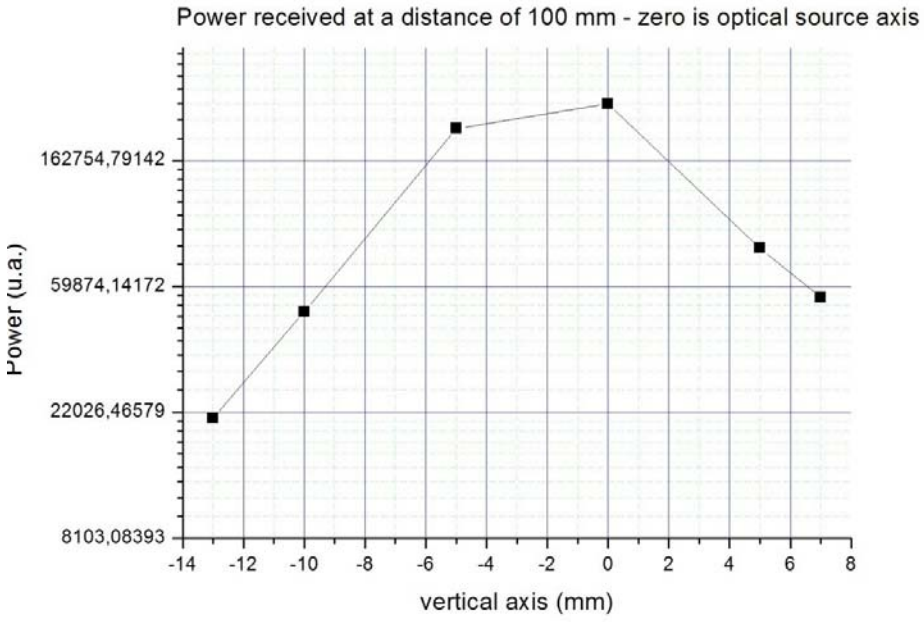

Figure 2.11: *Spatial distribution of power in front of the source at a distance of 100 mm along vertical axis. See text for details.*

The shape seems a truncated Gaussian function along vertical axis and an almost flat one, as it were a very large Gaussian function, along horizontal axis. This was compared to the shape provided by ZEMAX for this set up, displayed in the following picture. The shape observed are compatible with an emission comparable to that foreseen by ZEMAX, a little inclined toward the vertical axis but mainly along the horizontal axis. This is compatible with observation of physical position of emitting layer inside the source.

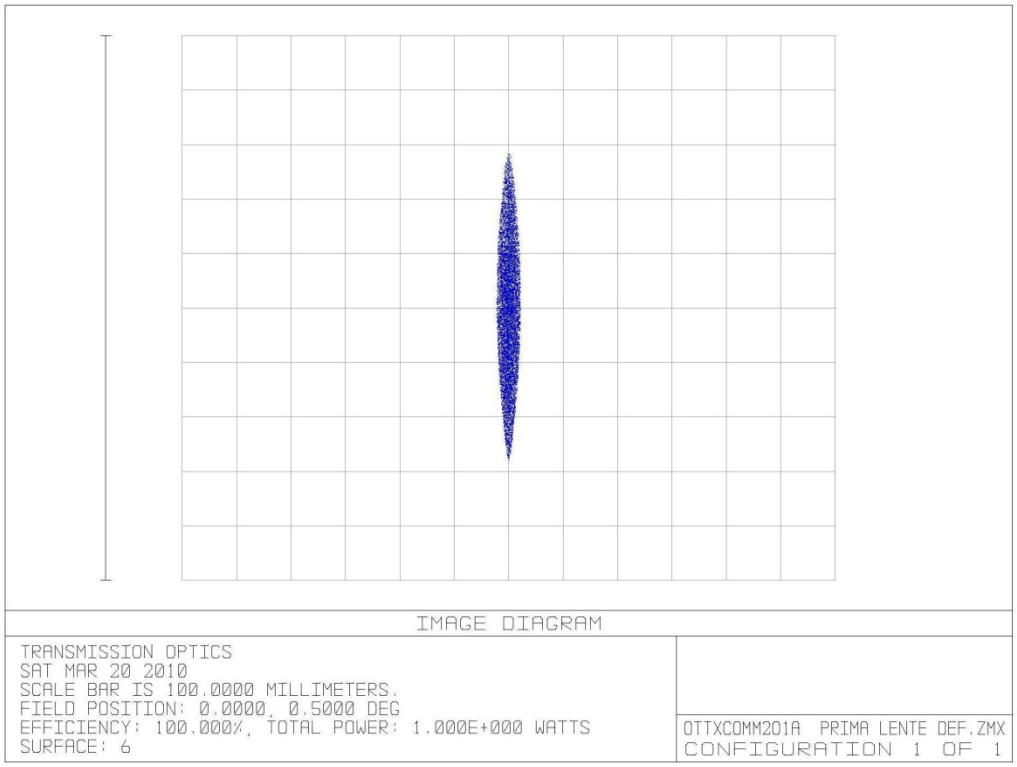

Figure 2.12: *Spatial distribution of power in front of the source at a distance of 100 mm as foreseen by ZEMAX. See text for details.*

In order to proceed with system set up testing, we decide to use a IR camera which is able to measure radiation emitted from diode laser, namely Hamamatsu C1000-03, so to have a quick and friendly system to see the shape of the beam without time consuming detector displacements. Image was computer analyzed using a USB 2.0 adapter and a digital converting software, which was further analyzed with image-J free software. We used a squared paper sheet to have a rough idea of physical beam dimension. We put this sheet in front of the source at a distance of 33,02 cm (8''), with the first lens mounted in the best position found with the previous method. Beam shape is almost circular with a diameter of 25 mm while ZEMAX foresaw an elliptical shape with a long axis of 70 mm and the short one of 7 mm. The reason is probably that mechanical handmade of first lens is too narrow and radiation is absorbed or scattered. The support was modified with a conical shape to avoid this effect.

The measurement obtained are only qualitative due to the lack of calibrations, but Full Width Half Maximum (FWHM) in horizontal, vertical and diagonal (45° respect to both axes) directions determined after noise suppression are measured, at a distance of 24 cm from the source. Using translating mount it was possible to move finely the lens in order to achieve best position in terms of peak power, shape and position both in horizontal and vertical axis.

Check of results with ZEMAX provided shape suggests to change again the handmade lens support so as to enlarge the conical hole as much as possible. Conical shape angle was 45° and the hole was depth until a distance of 1 mm from the lens, as visible in the following picture, where also source box is visible. A long set of measures to find best lens position were then performed in both axes.

The following picture is taken from our IR camera using visible light in order to set up focus and test system to see what is going to be measured using IR radiation.

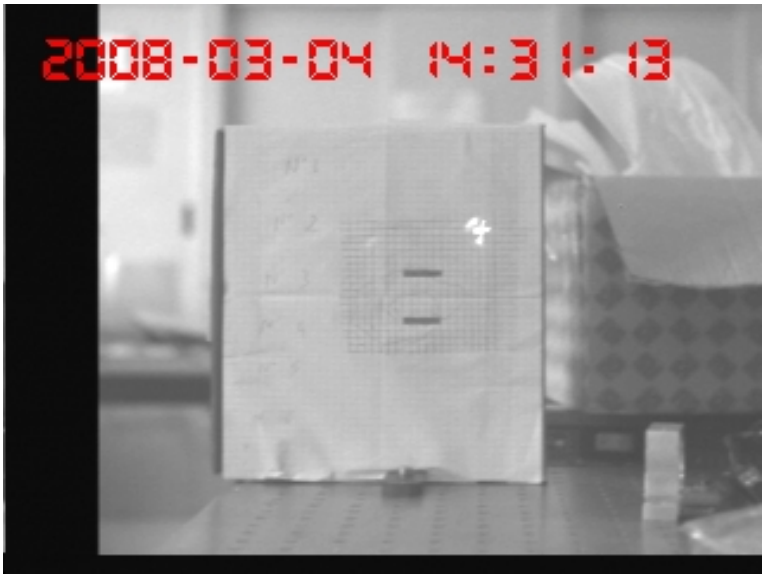

Figure 2.13: *Image taken with our IR camera using visible light during screen positioning and focus test. See text for details.*

A shot of the noise was always taken to have a reference above which calculate maximum value and FWHM. An example of such shot is reported in the following picture.

Figure 2.14: *Image taken with our IR camera before lighting on the source to have a noise reference level.*

An example of image taken during position optimization is provided in the next picture. IR camera sensitivity is not really high due to its general purposes design. Moreover it was impossible to fix a filter in front of receiving optics due to its out of standard diameter and mounts system.

Figure 2.15: *Image taken with our IR camera with source visible, only first lens mounted in front of the source. The high intensity spot is only a camera detector damage. See text for details.*

Finally in the next picture an example of image provided by digitalization is given. Radiation peak was calculated along axis determined by human eye discriminations. Pixel are associated to a determined distance in mm which is provided using a known distance in the screen. The maximum value and FWHM was then easily calculated.

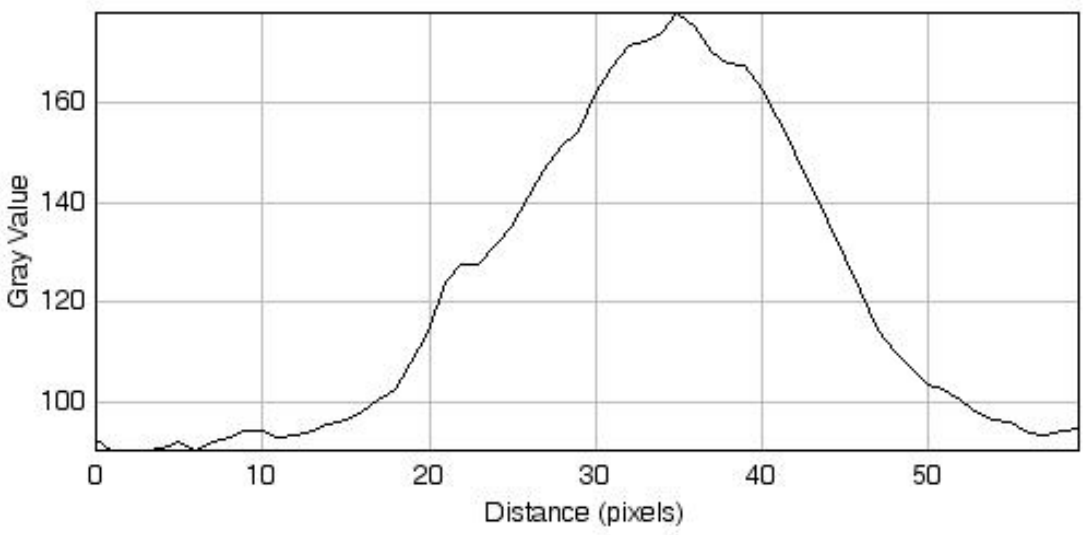

Figure 2.16: *picture of a typical Gaussian shape provided by image analysis along the shorter axis. See text for details.*

After first lens position optimization the second lens was mounted in a translating mount THORLABS, the same used for the first lens, so to adjust finely alignment. The two translating mounts were then linked using a thread tube which lets you change relative distance in a range which is centered on the ZEMAX prescribed position. Some difficulties in testing the system arose because it was not so simple to change relative distance between

lenses. Considering that second lens position in horizontal and vertical position is not so critical, we decided to fix second lens centered on optical axis and easily translate it using a properly designed zoom system. The screen was fixed at a distance of 1.1 m. One of the spot acquired with IR camera during our test is reported in the following picture.

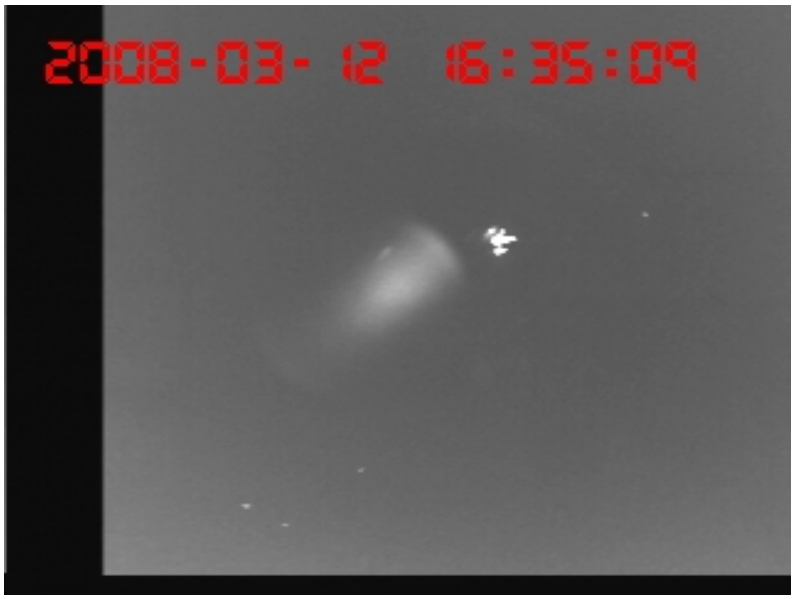

Figure 2.17: *Image taken with our IR camera with source visible, both lenses mounted in front of the source. The high intensity spot is only a camera detector damage. See text for details.*

After many experimental changes in distance and lenses arrange set up, no image finally is similar to that expected by ZEMAX calculus, reported in figure 2.12. Moreover, even ZEMAX determined different images depending on whether using normal "sequential component" set up or "non sequential component" set up. The main difference is determined by dramatic change in image quality determined by even little change in the relative distance of lenses in the second case. This is probably more realistic. In fact it was found that our best experimental image, reported in figure 2.17, determined a divergence and a shape not far from that obtained by ZEMAX. The last was obtained using non sequential component calculus, setting a distance of 2 mm from source and first lens and is reported in figure 2.18. It is not possible to measure such distance because the output window of the source is not the source itself and lens coupling is someway a "black box" since it is not possible to see and measure a distance inside aluminum box when connected to translating mount of first lens. Nevertheless, it is quite a realist distance, considering mounting set up and general source characteristics.

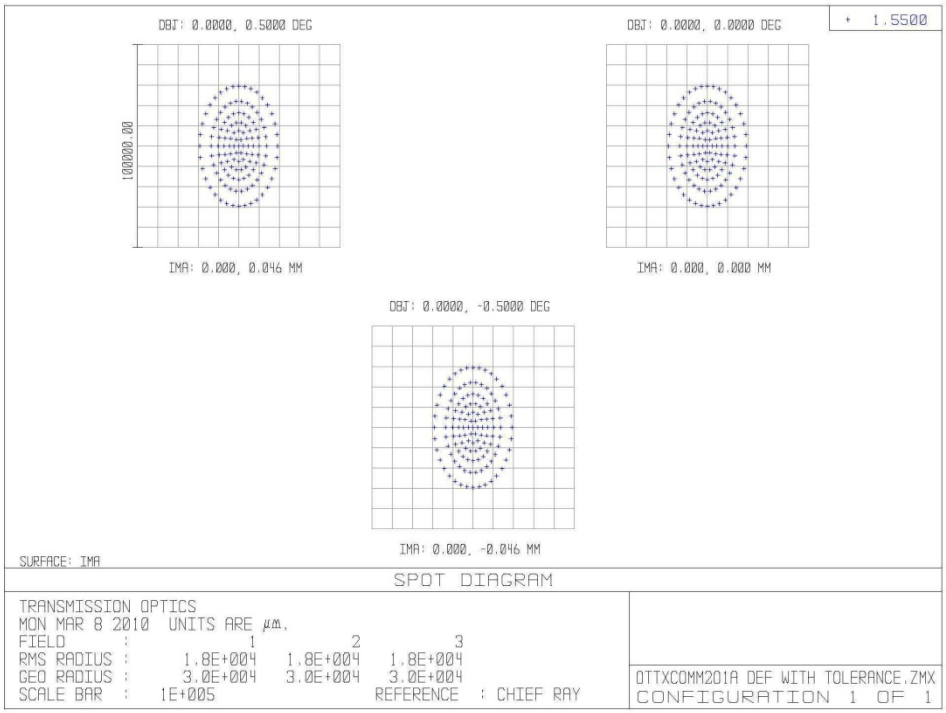

Figure 18: *Spatial distribution of power in front of the source with both lenses mounted in front, at a distance of 1100 mm as foreseen by ZEMAX, "Non Sequential Component", considering a distance of 2 mm between source and first lens. See text for details.*

The divergence has a value of 25 mRad, quite far from the one provided by ZEMAX for the ideal case 7.43 mRad, and also far from the maximum value allowed to full fitting our system performance, namely 10 mRad, both numbers already explained in the first paragraph.

The variation of system performance with the distance between source and first lens are reported in figure 16, where several FWHM were experimentally determined by changing lenses relative distance and compared to the one determined by ZEMAX by changing distance between source and first lens. A distance of two mm is not far from experimental results, confirming the mentioned theory. In this case some energy is lost not only considering beam divergence, which determines a big amount of energy is lost because not collected by receiving optics, but also taking care of vignetting, which costs a leakage of about 20% energy.

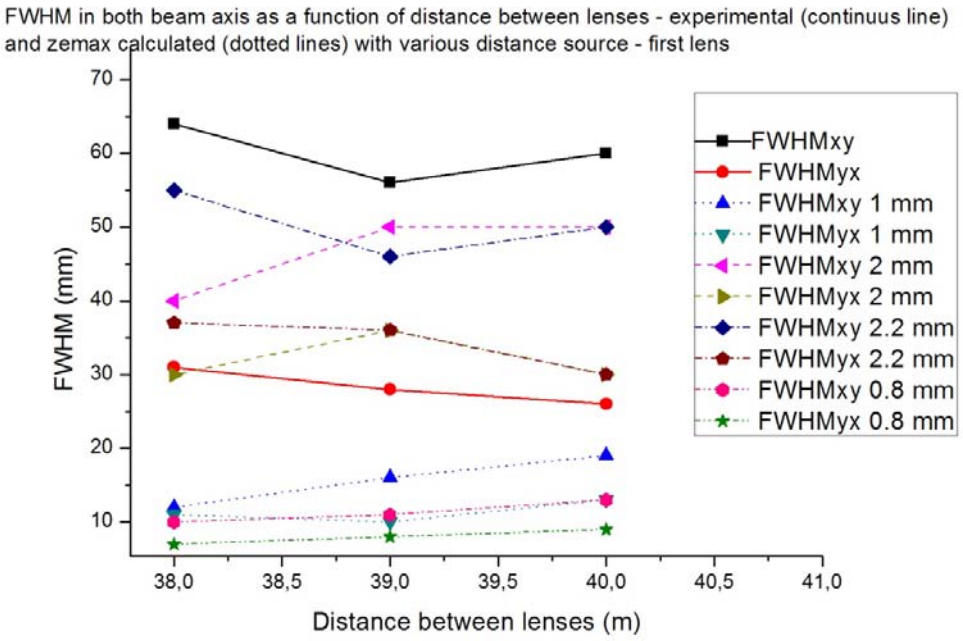

Figure 2.19: *ZEMAX FWHM prediction compared to experimental results changing lenses and source distances. See text for details.*

Future set up changing will be devoted to strictly control source distance and inclination from first lens. A tentative to use commercially available tools failed, so it is probably necessary a properly designed component. Even if system performances are not guaranteed, we decide to continue working on receiving optics and detector. Most of the job was done working on both subsystems during the same period.

2.4 Detector

A detector was initially chosen taking care of Signal to Noise Ratio (SNR) of the system and so looking for detectors with low Noise Equivalent Power (NEP) or high Detectivity and big surface to get an easier coupling to the receiving optics. Unfortunately, response time of the chosen detector is 1.6 μs, calculated inverting cut-off frequency from datasheet, is too long not only to acquire a data useful for range resolved measures but also to acquire intelligible data at all. Characteristics of this detector, made by Hamamatsu, are reported in table 2.3. Sensitivity and active surface are really good, thanks to an efficient cooling system. Response time, determined inverting cut-off frequency, is not good at all. Signal has not the time to rise at all.

Model	Opitical bandw. – λ (nm)	Cut off freq. (MHz)	NEP ($W/Hz^{1/2}$)	RESP. (A/W)	D^* (jones)	Price (€)
G8605-25	900-1650	0,6 MHz	$2x10^{-14}$	0.95	$3x10^{13}$	1155
A3179-01	Heat sink					98
C4159-02	Preamplifier					855
C1103-04	Temperature controller					979

Table 2.3: *characteristics of first chosen detector.*

A different detector was then chosen taking care of speed, sensitivity and coupling optics. The choice was an avalanche photodiode which is able to pick up even signal as fast as 1 ns. Namely it is model 1647 made by Newfocus and related accessories. Main features of our choice are reported in the following picture, taken from original data sheet. Even if detector active surface is really small, it is coupled to a fibre optics which is coupled to a 5 mm lens provided by the manufacturer. It is then possible to couple this lens to our designed receiving optics, as explained in the following paragraph.

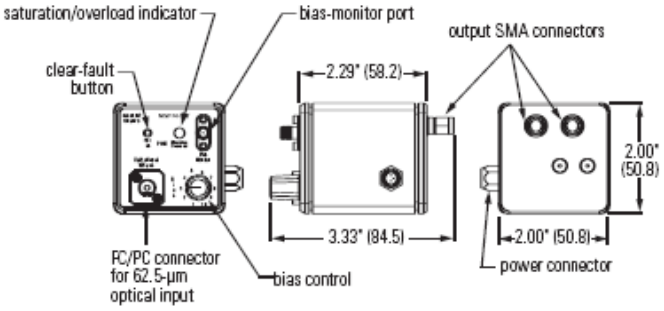

Model 1647

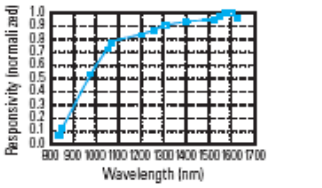

Typical responsivity of the Model 1647.

Wavelength Range	800–1650 nm
3-dB Bandwidth (typical)	15 kHz–1.1 GHz
Rise Time (typical)	250 ps
Peak Conversion Gain	28,000 V/W (differential outputs) 14,000 V/W (single output)
Output Impedance	50 Ω
NEP (typical)	1.6 pW/√Hz
Saturation Power, AC	6 µW
CW Optical Damage Threshold	200 µW
Power Requirements	±15 V, <200 mA (Model 0901 recommended)
Optical Input	FC, 62.5 µm
Electrical Output	SMA
Model #	**1647**
Price*	$2,250
Price, 3-yr Extended Warranty†*	$695

NOTE: Specifications are given at maximum gain setting. At lower gain settings, specifications will vary.
†*See our terms and conditions of sale for more details.*

Related Products: Power Supplies (page 144) ■ Electrical Accessories (page 145)
Breakout Cable (page 142) ■ VCSEL (page 47)

Definitions of Characteristics (page 148)

For international prices add 10%.

Figure 2.20: *Table taken from data sheet reporting main characteristics of high speed detector chosen. See text for details.*

2.5 Receiving optics

Receiving optics, as well as all the other components, were chosen taking care of cost, simplicity and reliability. A system which is able to ensure high receiving Area with low cost, simple to mount and high reliability could be made using a Fresnel lens coupled to traditional optics to avoid interfering fringes, also because second lens diameter and thickness are not

critical. The chosen Fresnel lens must not be confused with the one obtained using transmitting and absorbing area so as to use interference to collect light in some positions. The one we are speaking about were originally though by Fresnel for huge transmission optics as that needed inside lighthouses. The principle is that it is possible to "cut off" the thick part inside a lens because the ray bending effect is due to the surface separation of air and lens material. Further details can be found in ref 2.

These lenses are big, even 457 mm diameter for commercial ones, with a low weight, thickness is few millimeters even for the bigger ones, nowadays are made in plastic material. Image quality is not high due to aberration which are not simple to correct, but for our "energy collecting" application this is not so important. The second lens is instead a "traditional" lens. Both lenses have an high transmission at 1550 nm radiation. Their characteristics are listed in the following table.

Model	Manufacturer	Banda – λ (nm)	Thickness (mm)	NA	Focal. l. (mm)	Grooves for mm	Diam. (mm)	Price (€)
Acrilyc 48.4	Fresnel Technolog.	400-1600	2.8	0.37	457	5.6	457	220
45094	Edmund Optics	SF5	5,5		15		15	

Table 2.4: *characteristics of receiving optics chosen lenses.*

While first lens was chosen only taking care of diameter to have a big collecting surface, the second lens was chosen determining the best one to collect our photon on the smaller surface as possible with a commercial lens, chosen from that available on ZEMAX database. Commercial Fresnel lenses are not present in that database, so the lens was reconstructed starting from known data. Our reconstructed lens is worse than the real one because the last is aberration corrected while ours is not and so also focus ability simulated is worst than real one. Nevertheless quite good results were achieved. A side view of layout obtained including simulated rays in provided in the following picture.

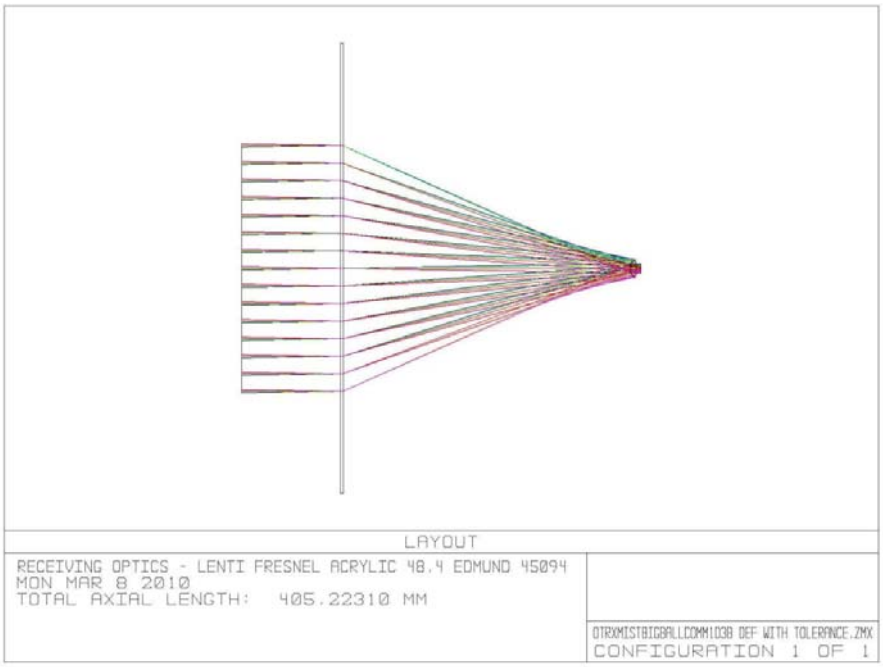

Figure 2.21: *Optical receiving system layout. See label for details.*

Receiving optics performances were determined calculating the energy collected inside a circle of various radius in the image plane, taking care of vignetting and considering shape of our source in image, reported in figures 19, 20 and 21 respectively.

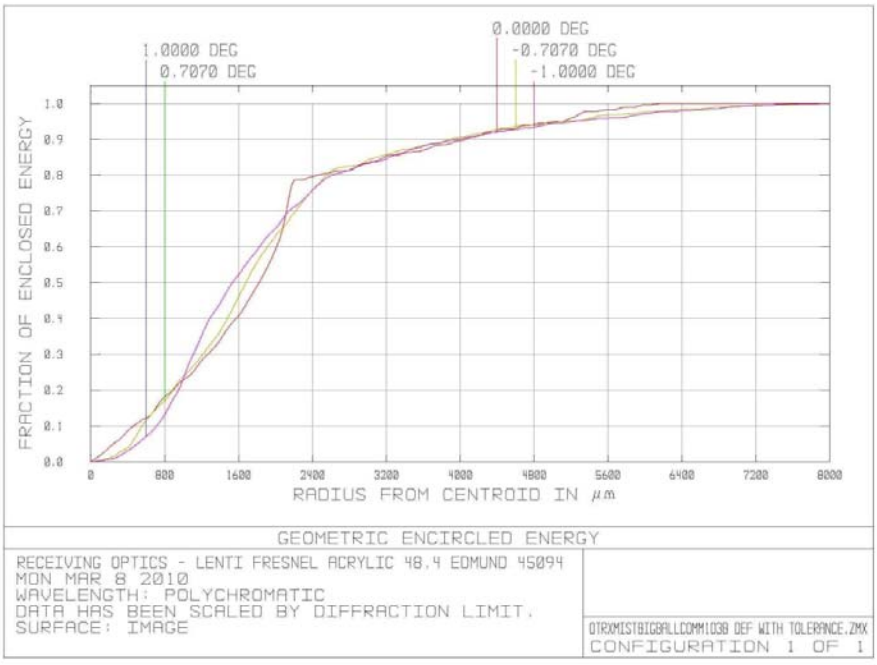

Figure 2.22: *Fraction of energy enclosed in a circle inside image plane. See label for details.*

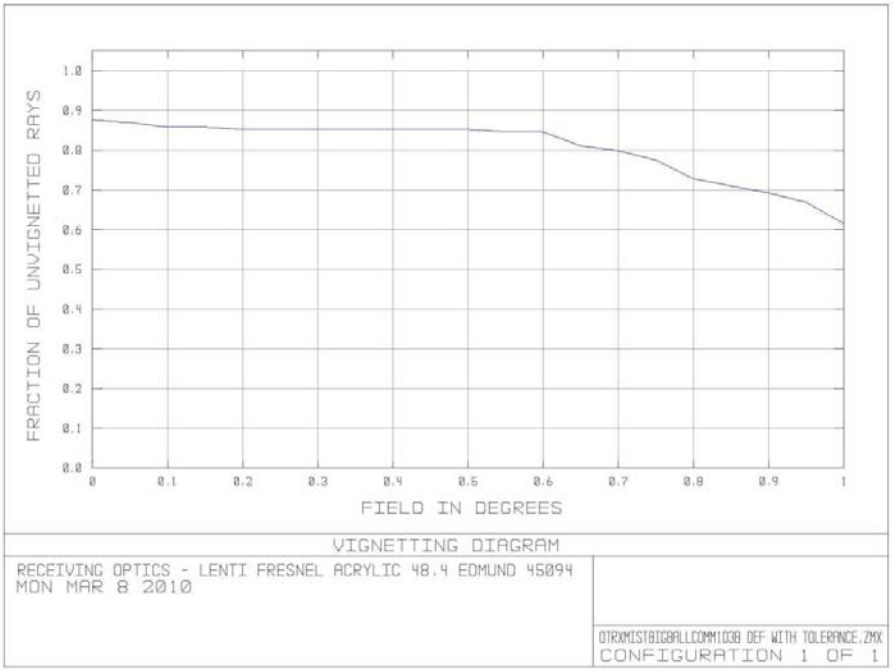

Figure 2.23: *Fraction of unvignetted rays in function of source inclination respect to optical axis. See label for details.*

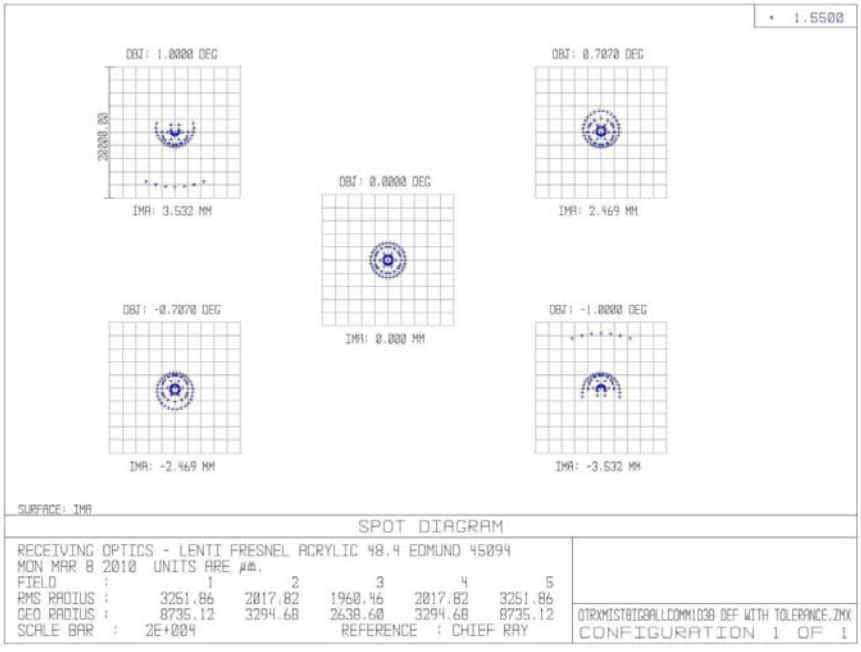

Figure 2.24: *Shape of source in the image plane. See label for details.*

System performances are generally good. More than 90% energy is focused on detector and loss due to vignetting is about 15%. Finally more than 75% energy is collected.

A tolerance study was performed also for this setup. Angle was varied till a value of 5° while centering was varied of 10 mm for Fresnel lens and 1 mm for traditional one. The spot image

where 90% of energy is collected varied from 1,14 mm to 3,44 mm. This is quite a good result considering big tolerances imposed.
Also a filter has to be inserted in order to lower noise determined by different source, also considering detector wide receiving band. Two filters were chosen, a laser line filter and a long pass filter. The first one is good because of its selectivity while the second for its high transmission value. Only the first one was finally used during system testing.

Model	Line center λ (nm)	bandwidth (nm)	Trasm. (%)	Thickness (mm)	Diam. (mm)	Price (€)
Thorlabs Laser line filter	1550	12	40	5,6	25,4	85,79
Thorlabs Long pass filter FEL 1500	1500		70	6,3	25,4	69,13

Table 2.5: *characteristics of chosen filters.*

2.6 Test of detector and receiving optics

Many affords had to be done to test detectors. A plural form is needed because we change detectors during tests, as explained in the previous subparagraph. The first detector has to be mounted also considering its cooling system and temperature controller. also some soldering and mechanical adjustments were done. Unfortunately this job did not give any results, as explained. An example of results determined trying to acquire a fast signal determined by a pulsed laser with our slow detector, pulse length of 50 ns, thus comparable to our chosen source, is showed in the following picture. Clearly there is no signal, just noise.

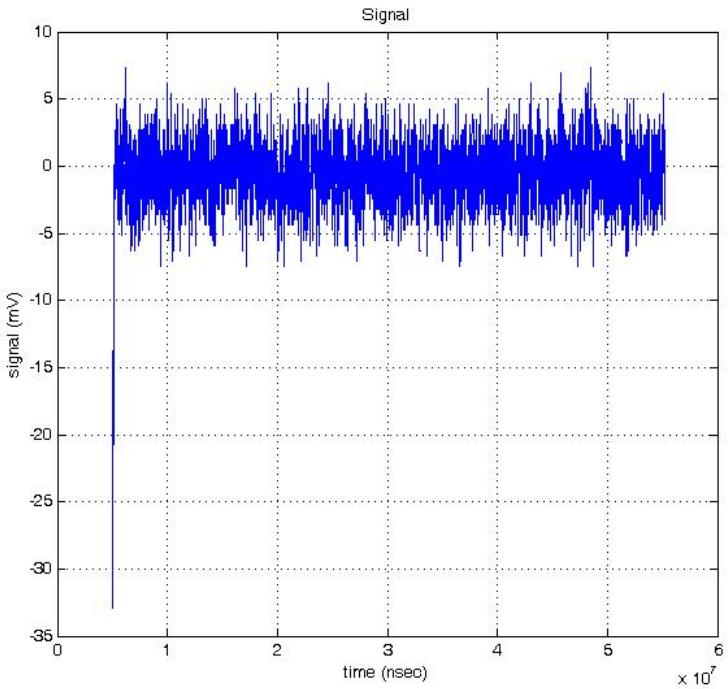

Figure 2.25: *Signal acquired during slow speed detector testing while illuminated by a short pulse laser (pulse length 50 ns). See text for details.*

Finally, a good signal was obtained only changing detector. The Newfocus detector gives quite a good signal in terms of time resolution, but SNR is even worse than expected. Theoretical prediction with this detector, explained in the following paragraph, gives a chance to see a lidar signal up to a range of 80 m. Instead it was impossible to see a lidar signal at all. The only visible signal was determined by reflection from a surface at a distance of about 10 m and properly organized to maximize reflection towards receiving optics. Perhaps it is possible to think about a DOAS, not a lidar for sure, with this system setup. The signal acquired is shown in the following picture.

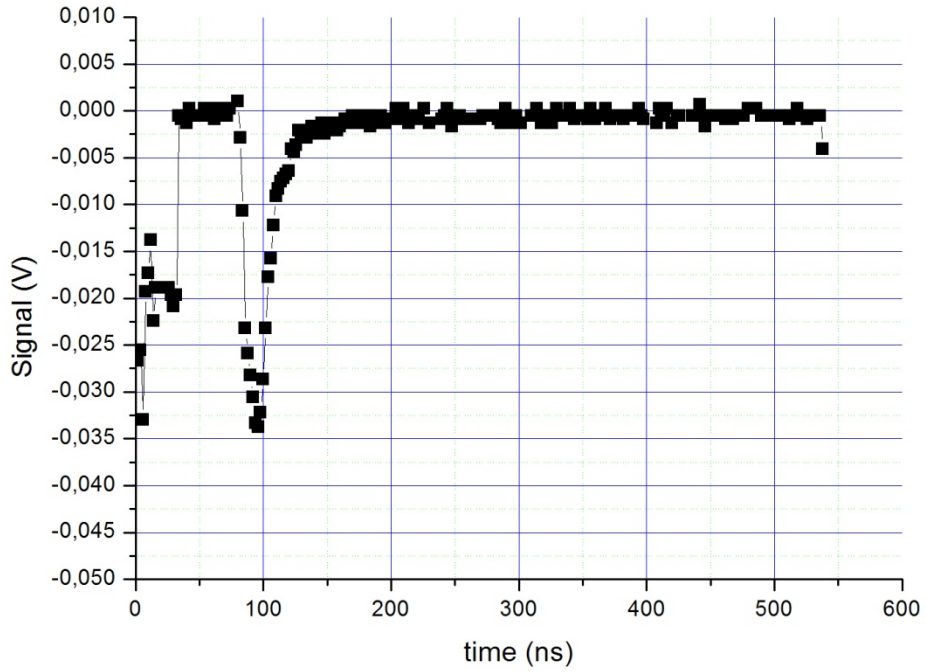

Figure 2.26: *Signal acquired during high speed detector testing while illuminated by radiation of our source retroreflected by a solid target.*

The last measures were performed after having mounted and tested receiving optics. This activity was performed for a long period because it is quite a hard job to properly align a huge Fresnel lens with a small traditional lens in turn coupled to a small detector. This result was achieved changing lenses support up to a reasonable system. Testing was done with a multiple traditional source, made with a lamp screened by a four hole thick paper such as to reconstruct our source dimension at the test distance. The focus position and image dimension were compared to the real object one. Image seems to be small enough that a big amount of incoming energy could be picked up by detector. Several Mask to rebuilt source dimension were rebuilt to reach longer distance. At 12,5 m of distance the image of the four holes is clearly visible inside a lapped glass put in detector theoretical position. Image in that point is 6 mm length, 4 mm wide. Detector diameter or final receiving lens diameter is 5 mm, so not all energy is picked up, but not so bad. Real Fresnel lens seems to be really better than the one used in ZEMAX and aberration corrections, not introduced as explained in the previous paragraph, work properly. The next step is to get a distance that is not so far from ideal working distance of our system and for this reason a multiple source was organized using two windows, whose distance is 250 cm, of the building block in front of laboratory at

a distance of 150 m. The values finally obtained are quite good. In the next picture the dimensions of the image, in our case the relative distances of source points from the windows, after the first and second lenses are used to calculate a virtual image surface and compared to the value of detector surface, just to have a rough idea of receiving optics performances. ZEMAX prediction is reported as well for the sake of clarity. Using both lenses 100% of energy is received, even if image area calculated by ZEMAX is even smaller. Receiving optics, considering its diameter, seems to work quite well.

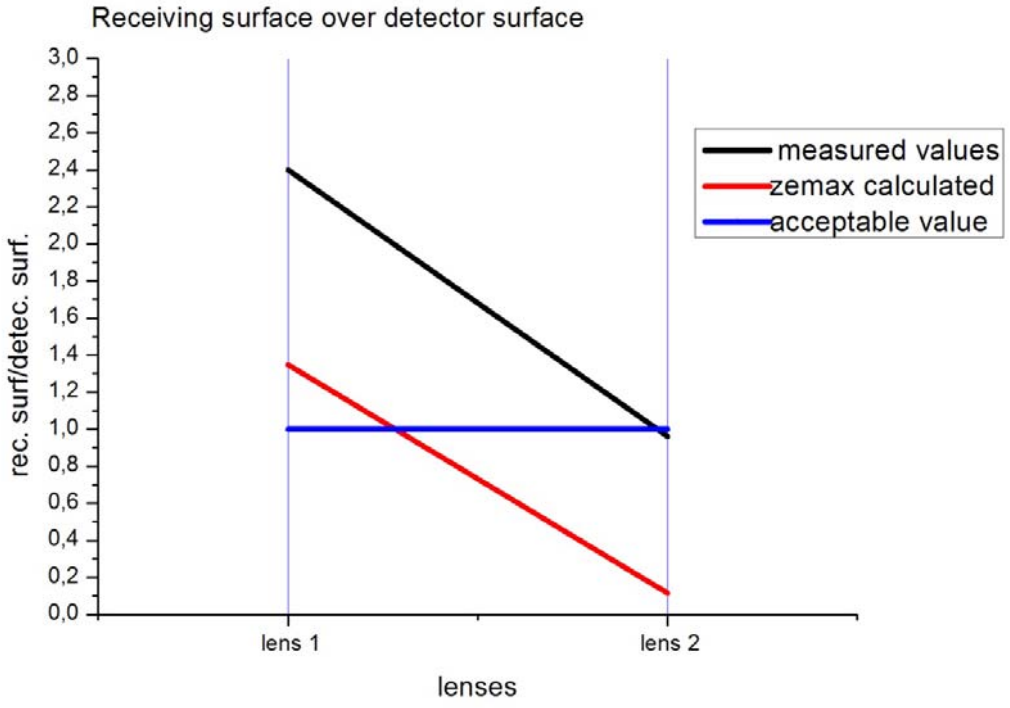

Figure 2.27: *Ratio of image surface as calculated by experimental points and detector surface. Same ratio for ZEMAX calculated image surface. Both calculus made considering one or two lenses in receiving optics.*

2.7 PHOTON BUDGET AND ENERGY CONSIDERATION

Let us summarize in the following table the main information about the system characteristics already provided and let us give some useful data for our task, for example atmospheric medium characteristics using our source wavelength. These information will be used to calculate system performance expected. Usually this calculus have to be done at the beginning of an experimental activity, so as to determine if a system set up is able to achieve desired performance or not; we put this calculus at the end because system configuration change during testing activity and in some way realistic calculus was performed only at the end.

Variable	Symbol	M.U.
Receiving optics radius	r_{oi}	m
Sensible detector area	r_s	mm
Output laser area	r_{las}	mm
Distance of target	R	m
target Displacement	d	m
Receiving optics focal distance	f	m
Circle of least confusion radius	r_{clc}	mm
Circle of least confusion displacement	d_{clc}	mm
Target image on detector radius	R_t	m
Laser image on detector radius	r_l	m
Receiving optics Acceptance radius	Θ_{acc}	rad
Laser Divergence, including transmitting optics	Θ_{las}	rad
Maximum laser divergence	Div_{las}	rad
Laser source transmitting optics focal distance	f_{las}	mm
Distance between optical axis	I	m
Detector Detectivity	D*	Jones
Laser pulse duration	t_l	ns
Detector integration time	t_s	ns
Minimum Signal to Noise Ratio	SNR_{min}	-
Receiving optics transmitting coefficient	T_r	-
Optical filter transmitting coefficient	T_f	-
Total transmitting coefficient	T	-
Absorption coefficient	K	m^{-1}
Backscattering coefficient	β	m^{-1}
Single pulse laser Energy	E_l	J
Minimum Detectable Energy	MDE	J
Energy received by detector	E	J
Speedo of light in air	c	m/s

Table 2.6: *Symbols used in calculation.*

Let us consider first of all energy received by detector due to backscattering. The following formula is achieved [ref. 3 page 241]:

$$E(R) = \frac{E_l T \pi r_{oi}^2}{R^2} \beta \frac{c t_s}{2} e^{-2kR} \qquad \textbf{equation 2.1}$$

This value has to be compared to the minimum detectable energy, which of course does not change with distance [ref. 3, page 231]:

$$MDE = \frac{1}{D^*}\left\{\frac{t_s \pi {r_s}^2}{2}\right\}^{\frac{1}{2}} SNR_{min} \qquad \textbf{equation 2.2}$$

Initially, we consider that the first detector, even if slow, would be able to pick up enough energy and only range precision would be affected. For this reason the following picture was considered to start reasoning on feasibility, which gives quite a good result up to a distance of 700 m:

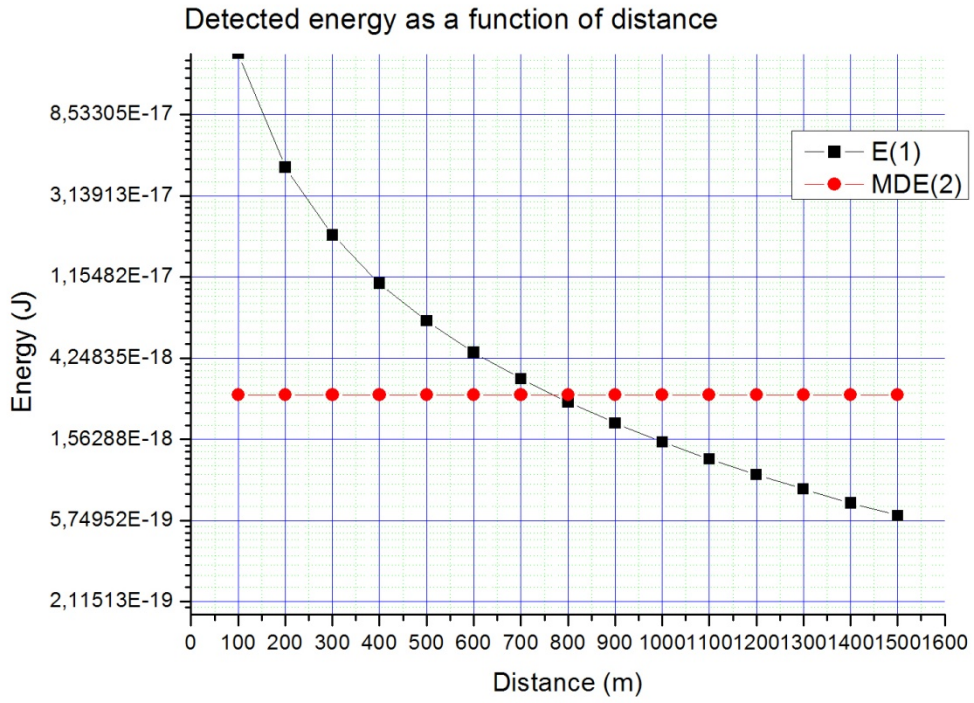

Figure 2.28: *Energy received by first chosen detector compared to Minimum Detectable Energy. See text for details.*

The previously explained idea was falsified only during real test activity. For this reason we turn our attention on an avalanche photodiode, Newfocus 1647 already described in the previous paragraph. This detector is fast enough and a real signal was acquired. It was chosen because an optical guide linked to a lens of 5 mm was also acquired from the same manufacturer which let us pick up energy received from our receiving optics. Unfortunately, the system was not able to pick up a real signal even from short distance. Theoretical calculation in fact predicts a range up to 40 m, but real LIDAR signal was not visible at all.

A new approach was used to reconsider our original idea. Our task is to have a low cost LIDAR. We turn our attention to recently developed source and different kind of detectors. A possible alternative to laser diode are fiber lasers, which use an optical fiber which has the active medium inside. Cost is rapidly going down and power is going up. Nuphoton Technologies NP2000MOPA laser source now has a peak power of up to KW level and a cost not far from 10.000 €. Main characteristics taken from manufacturer data sheet are reported in the following table.

NP2000MOPA Laser Source

Optical Performance

Parameter	Min.	Typ.	Max.	Units
Wavelength of operation	1528	-	1565	nm
Average power	-	-	0.4	W
Peak power	-	-	10	kW
Pulse width	1	-	3	ns
Rep rate	Single Shot	-	200	kHz
Stability	-	-	0.1	dB/min
Output fiber core diameter (single mode)	-	9	-	um
Input voltage rating	+4.75	+5	+5.25	V
Power dissipation	-	20	-	W
Temperature range of operation	0	25	65	°C
Output connector	Customer specific			

Table 2.7: *Main characteristic of a fibre laser which could be considered as a new source.*

Also detector could be changed considering different technologies. We tried to find an almost "plug and play" one, but turning our attention over scientific application detectors we found one which has a really High Detectivity with a cost of 50 € to which you add 1150 € for the preamplifier. Some characteristics taken from data sheet are reported in table 2.8. It seems an ideal solution, but it is probably not. First of all, they give you a "rough" detector which has to be linked to electrical and electronic devices, which are not provided. Even the connector does not exist. A preamplifier is sold but everything around detector and preamplifier have to be projected and realized. Moreover, it is projected for scientific application inside laboratory. Is it possible to have such low noise outside laboratory condition? Probably not. We want an easy to use and reliable system, so this detector is not ideal for our purpose.

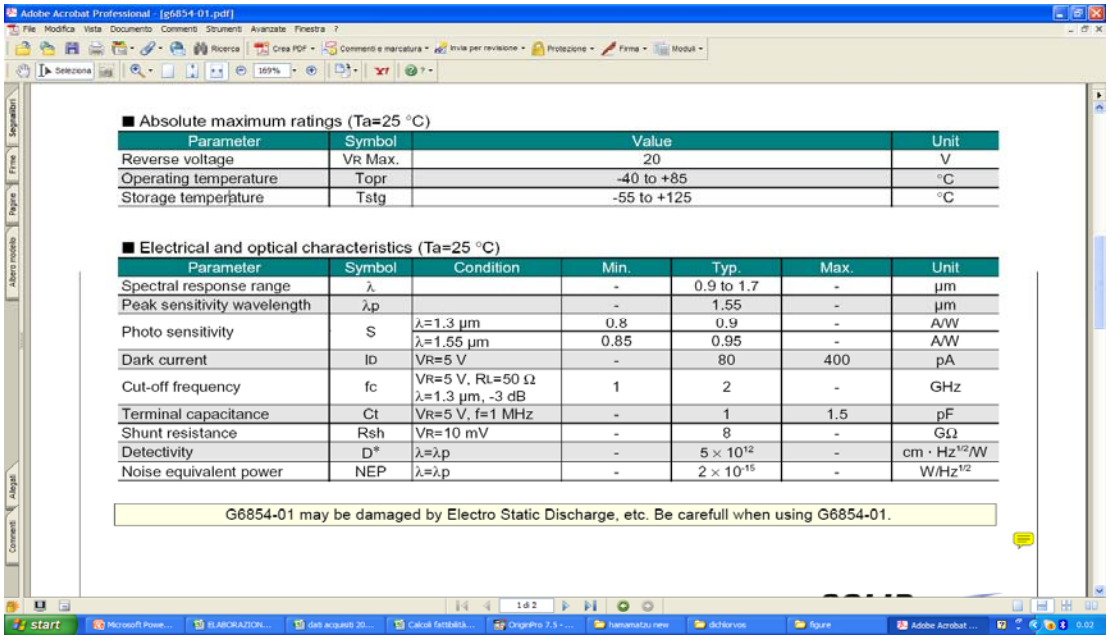

■ Absolute maximum ratings (Ta=25 °C)

Parameter	Symbol	Value	Unit
Reverse voltage	VR Max.	20	V
Operating temperature	Topr	-40 to +85	°C
Storage temperature	Tstg	-55 to +125	°C

■ Electrical and optical characteristics (Ta=25 °C)

Parameter	Symbol	Condition	Min.	Typ.	Max.	Unit
Spectral response range	λ		-	0.9 to 1.7	-	µm
Peak sensitivity wavelength	λp		-	1.55	-	µm
Photo sensitivity	S	λ=1.3 µm	0.8	0.9	-	A/W
		λ=1.55 µm	0.85	0.95	-	A/W
Dark current	ID	VR=5 V	-	80	400	pA
Cut-off frequency	fc	VR=5 V, RL=50 Ω λ=1.3 µm, -3 dB	1	2	-	GHz
Terminal capacitance	Ct	VR=5 V, f=1 MHz	-	1	1.5	pF
Shunt resistance	Rsh	VR=10 mV	-	8	-	GΩ
Detectivity	D*	λ=λp	-	5×10^{12}	-	cm · $Hz^{1/2}$/W
Noise equivalent power	NEP	λ=λp	-	2×10^{-15}	-	W/$Hz^{1/2}$

G6854-01 may be damaged by Electro Static Discharge, etc. Be carefull when using G6854-01.

Table 2.8: *Main characteristic of a new possible detector.*

Theoretical situation is clearly visible in the following picture, where LIDAR signal determined with already employed diode laser source and fiber laser source are plotted and compared with Newfocus already tested detector and Hamamatsu recently considered detector. All other elements of the system are the same already used.

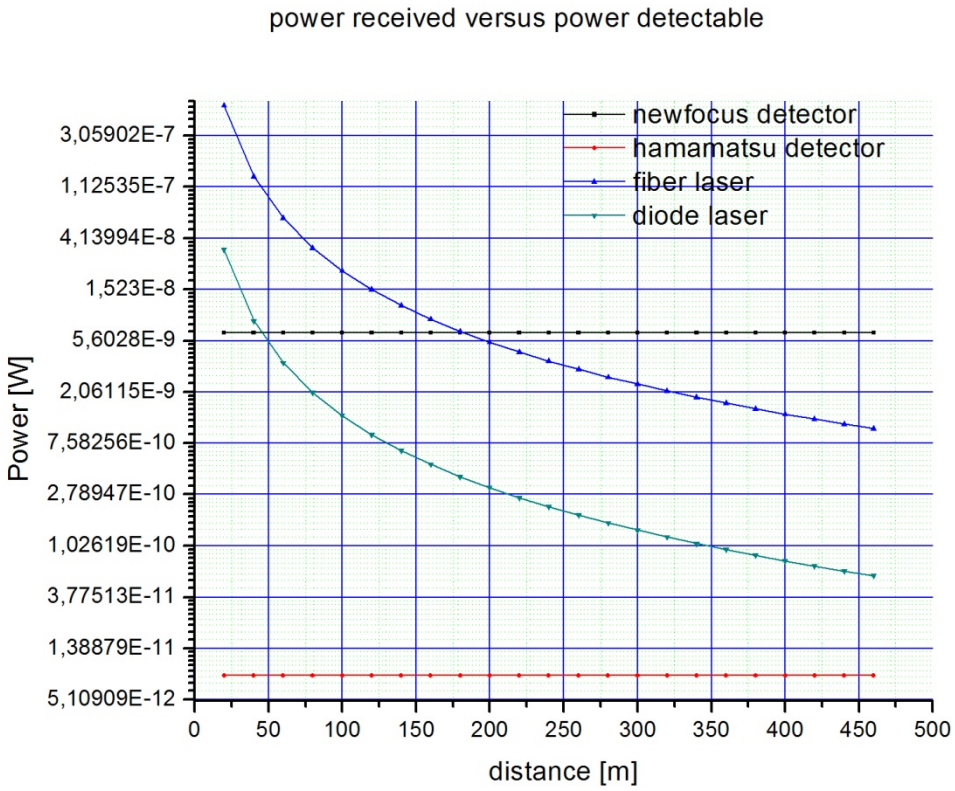

Figure 2.29: *Energy received by detector considering two different sources compared to Minimum Detectable Energy of two different detectors. See text for details.*

The system could reach our goal changing detector or source and reach much higher range changing both. But as previously explained change detector means change system original idea, so the best solution seems changing just the source, even if this means a theoretical result of 160 m range for the LIDAR signal much lower than the one theoretically reachable changing detector.

Some geometric consideration on realized LIDAR are also useful to fully explore this system. The maximum target radius which could be projected inside detector by receiving optics is determined by the following formula[ref. 3, page 258]:

$$R_t = r_{oi} + R\frac{r_s}{f} \qquad \textbf{equation 2.3}$$

Values determined for our system are reported in the next figure. A field of view determined by the angle seen by detector is then calculated starting from this value and it changes in the range from 0.011 to 0.013 Rad due to not negligible receiving optics radius. Each points emits a radiance which determines an image on detector focal plane which is completely or

partially inside detector itself as a function of the distance from optical axis. The border of this area is target radius already explained.

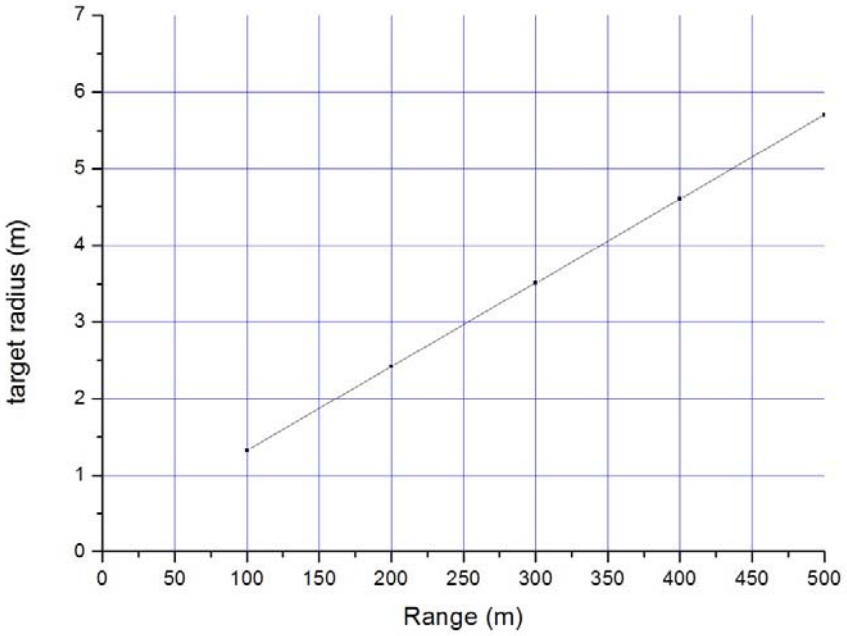

Figure 2.30: *Target radius as a function of range. See text for details.*

Another important variable is the circle of least confusion, which is in some way the best image available. Its distance from optical axis, called displacement, and its radius are provided by the following formulas[ref. 3, page 266]:

$$d_{clc} = \frac{rf}{R} \qquad \textbf{equation 2.4}$$

$$r_{clc} = \frac{r_{oi}}{R} f \qquad \textbf{equation 2.5}$$

The value of these variables at the distance from optical axis which determine geometrical limit of laser beam, fixed to a value of 2 meter, as a function of distance were calculated. A constant value of 4.57 mm is obtained for displacement and the radius value is reported in the following figure. So a value of 5 mm for detector diameter is good also considering experimental problem.

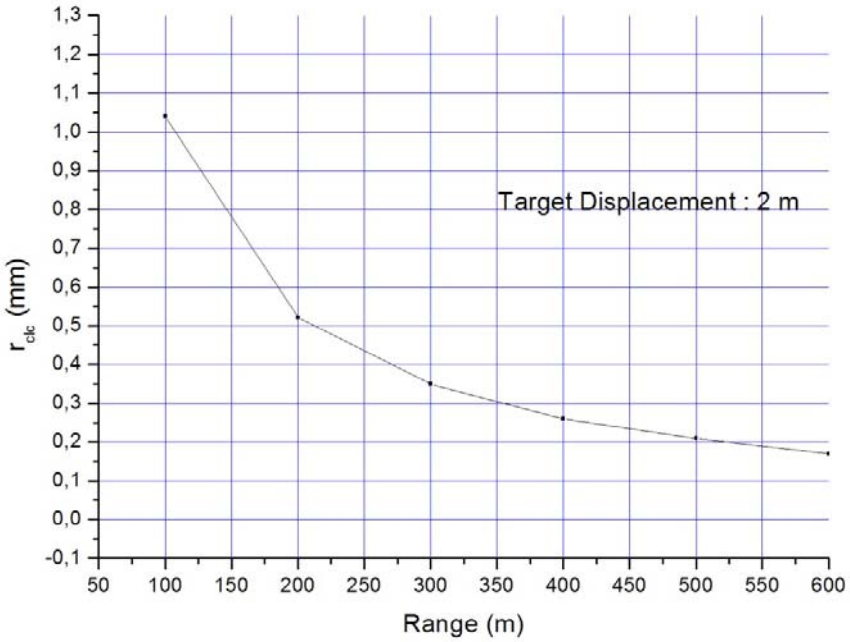

Figure 2.31: *Circle of least confusion radius as a function of range. See text for details.*

Real geometrical limit for our system is then beam divergence, which has to be lower than receiving optics field of view. If a divergence of 10 mRad is considered, a reasonable value optimizing tested system or considering a new source, the beam radius as a function of distance is provided by [ref. 3, page 258]:

$$r_l = (r_{las}^2 + R^2\theta_{las}^2)^{\frac{1}{2}} \qquad \textbf{equation 2.6}$$

Related calculated values are reported in the following figure. Surface hit by laser is always less than surface projected inside detector as prescribed for a working LIDAR. Considering a realistic value for the distance of the receiving and transmitting optical axis, 0.3 m, surface hit by laser radiation is completely inside the detector field of view also for short range. The previous sentence is demonstrated if beam radius and target radius difference are equal:

$$\left|\mathrm{r_{oi}} + \mathrm{R}\frac{\mathrm{r_s}}{\mathrm{f}} - (r_{las}^2 + R^2\theta_{las}^2)^{\frac{1}{2}}\right| = I \qquad \textbf{equation 2.7}$$

The minimum value of range for which this statement holds is 80 m, which is a reasonable value considering our application.

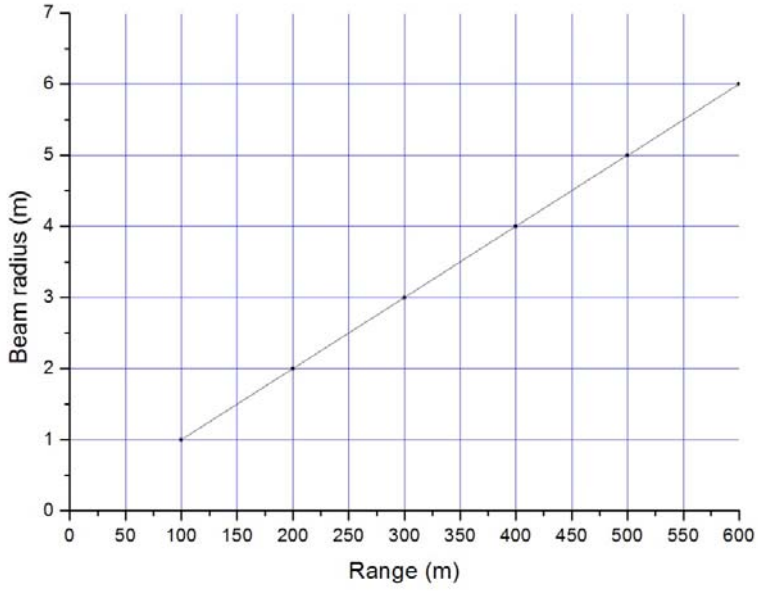

Figure 2.32: *Laser beam radius as a function of range. See text for details.*

Spatial resolution of the system is determined by pulse duration and acquisition time:

$$\Delta R = c\frac{t_l + t_s}{2} \qquad \textbf{equation 2.8}$$

In our case it is about 5 m.

Finally, let us suppose to reach a working system and that it is mounted on a mobile platform so to explore the entire sky. Considering a beam divergence of 10 mRad and lower divergence of 5 mRad on short axis, we need 314 steps to cover elevation from zero to ninety degree. In azimuth we have to consider a variable number from 628 at zero to 1 at ninety. Total points are 12340. Considering that possible laser source is able to work at KHz repetition rate, we could fix 1 ms for each point. Total time consumed by laser is then 125 s. This duration makes us suppose a less than 27 minutes total duration, also because a step motor is needed only in elevation movement. If one rotation is done in 5 s, then in 1 ms an angle of only 1.36 mRad is covered, reasonable error on general system setup. Total time employed is then 1570 s.

2.8 CONCLUSION: PERFORMANCES AND FUTURE DEVELOPMENT

A new idea of a mini Lidar project is described in this chapter. The system was projected and tested but some components were changed during testing. System prototype does not fit expected requirements because photon budget was initially wrong due to a not perfect consideration of the variable "time" in our calculation. Anyway, the experience done could be useful to develop a working system in the future. Many components in fact, could eventually be used also in a new system. In particular we investigated the possible choice of new components and changing the source seems to be the most reliable solution. This will rise cost of few thousand euro, but power will probably be enough to reach the expected goal.

The general task to achieve a low cost lidar will be safe increasing cost of about 30%. Of course only real measures will determine real performances and limits of the new system.

2.9 REFERENCES

[1] Zemax Development Corporation, www.zemax.com

[2] Fresnel lenses, www.fresneltech.com/pdf/FresnelLenses.pdf

[3] Measures R., Laser remote sensing Fundamentals and application, Krieger Publishing Company, Malabar Florida (1992)

MULTIWAVELENGHT DIAL AND MULTIVARIATE STATISTICAL ANALYSIS: THEORETICAL APPROACH AND PRELIMINARY DESIGN OF A POSSIBLE DEVICE

1. INTRODUCTION

We are thinking about a system which is, in some way, an evolution of DIAL. So let's start from Dial[1,2]. The choice of lines could be quite difficult. There is a high probability that the same couple of laser lines are absorbed by interfering substance producing ambiguous identification or false alarm. It is possible to find many of these molecules as environmental contaminants due to their use in civil activities. Many of these substances have little differences in their own absorption coefficients due to the presence of the same functional group. For this reason it is important to find, analyze and choose the best lines where the differences of absorption coefficients can be used for unambiguous identification. Obviously, this work has to be done matching several lines for each substance, but it is not enough.
So an experimental database of absorption coefficients is needed and must be linked to a properly developed identification software. Moreover, fingerprint database must be strictly correlated to the source to be used for Multiwavelenght-Dial technique.
Only one set of measurements is found in literature which refers to the use of CO_2 DIAL technique to measure concentration of highly toxic compounds, but of a different class[3]. Also in this case a fingerprint database was previously organized[4] and they were worried by the possible presence of interfering substances.
In this chapter the principle which leads to the identification software will be explained and its link to database outlined.

2. MULTIVARIATE STATISTICAL ANALYSIS AND NEURAL NETWORK AS A TOOL FOR COMPLEX DATA ANALYSIS

Multivariate statistical analysis is a method which is able to pick up the main characteristics of a complex data set. In this way it is possible to distinguish between different elements of a sample using their own characteristics put inside a vector, so to arrange a matrix that can be normalized and analyzed using a statistical method.
Let's start from some general statements to define pattern recognition and multicomponent analysis:

- *Pattern recognition* (PARC) refers to the *qualitative analysis* of the different compounds present in a certain mixture.
- *Multicomponent analysis* (MCA) refers to the *quantitative determination* of one or *more compounds in a mixt*ure.

Many concepts a*nd methods are used to extr*act information from complex data which are usually analyzed using such complex analytical tools. Usually it is necessary to process data to let mathematical instruments work properly, e.g. correcting drifts subtracting offsets, etc…. Moreover it is generally useful to preprocess data to normalize them. It is also often useful to display data in such a way that it is easily comprehensible the link between different elements of the same group, so as to simplify class organization. These instruments are not particularly useful in our applications because we are not dealing with data coming from different classes of sensors or which have to be correlated with a dedicated method. Our data are quite simple because the sensor is always the same. The real difficulty comes from different response analysis of different substances depending on wavelength and concentration. The analysis method to extrapolate information for identification using a Multiwavelength DIAL will be explained in the following chapter.
Generally, a qualitative or quantitative link between output signals of an instrument and the chemical information are found analyzing experimental data. This usually requires a

comparison of the sensor outputs with previously recorded calibration data. These calibration data consist of measurements in which sensor signals are correlated to concentrations of pure analytes or mixtures of analytes. Calibration function, which should make it possible to analyze unknown samples if present in the calibration database, is generated by this correlation, hopefully with small systematic errors and small standard deviations, concerning corresponding predictions[5]. A survey of the most popular numerical methods is given in Figure 3.1. All model-based and model-free methods used for qualitative and quantitative analyses are described by this scheme. Some approaches, however, do not fit exactly into one of these categories because the huge amount of different concepts cannot be described by a simplified classification and so it is just a first approximation. Measuring data are correlated with analyte during the calibration procedure by all these methods.

• *Model-based:* an exactly defined set of parameters describes this correlation function Physical variables are related to these parameters. A linear correlation between measuring data and concentrations is usually considered even if it is the simplest case. The measured sensor signals, after having explicitly determined the inverse calibration function, are used to calculate the concentrations or, for our purpose, identify unknown samples.

• *Model-free* methods: an implicit representation of this correlation is used in this case without definition of parameters which can be identified as physical variables.

• S*upervised* and *unsupervised* methods: the method of calibration is different. In the first case the sensor signals and the concentration values or substances identified are used for calibration. The calibration information is created by comparing sensor signals and analyte concentrations or name (linear or nonlinear algorithms, iterative adaptation of weights in back-propagation nets). sensor signals only are used for calibration in the second case. Similarities on the sensor signals and other criteria, such as differences, are used during calibration. Therefore, algorithms only qualify or classify the sensor signals. Supervised algorithms can be used for both qualitative and quantitative tasks.

<table>
<tr><td rowspan="5">Unsupervised, hidden correlation, qualitative</td><td colspan="2">model-based</td><td rowspan="5">Supervised, obvious correlation, quantitative</td></tr>
<tr><td>Projection method
Principal Component Analysis</td><td>Linear algebra Principal Component Regression</td></tr>
<tr><td>Qualitative</td><td>Quantitative</td></tr>
<tr><td>Topology conservation
Context conservation
Self Organizing Maps
Adaptive Resonance Theory
Cluster Analysis</td><td>Iterative learning Systems
Back Propagation Neuronal Networks</td></tr>
<tr><td colspan="2">model-free</td></tr>
</table>

Figure 3.1: *Survey on multivariate approaches. A more detailed description of these methods is given in text.*

Let's now have a deep glance over the most important methods.

Principal Component Analysis (PCA):

Multivariate data consisting of *m* sensor responses (variables) contain data which depend on more than one parameter, such as the signals of several sensors for the same composition of analytes or, in our case, the signal of the same sensor detected for different wavelengths emitted from the source. These data usually are not distributed over the entire m-dimensional vector space.

Data are cross correlated so that not all information are equally useful. The useful data space built from *m* signals will therefore always be smaller than the maximum dimension *m*. The aim of principal component analysis (PCA) is an optimum description of a given data set in a dimension smaller than *m.* If at all possible, the reduction should be made down to a two or three-dimensional space and in general dimensional number as small as possible. In this case, direct visualization of similarities and differences become simpler. Each coordinate represents a property (information) which is completely independent of the other properties as represented by the other coordinates, being uncorrelated and orthogonal in this reduced coordinates space. Principle component analysis is therefore a specific kind of orthogonal projection. The calculated orthogonal coordinate system is usually *called features space.*
Determination of eigenvectors and eigenvalues of the matrix of covariance X^TX, which is built from the data matrix X, is the most used possibility for determining such a coordinate system.
Eigenvectors are denoted as principal components (PC) or as factors in the terminology of principal component analysis. The data matrix rank *R* is usually smaller than the maximum rank *(t,m)* because of noise in any analysis of measuring data. Primary components are called the principal components describing the systematic variation in the data. The rest of the principal components represents only noise contribution and are called secondary components. The absolute amount of the singular values is considered a measure of the particular contribution to the systematic variance of the respective principal component. Evidently, the original coordinate system bigger variation is determined by the first principal component direction. The *loading* of a variable *i* with respect to a principal component f is defined as a product of the coordinate of this principal component with respect to the original variable and the corresponding singular value[6] according to

$$\text{Loading}\ (\text{Var}_i, PC_f) = s_f \bullet v_{if} \quad \textbf{equation 3.1}$$

High loadings of a variable for a principal component analysis indicate that the new principal component is strongly influenced by the original variable because the axis as
defined by the principal component is aligned close to the direction of the original coordinate axis. Consequently, a selection of adequate variables from the original array is easy. On the other hand, the variables are not very useful if they exhibit only small loadings for all principal components.
The *score* of an object *r* for a principal component *f* is defined as the coordinate of this object relative to the principal component:

$$\text{score}(\text{ob}_r, \text{PC}_f) = u_{rf} \quad \textbf{equation 3.2}$$

In gas sensorics, for example, the scores describe the position of the gas mixtures in the features space. The plot of scores as a function of a selected number of primary principal components leads to the desired orthogonal projection. This projection may be used for pattern recognition by visualizing clusters. It provides the base for a subsequent cluster analysis (CA). Further descriptions on this topic are available in the literature[7,8,9].

Principal Component Regression (PCR):
Principal component regression (PCR) starts linking the physical information which is looked for, for example analyte concentrations P_{txn} (P_{txn} is the matrix of *n* analyte concentrations present in *t* measurements, p_{rk} denotes the concentration of analyte *k (k* = l, ... *n)* in the rth measurement/object *(r* = l, ... t)) of *t* mixtures consisting of *n* analytes (gases, substances)

and measuring data X_{txm} of m variables (sensor signals) for these mixtures (inverse calibration[10]) according to

$$P_{txn} = X_{txm} b_{mxm} \quad \textbf{equation 3.3}$$

Based on the orthogonal separation of the data matrix, the parameters **b** may be estimated inverting the previous equation using useful concentration for calibration.

$$\tilde{b}_{mxn} = P_{txn} Z^{-1,q}_{mxt} \quad \textbf{equation 3.4}$$

The matrix $Z^{-1,q}_{mxt}$ is denoted the inverse regression matrix of q factors.

A small systematic error is introduced disregarding secondary factors in the calculation of the inverse regression matrix. This is related with a reduced uncertainty in the result *(mean square error* (MSE) criterion).

The primary goal of PCR is the selection of an optimum subset of factors from all the principal components. An often used and robust approach is *cross validation* (CV). In this approach, the data set X and P is separated into a certain number t_{model} of independent combinations of subsets X^K_r , P^K_r (calibration) and X^π_r, P^π_r , (testing) with t^k and t^π data points, respectively. Subsequent to this separation, a Predicted Error Sum of Squares (PRESS) is calculated which is based on a factorial combination adding up all the errors in the calculation of P^π_r in the framework of a model built from X^K_r , P^K_r according to

$$H_{nxn} = \frac{\sum_{r=1}^{t_{model}} \left(P_r^\pi - Z_r^k \tilde{b}_r^k\right)^T \left(P_r^\pi - Z_r^k \tilde{b}_r^k\right)}{t^\pi}; PRESS = \sum_{K=1}^{N} h_{kk} \qquad \textbf{equation 3.5}$$

The numbers h_{kk} denote diagonal elements of the error matrix H of the model. The most robust results are obtained for $t^\pi = 1$ ("leave one out" technique). The optimum number of factors is obtained if the consideration of further factors does not significantly reduce PRESS. For comparison of this method with the multilinear regression method, see ref. 11.

Partial Least Squares (PLS):

Equation 3.4 may also be solved by other orthogonal separations of the data matrix. One approach is the *partial least-squares* (PLS) method according to Equation 5-8, which, for example, was performed by Lanczos bidiagonalization[12]:

$$X_{txm} = O_{txm} L_{mxm} W^T_{mxm} \quad \textbf{equation 3.6}$$

Here, two orthogonal (with respect to the columns) matrices O and W are obtained which are linked by a bidiagonal matrix L. Fundamental differences as compared to the principal component regressions include the following points:

- The PLS factors are not independent of each other.
- The bidiagonalization is calculated by taking into consideration the concentration vector p_k of one component (PLS1) or the concentration matrix P of all components (PLS2). In contrast to PCR, this approach takes into account the concentrations already present in the model building.
- The selection of the optimum subset of PLS factors is significantly simplified compared with the situation in the PCR approach. In the PCR approach, all possible

combinations of multicomponents have to be checked. The PLS factors, on the other hand, are a priori ranked with regard to their contribution to the prediction (MSB criterion) whereas the PCR factors are ordered with respect to their variance content and not with respect to their MSB prediction power. The optimum subset therefore always consists of the first q PLS factors. The validation of the model in this case may also be performed by cross validation.

The limits of both regression methods are given by the prerequisite of a linear correlation between concentrations and measuring data. More sophisticated approaches which consider deviations from this linear behavior already in the model building have been described (see, e.g., the polynomial approach[13] or splines approach[14]).

Nonparameterizing Approaches:

In contrast to the approaches described so far, the nonparameterizing approaches do not require any model and hence do not require any assumptions about statistical distributions and linear correlation between the data. In the framework of these approaches, *artificial neural networks* (ANN) and their fundamentals may be treated. In the following, any analogy with natural neural networks is avoided and, in particular, terms such as neurons and synapses are not used here. The adaptation of these approaches to a specific problem is given by iterative adjustment of weights in a net during the learning process. This adaptation may be done either by comparison of the desired result with the data at the output of the net(supervised learning) or by maximizing differences in the learning data based on an arbitrary criterion of similarity (unsupervised learning).

In the following, two network architectures are chosen as prototypes representing the numerous different approaches described in the literature. *Self-organizing feature maps* with *Kohonen algorithms* form the basis of a method with topology conservation in pattern recognition. They serve as one example of the application of unsupervised learning procedures. As examples of supervised *learning, feed forward nets* (perceptrons) with *back propagation algorithms* according to Rumelhart et al.[15] and Parker[16] are described.

Kohonen's "Self-Organizing Map" (SOM for Unsupervised Competitive Learning):

Topology-conserving nets may be realized according to an architecture as illustrated in figure 3.2. The continuously varying values x_i of the input vectors (the normalized sensor data) are linked with every knot $\xi_{\beta\gamma}$ of the output layer via weights $w_{i\beta\gamma}$. *"Neighbor relations"* occur between different elements of the output because of geometric arrangement of knots in the output layer. Perceptrons, which will be discussed later, have a completely different arrangement. This geometric arrangement to cluster the input data is used by the algorithm of Kohonen according to a similarity criterion. Similar patterns at the input determine elements at the output which are in close vicinity. The information are stored in the position of the respective output unit on the Kohonen map.

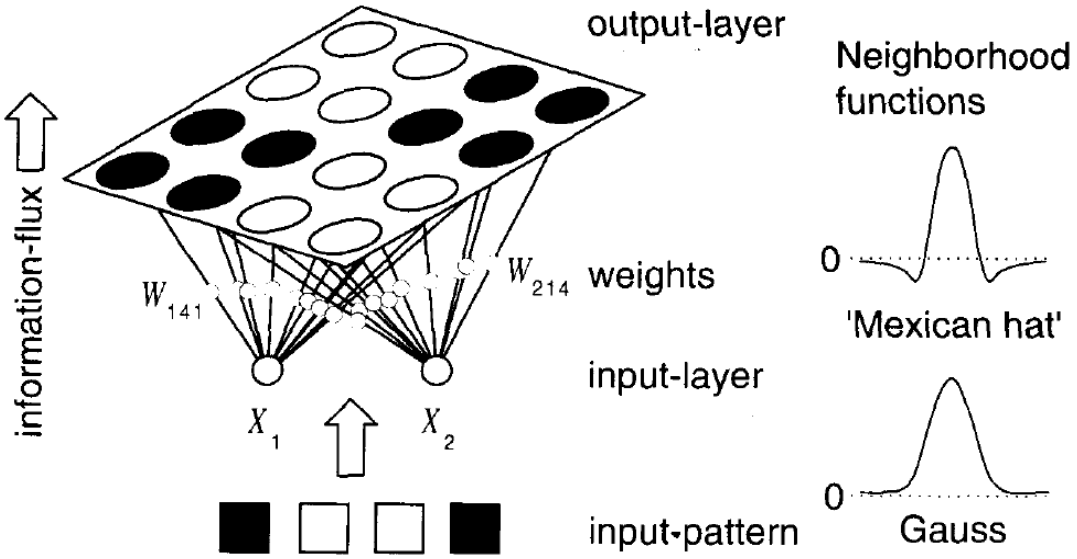

***Figure 3.2**: Schematic view of a topology-conserving Kohonen map. In this special example, four distinct input patterns are grouped in four different regions of the 4x4 map. Two sensor inputs X_1 and X_2 are evaluated.*

Such an arrangement may be realized by competitive learning algorithms[17]. As a starting point, a specific architecture is chosen. The *m* continuous input elements x_1 to x_m are arranged and then projected on to a two-dimensional output space (Kohonen map). This corresponds to a reduction of the dimension of the data space from *m* to 2. The input patterns are given as vectors:

$$x_r = (x_{r1}, x_{r2}, ..., x_{rm}) \qquad \textbf{equation 3.7}$$

which are normalized to the same length (ie, variance 1, "input function"):

$$f_{input}(x') = x = \frac{x'}{|x'|} \qquad \textbf{equation 3.8}$$

The map is described by weight vectors:

$$w_{\beta\gamma} = (w_{1\beta\gamma}, w_{2\beta\gamma}, ..., w_{m\beta\gamma}) \qquad \textbf{equation 3.9}$$

For each element at the output of the map there is just one weight vector. At the beginning of the training all the weights are selected randomly with values $-1 < w_{i\beta\gamma} < +1$ and the resulting vectors are normalized to length 1. As a result, all weight vectors show statistical orientations at constant length. As a next step, the input vectors are chosen in a statistical order and for each input vector x_r the weight vector $w_{\beta\gamma}$ (or the element at a position $\beta\gamma$ on the map) is chosen as the "winner", which is more similar to the input vector following a previously defined algorithm. Kohonen uses the definition of the Euclidean distance $|w_{\beta\gamma} - x_r|$ to characterize similarities (similarity criterion).
For the winner, Equation 3.10 holds:

$$\left|\omega^{+}_{\beta\gamma} - x_r\right| \le \left|\omega_{\delta\varepsilon} - x_r\right| \qquad \forall \ \delta, \varepsilon \ \textbf{equation 3.10}$$

Around the winner output element as the center, the weight vectors of the adjacent output units are thereafter turned into the direction of the input vector by a certain factor. The degree of turning is smaller for output elements which are far away from the winner according to

$$\Delta\omega_{\delta\varepsilon} = \eta\Lambda(\delta\varepsilon, \beta\gamma)[\omega_{\delta\varepsilon} - x_r] \quad \textbf{equation 3.11}$$

The maximum factor of adaptation is given by the *learning rate η.* The radial dependence of the adaptation is defined by the neighboring functions *Λ(δε,βγ).* This function is 1 for $\delta = \beta$ v $\varepsilon = \gamma$ and slopes radially with the distance $|r_{\delta\varepsilon} - r_{\beta\gamma}|$ of the output element *δε* from the winner element with the position *βγ (r* denotes the distance vector on the Kohonen map). The winner element thereby undergoes the maximum change. Elements which are far apart from the winner element at this map are adapted only slightly.
Commonly used neighboring functions include the "bell" function:

$$\Lambda(\delta\varepsilon, \beta\gamma) = \exp\left[\frac{-\left|r_{\delta\varepsilon} - r_{\beta\gamma}\right|^2}{2\sigma^2}\right] \qquad \textbf{equation 3.12}$$

or the "Mexican hat" function:

$$\Lambda(\delta\varepsilon, \beta\gamma) = 2\exp\left[\frac{-\left|r_{\delta\varepsilon} - r_{\beta\gamma}\right|^2}{2\sigma^2}\right] - \exp\left[\frac{-\left|r_{\delta\varepsilon} - r_{\beta\gamma}\right|^2}{4\sigma^2}\right] \qquad \textbf{equation 3.13}$$

The width (ie, the size of the neighboring area) is determined by the parameter *σ.* Differences between the two types of functions refer to the kind of limits which define the size of the different clusters. In the "bell" approach there are smooth transitions whereas the "Mexican hat" approach leads to very sharp boundaries.
This procedure is repeated for all vectors of the learning data set until a given number of learning cycles t_{max} is reached. One learning cycle includes the presentation of all learning vectors once in a statistical order. Usually one begins with a high learning rate η_0 and a broad neighboring function σ_0. The parameters η and σ are then reduced step by step during the learning process. As a result, the net has a chance to reach quickly a certain degree of order in the beginning and a slow convergence at the end. The correlation between both parameters and the number of cycles *t* may be chosen linearly according to

$$\eta(t) = \eta_0\left(1 - \frac{t}{t_{\max}}\right), \qquad \sigma(t) = \sigma_0\left(1 - \frac{t}{t_{\max}}\right) \qquad \textbf{equation 3.14}$$

If the input vectors after finishing the training are given specific meanings (i.e., by a certain classification), it is possible to prove the capability of a map to form clusters. For this procedure, a plot of the distribution of the different classes as a function of the position at the map has to be made. The number of necessary output elements, i.e., the size of the map, may be judged by considering the distribution of learning data on the map. The optimum size of the map is obtained if only a few output sites of the map remain empty without deteriorating the overall result in minimizing the map size.

Multilayer Perceptrons (Supervised Learning):
A simple approach of supervised learning may be realized in a *multilayered feed forward net* according to the *back-propagation* algorithm[18]. The architecture and notation for a two-layered completely linked perceptron are illustrated in Figure 3.3. The following discussion is restricted to this particular case with only one interlayer and one output layer for continuously varied input and output values. The equations may easily be adapted to nets with arbitrarily chosen numbers of interlayers.

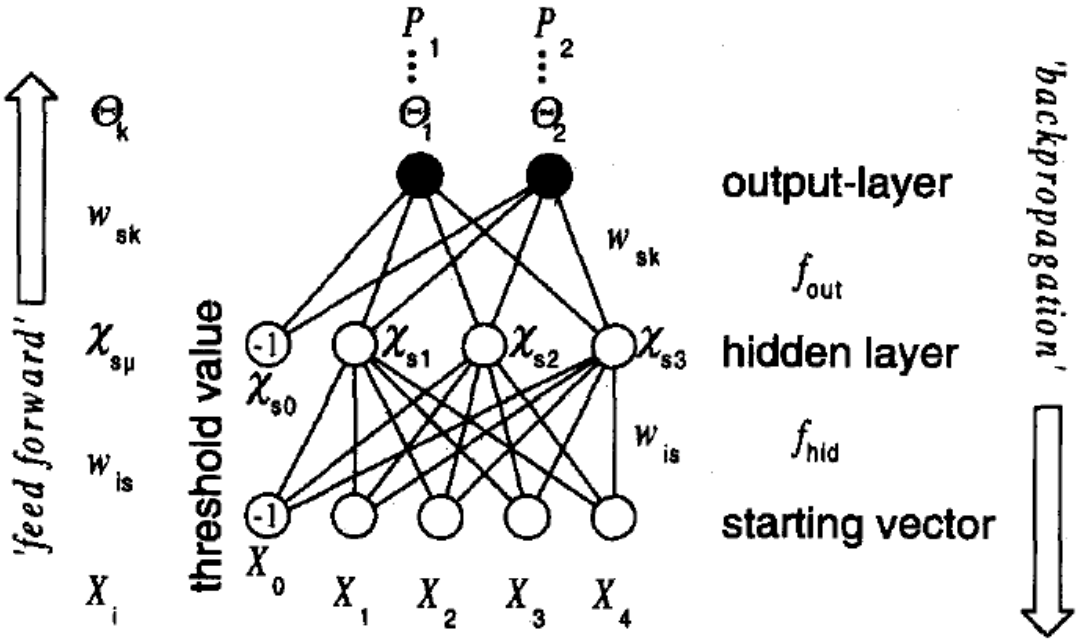

Figure 3.3: *Perceptron architecture and notation of the different knots and weights. The direction of signal processing (feed forward) and network adaptation (back-propagation) are ndicated. This example includes four sensor inputs X_1-X_4 and two analyte concentration outputs P_1 and P_2.*

As for Kohonen maps, the normalized input patterns are arranged as m-dimensional vectors X_r. To construct the net during the training procedure, a corresponding n-dimensional output vector θ_r is required for each input vector. If these input vectors are identified as sensor signals, the output knots may have different meanings which depend on the particular measuring problem. In the spirit of pattern recognition one may, for example, attribute to each knot at the output layer the identification of a certain analyte with values between 0 (i.e., the analyte is not present in the test mixture) and 1 (i.e., the analyte is present). The input values are linked by weights w_{is} with the knots $\chi_{s\mu}$ in the interlayers (hidden layers). The knots in the interlayers are correlated by weights w_{sk} with the output layer. Each knot in the interlayer and output layer is in addition described by a (nonlinear) *transfer function* f_{hid} and f_{out}, respectively, and by a threshold value. Both control the calculation of the output signal from the input value. The transfer function is usually defined prior to the learning phase and remains constant during the learning phase. The threshold value is usually adjusted by an additional link between the knots of the net with a further element in each layer (index 0) with a fixed value of -1. The interlayer does not occur directly and is therefore usually denoted as hidden layer.
The architecture shown here makes it possible to create an output pattern θ_r for each input vector x_r by feed forward calculation. The system transfer functions are adapted to the specific problem. Specific examples include:

• pattern recognition for qualitative analytical problems:

$$f_{hid}(x) = f_{out}(x) = \tanh(\beta x) \quad \text{or} \quad 2/\left(1 + e^{-\beta x}\right) - 1 \qquad \textbf{equation 3.15}$$

• nonlinear regression for quantitative analytical problems:

$$f_{hid}(x) = \tanh(\beta x) \quad \text{or} \quad 2/\left(1 + e^{-\beta x}\right) - 1 \quad ; \; f_{out}(x) = x \qquad \textbf{equation 3.16}$$

• and linear regression:

$$f_{hid}(x) = f_{out}(x) = x \qquad \textbf{equation 3.17}$$

The parameter β influences the slope of the transfer function and hence the degree of nonlinearity of the net. The choice of the different transfer functions is in principle arbitrary. The transfer functions listed above have the advantage that their derivations needed for adapting the net may be calculated in a simple way from the values of the functions themselves according to

$$f_{hid}(x) = tanh(x) \leftrightarrow f'_{hid} = 1 - f^2_{hid}(x)$$

$$f_{hid}(x) = \frac{2}{1 + e^{-x}} - 1 \leftrightarrow f'_{hid} = 2 f_{hid}(x)[1 - f_{hid}(x)] \qquad \textbf{equation 3.18}$$

If in the beginning the weights are statistically chosen in the range between +1 and -1, the output pattern θ' will in the most general case not be correlated with the wanted pattern θ. One possibility of an adaptation of the net to a specific problem consists of an iterative adaptation of the weights $\omega_{\delta\varepsilon}$ during the training, which is determined by the difference $\delta = \theta' - \theta$ between the actual output and the desired output in this specific case *(error back propagation)*. One possibility is an adaptation along the largest gradient

$$E(\omega) = \frac{1}{2}\delta^T \delta \qquad \textbf{equation 3.19}$$

of an area defined by the error function *(cost function)* in the space of the different weights. This approach is known in the literature as the *gradient descent* algorithm. For a further description and list of the different weight adaptation functions $\Delta\omega_{\delta\varepsilon}$, see ref 19.
The calculated adaptation factors have to be interpreted as maximum values. Using these values, a convergence of the net with respect to the desired solution of the problem is not very probable. In practical cases, the adaptation during each iteration is done only by a small fraction of the calculated values (the iteration concerns the presentation of one pair, ie, of an input vector and output pattern). This fraction is determined by the learning rate η as in the case of self-organizing maps. If, in addition, a parameter a is defined which takes into consideration the values $\Delta\omega_{\delta\varepsilon}^{past}$ of past iterations one obtains the real weight adaptation from the equation

$$\Delta\omega_{\delta\varepsilon}^{true} = \eta\Delta\omega_{\delta\varepsilon} + \Delta\omega_{\delta\varepsilon}^{past} \qquad \textbf{equation 3.20}$$

The learning phase is then realized by the presentation of pairs of learning data in random order. One learning cycle includes one presentation of all existing data pairs. Usually, one begins with a relatively small learning rate of 0.01 and a mean moment of 0.5. The learning process may be speeded up significantly by a suitable change of the learning parameter during the training.

Adaptive Resonance Theory (ART):

A good introduction to adaptive resonance theory (ART) is given by Wienke and Buydens[20]. ART-based neural networks were first introduced by Grossberg[21] as a theoretical model of a classification principle in biological brains.

The starting points in ART again are *t* multivariate described samples X (dimension *t* x *m),* each given by measurements taken of *m* different variables. A typical example is a set X of *t* single gas or gas mixture measurements, whereby each x_i, has a length *m (m* variables or sensor signals). Each multivariate measurement x_r is thus a directed vector in the *m* dimensional space[22]. Some of the *t* vectors can be closer to each other in this space, forming groups if they are similar to each other (Figure 3.4). The aim of ART networks is to find groups with similar sample vectors *x* among the *t* vectors, whereby the number of groups *c* is not known a priori. Therefore, ART is a multivariate data-clustering method somehow comparable to SOM. A significant difference from SOM is that ART conserves the original dimension *(m* variables) whereas SOM usually gives clusters in a two-dimensional map.

The clustering process, called *network training,* starts with a random selection of an arbitrary r^{th} sample x_r, out of the entire set of training samples X and copying it into a future "long-term memory (LTM)" of "weights". In the easiest case, this will be simply a new vector *w* (dimension m) representing a raw estimate of a first (new) cluster (Figure 3.4). In other cases, several scaling operators follow this copy step. Anyway, the weights in ART are thus also vectors describing the direction of the clusters in the features space (normally the weight vector w_r is linearly dependent on the original input vector x_r). After the initialization of a new (or first) cluster, another x_j is randomly selected and compared mathematically with all the hitherto existing a clusters, W *(network weights).* During such a comparison, a virtual image x_j* of x_j is generated internally within the network. This virtual image either fits the original image or it deviates significantly from it. Both cases will be discussed later. Simultaneously, x_j* also forms a kind of temporary short-term memory(STM) for x_j. After comparison to all clusters *(weights),* a *winner* among them can be found, providing a virtual image $x_j^{*,winner}$ having the highest similarity (lowest dissimilarity) to x_j. Dissimilarity is expressed in ART as ρ^{calc} via distinct equations. One may think in the simplest version about a Euclidean angle between x_j and each w_i. At this point, classical cluster analysis would stop with further similarity comparison.

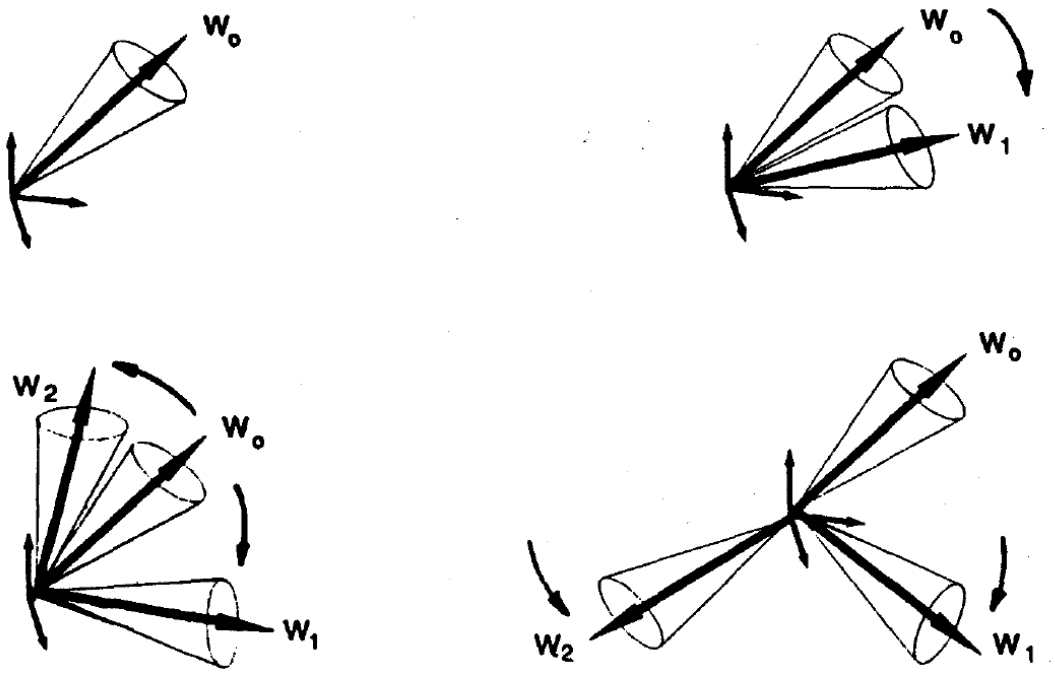

Figure 3.4*: Cluster formation in the features space during training an ART neural network.*

But in ART, the highest similarity between sample x_j, and cluster w^{winner} *is* not the only satisfying criterion for their future fusion. In a second crucial step there is a check to find whether the virtual image $x_j^{*,winner}$ generated by the network is similar enough to the original actual input x_j. Technically, this is achieved by comparing the numerically calculated dissimilarity ρ_{winner}^{calc}, between x_j and w^{winner}, using a constant, defined in advance, called a *vigilance* parameter, ρ^{max}. This ρ^{max} forms a fixed spatial limit around each cluster. Thus, if

$$\rho_{winner}^{calc} \leq \rho^{\max} \quad \textbf{equation 3.21}$$

then $x_j^{*,winner}$, is similar enough to x_j or classically expressed, x_j is located inside the borders of the existing cluster w^{winner}. For simplicity, ρ_{winner}^{calc} and ρ^{max} are always given values 0-1 (achieved by suitable scaling procedures within ART). A value of ρ^{max} close to unity means a high dissimilarity. Even a large difference between w^{winner} and x_j allows classification in the same cluster. High dissimilarity will thus provide few large clusters.
In the reverse case, where ρ^{max} is chosen close to zero (low dissimilarity) a small deviation between w^{winner} and x_j is the reason for opening a new separate cluster. The classification will consequently end up in many small clusters. If Equation 3.21 is fulfilled, one says that the network is in *resonance* with this type of input, or that it already *knows* this phenotype. In the other case, if

$$\rho_{winner}^{calc} > \rho^{\max} \quad \textbf{equation 3.22}$$

the network discovered a *novelty.* Here, $x_j^{*,winner}$ is not close enough to the closest w^{winner}. After the resonance check according to Equations 3.21 and 22, the third crucial step follows, called *adaptation.* If Equation 3.21 is fulfilled, the network changes the weights of the winning cluster by a small step, given by a step width denoted η (the *learning rate),* towards the spatial position of the actual input vector x_j. This step is comparable to the learning step in SOM. The entire calculation formula for adaptation of the weights containing η is called a

learning rule. In practice, η can be chosen between 0 and 1, whereby a value of η close to zero will provide only small changes in the weights. In this way, an ART network stores a weighted part of the present input vector in the LTM, just as any other artificial neural network does. If Equation 3.21 is not satisfied but Equation 3.22 is fulfilled, the network does not adapt its weights but adapts its structure to the discovered novelty. Structure adaptation means simply adding a new cluster to the existing ones. The novelty is immediately stored in the additional weights. This is another Grossberg's unique idea: ART neural networks not only use their weights but also their structure for information storage and for data fitting.
After this step of adaptation, another input vector is randomly selected from training data, and the entire process of *resonance* and *adaptation* is repeated, whereby the former content of the STM is repeatedly overwritten by new virtual inputs, as it happens in the biological brain. Random sampling of t times the training data matrix X is called one *epoch* of training. Simultaneously, the contrast between clusters in the LTM increases *(generalization).* The process converges within a few epochs of training, with the formation of c clusters, whereby the previously chosen constants of learning rate η, and vigilance parameter ρ, determine how many clusters c are formed (Figure 3.4). In other words, by a suitable choice of η and ρ the data cloud X can be approximated by (or resolved to) a number c *of* clusters. In this way, a variation of η and ρ can serve as an active data exploration of X. Like using classical pattern recognition, it also holds for ART that the more compact, point-shaped and well-separated the subclusters are, that are hidden in the t data vectors, the less important is the ART user's choice of η and ρ. In this situation, ART will always find the true number c of hidden clusters. However, the more the data are scattered, or the more they form a continuous hypersurface of equidistant points, the greater is the influence of η and ρ on the clustering result and on the number c.

3. MULTIVARIATE STATISTICAL ANALYSIS OF MULTIWAVELENGHT DIAL SIGNALS

In general, as already said, there is no way to choose the right couple of "on" and "off" lines for DIAL technique from those found in literature. The only chance to choose correctly is to analyze all the IR spectra and absorption coefficients taken with our CO_2 source both of interfering substances and substances used as chemical weapons. Nevertheless, many difficulties could arise if clear identification is a must. The only chance to identify a substance is to use Multiwavelenght-DIAL technique, where many lines of the source have to be checked and a computer can help us to scan database in real time in order to look for the substance compatible with observed absorption coefficients. Even in this case the system could not work well if different substances are mixed in the same area, but this is quite a rare case. A smart software tool, based on the method previously analyzed, which will be presented in its early steps in chapter five, will identify chemical weapons or dangerous substances with great accuracy minimizing the rate of false alarms. There is a patent pending that comprise the described methodology of remote sensing[23].
For our application we need to understand if it is possible to use multivariate statistical analysis, and the other high persomance analysis method described in the previous paragraph, and which tools need to be implemented for this purpouse. First of all we want to distinguish, using the power of retroreflected radiation at different wavelenghts, which is tha substance present in atmosphere. In order to achieve this goal we start from LIDAR equation without taking care of usual DIAL approach. The initial LIDAR equation is:

$$P(\lambda,R) = P_l \frac{A}{R^2} \xi(\lambda) \beta(\lambda,R) \frac{c\tau_l}{2} e^{-\int_0^R k(\lambda,R)dR}$$

equation 3.23

Symbols are explained in the following table:

Symbol	Meaning
P_l	Power emitted from source
A	Surface of receiver
R	Distance from receiver of radiating volume
$\xi(\lambda)$	Receiver spectral transmission factor
$\beta(\lambda,R)$	Backscattering coefficient dependent on atmospheric characteristics
τ_l	Source pulse duration
C	Speed of light
$k(\lambda,R)$	Extinction coefficient of atmosphere

Table 3.1: *variables and constant of LIDAR equation*

Let us now make some consideration that help us finding a proper solution for our task, that is just recognizing substances in atmosphere (if present in the database).

First of all, let the distance R be fixed, for instance where the system, just used as a LIDAR, recognizes something strange. So let us consider just the power retro reflected from that tiny slice of space (in our case the information on space are derived from that in time).

Let moreover suppose that atmospheric extinction coefficient k does not change sensibly with λ, quite common consideration using DIAL technique. This statement is not exactly true in our case because we have to use many lines and some of them could be quite far to apply this approximation. However the changes in spectra obtained are the same for all the substances and this may involve a correction in the database but the method could work the same. The value chosen could be the one measured and found in the literature or the one obtained from the same instrument from a "normal" atmosphere. Another choice could be using a different constant for each wavelength, thus becoming a more realistic method but with more complicated calculus.

Finally let us suppose that, at least during the development of the method, only one substance at a time is present along a path on a single analysis.

Starting from this assumptions LIDAR equations become the product of a constant and few variables. In details, we have:

$$P(\lambda_i) = C_i \beta(\lambda_i) = C_i N \frac{d\sigma(\lambda_i)}{d\Omega} \qquad \textbf{equation 3.24}$$

In this equation we also describe the terms inside backscattering coefficient, where N is concentration and σ is backscattering cross section. Concentration usually depends on distance, but in this case R is a constant. The other part is the differential cross section. The constant C is put with an index meaning that it follows wavelength so to remain in the general case. The constant is reported in the following expression:

$$C(\lambda_i) = P_{\lambda_i} \frac{A}{R^2} \xi(\lambda_i) \frac{c\tau_l}{2} e^{-\int_0^R k(\lambda_i, R)dR}$$ **equation 3.25**

For our purpose the unknown element is the product of concentration and cross section that we achieve from equation 3.24:

$$N \frac{d\sigma(\lambda_i)}{d\Omega} = \frac{P(\lambda_i)}{C_i}$$ **equation 3.26**

Multivariate statistical analysis and the other method for our purpose have to be performed with "pure" fingerprints, that means they do not depend on intensity and rely only on relative values, let us say we do not care about dimensions but we care about shapes, because in some way we are applying a sort of pattern recognition. For this reason we have to normalize each element of the vector whose elements are determined by the previous equation by dividing for the sum of all the elements, so we have the following formula if we use m different wavelength:

$$C_{Norm} = \sum_{i=1}^{m} \frac{P(\lambda_i)}{C_i}$$ **equation 3.27**

In this way the relationship of intensity and concentration is avoided and the meaning of vectors values refers only to relative variations of different components and so we can use the most relevant information for our purpose that is the shape.

One of the steps of the software able to identify a substance is to calculate the coefficients with previous equation just after something strange is found so to be able to perform multivariate statistical analysis.

After a substance in atmosphere is recognized with a good probability (the edge need to be chosen) "classical" DIAL method could be used using "on" and "off" lines chosen during database built up.

The starting point data of multivariate statistical analysis in our case are absorption coefficients normalized as explained in the previous section so to avoid the intensity as the dominant element of analysis. The software used is a toolbox of MATLAB[24]. MATLAB is also used to perform calculations needed before analysis. In details we transpose the matrix so to have different substances along the rows and absorption coefficient for each wavelength along the columns and then normalize each element with the sum along the row.

The method relies also, among several other elements, on the analysis of principal component, so the components of vector space are chosen so to better represent differences inside elements of the database. After the transformation of matrix is usually carried out on analysis of the first few components, that means usually 20% of original number of variables, is enough to have useful piece of information available. A powerful tool of the method is done through figures which represent the position of the substances, symbolized with

numbers, in a diagram with the first and second principal component, and the first and third if necessary. The distances between the point is a qualitative measure of the probability to distinguish the corresponding substances. All the method used will be explained in detail in chapter 5, where they are applied to our real data.

4. PROJECT OF THE SYSTEM AND POSSIBLE CHOICE OF COMPONENTS

It is generally possible to realize a DIAL system, also a Multiwavelenght DIAL, choosing from a wide range of possible sources and detectors. In order to choose our source, which in some way forces all the other components of the system to follow, we use the following criteria:

1. There must be a relevant absorption of interesting compounds on the emitting wavelength.
2. The source must be easily scalable, that means there must be the chance to use different systems, working with the same principle but covering different working range, and so it has to work from relatively low power to huge power.
3. We need as much different wavelength as possible in order to increase the chance of discrimination with our method.
4. It is preferable to have some experience in using that source for a DIAL system so as to increase the chance to achieve the new goal of our system.

For these reasons the choice has fallen naturally on CO_2 laser source. In fact there is quite a big absorption on the wavelengths provided by this class of sources for many of the interesting compounds, as easily confirmed by a quick investigation on IR database, e.g. HITRAN[25]. Moreover in laboratory but also as COTS exists numerous sources with power ranging from mW to MW.

CO_2 laser source tell us nothing more than a full class of sources. Let us now go into details in order to choose the best source for our application. We need to focus on the following elements:

1. Power must be enough to be useful for a DIAL system, that means signal higher than noise even in clear atmosphere up to a distance not lower than one Kilometre.
2. Pulse length must be as short as possible, to increase spatial resolution of the system.
3. It is highly recommended that source divergence is low enough so that all energy retroreflected is picked up by receiving optics, that means source divergence is lower than Field of view. Otherwise a divergence correction through an optical system is needed.
4. Source must be tunable, that means that is possible to choose the wavelength. There must be as many lines as possible, as explained at the beginning of this paragraph. Moreover, the tuning system must be fast so to change wavelength and measure over several ones while atmosphere can be considered “frozen”.
5. Also Pulse Repetition Frequency (PRF) must be high enough to rapidly acquire a statistically considerable number of shots for each wavelength.

6. For our current purpose, dealing with measures over very dangerous compounds, we must consider also physical dimensions so that the system can be used inside a chemical laboratory under a standard fume hood.
7. Last but not least, it is highly preferable to use a COTS source. Our final goal is in fact to built a prototype of the system which could easily become a real and used system and this task is much simpler using already projected subsystem.

Our real experimental set-up, explained in detail in the following chapter, rely on a source which does not match all these requirements because it was initially acquired thinking of a local sensor.

For the real system the best choice found till now on the market which fits with all requirements is Edinburg instruments MTL-3. In the following picture the system and its main characteristics are displayed. It fulfils our requirements because of its dimensions which allow the use under a fume hood, energy is enough for a short range system (about 1 Km), pulse length declared is 100 ns and beam divergence is very low since they declare an M^2 of 1.2 (20% above diffraction limit). Moreover PRF is up to 100 Hz and there is an agile tuning options to quickly change wavelength. Also the price, which could be considered an interesting point looking at real world application, is reasonable, around 70.000 euro.

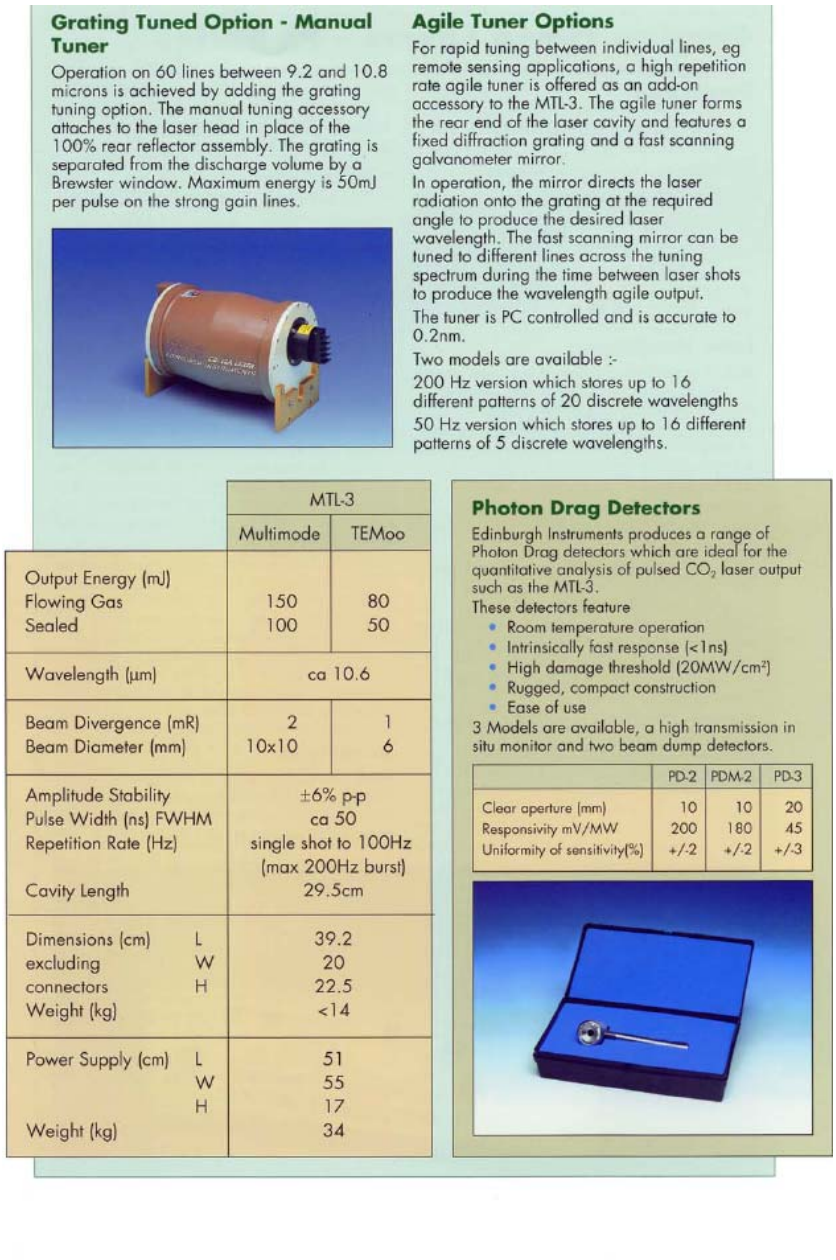

Grating Tuned Option - Manual Tuner

Operation on 60 lines between 9.2 and 10.8 microns is achieved by adding the grating tuning option. The manual tuning accessory attaches to the laser head in place of the 100% rear reflector assembly. The grating is separated from the discharge volume by a Brewster window. Maximum energy is 50mJ per pulse on the strong gain lines.

Agile Tuner Options

For rapid tuning between individual lines, eg remote sensing applications, a high repetition rate agile tuner is offered as an add-on accessory to the MTL-3. The agile tuner forms the rear end of the laser cavity and features a fixed diffraction grating and a fast scanning galvanometer mirror.

In operation, the mirror directs the laser radiation onto the grating at the required angle to produce the desired laser wavelength. The fast scanning mirror can be tuned to different lines across the tuning spectrum during the time between laser shots to produce the wavelength agile output.

The tuner is PC controlled and is accurate to 0.2nm.

Two models are available :-

200 Hz version which stores up to 16 different patterns of 20 discrete wavelengths

50 Hz version which stores up to 16 different patterns of 5 discrete wavelengths.

	MTL-3	
	Multimode	TEMoo
Output Energy (mJ)		
Flowing Gas	150	80
Sealed	100	50
Wavelength (µm)	ca 10.6	
Beam Divergence (mR)	2	1
Beam Diameter (mm)	10x10	6
Amplitude Stability	±6% p-p	
Pulse Width (ns) FWHM	ca 50	
Repetition Rate (Hz)	single shot to 100Hz (max 200Hz burst)	
Cavity Length	29.5cm	
Dimensions (cm) L	39.2	
excluding W	20	
connectors H	22.5	
Weight (kg)	<14	
Power Supply (cm) L	51	
W	55	
H	17	
Weight (kg)	34	

Photon Drag Detectors

Edinburgh Instruments produces a range of Photon Drag detectors which are ideal for the quantitative analysis of pulsed CO_2 laser output such as the MTL-3.

These detectors feature

- Room temperature operation
- Intrinsically fast response (<1ns)
- High damage threshold (20MW/cm²)
- Rugged, compact construction
- Ease of use

3 Models are available, a high transmission in situ monitor and two beam dump detectors.

	PD-2	PDM-2	PD-3
Clear aperture (mm)	10	10	20
Responsivity mV/MW	200	180	45
Uniformity of sensitivity(%)	+/-2	+/-2	+/-3

Figure 3.5: *a page taken from brochure of the chosen laser source.*

The choice of fast sensor which can be used in order to detect radiation from an IR source emitting in the band of a CO_2 laser is very simple because, unless we decide to produce a new one, there is only one company which manufactures a sensor able to be used for a DIAL in term of speed and sensitivity. This company is Kolmar technologies and the chosen sensor, KV104 has a Detectivity of $D^*=3x10^{10}$ Jones, a conversion factor of 4 Amp/Watt and an acquisition band of 100 MHz, thus useful for pulse length higher than 10 ns. It is cooled using a Dewar system cooled with liquid nitrogen, but we are thinking to change the cooling system using an electric one already developed for nuclear sensors applications. The following picture is part of a brochure, taken from internet, of the chosen sensor. The price, considering the technology, is really affordable, around 4000 USD.

KOLMAR TECHNOLOGIES

Series KV104: HgCdTe Photodiodes

Series Configurations

Model*	Wavelength (µm) Peak	Cutoff	Size (mm)	Bandwidth (Hz)	D*(60FOV) (Jones,typ)	Responsivity (Amps/Watt)
KV104-1-A-3/11	10.5	>11.5	1 x 1	>20M	3E10	>4
KV104-1-A-3/12	11	>12.3	1 x 1	>20M	3E10	>4
KV104-1-A-3/10	9	>10	1 x 1	>20M	5E10	>4
KV104-0.5-A-3/11	10.5	>11.5	0.5 x 0.5	>50M	3E10	>4
KV104-0.25-A-1/11	10.5	>11.5	0.25x0.25	>100M	3E10	>4
KV104-0.1-1-E/11	10.5	>11.5	0.1 x 0.1	>500M	3E10	>4
KV104-0.5-A-2/8	7.2	>8	0.5 x 0.5	>30M	7E10	>3
KV104-1-A-7/11/TS	10.5	>11.5	1 x 1	>20M	3E10	>4
KV104-1-A-5/11/TS	10.5	>11.5	1 x 1	>20M	3E10	>4

*Key: model-size-package-window/wavelength/options

Options

Various cryogenic packages
- hold times up to 24 hours

Temperature sensor
Windows
ZnSe
ZnSe wedge
Ge

Coatings
10.6 µm
2 µm –13 µm
Cold-filters
Cold stops
- 60°, 45° ,30°

Pixel sizes 2.0 mm to 0.05 mm
Matched amplifiers available

Custom Configurations on Request

Standard Dewar Configuration

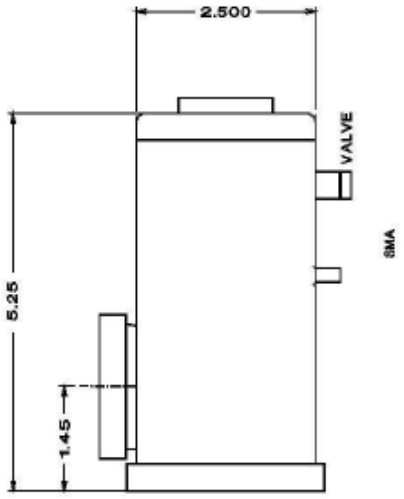

Figure 3.6: *A part of the brochure concerning the chosen sensor.*

The cooling system that could be arranged for our application is made by ORTEC. Its main characteristic and a picture are found in the following figure.
The system demonstrator will probably work looking in a certain direction, so there will be no need to project particular mechanics even if care must be taken to organize a good system to align transmitting and receiving optics or, better, to choose the wanted angle of intersection. Transmitting optics is provided by source manufacturer, but it is not the same for receiving optics which will be properly projected using commercial lenses or mirrors. Among other needed subsystem there will be the unit to give electrical power to source and detector and other devices, the electronic related to source and to change wavelength in particular, and a computer to control all the system, acquire and store data.

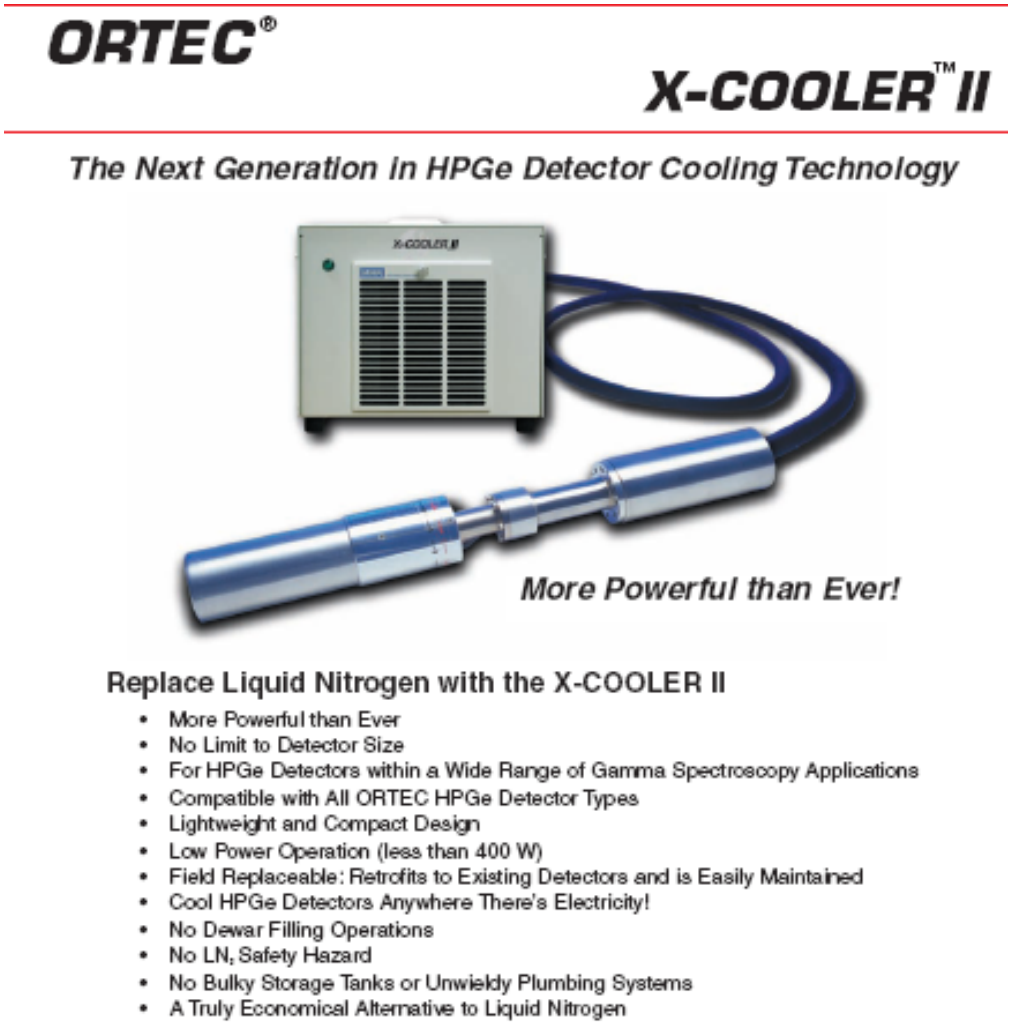

***Figure* 1.7:** *picture and main characteristic of cooling system taken from internet.*

5. FINGERPRINT DATABASE AS A FUNDAMENTAL PART OF THE TOOL AND OTHER USEFUL DATABASE

The Hardware is important, of course, but what really makes a system new is the knowledge that is under its use. In this case the real big improvement of our device is the use of a database and the properly designed software for identification. Thus the fingerprint database is the fundamental part of the tool. Database are difficult to make because it is not possible just to extrapolate information on absorption coefficient using already existing IR spectroscopy database. In fact there is a strong correlation of the source with absorption coefficient due mainly to difference in line bandwidth. Moreover many of these database are made in liquid phase to meet other needs, but there is a big difference in a spectrum acquired in liquid phase or gas phase, apart from conversion difficulties.

Only one paper is found in literature[26] which refers to a database useful to recognize organophosphorus compounds, an useful class because used in pesticides, petroleum additives and solvents, but it was done to be used in a traditional IR spectrometer and just a core of knowledge based system was presented.

A different but also important database is made taking care of different extinction coefficients. These data may be calculated by well known software FASCODE[27]. Extinction coefficient or transmittance are not constant. Their values depend on wavelength, weather

condition, elevation of optical axis of receiving optics, temperature, pressure and many other parameters. Just to have a starting point, optical depth, radiance and transmittance were calculated considering an horizontal firing (so to avoid any calculation due to temperature or pressure change with altitude) and “medium” rural condition on western countries. All typical CO_2 laser source were considered in our “first approach” database. The software is so detailed that for each wavelength introduced there is a fine structure analysis of atmosphere such that for each laser lines there are tens of values, the exact number depending on laser line bandwidth and generally different line to line even for the same source. The number used for concentration calculation or for system performance evaluation is then determined with a weighted means around the peak value of the laser line.

Real use of this numbers is quite straightforward because it must be considered how difficult could be to use the “right” number not in a scientific background, were many other instruments and skilled people determine the final results, but in an automatically working device or generally when the device has to work as a rough instruments handed by poorly skilled personnel. Nevertheless, a database which can give a rough idea of the number expected based on few and simple information (weather condition, region and altitude of employment, temperature and pressure near the device, elevation given by the system itself) could be useful to reduce the expected error in concentration calculation.

The best thing to do is of course to automatically determine the useful numbers, if there is a fast enough calculator at your disposal. On the other case it is possible to use already calculated numbers and the system just choose the right one for the actual situation.

An example of already calculated transmittance and radiance results (this last of course useful for signal to noise evaluation) is given in the following table with the same format as calculated by FASCODE. FASCODE can give a medium value calculated over a bandwidth if requested. This could be useful in our case to give directly one value for each laser emitting wavelength instead of calculate separately a weighted one.

Wavelength **(cm^{-1})**	Wavelength **(μm)**	**Radiance**	**Transmittance**
1081.53999999	9.2460750412	7.06576747689e-006	0.0748308375478
1081.56159999	9.24589038671	7.03402020008e-006	0.0789451524615
1081.58319999	9.24570573959	7.00336568116e-006	0.0829167440534
1081.60479999	9.24552109985	6.97458699506e-006	0.0866429954767
1081.62639999	9.24533646748	6.9502129918e-006	0.0897928252816
1081.64799999	9.24515184249	6.93112633599e-006	0.0922504961491
1081.66959999	9.24496722486	6.91793320584e-006	0.0939363762736
1081.69119998	9.24478261462	6.90759225108e-006	0.0952489152551
1081.71279998	9.24459801174	6.90056413077e-006	0.0961277037859
1081.73439998	9.24441341624	6.89677744958e-006	0.0965818241239
1081.75599998	9.24422882811	6.89552234689e-006	0.0967044755816
1081.77759998	9.24404424735	6.89706212142e-006	0.0964610129595
1081.79919998	9.24385967396	6.89974058332e-006	0.0960682034492
1081.82079998	9.24367510794	6.8991516855e-006	0.0961035713553
1081.84239998	9.2434905493	6.89200487614e-006	0.0969981998205
1081.86399997	9.24330599802	6.88143381922e-006	0.0983414202929
1081.88559997	9.24312145411	6.87092096996e-006	0.0996772944927
1081.90719997	9.24293691757	6.86275370754e-006	0.100705884397
1081.92879997	9.2427523884	6.85705117576e-006	0.10141145438
1081.95039997	9.24256786659	6.85460190653e-006	0.101691104472
1081.97199997	9.24238335216	6.855335414e-006	0.101553454995
1081.99359997	9.24219884509	6.8579024628e-006	0.101175434887
1082.01519996	9.24201434539	6.86168823449e-006	0.100637666881
1082.03679996	9.24182985305	6.8672825364e-006	0.0998627394438
1082.05839996	9.24164536808	6.87623105478e-006	0.098648019135
1082.07999996	9.24146089047	6.88888439981e-006	0.0969476550817
1082.10159996	9.24127642023	6.90727802066e-006	0.0944945067167
1082.12319996	9.24109195735	6.93111951477e-006	0.0913270115852
1082.14479996	9.24090750184	6.96428242009e-006	0.08693703264
1082.16639996	9.24072305369	7.00598138792e-006	0.0814275071025
1082.18799995	9.2405386129	7.06460014044e-006	0.0736989229918
1082.20959995	9.24035417948	7.13534245733e-006	0.0643800422549
1082.23119995	9.24016975342	7.21986816643e-006	0.0532527603209
1082.25279995	9.23998533472	7.31418731448e-006	0.0408402271569
1082.27439995	9.23980092338	7.38438393455e-006	0.0315899439156
1082.29599995	9.2396165194	7.4135664363e-006	0.0277179256082
1082.31759995	9.23943212278	7.388555332e-006	0.0309531781822

Table 3.2: *Radiance and transmittance and calculated by FASCODE (see text for details).*

6. CONCLUSION: PERFORMANCE EXPECTED AND POSSIBLE PROBLEM

The real limits of the system depends of course on the real discrimination ability of proposed setup. Real tests of the system could be made only with "on field" experimental activity using a real case of study. The system is strongly dependent also on the tool set up; power of the source depends also on wavelength but wavelength's number is important to build an accurate discrimination tool. Each compound has its own spectrum which will be used to identify the compound itself; of course if some wavelength absorb very low, starting from some range there could be identification problem due to the signal comparable to the detector noise.

In order to have a rough idea on performance expected, we can use the well known method to calculate a DIAL system performance. Let us use absorption coefficients calculated for the choice "on" and "off" lines using the data taken for our database described in the next chapter.

The system ability of detection is determined by two different factors, one affecting long range measurements, the other affecting short range ones. All details can be found in ref 28. In general, a signal must be compared to the sensor noise to determine if it is possible to have a good measure or not. This is done calculating the power retroreflected by target compounds at the two wavelengths ("on" and "off") and achieved by our sensor. The difference must be greater than noise and in general must be detectable. The signal retroreflected depends of course on absorption coefficients, which may be considered fixed, and concentration, which is not.

Concentration is, in general, calculated using DIAL equation:

$$n(R)=\frac{1}{2\sigma}\left[\frac{d}{dr}\left\{\ln\left(\frac{P(\lambda_w,R)}{P(\lambda_0,R)}\right)\right\}-\left\{\ln\left(\frac{\beta(\lambda_w,R)}{\beta(\lambda_0,R)}\right)\right\}\right]+k(\lambda_w,R)-k(\lambda_0,R) \qquad \textbf{equation 3.28}$$

Where:

σ is the cross section difference between on and off lines.

P is the power, in this case retroreflected from R considering on line, "*w"* indices, and off lines, "0" indices.

β is reflectivity of target with same indices as power.

k is the total attenuation coefficient, given by $k=\underline{k}(\lambda,R)+N(R)\sigma(\lambda)$, where $\underline{k}$ is attenuation coefficient without the absorption contribution from the molecular species of interest, same indices again.

R is the range.

Minimum detectable concentration is not determined by the previous formula but from the minimum detectable change in power received dealing to on and off lines, identified by P and P' in the following calculus. Let's start again from LIDAR, equation 3.23, rewriting it so to empathize contribution of compound present in atmosphere:

$$P=\frac{P_0\xi A\rho}{\pi R^2}e^{-2\int(\sigma N+\beta)dR} \qquad \textbf{equation 3.29}$$

Where ρ is used for target reflectivity.

Appling it both to on and off lines, denoting with ‘ each formula element which refers to off line, we have:

$$\Delta P = P' - P = \frac{\xi \beta A P_0 e^{-2\beta' R}}{R^2}\left[1 - e^{-2\sigma N R}\right] \qquad \textbf{equation 3.30}$$

Where σ' and $\beta-\beta'$ have been assumed to be negligible.

After few manipulation, considering the case that the noise is the limiting factor and assuming that $exp(-2\sigma N_{min}R) \approx 1-2\sigma N_{min}R$, the following equation is found for the minimum detectable concentration:

$$n_{\min} = \frac{\mathrm{NEP} \cdot \pi \cdot \mathrm{R}}{2 \cdot \xi \cdot \rho \cdot \mathrm{A} \cdot \mathrm{P}_0 \cdot \Delta\sigma \cdot \exp\left(-2\alpha R\right)} \qquad \textbf{equation 3.31}$$

Where:

NEP is the Noise Equivalent Power, for our sensor calculated dividing the active area by the Detectivity.

ξ, the efficiency, is set to a general value of 0.9.

ρ is set to the value of 0.01.

A is set to a reasonable value of 0.1 m^2.

P_0 is set to the value of $5*10^5$ W, as calculated from single pulse energy.

$\Delta\sigma$ is the difference of absorption coefficients of “on” and “off” lines.

α is extinction coefficient for these wavelengths calculated by FASCODE, in this case set to the value of 0.5228 atm^{-1} cm^{-1}.

On short range the limit is instead determined by the minimal fractional change in the lidar return that can be measured accurately.

In this case, after some manipulation, we finally found the following formula:

$$n_{\min} = \frac{5 \cdot 10^3 \cdot \left(\Delta \mathrm{P_r} / \mathrm{P_r}\right)}{\Delta\sigma \cdot R} \qquad \textbf{equation 3.32}$$

Where:

$\Delta P_r/P_r$ is the fractional change of power received, which is set to the value of 0.01.

Let us now consider a practical case taken from our database. Tetrachloroethene for example has a difference of 14 cm^{-1} atm^{-1} from the strongest line, with a wavelength of 10.159 μm, and the next one, with a wavelength of 10.170 μm. Putting the data previously explained in the formulas above, the following graph is obtained where both concentration limit curves corresponding to long and short range formulas are displayed.

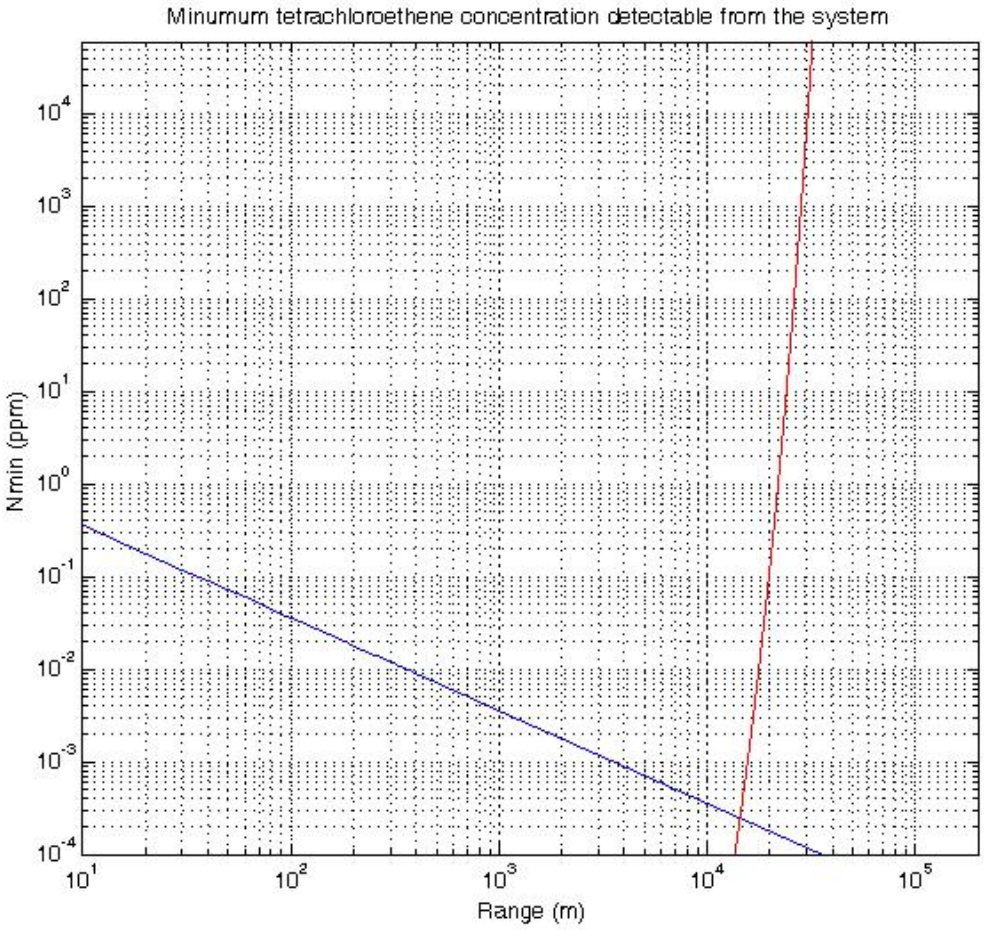

Figure 3.8: *Minimum concentration detectable from the system for Tetrachloroethene, where blue line is determined through equation 3.32 whereas red one through equation 3.31 (see text for details).*

Real performance for our method, which is really different from DIAL, not clearly measurable and not even predictable theoretically, are unknown. Only real tests, as already said, will show real performance. The final number is expected to be a probability of identification. After identification concentration measures is possible and performance on this point can be calculated as in the previous example.
Real difficulties, apart from the method development itself, could arise from the relatively slow scan of the atmosphere. In fact even supposing to be able to fire at 100 Hz, so to acquire on a single wavelength in less than one second, at least five seconds must be considered to change wavelength, acquire and store data. With 6 seconds on each wavelength, we need five minutes to cover fifty wavelengths, which is not enough to consider a frozen atmosphere in many cases.
It must be underlined that our method performances are much greater than any other remote sensing method realized since know. This point was already explained in chapter one while explaining passive remote systems.

7. REFERENCES

[1] C. Bellecci, G. Caputi, F. De Donato, P. Gaudio, M. Valentini, CO_2 Dial for monitoring atmospheric pollutants at the University of Calabria, Il Nuovo Cimento, **18**, 5, 463-472 (1995).

[2] C. Bellecci, P. Aversa, G. Benedetti Michelangeli, G. Caputi, F. De Donato, P. Gaudio, M. Valentini and R. Zoccali, Improvement of Calabria University CO_2 laser DIAL system, Proceeding SPIE, **3104**, 154-157 (1997).

[3] D.K. Killinger and N. Meniuk, Remote probing of the atmosphere using a CO_2 DIAL System, IEEE Journal of quantum electronics, Vol. QE-17, n° 9 september 1981.

[4] G.L. Loper, A.R. Calloway, M.A. Stamps and J.A. Gelbwachs, Carbon dioxide laser absorption spectra and low ppb photoacoustic detection of Hydrazine fuels, Applied Optics, Vol. 19, 2726 (1980).

[5] Cammann, K., *Sens. Actuators B* 24-25 (1995) 769-772.

[6] Massart, D. L., Vandeginste, B. G. M., Deming, S. N., Michotte, Y., Kaufman, L., *Data Handling in Science and Technology 2: Chemometrics: a Textbook;* Amsterdam: Eisevier, 1988.

[7]Malinowski, E. R., Howery, D. G., *Factor Analysis in Chemistry;* New York: Wiley, 1980.

[8] Rasmussen, G. T., Isenhour, T. L., Lowry, S. R., Ritter, G. L., *Anal. Chim. Acta* 103 (1978) 213-221.

[9] Wold, S., Esbensen, K., Geladi, P., *Intell. Lab. Syst. 2* (1987) 37

[10] Marbach, R., Heise, H. M., *Chemometr. Intell. Lab. Syst.* 9 (1990) 45-63.

[11] Carey, W. P., Beebe, K. R., Sanchez, E., Geladi, P., Kowalski, B. R., *Sens. Actuators B* 9 (1986) 223-234.

[12] Golub, G. H., van Loan, C. F., *Matrix Computations;* Baltimore: John Hopkins University Press, 1983.

[13] Wold, S., Kettaneh-Wold, N., Skagerberg, B., *Chemometr. Intell. Lab. Syst. 7* (1989) 53-65.

[14] Wold, S., Kettaneh-Wold, N., *Chemometr. Intell. Lab. Syst.* 14 (1992) 71-84.

[15] Rumelhart, D. E., McClelland, J. L., *Parallel Distributed Processing: Explorations in the Microstructure of Cognition, Vol. 1: Learning Internal Representations by Error Propagation;* Cambridge, MA: MIT Press.

[16] Parker, D. B., in: *IEEE First International Conference on Neural Networks (San Diego),* Caudill, M., Butler, C. (eds.), New York: IEEE, 1987, Vol. II, pp. 593-600.

[17] Kohonen, T., *Self-Organization and Associative Memory,* 3rd edn.; Springer: Berlin, 1989.

[18] Hertz, J., Krogh, A., Palmer, R. G., *Introduction to the Theory of Neural Computation, Lecture Notes,Vol. 1;* New York: Addison-Wesley, 1991.

[19] Hertz, J., Krogh, A., Palmer, R. G., *Introduction to the Theory of Neural Computation, Lecture Notes, Vol. 1;* New York: Addison-Wesley, 1991.

[20] Wienke, D., Buydens, L., *Trends Anal. Chem.* 14 (1995) 398-406.

[21] Grossberg, S., Bio/. *Cybernet.* 23 (1976) 121-134 and 187-203.

[22] Weimar, U., Schierbaum, K. D., Göpel, W., *Sens. Actuators B 2* (1990) 71-78.

[23] Italian Patent request n° RM2010A000211 dated 03/05/2010 "Metodo di analisi di gas in atmosfera mediante una tecnica di tipo DIAL"

[24] www.mathworks.it/products/matlab

[25] www.cfa.harward.edu/hitran

[26] Zhahyang M. and Yuanjun M., An expert system Knowledge Base for the analysis of Infrared Spectra of organophosphorus compounds, Microchemical Journal 53, 371-375 (1996)

[27] H. J. P. Smith et al., Fast Atmospheric Signature Code (Spectral Transmittance and Radiance), Air Force Geophysics Laboratory Technical Report AFGL-TR-78-0081, Hanscom AFB, MA (1978)

[28] D. K. Killinger and N. Menyuk, Remote probing of the atmosphere using a CO_2 DIAL system, IEEE, Vol. QE-17, NO 9, 1917-1929 (1981)

EXPERIMENTAL SET UP, DATA ACQUIRED AND CALCULUS FOR THE FINGERPRINT DATABASE

1. DESIGN AND DEVELOPMENT OF EXPERIMENTAL SETUP

The experimental set up is made with the following components:

- A cell, to be filled with investigated molecules. Two ZnSe windows close the cell and let radiation cross the cell itself.
- A CO_2 laser source.
- A controller to change laser lines automatically.
- A function generator to lead laser gas discharge, e.g. control laser Pulse Repetition Frequency (PRF) and pulse length.
- Two piroelectric detectors.
- Two signal analyzer (one for each detector).
- A vacuum pump.
- A pressure measurement device.
- A mirror in order to send the beam in the proper direction.
- A beam splitter, to split the beam in two parts, one sent inside cell and the other directly to a sensor in order to normalize measures.
- A computer where data are collected and stored.

A scheme of the system is shown in the following picture.

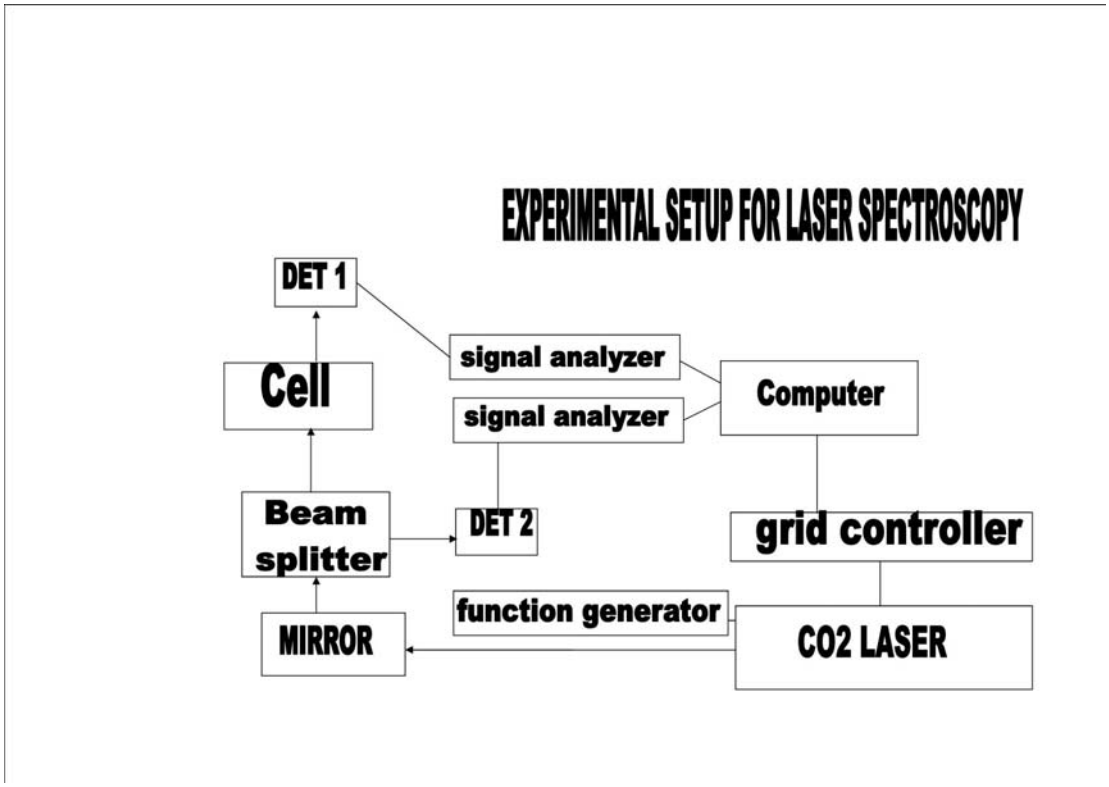

Figure 4.1: *Sketch of experimental set up used to measure absorption in cell.*

Preliminary measurements were carried out using a 3 m long cell and a big source. These measurements were compared to many measurements made using a traditional IR spectrometer with substances in liquid phase. The need of a different set up as well as of a powerful recognition method quickly arose[1].

Measurements have been carried out making use of a 0.3 m long cell, so to be used under a fume hood to avoid dispersion of substances, with a diameter of 0.045 m. This cell was filled with a known amount of investigated substance, using all precautions for safety compliance.

A different cell, based on a system of mirrors so to have a variable optical path from 1 m to 30 m has been projected, but still not realized, to increase system performance allowing measurement of low absorption or low vapour pressure substances. This cell project will be presented in chapter 5.

The source was chosen so to fit the following constraints:

- A small source is needed to carry on our measures under a fume hood, for safety compliance;
- A cheap dial system must be based on "COTS" components, in order to develop something to be commercialized in the future;

Detectors are two equal energy meters made by GENTEC, model QE12LP-H-MB, with a responsivity of 10 V/J and a Noise equivalent energy 0f 0.7 μJ.

This sensors could be connected directly to a PC using an analyzer named SOLO-X. For this reason we do not use oscilloscope. The system is controlled through a labview program so to automatically change laser lines and acquire some data.

The main characteristics of source are summarized in the following table.

Transmitter	
Active medium	CO_2
Emission type	Pulsed
Spectral range	9.2-10.8 μm
Pulse repetition rate (used 1 Hz)	1 – 15 KHz
Beam divergence	5 mRad
Beam waist diameter	3 mm
Pulse duration	200 μs
Pulse energy	1 mJ

Table 4.1: *Characteristics of source.*

The source was fully characterized through a series of measures in order to understand power performance for each wavelength. The values obtained were compared to those given by the manufacturer. In theory eighty-one wavelengths were possible, but only sixty-two were considered strong enough to be used. Among these, some are instable in power resulting in reliable data not for all measures. The following picture shows the power value versus wavelength. A blue value refers to manufacturer given value, red value refers to direct measures made by sensor proprietary system and black value refers to labview analyzed data. The differences in measured value are probably due to some "zeroes" which are not considered as zeroes by proprietary software because of noise and put inside calculation, thus providing lower value than real value. The difference of labview data from manufacturer is not explained, but, since general behavior is the same and we are going to work with energy ratios, it is not really important to understand this particular difference.

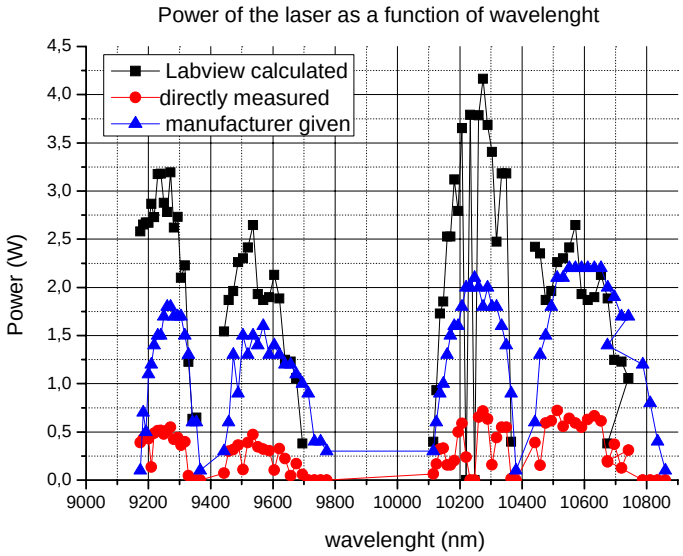

Figure 4.2: *Laser source power as declared by manufacturer and measured with our sensor.*

Also the pulse duration and shape, referred to time, were analyzed using a very fast photoconductive type VIGO sensor, namely model PCI 10.6. Duration measured is very similar to the one provided by the manufacturer, as it is clearly visible from the following picture.

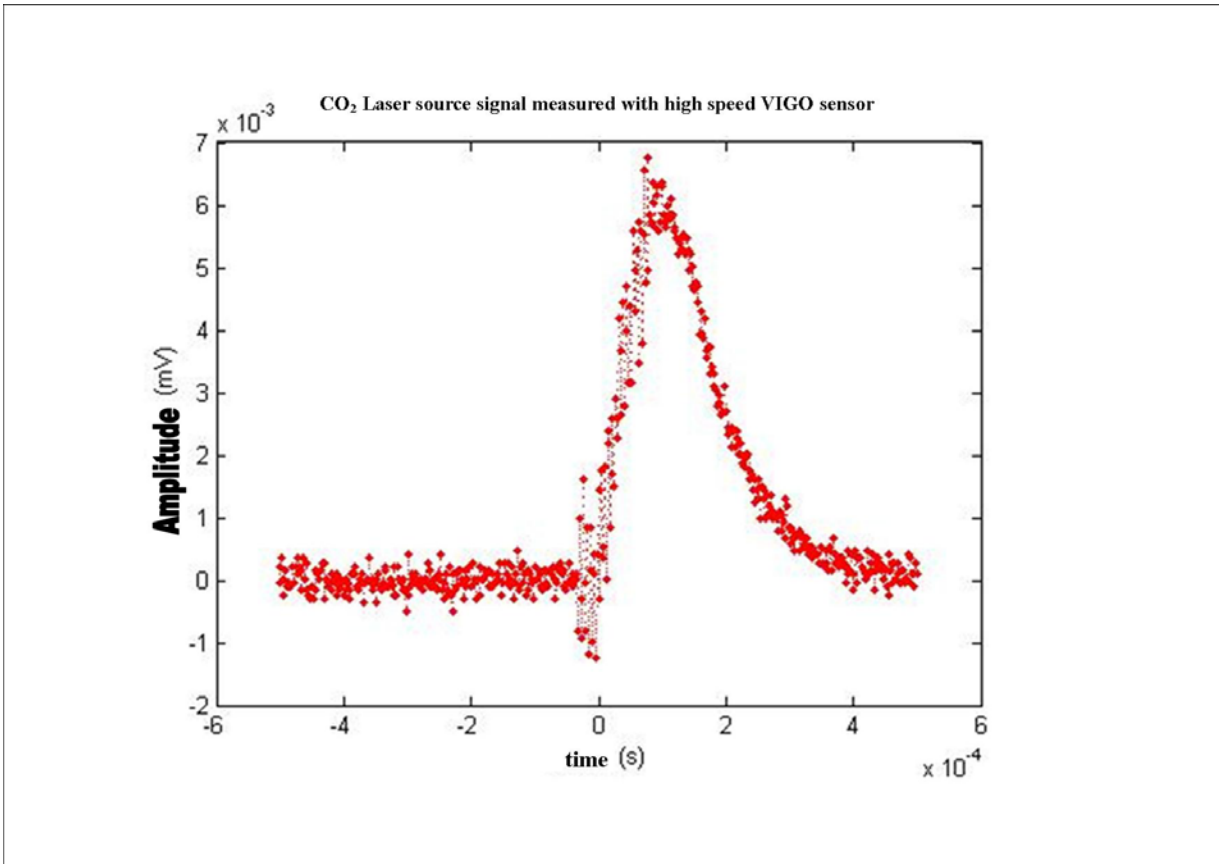

Figure 4.3: *Laser source pulse shape as measured with a VIGO high speed sensor.*

Measurements were fully automatized using a labview[2] program which allows to change laser lines, acquire and store data, change measurements settings, show measurements in real time and have full control of the system. The main program front panel is shown in the following picture.

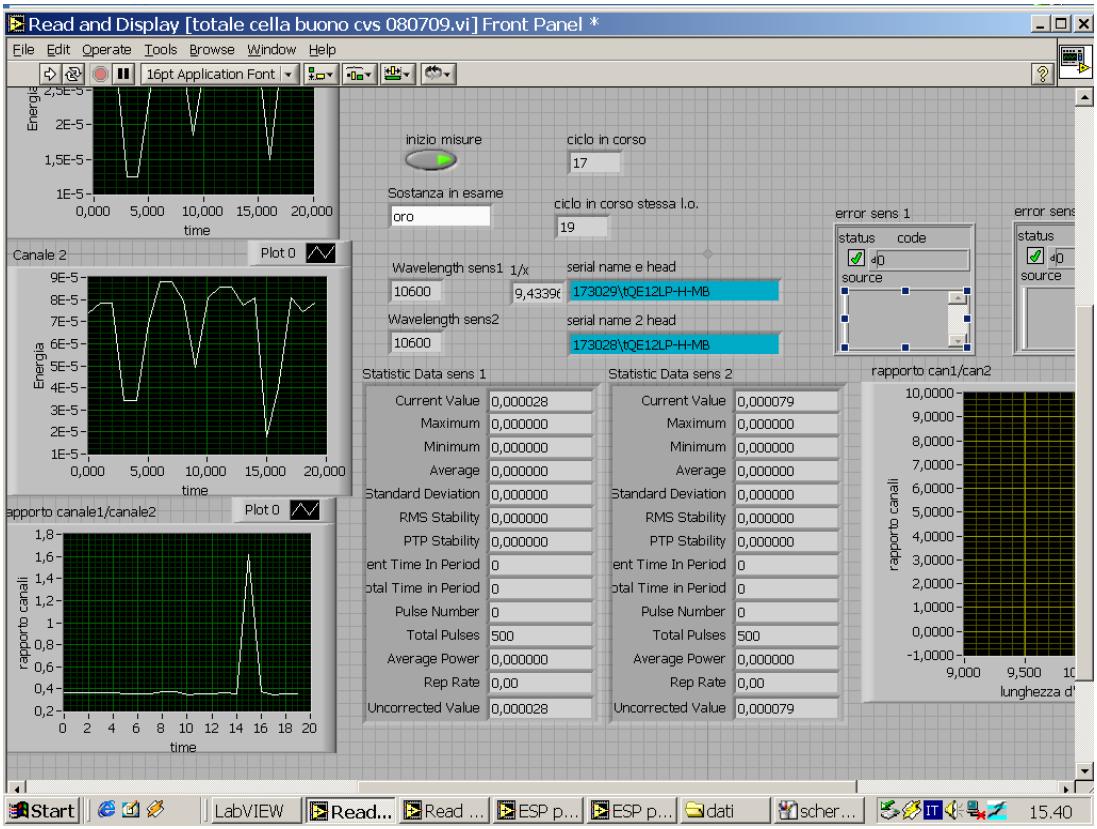

Figure 4.4: *front panel of labview program to automatize measures.*

The program is organized so that the system, namely all devices used for measurements, operates the following instructions:

1. switching on controller;
2. moving laser to the next line (the first if measure is already started) using the file with controller position corresponding to chosen wavelenght;
3. switching off controller;
4. starting sensors acquiring and send it useful data (wavelenght for calibration, taken from wavelenght database file);
5. acquiring data and store it twenty times (changeable if desired), that means stop signal with the frequency of 1 Hz so to follow laser emitting time and save values (laser emission wavelenght, cycle number, energy, time) to a given file;
6. calculating medium value and error;
7. calculating the number of "good" measures taking care if one sensor or both are failing so to calculate properly statistical value;
8. showing sensors energy value;
9. showing sensor state, that means working or in error state and in this case error message;
10. showing sensor energy and sensor ratio graphic value at the end of measure for each laser lines (number of cycle on x axes, value on y axes).

The main program relies also on subprograms. One was devoted to control sensor and the other to control position controller. Both were taken from manufacturer but modified to be adapted to our purpouse. Front panels of both are shown in the following pictures.

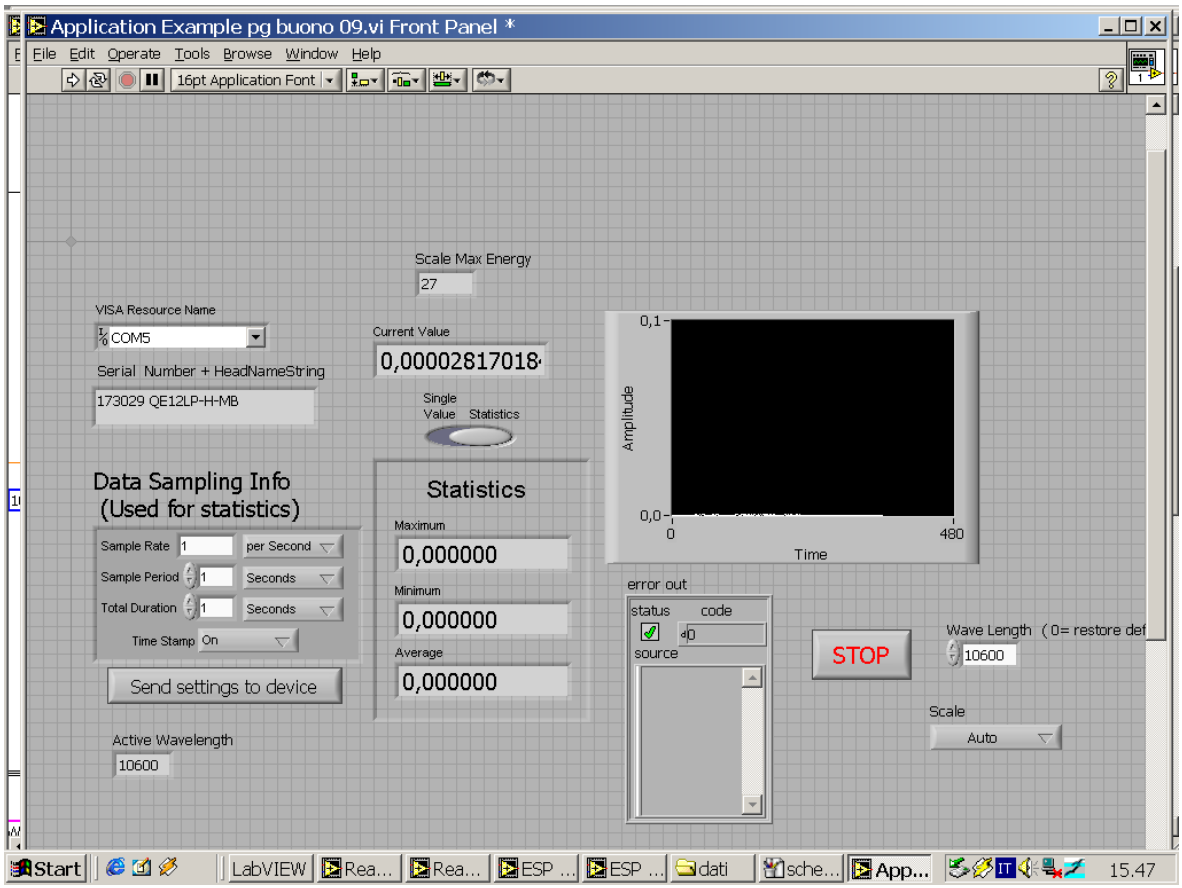

Figure 4.5: *Front panel of sensor driver and controller.*

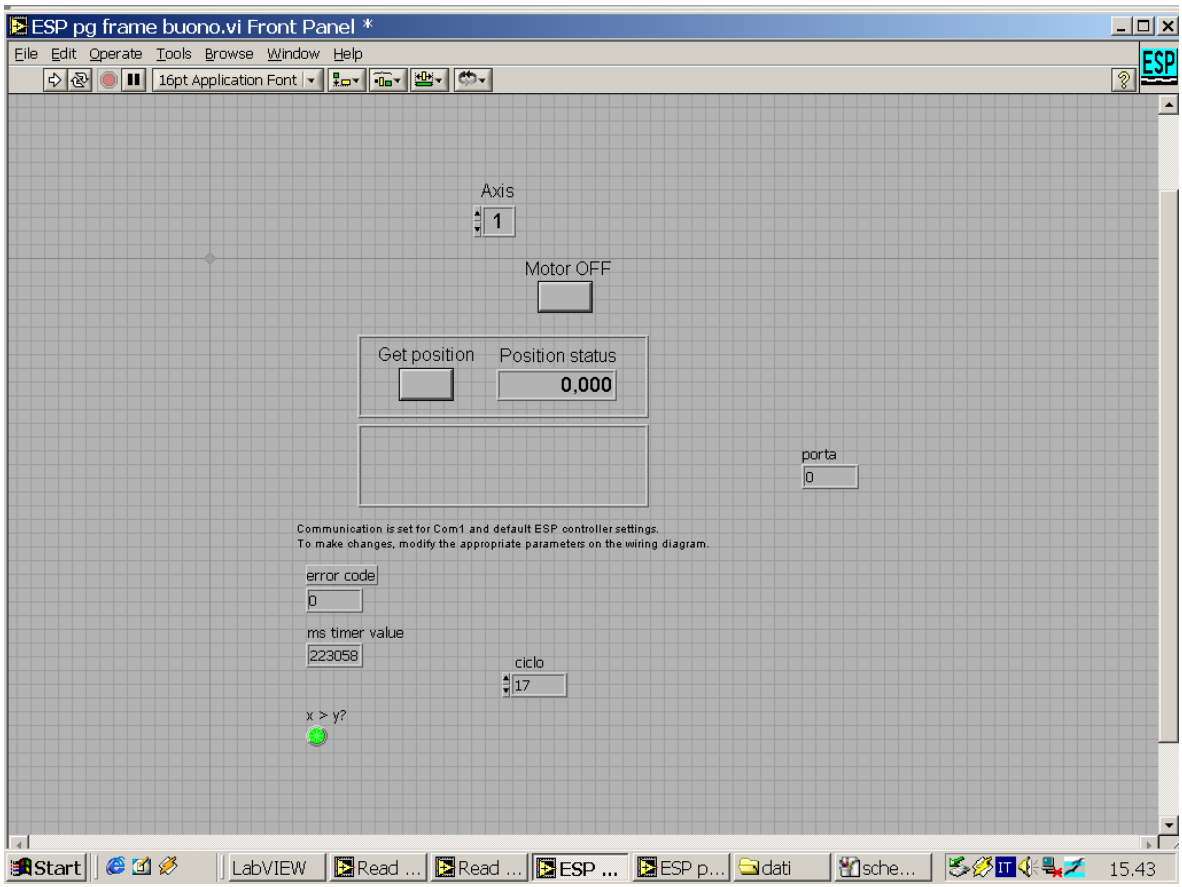

Figure 4.6: *Front panel of grid controller.*

2. BUILT UP, TEST OF EXPERIMENTAL SET UP AND SOFTWARE ANALYSIS TO REDUCE ERROR

Many affords had to be done in order to avoid great standard deviation in the channels measurements. In fact, as is known, laser source energy is not stable and so Standard Deviation on energy measurement over several shot is high. For this reason we decided to shot with only one Hz frequency and made channel ratio shot by shot. Since it was impossible with our slow sensor to have a properly chosen trigger, we needed to filter data during analysis so to avoid ratio of different shots. For each wavelength a set of twenty measurements were performed. then the ratio of two channels was calculated. Ratios were compared to the median of their set, which resulted to be a reliable data (few other corrections performed). If data is comparable to median, which means it is ten percent inside the value, it is used to perform all calculus (media, standard deviation); otherwise data are recalculated comparing to data taken in the previous or following second, e.g. data of sensor one taken during i-cycle is compared to data taken from sensor two in cycles i+1 and i-1. If one of these data are again comparable to median, this value is considered for the calculus, otherwise it is rejected. All these calculation were made using a properly programmed software using MATlab[3] programming language. The program is devoted also to calculate absorption coefficients and related error with the method described later.
A flow or hot air was organized to increase cell temperature. The cell was put in a box of insulating material and the hot air flow was sent to the bottom of the box. Two different sensors are used to check temperature, one as a reference to switch on and off air flow and measure air temperature, the other is a thermocouple which measures cell temperature. This last was used as reference temperature for the gas inside the cell. Maximum temperature is 60 °C and usually oscillation around the chosen value are 1°C.

A critical point in this kind of measure is safety. Compound used for chemical weapons and some used in civil activity must be handled with care. Mustard is critical also because really corrosive. For this reason measurements were made with special attention; All substances employed for measurements were put inside the cell with safety procedure of the chemical laboratory. In this case measurements were performed indoor under a fume hood, after that specialized personnel put mustard inside the cell and the area was under strict control. The following pictures show experimental area, cell and the cell during clearing.

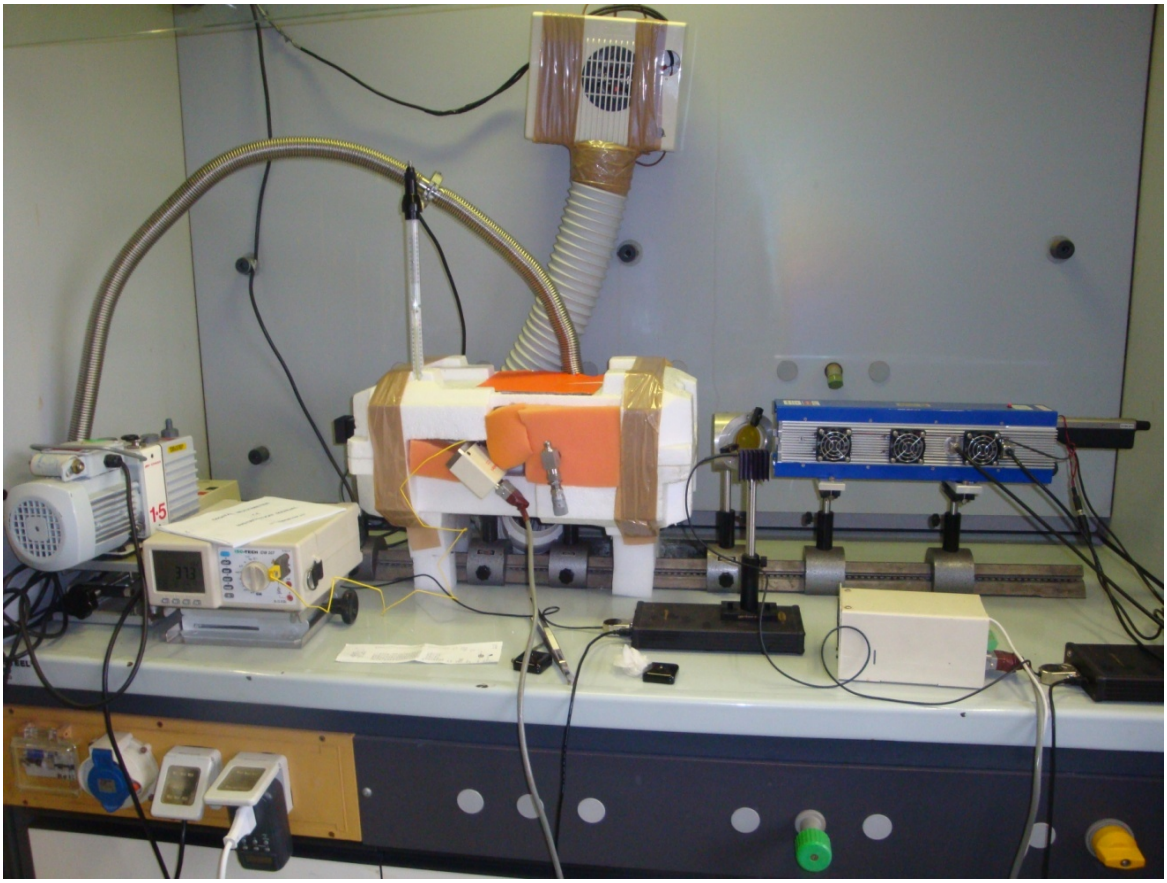

Figure 4.7: *Picture taken inside laboratory in Civitavecchia during measurements.*

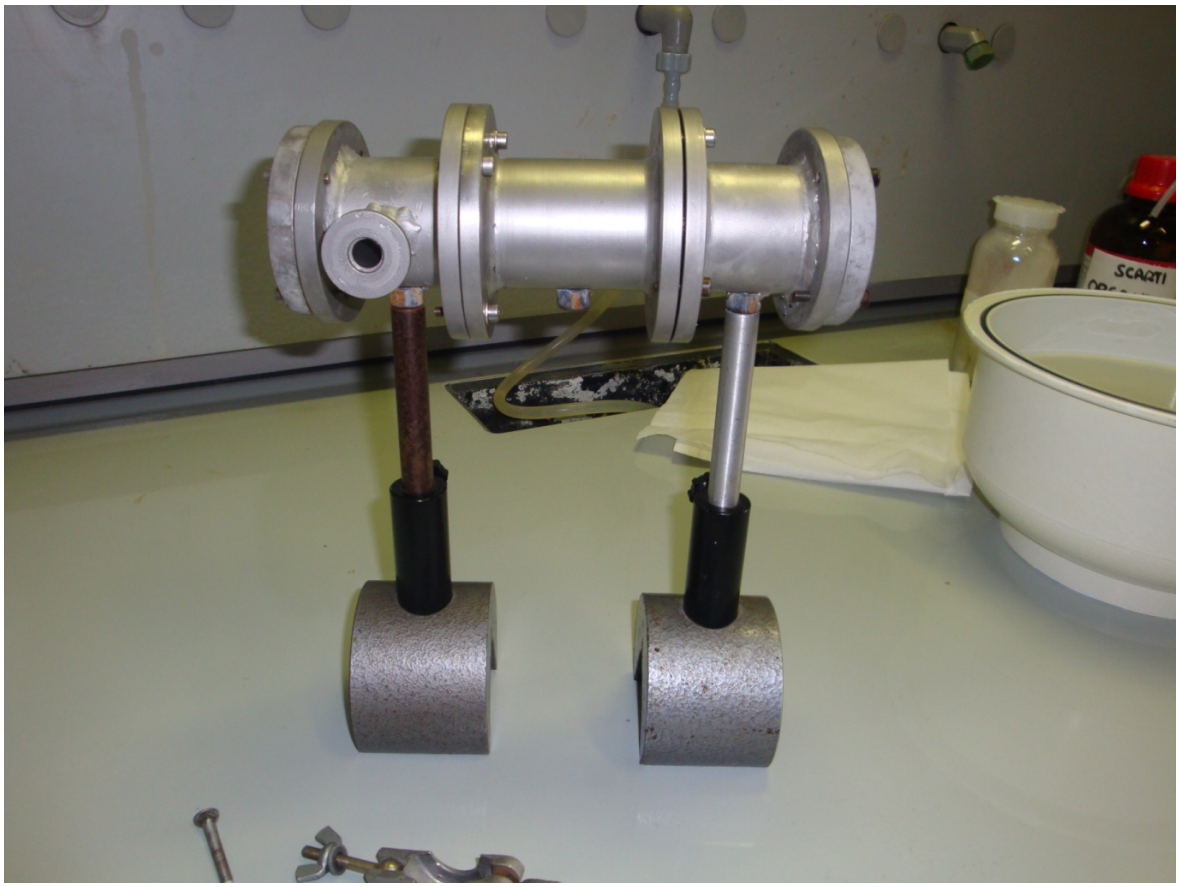

Figure 4.8: *Details of the cell inside laboratory. Damage due to chemical agent are clearly visible.*

Figure 4.9: *Picture taken during clearing of the system.*

3. CHOICE OF SUBSTANCE TO ANALYZE, ANALYSIS METHOD AND DATA REJECTION

The choice of the substance to analyze with our system was determined principally considering two conditions:

1. Vapor pressure high enough so that there is quite a real chance to find it in atmosphere and so to allow absorption calculation in gas phase. This limit value was chosen in 10^{-2} mm Hg.
2. Absorption in the IR spectral range not negligible. This was verified before by mean of IR spectrum made in liquid phase with spectrometer. Sometimes real measures were made and data rejection was made after. Sometimes also a library of already done IR measures was consulted.

These conditions depend also on the experimental set up. A different system, using a powerful laser and a longer path length may let some of the excluded substance be included, being sure to have some chance to measure it in the atmosphere. Considerations on the upgrade needed to increase system performance will be made in chapter 5.

Until now, thirty two compounds were analyzed. Ten compounds are dangerous molecules which could be considered chemical weapons or toxic industrial compounds, the others are volatile organic compounds (VOC). We start our database choosing compounds which are quite widespread in human activity and have a good absorption in IR band. This last condition was verified also for the first class of compounds, so that only if volatility and IR absorption were high enough they were considered for the database.

Measures made with IR spectrometer in liquid phase were compared with measures made within the cell to have a quick reference to a different system. Moreover, these data could be useful to understand, quickly and cheaply, which substance could really be a source of interference and which not. Last but not least, these data could be useful also for the database itself because IR spectroscopy could be used, designing a dedicated equipment, in order to quickly recognize chemical substances in the area of deployment. Some commercial devices are already available, as the one described in chapter 1, paragraph 2.2.4.2., and several researches[4,5] are studying this last possibility which will be investigated in chapter 6. In the following picture the spectrum obtained for mustard is displayed[6]. The peak at 1037 cm^{-1} is inside the band of our laser source output.

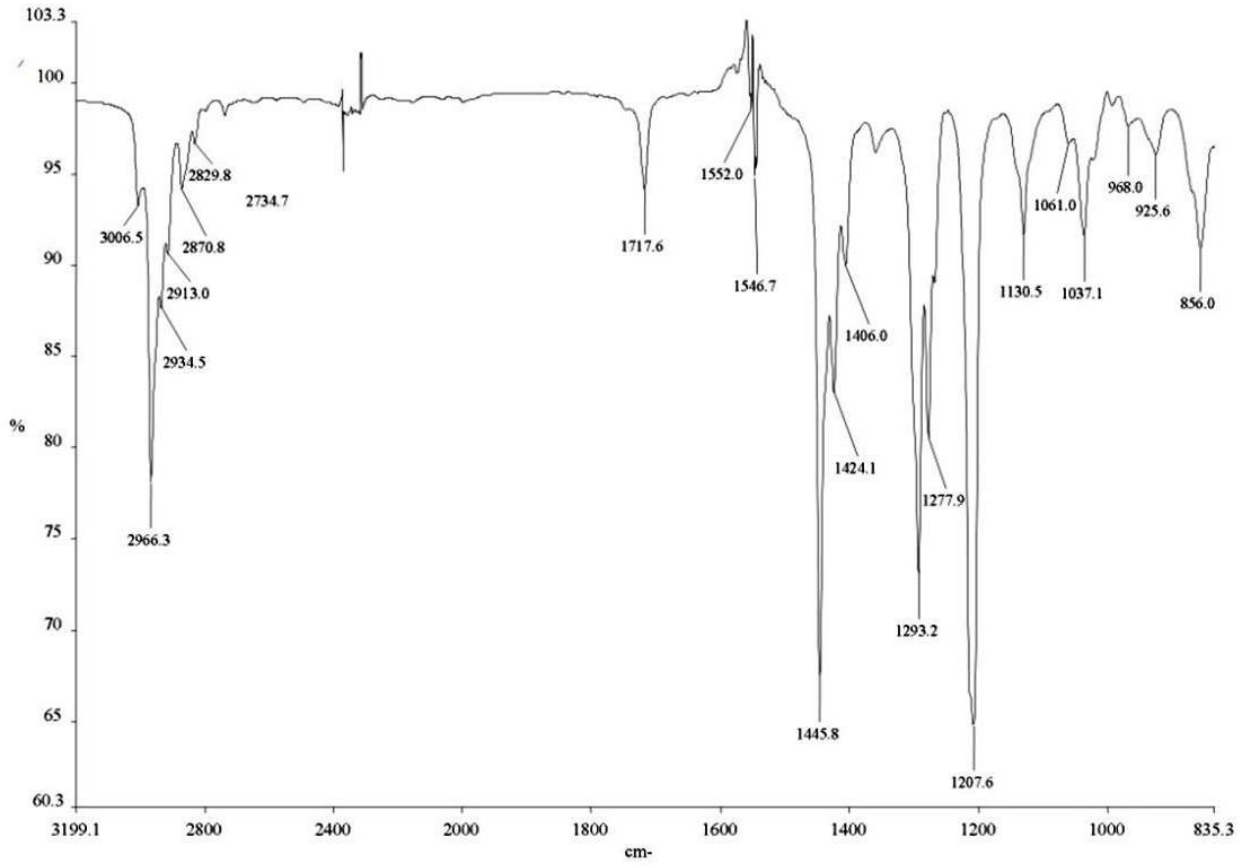

Figure 4.10: Experimental transmission spectrum of mustard from 835 to 3199 cm^{-1}.

All the compounds analyzed till now are listed in the following table containing also their main physical properties. They are all dangerous molecules or interferents, as explained in the first chapter.

No data was really rejected even if some data are really poor and their use in discrimination method does not give any satisfying results. Many of the chemical weapons investigated, due to their low vapour pressure, do not give really good data as it is clearly visible from the picture later in this chapter. Nevertheless the multivariate statistical analysis seems to perform good discrimination for some of them, as explained in the following chapter.

Finally, many substances were not analyzed according to this criteria and none was really rejected. Only Coumaphos, a pesticide, gave such a bad result in terms of repeatability and error to force us into rejecting performed measures at all.

Compound	density	Molecular Weight	Vapor Pressure (mm Hg)	Boiling Point (°C)	Compound classification
CH3CN (acetonitrile)	0,7830	41,0500	72,80	81,60	VOC
CH2Cl2 (dichlorometane)	1,3255	84,9300	6.83psi (20°C) 336.25 (20 °C) 24.45 psi (55°C)	39,75	VOC
Ethilbenzene	0,8660	106,1700	10 (20 °C) 19 (37.7 °C)	136,25	VOC
N-eptane	0,6840	100,2000	40 (20 °C) 83 (37.7°C)	98,40	VOC
N-esane	0,6600	86,1800	5.2 psi (37.7°C) 256 (37.7°C) 132 (20°C)	69,00	VOC
N-nonane	0,7180	128,2600	0.18 (psi) (37,7°C) 8.86	151,00	VOC
N-ottane	0,7028	114,2300	11 (20°C)	125,60	VOC
Undecane	0,7400	156,3100	<0,4 (20°C)	196,00	VOC
Clorobenzene	1,1070	112,5600	11,8 (25 °C)	131,50	VOC
Cicloesano	0,7781	84,1600	77 (20°C) 168.8 (37.7°C)	80,70	VOC
Toluene	0,8660	92,1400	22 (20°C) 26 (25°C)	110,60	VOC
111-tricloroetano	1,3376	133,4000		74,10	VOC
Acetone	0,7910	58,0800	184 (20°C)		VOC
Benzene	0,8800	78,1100	74.6 (20°C) 166 (37.7°C)	80,10	VOC
Methanolo (CH3OH)	0,7900	32,0400	97.68 (20°C) 410 (50°C)	64,96	VOC
Chloroformio (CHCl3)	1,4760	119,3800	160 (20°C)	61,50	VOC
Ndecane	0,7300	142,1500	1 (16.5°C) 3.77 (37.7°C)	174,00	VOC
Npentane	0,6260	72,1510		36,10	VOC
Tetrachloroetilene	1,6200	165,8300	13 (20°C) 19 (25°C)	121,00	VOC
Trimethilbenzene	0,8940	120,2000	3.4 (37,7°C)	175,50	VOC
Xilene	0,8700	106,1700	9 (20°C)	138,00	VOC
Dibromomethane	2,4770	173,8300	34.9 (20°C)	97,00	VOC
2-Butanone	0,8050	72,1080	71 (20°C)	80,00	VOC
4-methil-2pentanolo (isopropilmethilcarbinolo)	0,8020	102,1700	3.7 (20°C)	132,00	VOC
Dichloroetane	1,2560	98,9600	87 (25°C)	83,50	VOC
Allyl alchol	0,8540	58,0800		95,97	TIC
Mix dichlorometane diisopropylfluorophosphate	1,0550		0,579 (20°C)	183,00	
Carbon disulphide	1,2632	76,1400		46,50	TIC
Phosgene	1,3800	98,9200		8,20	CW
Chloropicrin	1,6579	164,3800	18.8 (20°C) 50.00 (40°C)	112,40	mix ccl4 – CW
Lewisite	1,8900	207,3200	0,394 (20°C)		mix chloro formio – CW
Nitrogen mustard gas	1,2400	204,5400	0,03 (25 °C)		CW
Allyl isothicyanate	1,0240	99,1600		152,00	TIC
Mustard gas	1,28	159,08	0.346 (40°C)	218,00	CW
Chloroethylphenyl sulfide	1,182	172,67	0,0186	146,00	TIC (Pesticide)
Dichlorvos	1,41	220,98	0,012 (20 °C)		TIC (Pesticide)

Table 4.2: *List of compounds analyzed and some chemical properties.*

4. ABSORPTION COEFFICIENTS CALCULATION AND ERROR ANALYSIS

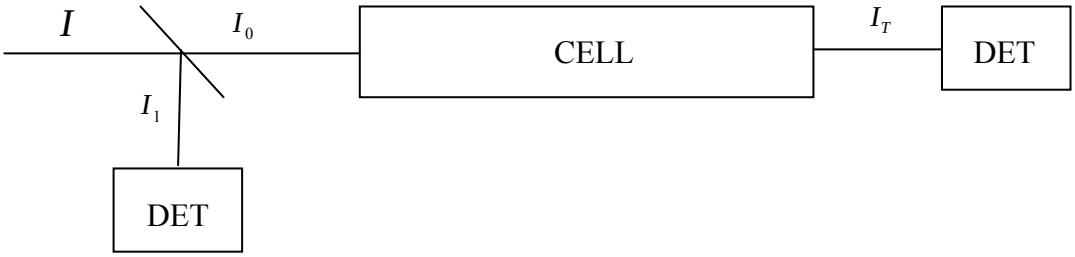

figure 4.11: *Sketch of experimental apparatus.*

The laser beam is split in two parts before entering the cell using a 45° tilted ZnSe Beam Splitter. This is useful because a fraction β of intensity is sent towards the reference detector and the other fraction $(1-\beta)$ is sent inside the cell and hits the main detector which measures the transmitted intensity.
The absorption coefficient $\alpha(i)$, which refers to the i[th] line of the laser source, was calculated by the ratio of beam energy before (I_0) and after (I_T) the cell. If β is the reflectance of the beam splitter, as stated before, without taking care of leakage, the following calculations are obtained:

$$I_T = I_0 A_w A_g = (1-\beta)\cdot I \cdot A_w A_g \qquad \textbf{equation 4.1}$$

where I is the input pulse energy from the source, A_w and A_g are the percentages of attenuation due respectively to windows and gas inside the cell.
In order to avoid the link that β and A_w have with the ratio I_T/I_0, which is critical because there is a strong relation with wavelength and polarization, the ratio I_T/I_0 was determined also with the cell empty.
Performing the same calculation in the latter case we have for the intensity with empty cell:

$$I_T^{EC} = I_0 A_w = (1-\beta)\cdot I \cdot A_w \qquad \textbf{equation } 4.2$$

The ratio in this case is:

$$\left(\frac{I_T}{I_0}\right)_{EC} = \frac{(1-\beta)\cdot I \cdot A_w}{(1-\beta)\cdot I} = A_w \qquad \textbf{equation 4.3}$$

After the substance is introduced the ratio with the filled cell is again performed, leading to the following results:

$$\left(\frac{I_T}{I_0}\right)_{FC} = \frac{(1-\beta)\cdot I \cdot A_w \cdot A_g}{(1-\beta)\cdot I} = A_w \cdot A_g \qquad \textbf{equation 4.4}$$

The attenuation coefficient is then calculated performing the ratio of the previous calculations:

$$\frac{\left(\frac{I_T}{I_0}\right)_{FC}}{\left(\frac{I_T}{I_0}\right)_{EC}} = A_g \qquad \textbf{equation 4.5}$$

The value of i^{th} line absorption coefficient was then calculated starting from the well known Beer-Lambert law.
Performing the calculation we have:

$$\alpha(i) = \frac{1}{c \cdot l} \ln \frac{1}{A_g} \qquad \textbf{equation 4.6}$$

where l is the length of the cell and c is concentration, calculated in terms of partial pressure.
In order to improve measures accuracy, the mean value over 20 measures was calculated for each of the sixty two laser lines emitted from our source.
Measures were performed at fixed temperature for several reasons using a thermalized system. First of all, we wanted to verify absorption coefficients variation with temperature. It seems that there is not a great fluctuation on the range considered, namely 25- 50 °C. A detailed study is beyond the purpose of this work. Second, we want to know how many molecules are inside our cell in partial pressure. This information is achievable with different methods and we choose the best one depending on measurement conditions. The first is direct measurement of pressure variation before and after introducing the compound inside the cell. This is reliable if the change in pressure is high enough to let relative error remain under 5% and if experimental set up is reliable itself, e.g. there is not air insertion while introducing the investigated compound. The second is to use vapor pressure value. This is possible if there is enough material inside the cell to let some material in liquid phase. Temperature control is important in this case to use tabulated vapor pressure value. The third method is to use perfect gas law to calculate pressure. This method is good if there is not enough material to reach vapor pressure and if quantity of material and temperature are measured with good accuracy. The direct measurement could be used to confirm second and third method.
The error calculus was performed using error propagation on the previous formula of absorption coefficient. We obtain the following result for the relative error:

$$\frac{\Delta\alpha(\nu)}{\alpha(\nu)} = \frac{\Delta P}{P} + \frac{\Delta l}{l} + \frac{I_0}{I} * \frac{1}{\ln(\frac{I}{I_0})} * \Delta(\frac{I}{I_0}) \qquad \textbf{equation 4.7}$$

The error in length is essentially due to possible misalignment of the cell or little change in length because of different compression of the rubber O-ring. It is fixed to the value of one mm.
The error in pressure depends on the method used to obtain the value. In case "measured value" is used the instrumental error fixed to 0.5 mBar. On the other hand, if vapor pressure is used the error is half the value of the last decimal used. Finally if perfect gas law is used the error depends on temperature and volume, which is related to moles, introduced. For the temperature an error of 1 K is fixed, depending not on the sensor used but on the possible difference of medium value since we are dealing with a point measures. The error in volume value is determined by the chemical syringe used and it is usually 0.5 µl.
The error in the ratio intensity or energy is determined by calculation of standard deviation and adding the value of sensor noise, divided by the medium value, to be conservative. Corrections on

this point were explained in the previous paragraph. The choice of error source must be made before performing MATlab calculation listed in picture 4.7.

As an example of absorption coefficients of some of the listed substances are displayed in the spectral range of our CO_2 laser and compared to the other taken with traditional spectroscopy in liquid phase. Data are normalized to be comparable one with each other and with data coming from CO_2 laser that will be described later. The equation 4.5 is used also in liquid phase. The main differences are now explained. Concentration is measured in mol/l so that absorption coefficient is measured in $[(mol/l)^{-1}\ cm^{-1}]$ both for liquid substances, as in the present case, and for substances in gas phase, as in the other one. It is of course necessary to subtract the effect of solvent from the spectrum. This is quite a simple operation since the solvent concentration is always the same.
The conversion system used is described as follow. Density and volume of substance introduced are known, so it is possible to calculate the mass; dividing for the molecular weight it is then possible to calculate the number of moles. It is then possible to calculate the number of moles for unit concentration. In gas phase a conversion is needed from pressure, obtained with one of the method previously described, to *mol* per *liter*. It is quite simple to calculate the number of moles from perfect gas law:

$$n = \frac{P*V}{R*T} \qquad \textbf{equation 4.8}$$

This is used to calculate molar density. If you trust measure of volume introduced more than pressure, it is possible to calculate the number of moles starting from the density value as it is done when measuring in liquid phase. Number of moles per volume is then easily calculated.

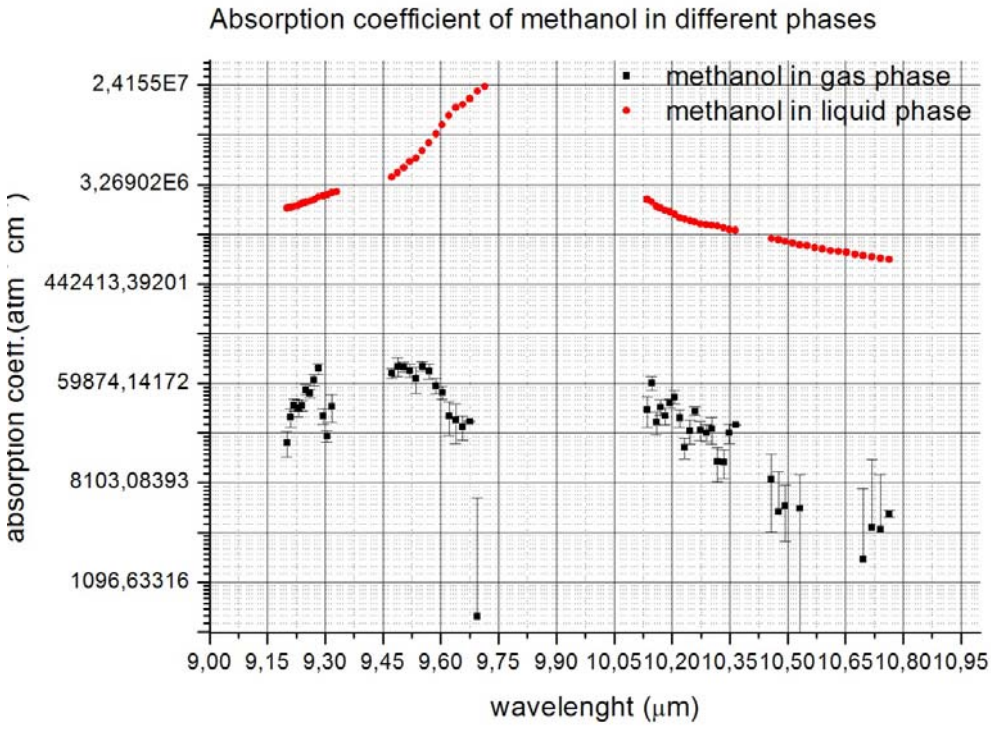

Figure 4.12: *Experimental absorption coefficients of methanol. Data are taken with two different method (see text for details).*

5. SPECTRA ANALYSIS: DIFFERENCE IN DIFFERENT CLASS OF COMPOUNDS OR DUE TO TEMPERATURE AND CONCENTRATION DEPENDENCES

In the following pictures absorption coefficients measured with our experiment are shown for many of the compounds cited in the previous table. Not all are shown since some are still being analyzed for further error analysis or are not really significant because of their low absorption value. Many of these pictures have the same substance measured alone or in air at the same temperature. Other are devoted to illustrate changing due to pressure or temperature in details. Comments are added after each picture if necessary. Analysis related to identification will be explained in the next chapter.

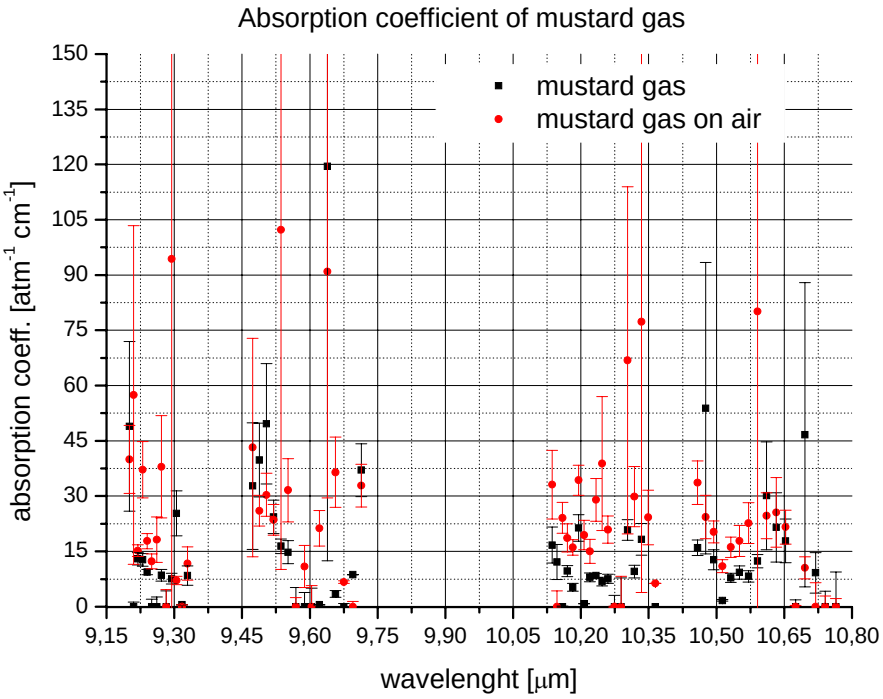

figure 4.13: *Absorption coefficients of compound cited in text vs. wavelength with error bars.*

For this chemical weapon, even if absorption coefficients are quite high compared to other substances, the vapor pressure is so low that a big error was obtained. Our instrument was not able to measure a difference in pressure before and after insertion in cell, so calculus were performed using theoretical vapor pressure at the temperature forced in the cell. Really good measure could be performed only with a much longer optical path and a powerful source. Some lines are clearly visible, but confusion is still the main impression. Nevertheless software recognition is possible, as explained in the following chapter.

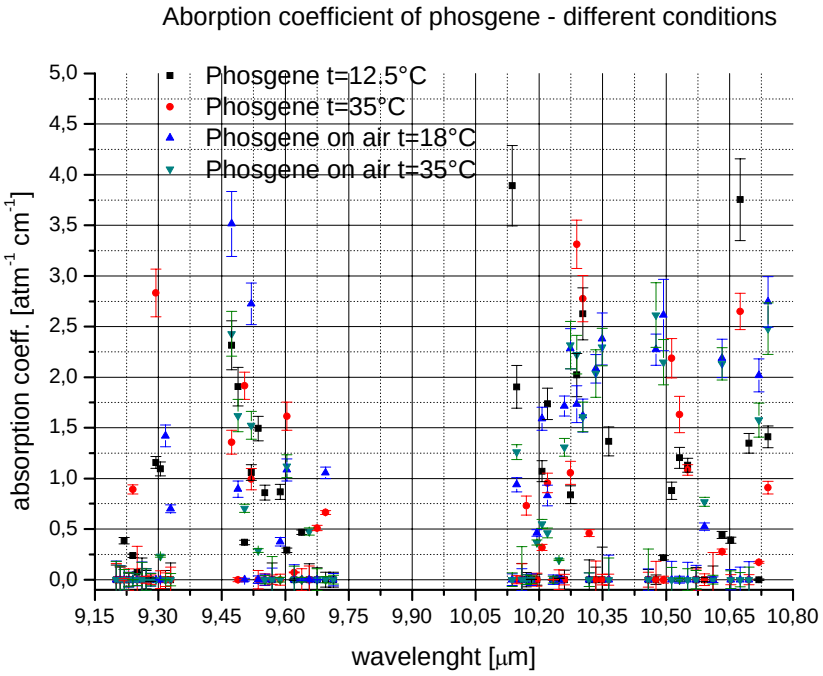

figure 4.14: *Absorption coefficients of compound cited in text vs. wavelength with error bars.*

On the opposite phosgene is a very high vapor pressure liquid such that it is unsafe to manipulate at low temperature. Different measures were performed. There is not a clearly recognizable behavior since there is a big difference of each line to the next one and temperature or air presence in cell could change the absorbed value from one to the next. Also in this case software recognition seems to be a reliable tool.

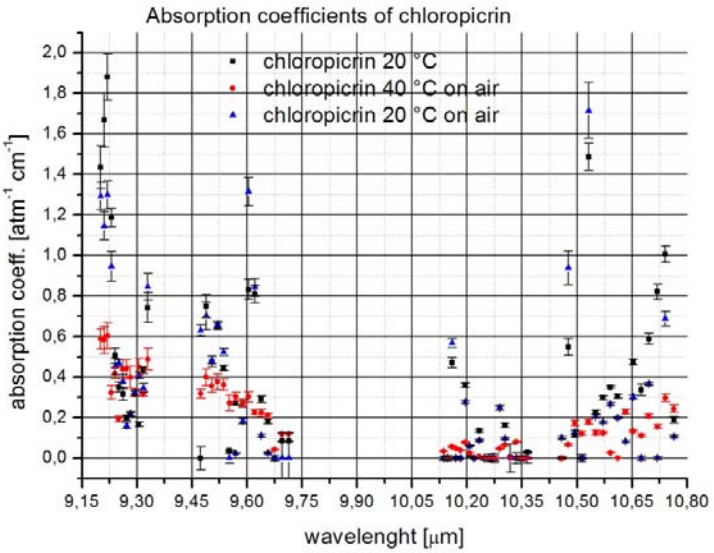

figure 4.15: *Absorption coefficients of compound cited in text vs. wavelength with error bars.*

Chloropicrin is a chemical weapon which is not as volatile as phosgene but much more than mustard gas. Difference between different measures seems related to air presence in cell more than temperature variation. Also this compound is identified using our software tool.

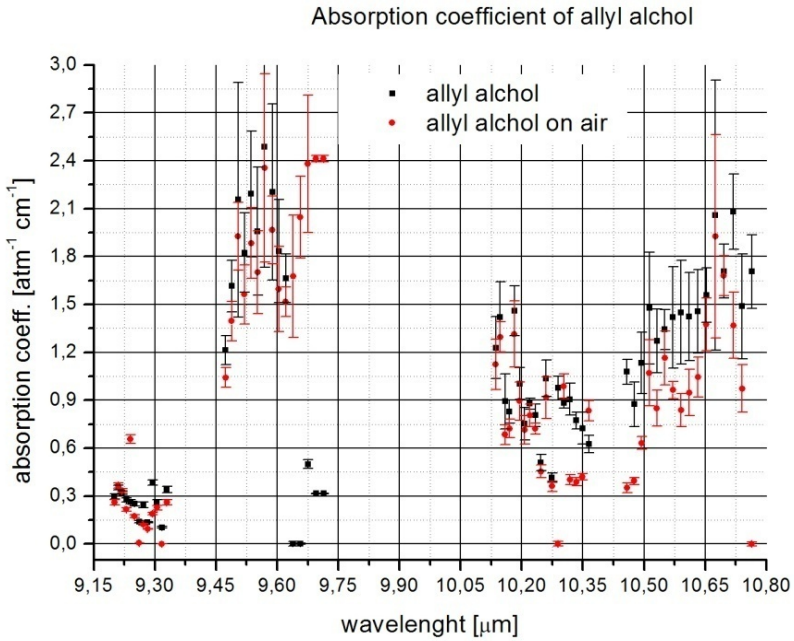

figure 4.16: *Absorption coefficients of compound cited in text vs. wavelength with error bars.*

Allyl alcohol is a TIC and for this reason it is identified using our identification tool. Error bars are higher than other similar compounds in terms of absorption coefficients and volatility for unknown reasons.

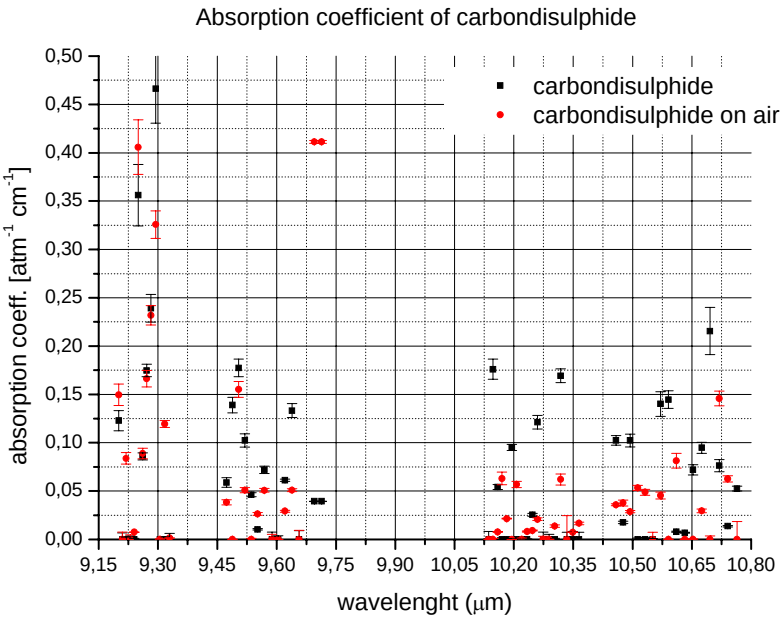

figure 4.17: *Absorption coefficients of compound cited in text vs. Wavelength with error bars.*

Carbondisulphide is a dangerous compound still used in some civil activity but generally prohibited due to its high toxicity and is thus considered a TIC. IR absorption is generally quite low. Air seems to smooth absorption on 10 μm bands. Few lines on the 9R band could help recognize this compounds. The last two values on the 9P band, even if reported, must probably be rejected due to poor laser emission in some of the measure involved. For this reason the great discrepancy in values, although not followed by a big error, is not to be considered. Due to its dangerousness, this compound was considered among the one to be investigated by our software tool. It is quite well recognized as the previous one.

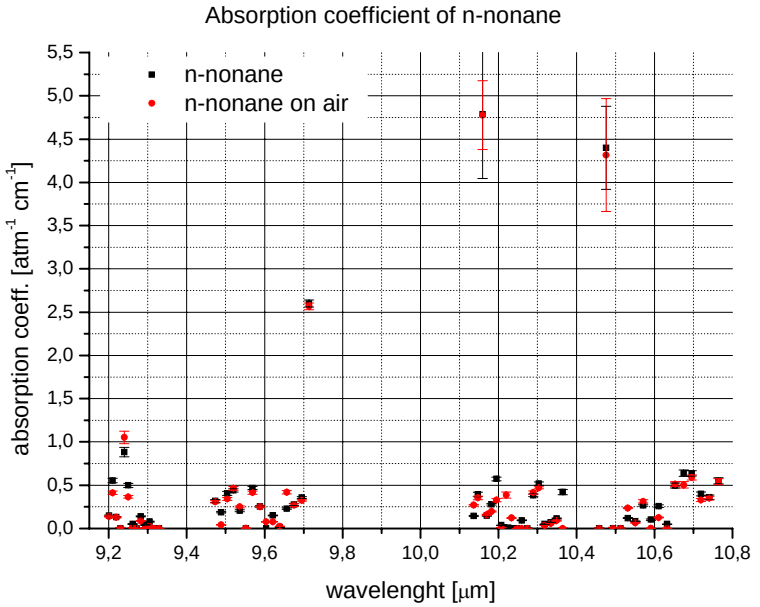

figure 4.18: *Absorption coefficients of compound cited in text vs. Wavelength with error bars.*

N-nonane is a VOC and for our main purpose it must be considered as an interferent. Its absorption coefficients are interesting because some lines have a value much higher than the other and so this is a perfect compounds to be investigated in atmosphere with classical DIAL as well as multivariate statistical analysis. This is considered just as interferents in our recognition model, as well as all other VOC.

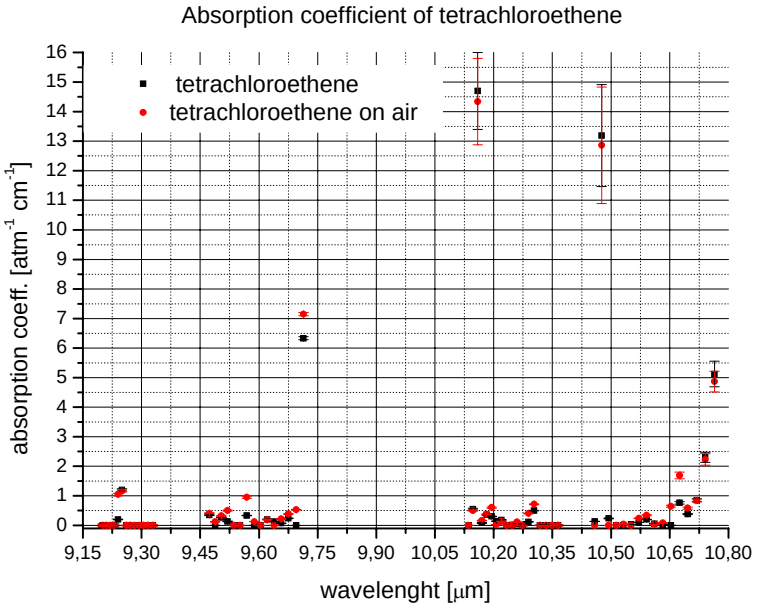

figure 4.19: *Absorption coefficients of compound cited in text vs. Wavelength with error bars.*

Tetrachloroethene is another VOC and so it is considered an interferent as well. It is an interesting compound because some frequencies have absorption coefficients much higher than all the others. It could be identified quite simply and moreover its concentration can be calculated very easily using DIAL technique.

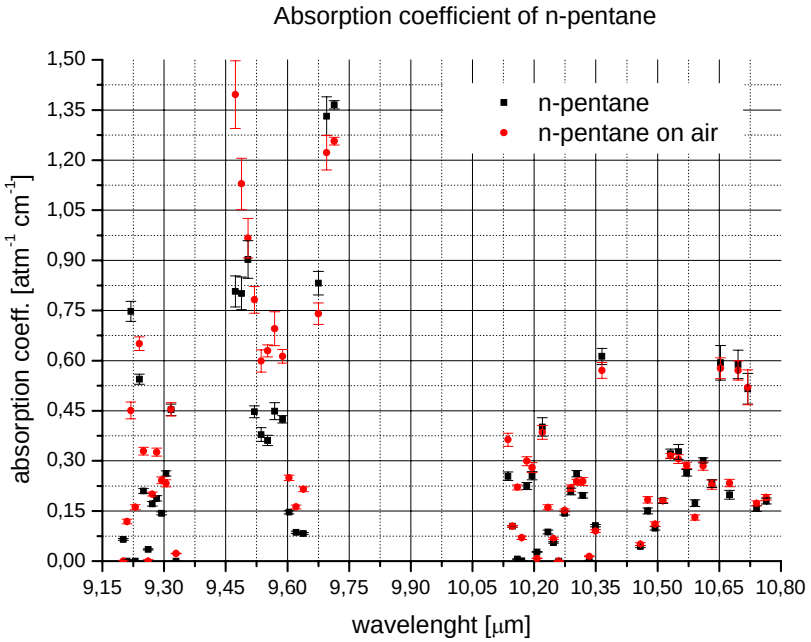

figure 4.20: *Absorption coefficients of compound cited in text vs. wavelength with error bars.*

N-pentane is a VOC as well. Its spectrum is not characterized by high or low peaks and its medium absorption coefficient is not high. Probably this is quite a difficult compound to be investigated.

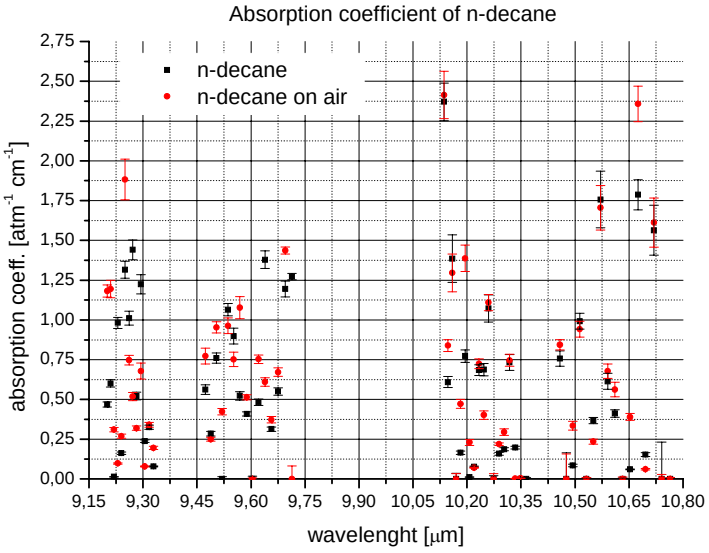

Figure 4.21: *Absorption coefficients of compound cited in text vs. wavelength with error bars.*

The behavior of N-decane is similar to that of N-pentane and comments are the same. This is probably due to the fact that molecular structure is quite the same.

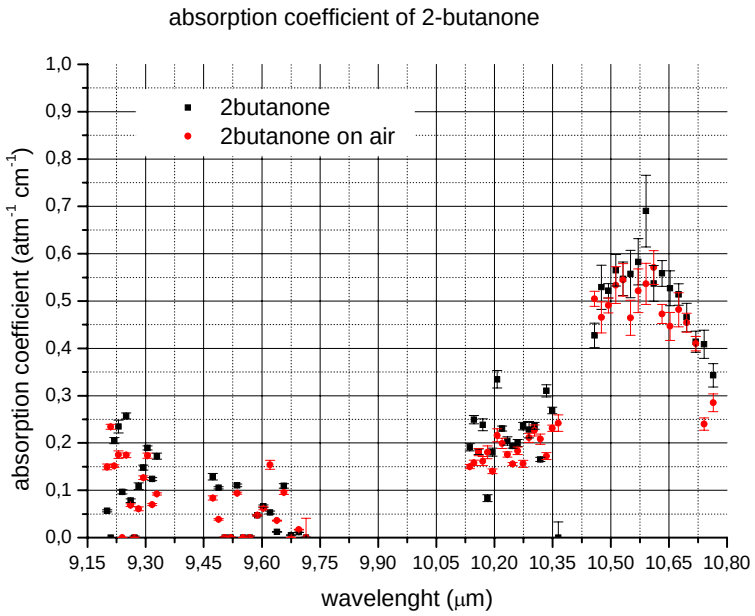

Figure 4.22: *Absorption coefficients of compound cited in text vs. wavelength with error bars.*

2-butanone is a VOC is quite different from others because its spectrum is almost flat apart from a really smooth and large peak around 10.6 μm. It is probably quite easy to be recognized if investigated.

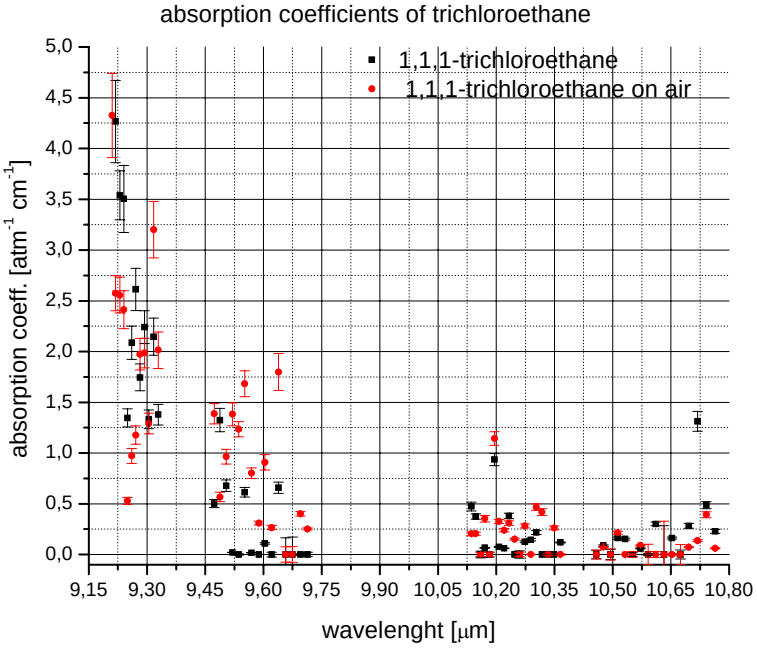

Figure 4.23: *Absorption coefficients of compound cited in text vs. wavelength with error bars.*

Trichloroethane is a VOC and is characterized by a decreasing value of absorption coefficients probably due to a peak just out our band at about 9 μm wavelength. Probably it could be easily investigated with our software tool if considered an interesting compound.

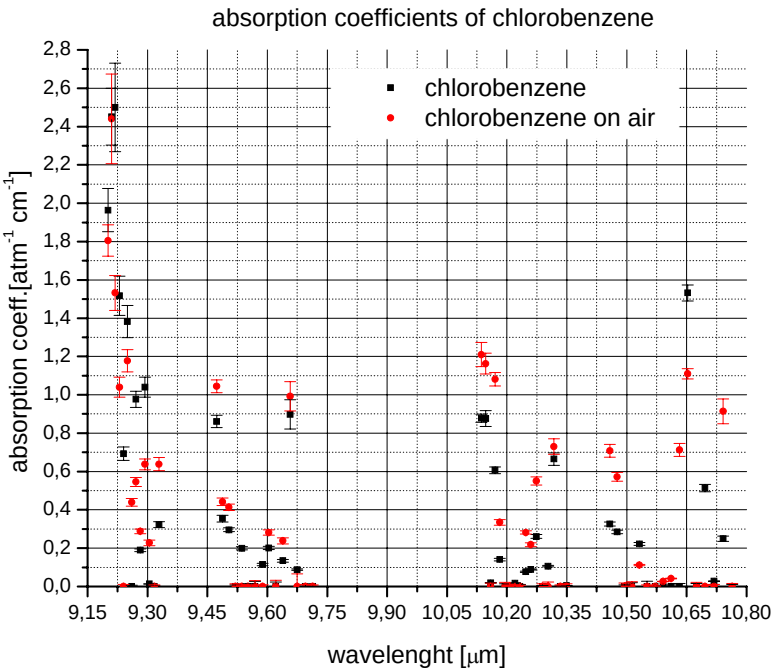

***Figure 4.24**: Absorption coefficients of compound cited in text vs. wavelength with error bars.*

Chlorobenzene has a general behaviour similar to the previous compound, probably due to the same characterizing element (chlorine) on an organic baseline. The presence of absorption in 10R and 10P band could help in discrimination among the two.

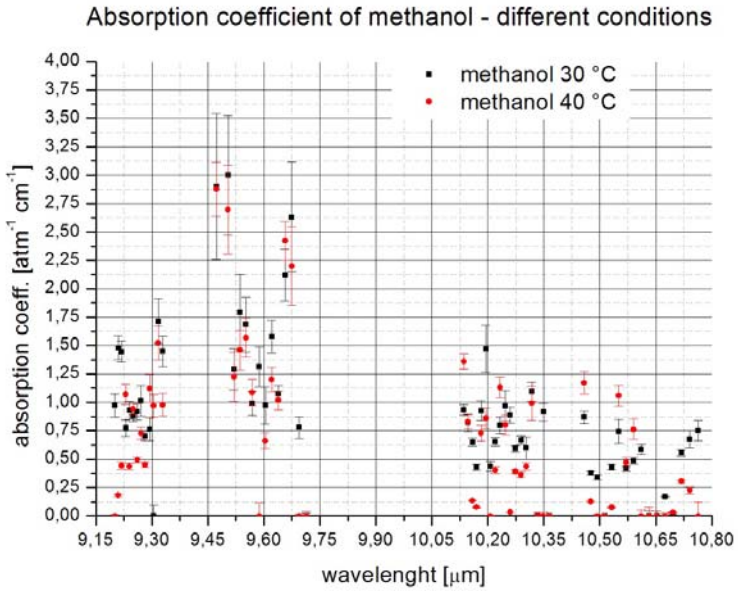

***Figure 4.25:** Absorption coefficients of compound cited in text vs. wavelength with error bars.*

Methanol is a quite widespread VOC. It was studied in various condition of temperature and concentration, inside the limits determined by our experimental set up, but differences are not really appreciable. The previous picture shows two of these measures.

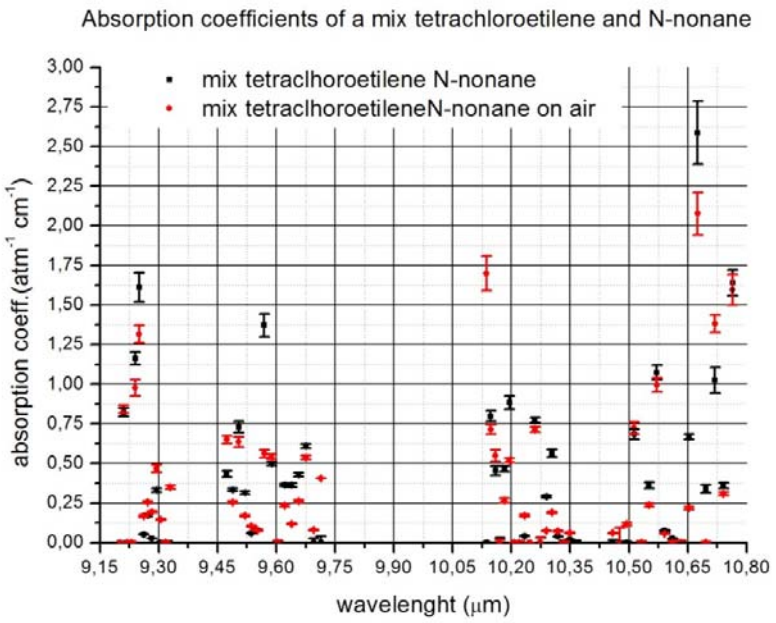

Figure 4.26: *Absorption coefficients of mix cited in text vs. wavelength with error bars.*

Mix of different compounds may be found in the atmosphere, also because many times they are used together in human activity. For this reason mixes of different compounds were also investigated. The compounds to be mixed were chosen so to have vapor pressure of the same order of magnitude and comparable absorption coefficients, so that none could completely obscure the other one. Absorption coefficients is calculated considering theoretical value of the ratio of molecules present and considering the pressure measured, so it is not as precise as that calculated for a single compound. The ability of our system to understand if a spectrum is made mixing different compounds will be further investigated in the next chapter.

6. CONCLUSION: WHY IT IS IMPOSSIBLE TO USE "CLASSICAL" DIAL, PERFORMANCE OF EXPERIMENTAL SETUP AND PROBLEM TO BE SOLVED

From the spectra analyzed in the previous paragraph it is quite clear that it is impossible to use classical DIAL to recognize substance. Each line is absorbed by many different substances and the ratio of power received by only two lines is not useful at all. It is not only possible that the same ratio belongs to different substance, but also that the presence of interferents or mixing give an unacceptable rate of false alarm.

DIAL method is based on the assumption that all the effects of the other compounds are subtracted by the "off" line, in other words the difference of the other compounds present in atmosphere is the same in both lines. This is a rough assumption that could be valid only in a standard atmosphere, and it is also the reason why many affords have been made since now to achieve a multiwavelenght method which is able to reduce error while measuring one substance, as explained in chapter one.

For these reasons we thought to use a different method, which goes over the Multiwavelenght dial, and will be explained in the following chapter.

The experimental set up is limited mainly by three constrains:

1. Length of cell, which affects the path length thus reducing the power absorbed by compound following Beer-Lambert law.
2. Power of source used, which reduces the system dynamic because in some case substance absorption coefficient and concentration could be so high that their product, put inside Beer-

Lambert law, produces a value of power comparable to the noise, that means a big error due to noise fluctuation, or lower than the noise, that means a measure without meaning such that it is possible to understand only that absorption coefficient is higher than a certain value. These problems are related to the following point as well.

3. Sensors intrinsic noise is related to the laser power described in the previous chapter, but noise is important also, on the other hand, if absorption is very low. If the difference between empty cell and full cell is lower than noise no absorption will be measured at all even if present.
4. Electronic components of the system. This point is important in case of high performance sensor, because in this case the system is limited by the byte used to acquire data and the problem is inside digitalization. This is not the present case, but could be if system will be improved. Details on this analysis will be given in chapter six where one of the possible local sensor application of a similar set up will be analyzed.

Let's now analyze each point providing a possible solution:

1. The path length could be changed providing a multipass cell which, using a properly projected optical system, is able to give a long path in a small volume so to fit under a fume hood. The best thing is to have a variable path length so to optimize its value to the substance under investigation. A possible cell was already projected but still not realized. The project is explained in detail in the following chapter.
2. The laser power is going to be increased, also thinking forward to real field use, and one of the possible laser system was analyzed in the previous chapter. The system considered has a power high enough to let us forgive this limitation.
3. Sensor's limitation is the one which will probably remain in the future. In fact a real improvement could be achieved only changing the class of sensor, so to overcame thermal based one and use nitrogen cooled one, as the one considered for the real projected system described in the previous chapter. But this means that we need two of such system working under a fume hood, which is really unpractical.
4. Electronic changing is related to the previous point, so also electronic will probably remain the same in the near future. Nevertheless, the solution on possible electronic which will be given in chapter six for the other system can be considered also to solve this problem.

7 REFERENCES

[1]C. Bellecci et al., Database for chemical weapons detection: first results, Optically Based Biological and Chemical Detection for Defence IV, Proceedings of the SPIE, Volume 7116 (2008).

[2] LABWIEW www.ni.com/labview

[3] www.mathworks.it/products/matlab

[4] Stephen S. et al. Optical detection of chemical warfare agents and toxic industrial chemicals: Simulation, Journal of Applied Physics 97, 113101 (2005)

[5] NATO - Science for Peace, SfP 982671, http://ppam.inflpr.ro/NATO/Sfp982671.htm

[6] Organization for the Prohibition of Chemical Weapons, IR data adopted by the first session of the conference of the states parties, approved at first and second session – (1997).

EXPERIMENTAL RESULTS AND MULTIVARIATE STATISTICAL ANALYSIS

1. FIRST ANALYSIS BASED ON DATABASE PARTIAL DATA

Multivariate statistical analysis was initially used on the first data acquired as described in the previous chapter. A list of compounds used in this preliminary analysis is found in the following table where a number is assigned in order to recognize each compound inside pictures and tables used for analysis.

Compound	N° used for analysis
N-epthane	10
Chlorobenzene	9
Toluene	11
111-trichloroethane	8
Benzene	12
Methanol (CH3OH)	1,2,3,4,5,6,7
1,1,1 Trimethylbenzene	13
Xylene	14
bis (2-chloroethyl) sulphide) - HD	15
2-chloroethylphenylsulphide	16 - 17
Dichlorvos	18

Table 5.1: List of compounds analyzed during first analysis.

Let's start considering the value of absorption coefficients ant their related measurement error. We need to generate many different measures in order to test our system, but real measures for each substance are too few, usually two, to perform accurate statistical analysis. For this reason we decide to generate random measures adding a random value inside limits determined adding or subtracting double statistical error, as explained in the previous chapter, to original absorption coefficient value. This method was applied of course to the full set of absorption coefficients related to the used wavelength. Ten of such "virtual" measurements are generated for each original measures related to a substance. Methanol, for example has seven different measures which generate 70 virtual measures. Each of the virtual measures are displayed in the same picture to understand if each substance is clearly distinguishable from the others. Dataset is then composed of all virtual measures of each substance. Each vector, composed by the generated set of values, one for each wavelength, was previously normalized as explained previously and PCA performed. PCA is able to change the vector space so to arrange data in a reference system where differences are empathized as explained in details in chapter 3, which, being an unsupervised method, shows data characteristics of grouping in class, even if for the same reason it is impossible to empathize the wanted information. The percentage of information related to each vector is descending, so it is usually enough to analyze few coefficients to understand the general behavior. Substances are identified with numbers, the ones used in table one and two, inside the following pictures. In the first picture there are the coefficients of the first two components for each substance considering ten "virtual" measurements as explained, while in the second picture there is an enlargement of the signed area inside the previous picture. Data refers to the first two components that have 68.87% of information. As it is clearly visible, each substance is quite away from each other, that means it is clearly recognized also automatically just dividing in class the area and assigning a name to each area.

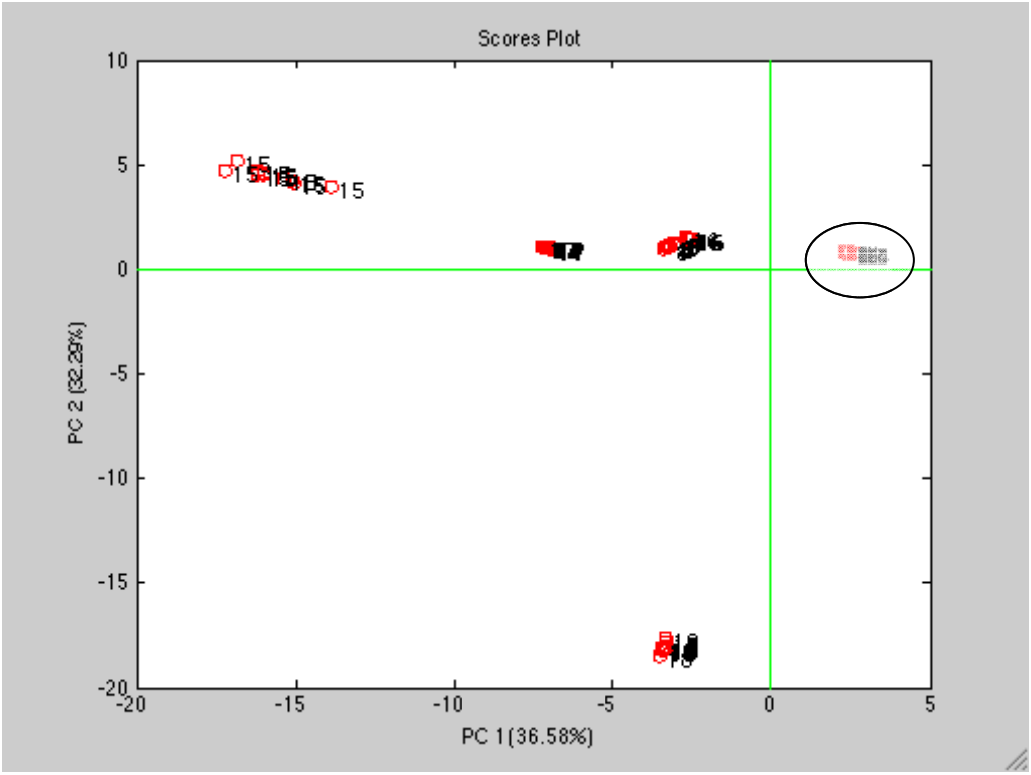

Figure 5.1: *Plot Diagram of Principal Component 1 versus Principal Component 2 of compounds PCA.*

Let us now consider only one compound, methanol, and analyze what the behavior of absorption coefficients is changing temperature or concentration. This Data will be analyzed inside the database, so to leave the same general condition of analysis and the same model, to see in which way different conditions could ruin identification. The identification number follows the other assigned so that the numbers explained in the following table are assigned to different conditions. Condition 3 is the worst one, probably due to severe condition for good measurements with our instrument because concentration is too low. The others appear to be close enough not to be confused with other compounds.

10 µl 28 °C	10 µl 28 °C on air	1 µl 28 °C	3 µl 50 °C	29 µl 50 °C	3 µl 30 °C	3 µl 40 °C
1	2	3	4	5	6	7

Table 5.2: *Numbers assigned to different conditions of methanol for Principal component Analysis.*

A further step in identification is made not only considering a qualitative ability in recognizing substances by human eye check of the previous pictures, but also making real model of identification using PLS – DA. This kind of classification was explained in chapter 3. In order to properly classify substances, the model used to perform analysis with PLS-DA is built using eleven class. All Methanol measures are considered in the same class, as well as mustard gas measures.
A full list of the class used follows:

1. Methanol
2. 1,1,1 Trichloroethane
3. Chlorobenzene
4. N-heptane

5. Toluene
6. Benzene
7. Trimethylbenzene
8. Xylene
9. Chloroetilfenilsulfide
10. Mustard gas
11. Dichlorvos

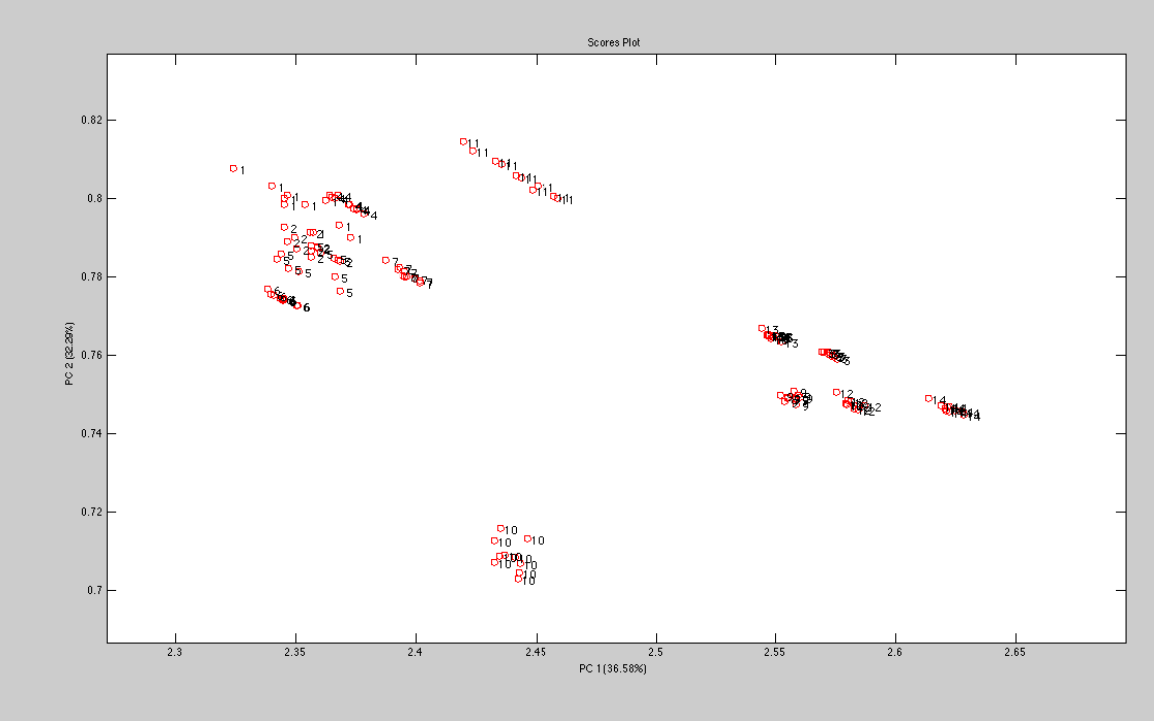

Figure 5.2: *Zoom of the previous picture circled area. several data refers to variation of physical data of methanol.*

Figure 3 reports the prediction error determined by PLS-DA using the Leave One Out Cross Validation method, already described in chapter 3 when explaining PCR, in order to validate PLS-DA itself. It builds N models starting from N measures. After N-1 measures are used to build the model and one is used for testing the model. With this method it is then possible to determine system ability to recognize substances. Measures were generated using error as already explained inside the class listed above.

Correct classification is more than 97%. It was achieved after choosing 19 latent variables, which lead to the lowest error during validation.

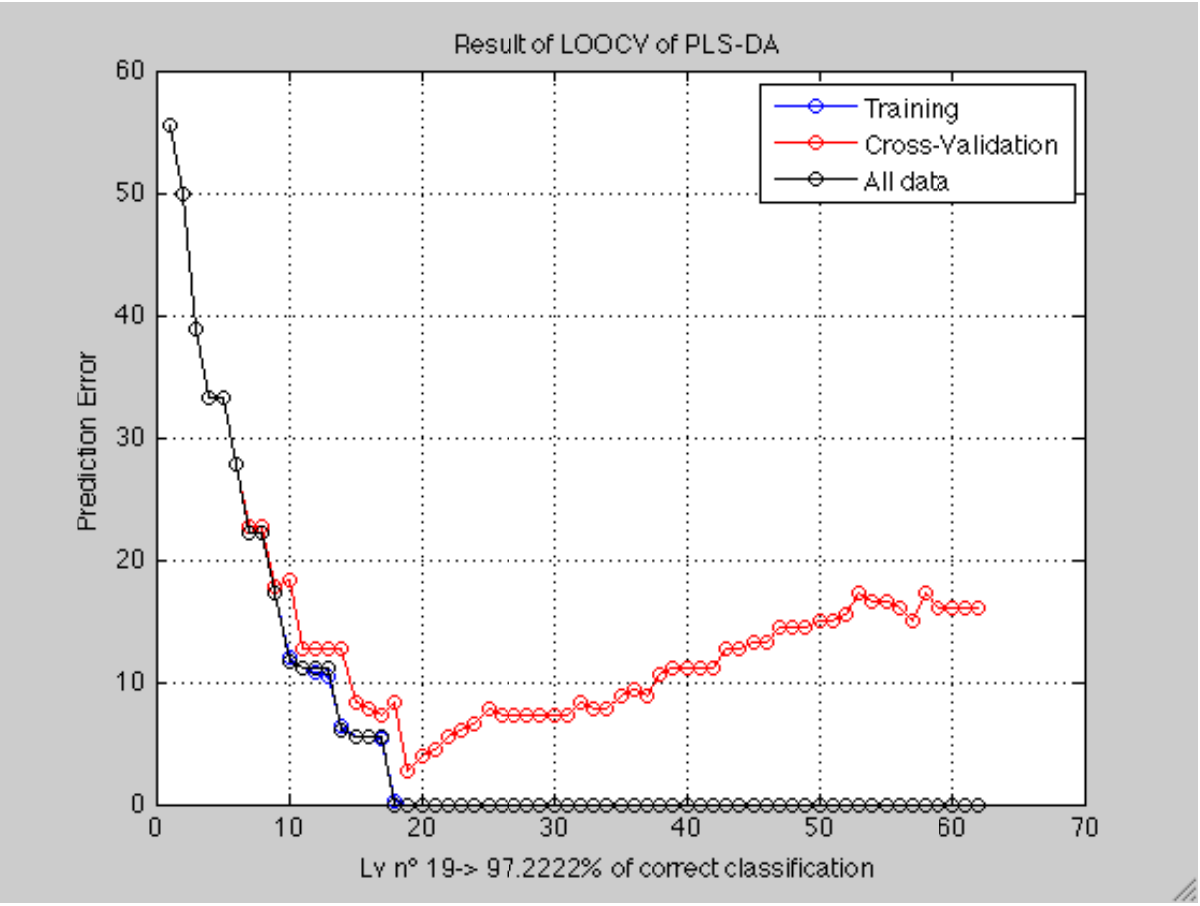

Figure 5.3: *Results concerning prediction error of the model built with eleven classes using the leave one out cross validation of PLS-DA. Both training and cross validation are reported.*

Confusion Matrix is reported in table 3. It is the best instrument to understand which part of the data are not well classified. Each measure is classified and if classification is properly made by the system then all data are founded in diagonal elements of the matrix. The errors are always determined by the same substance corresponding to number nine and class nine and so found in row number nine, Chloroetilfenilsulfide to be precise. It is confused with more than some different substances five times over the ten virtual measures considered. This is probably due to the big error determined by the low vapor pressure that determines a window too wide for many wavelengths.

70	0	0	0	0	0	0	0	0	0	0
0	10	0	0	0	0	0	0	0	0	0
0	0	10	0	0	0	0	0	0	0	0
0	0	0	10	0	0	0	0	0	0	0
0	0	0	0	10	0	0	0	0	0	0
0	0	0	0	0	10	0	0	0	0	0
0	0	0	0	0	0	10	0	0	0	0
0	0	0	0	0	0	0	10	0	0	0
2	0	1	0	1	0	0	1	5	0	0
0	0	0	0	0	0	0	0	0	20	0
0	0	0	0	0	0	0	0	0	0	10

Table 5.3: *Confusion Matrix of PLS-DA performed with eleven classes. Identification error are clearly visible because are out of diagonal elements.*

We have decided to leave these compounds out and perform our analysis again using ten classes instead of eleven. Results obtained are shown in the next picture.

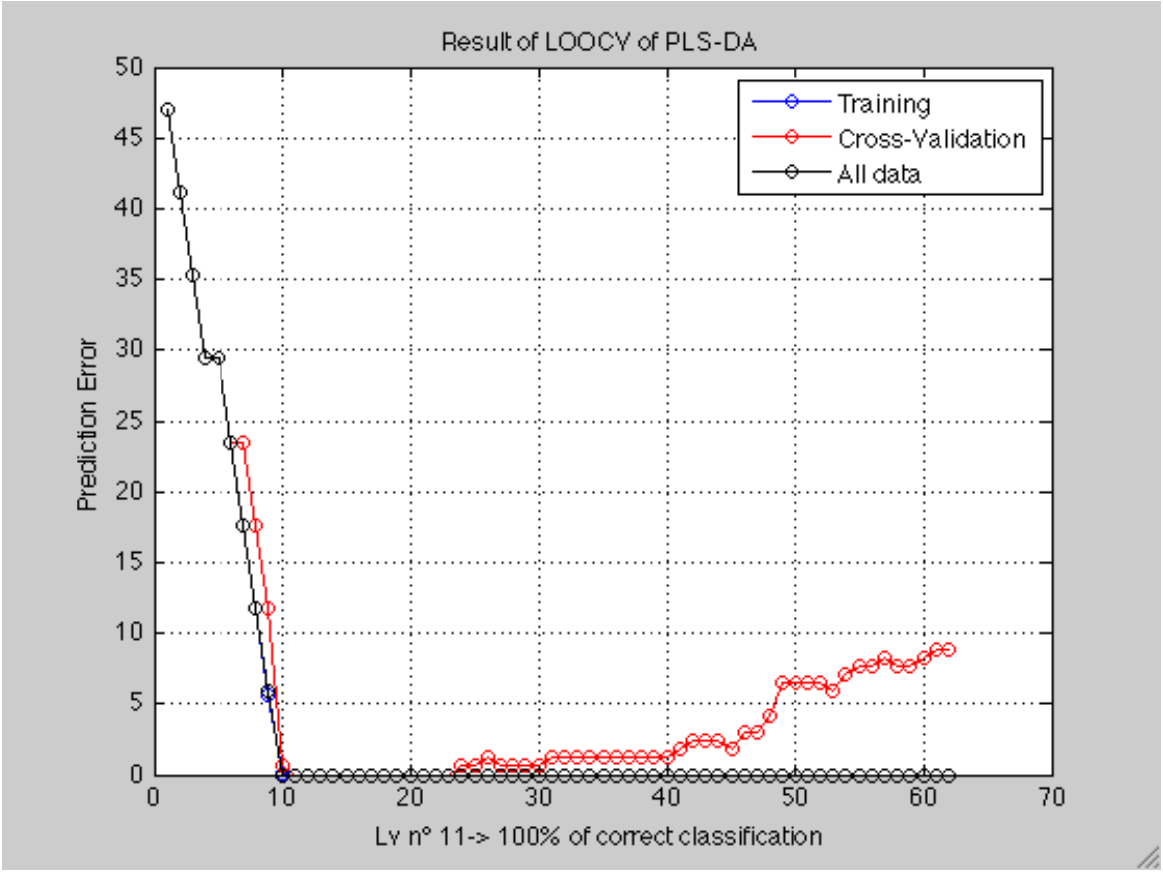

Figure 5.4: *Results concerning prediction error of the model built with ten classes. Both training and cross validation are reported.*

Confusion Matrix determined in this case is reported in the following table. All Compounds are well classified as clearly visible because all elements out of diagonal are zeroes.

70	0	0	0	0	0	0	0	0	0
0	10	0	0	0	0	0	0	0	0
0	0	10	0	0	0	0	0	0	0
0	0	0	10	0	0	0	0	0	0
0	0	0	0	10	0	0	0	0	0
0	0	0	0	0	10	0	0	0	0
0	0	0	0	0	0	10	0	0	0
0	0	0	0	0	0	0	10	0	0
0	0	0	0	0	0	0	0	20	0
0	0	0	0	0	0	0	0	0	10

Table 5.4: *Confusion Matrix of PLS-DA performed with ten classes. Identification error are absent because elements out of diagonal are all zeroes.*

2. ANALYSIS BASED ON DATABASE DATA WITH 36 SUBSTANCES

The number of substances considered in this case is much bigger than the previous one. The work needed to achieve an instrument which is able to recognize each substance is quite hard and long. It will be done whereas new resources will be available to speed up this research field. For this reason, also considering the main task of our instrument, that is to recognize chemical weapons or dangerous substances without confusion with interfering compounds, the classes were reduced to ten. Measures considered were 62, all of them generating a set of virtual measures, ten for each original measure, exactly the same as made for the first dataset and explained in the previous paragraph.

The class considered are the following:

1. Nitrogen Mustard gas
2. Chloroform and lewisite mixed up
3. Chloropicrin
4. Phosgene
5. Carbon disulphide
6. Allyl alcohol in air
7. Dichlorvos
8. Mustard gas
9. Chloroetilfenilsulfide
10. All other compounds.

Considering the high number of measures and classes involved for the first nine classes other data are provided so to have a good number for training set and test set. Finally considering all the substances and the class in which they are divided, the number used to generate discrimination method are the following:

1. Training set: 475 measures
2. Test set: 950 measures
3. After processing this data, only ten Principal Component determined by PCA are used for the next step, which is a Neural Network.

A feed forward neuronal network, which is in some the simplest to be implemented, has been used to build a non linear classifier, thus changing the analysis method used previously. The net has one hidden layer with eleven neuron working. The function used to get the hidden layer active is “tansig” while output layer is “purelin”.

Finally a confusion matrix is achieved with the same meaning as the previous paragraph.

Classification rate during this step is 98.9474%, thus a good level of classification. Some of the elements of the class “other compounds” are confused with other classes. This is probably due to the fact that one of the class concerns “lewisite”, a chemical weapon, which was mixed to chloroform and we cannot purify it. Much of the confusion could probably arise because the difference in spectra of this mix and pure chloroform is not really high.

A confusion matrix is obtained also after the training is considered ended. This is obtained while testing the Net to recognize substances. It is shown in the following picture.

In this case classification rate is 98.10%, thus not really far from the training one. The real novelty is that not only “other compounds” are confused, probably for the same reason explained for the training set, but also other two compounds, classes 7 and 9, namely dichlorvos and chloroetilfenilsulfide.
This is probably due to the fact that we decide not to reject some data which are not completely reliable, for the sake of clarity, because of the fact that they were taken near the boundary of our measurement set up working range. The limits of our system were outlined in the previous chapter.

100	0	0	0	0	0	0	0	0	0
0	100	0	0	0	0	0	0	0	0
0	0	100	0	0	0	0	0	0	0
0	0	0	150	0	0	0	0	0	0
0	0	0	0	50	0	0	0	0	0
0	0	0	0	0	100	0	0	0	0
0	0	2	1	0	2	45	0	0	0
0	0	0	0	0	0	0	100	0	0
0	0	0	0	0	0	0	0	47	3
0	0	0	0	0	0	0	0	0	140

Table 5.5: *Confusion Matrix obtained after test of the neural network. See text for details.*

3. SOFTWARE ANALYSIS TO INCREASE SYSTEM PERFORMANCE AND AUTOMATION

Further steps could be performed to increase system performance. Naturally all the steps already done, described in the previous paragraph, have to be repeated in case of new database based on a different source or upgrade of the present database. For this reason, considering that many affords are needed to achieve the goal which will be described, these steps were not implemented until now.
One step is to implement a statistical classifier. This is a classifier which not only assigns each measure to a possible substance, but also gives a confidence indicator on reliability of this identification, usually expressed as a probability of identification or accuracy identification percentage. This could be done through discrimination method based on various kinds of algorithmic, usually based on the Euclidean distance of the vector

representing the substance from the one representing the measure and similar geometrical based method. Some of these methods are described in ref. 1.
All these methods, including the one already used, have to be tested in "field" conditions and not only using a cell inside a laboratory. Real system performance has to be tested experimentally and probably some adjustments will arise from such tests.
A natural extension of the method is the use of different lasers which use different bands of electromagnetic spectrum. This improvement could increase the number of substances identified by the system because many substances have an almost zero cross section in the entire band of one source but generally this is not true considering two different bands. If a substance has an absorption cross section different from zero in both bands, its identification probability will be strongly increased by the use of both lasers. Two different database are needed to be used by each subsystem or by a main computer properly arranged for identification. Final result is total accuracy percentage of identification.
A sketch of a device based on more than one source, and of course more than one sensor, is shown in figure 5 where just two different sources and related sensors are used for the sake of simplicity. The two Multiwavelenght DIALs are completely independent, that means they could work also separately. Only information are sent to a main computer which is able to compare information and give an output which is made using all data. Data could be partially arranged by each local computer or completely elaborated by the main one. The main computer task is to use all the instruments provided (PLS-DA, Neural network, etc..) to recognize the substance.

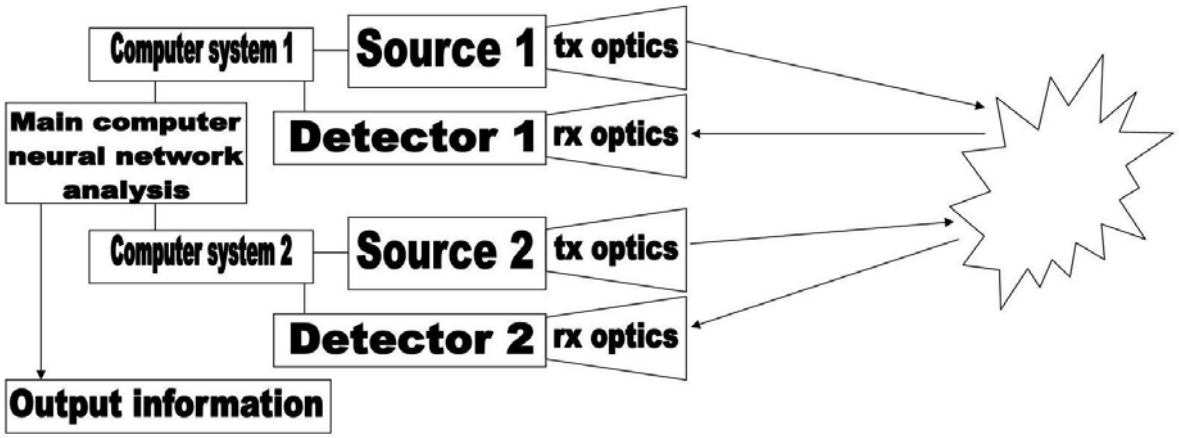

Figure 5.5: *Sketch of the system made with two Multiwavelenght DIAL. See text for details.*

4. UPGRADE OF EXPERIMENTAL SET UP: A PROJECT OF A MULTIPASS CELL

One of the improvements which could help in increasing system performance is the multipass cell. As previously explained in chapter 4, one of the limits is determined by optical path and so we need a method to increase optical path without increasing cell length, so to fit under a fume hood as the currently used set up. The best solution is the one that lets you choose the path length depending on the substance or, for detailed study, even on the wavelength.
At the beginning we tried to find possible device already available in commerce that could fit our needs, so to avoid wasting time and money for an already available device. We found only a Herriot cell, namely SCINTEC CMP30[2], which is not good for our purpose because the manufacturer does not guarantee that there is no cross energy change above 3 μm. So it is possible that some rays perform a shorter optical path and this is, for our purpose,

unacceptable. Also some modifications are needed; external window, for example, does not let ray with wavelength higher than 9 μm come inside the cell.
For these reasons we decide to project a completely new cell setup. Project is based also on other consideration which will be explained in the next chapter, the maximum path length was fixed to 30 m while physical length of the cell must not exceed 1 m. We also decide to use commercial mirrors, to get cost low.
We used optical project software ZEMAX[3] to arrange, test, modify and develop our cells to arrive at a good design. After some attempts to use two big commercial found mirrors, we decide to use several smaller mirrors on both sides of the cell for the following reasons:

1. It is possible to change inclination on some mirror to achieve the same results and correct little misalignments if needed;
2. It is possible to pick up the signal everywhere, just removing one mirror and putting a window to extract the beam from the cell. In this way the cell becomes a discrete multipass cell with path length variable from 1 m to 30 m with step of 1 m;
3. It is possible to mount buffer to avoid even partial energy crossing to the next mirror which could determine different path length, if necessary.

The first project that reached the goal, fully fitting our requirements, was a cell made with 29 mirrors made by Edmund optics, namely NT32-822. Each mirror has a diameter of 2'', a focal length of 508 mm and obviously a gold layer is provided in order to reflect IR radiation. Reflectivity, in fact, is 96%, thus considering 29 mirrors we lose less than 70%, without considering other leakage. Each mirror is inclined so to send the ray towards the following one until the exit window is reached. After some fine revision we have lowered the number of inclinations, originally many different values were allowed, down to four, the first three to different values and after fixed to 0.2°. This last work really simplifies the mechanical job needed to realize the cell. We finally test tolerance in mechanical or mounting precision which does not ruin system performance. An error of 0.01°, even if randomly applied to all mirrors, is compatible with our system requirements.
In the following pictures side view, frontal view and diagonal view are shown to give an idea of system set up. Source is not explicitly represented, but a laser source which has the same features of the one used is simulated, namely a TEM00 with divergence of 5 mRad. The output ray is visible as a blue one in the upper side of the pictures. After each reflection ray changes its color so to explicit the effect of reflections. Finally after 29 reflections, during which the beam is refocused thanks to the properly chosen focal length to correct original divergence, the beam hits a detector of 1 cm^2 with 100x100 pixels in order to have an idea of the beam shape which hits the real sensor, the area involved and sensor positioning options. A false color picture determined by this sensor is shown in figure 13. The total power collected is 1 W and it is equal to the power emitted by the source because total reflection is assumed. Thus no ray is lost due to vignetting or other optical reasons.

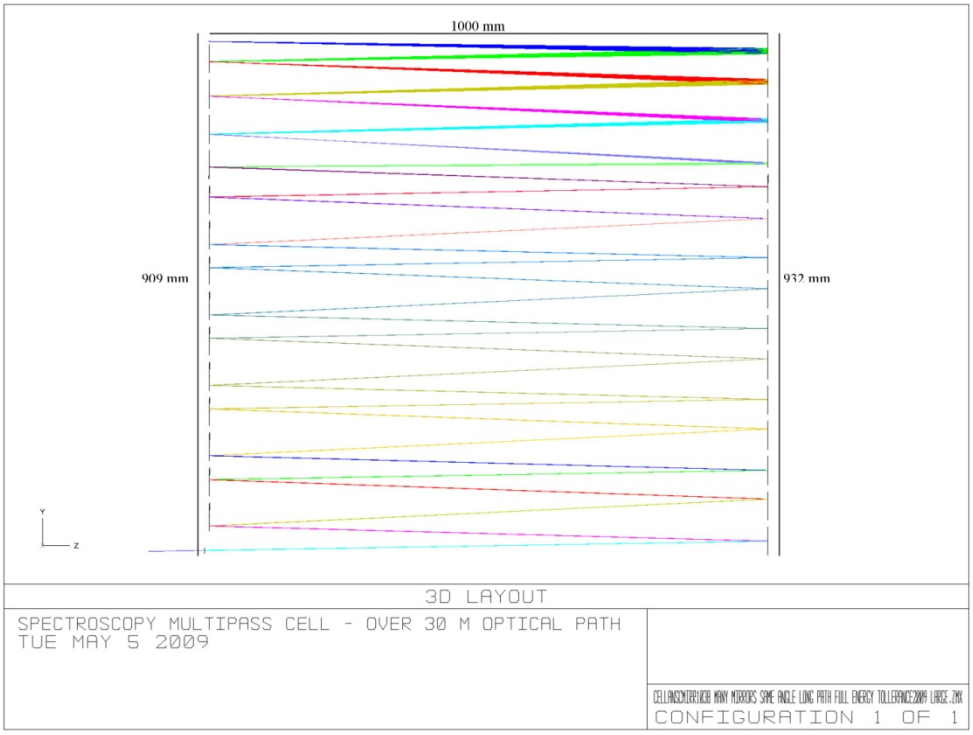

Figure 5.6: *Side view of the multipass cell. See text for details.*

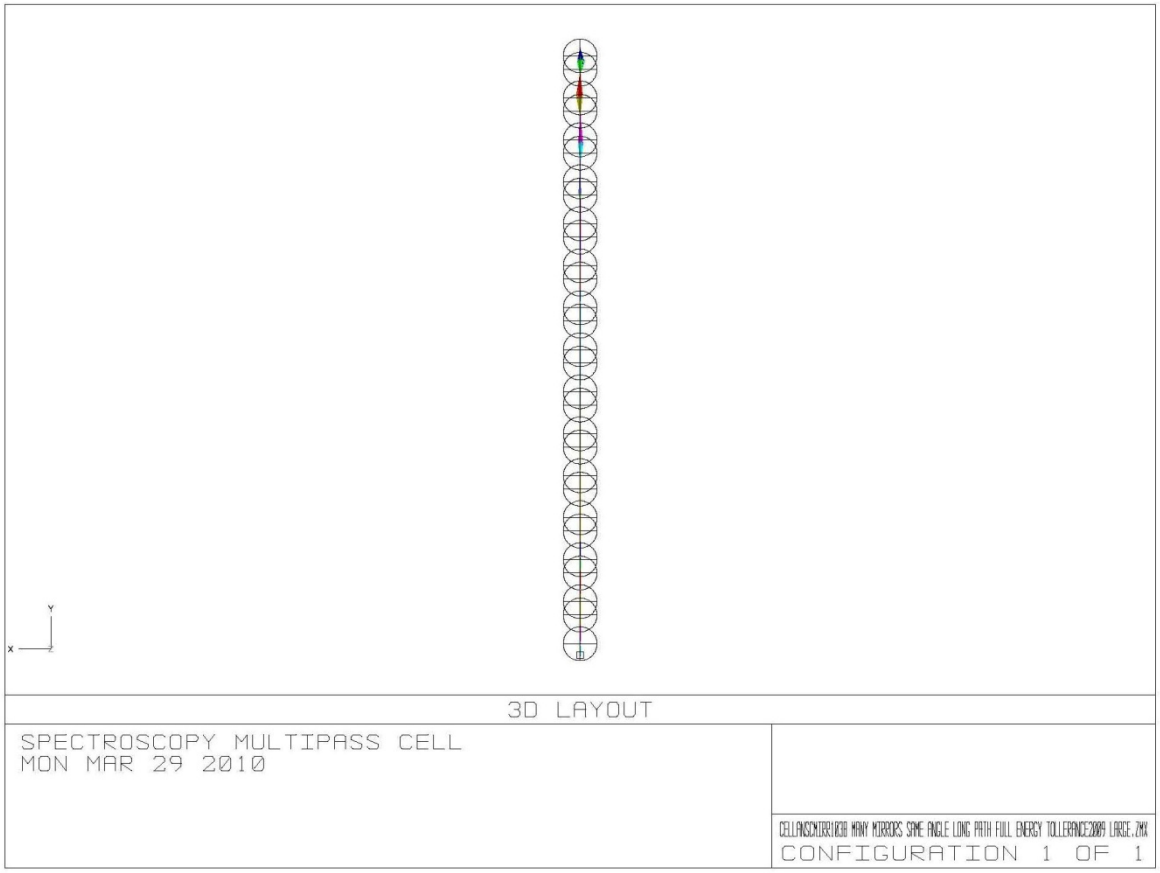

Figure 5.7: *Front view of the multipass cell. See text for details.*

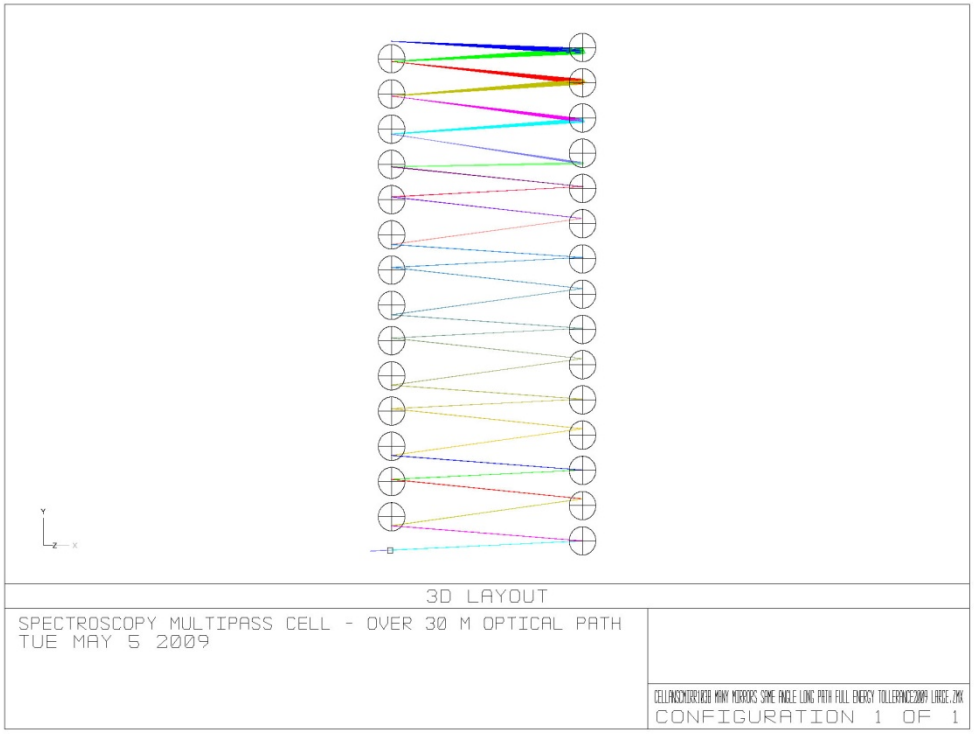

Figure 5.8: *3d view of the multipass cell. See text for details.*

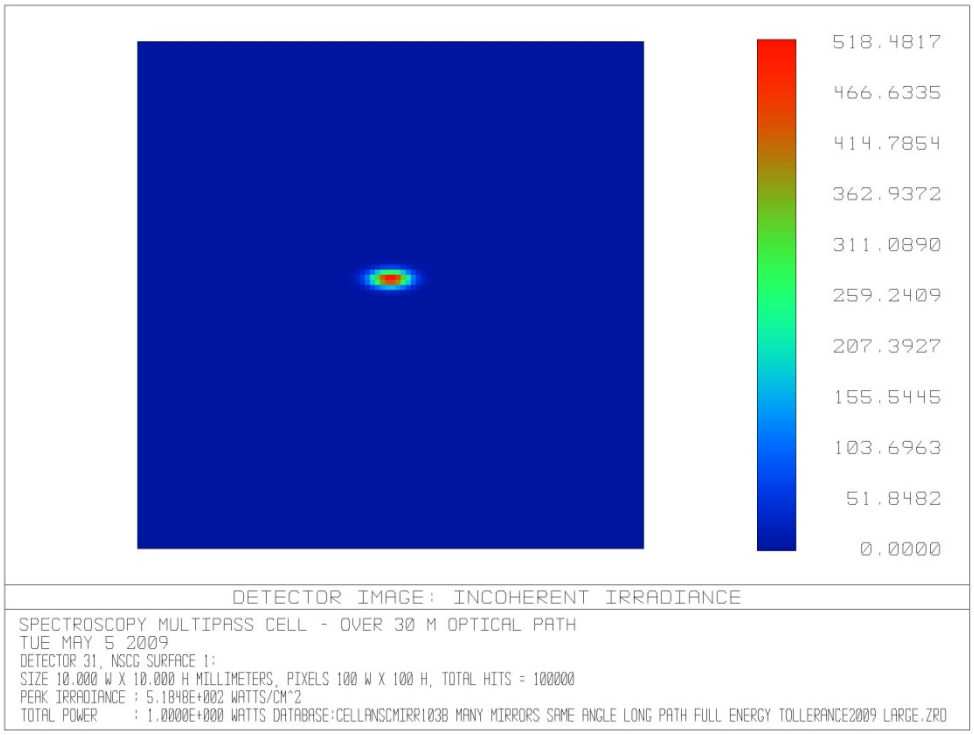

Figure 5.9:*False color irradiance acquired by a detector in correspondence of the output window of the multipass cell. See text for details.*

Mechanical consideration induced us to change this first set up. This cell, indeed, has to work also with quite high vacuum conditions and thus mechanical stress has to be considered. But optical precision needed is the same both at ambient pressure and vacuum condition and thus almost no mechanical stress is allowed. This condition has determined a really heavy box which is also technically difficult to realize. Moreover, even if the total volume is not so high, practical use could be not simple due to the difference of width, 909 mm minimum, compared to depth, 51 mm minimum. For these reasons the set up described, even if optically working, was modified so to allow the use of a cylinder shape mechanical support. Obviously, a cylinder is much more simple to realize for this kind of use.
A natural evolution of the previous set up is to just modify mirrors position so to have two arrays of mirrors in both circular side of the cylinder. Of course, a matrix means a rectangular shape which in our case is almost a square and could fit well inside a circle. In the next figures side, front and 3d view of the new set up are shown. Also irradiance picked up by virtual sensor is shown in figure 17 as in the previous case. Optical performances are almost the same. Mechanical work of support is critical because in this case four different angles of mirrors inclination are needed along one axis and seven mirrors have to be inclined also along the other axis to change column with four different angles, such that eventually at least eleven different angles have to be considered instead of four. Obviously a different angle is needed wherever a "column" change is prescribed. Moreover it was impossible to reduce the angle to the same number even in the same column because after each change corrections are needed.
Finally tolerance was also studied and the same results in angle precision, 0.01°, were achieved.

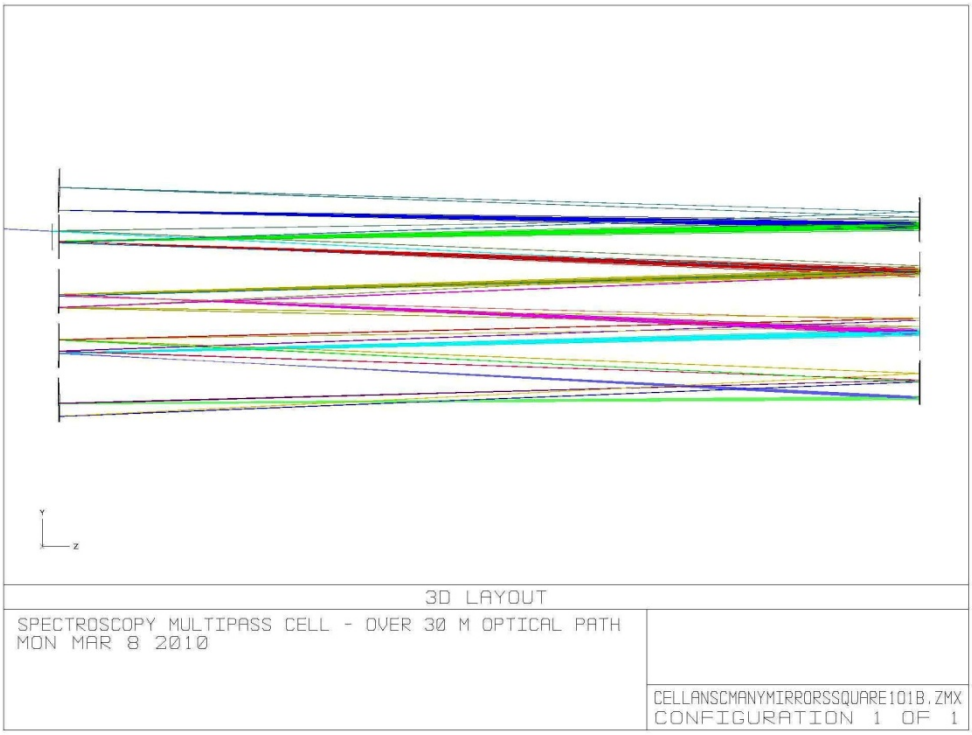

Figure 5.10: *Side view of the new multipass cell. See text for details.*

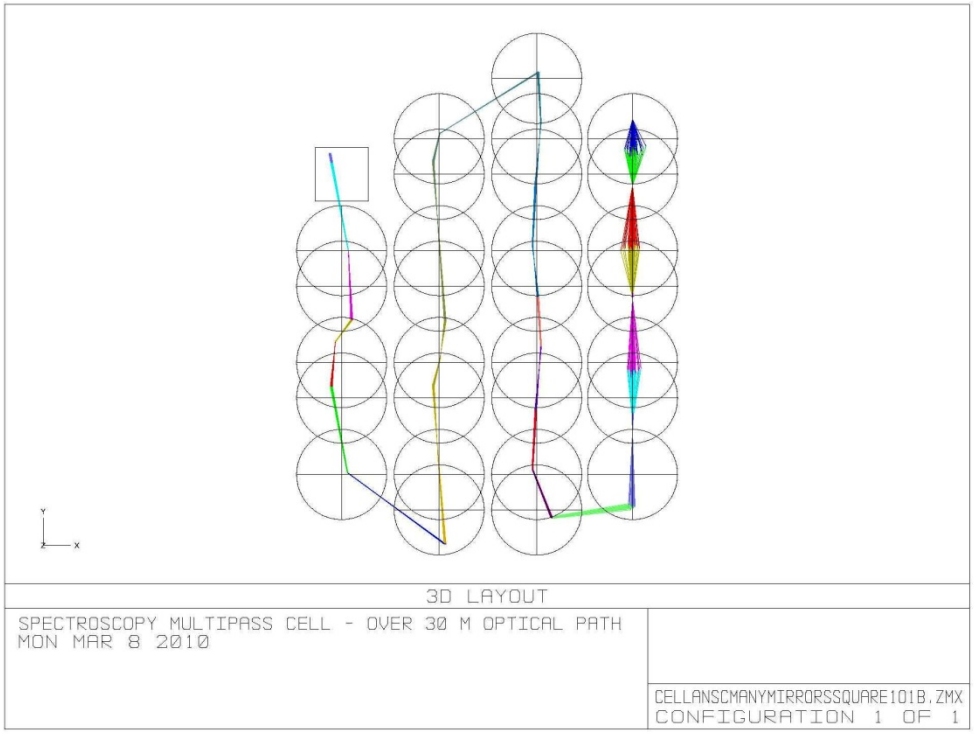

Figure 5.11: *Front view of the new multipass cell. See text for details.*

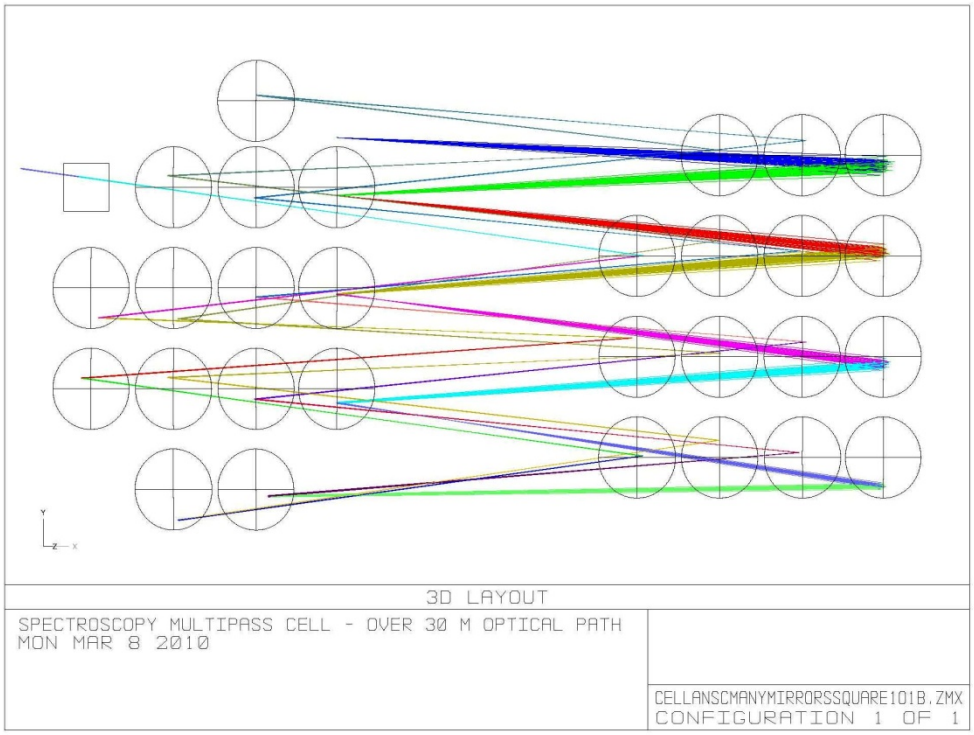

Figure 5.12: *3d view of the new multipass cell. See text for details.*

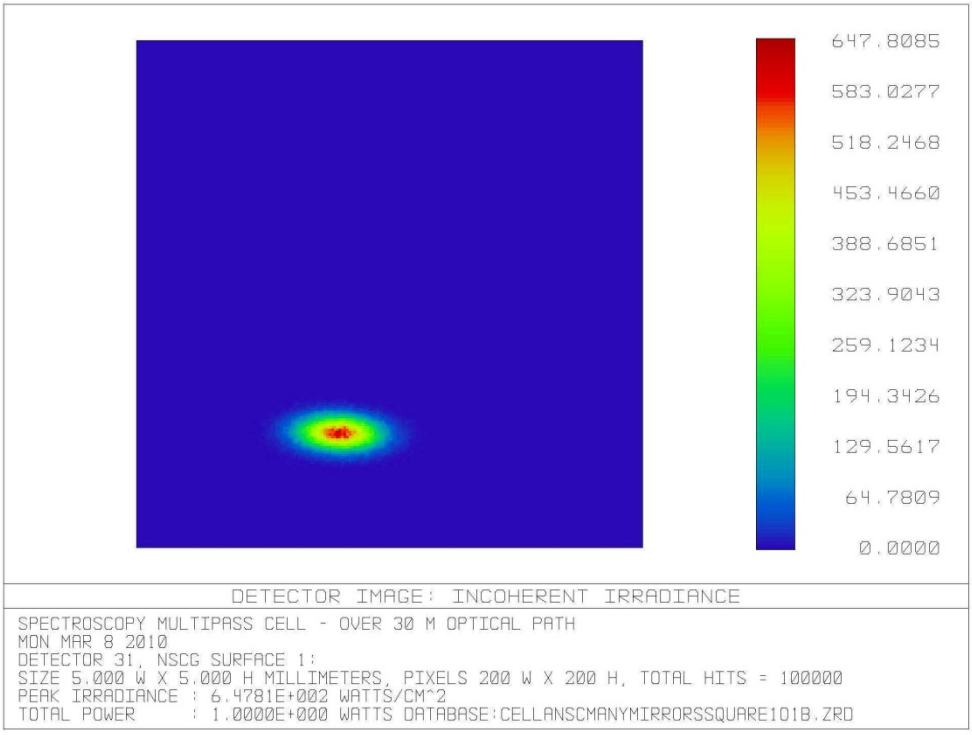

Figure 5.13: *False color irradiance acquired by a detector in correspondence of the output window of the new multipass cell. See text for details.*

5. REFERENCES

[1] K. Fukunaga, introduction to statistical pattern recognition, second edition, academic press (1990)

[2] www.scintec.it/prodotti/cmp/data_sheet_cmp30.pdf

[3] Zemax Development Corporation, www.zemax.com

POSSIBLE USE OF THE IDENTIFICATION METHOD AND DATABASE DEVELOPED FOR PUNCTUAL OR LOCAL DETECTION

1. INTRODUCTION

Until now, we have showed only devices and methods which are useful to give an alarm or recognize a substances remotely. But a big amount of technologies which has been presented could be developed in order to project and realise a local/network detector. Our database, presented in chapter 4, is developed using an experimental set up which could be used to identify a substance with almost no modification. The only job to do is to use the database and the software developed and explained in chapter five to recognize the substance. The hardware is exactly the same, the software is different. Of course, minimum detectable concentration, measurements error and many other elements related to the technique are different.

Another important element already projected but still not realized is the multipass cell. The cell was presented in chapter three. The project was developed thinking to the already explained extension of database but also with the aim to develop a local detector able to detect low concentration using a long optical path.

So, having technologies and a project of a multipass cell, we need calculus to understand real capabilities and limit of the method. While recognition limit is determined by software analysis of differences among the substances, being the developed method more related to this application than to Multiwavelenght DIAL, concentration limits of detection are completely different and they will be dealt with in this chapter. A real case is presented because it was studied for its applications in different fields. Ethylene is an interesting example of substance to be detected because it is a plant hormone which is released when plants are stressed or when fruit is coming to maturity. This could lead to application in experimental activity for aerospace application thinking of long term human exploration of space or in human activity connect to transport of vegetable and fruits. In this case the task is to quickly understand if plants in the space shuttle are stressed or not[1]. Another application is to monitor fruit maturation during storage or transportation[2,3]. Last but not least, ethylene is a stress indicator also for human body and is emitted out of lungs in different concentration depending on individual health and other factors. In this case an instrument to help diagnostics could be developed with the same principle[4,5]. For all these reasons we focus our attention on ethylene, but the same method could be applied to other substances.

1.1. Preliminary analysis of feasibility and definition of requirements

Let us focus on spatial application. A good alarm system must be able to measure concentration of ethylene down to fifty ppb. Moreover, electrical power requirements must be lower than 100 W (medium value) and volume needed by the system lower than 0.02 m^3. Let's consider just beginning as if we could use just two lines. The chosen lines correspond to the same lines chosen for the CO_2 DIAL system as "on" and "off" lines, that means 10P14, corresponding to a wavelength of 10.529 μm , and 10P16, corresponding to a wavelength of 10.549 μm. The lowest measurable concentration is determined calculating the concentration that is able to change the intensity collected at the detector due to the absorption through the path. Another approach is to measure absorption on several lines and in this case you can select line where there is quite a good absorption. In this case the calculation on minimum path needed has to be done considering the line with the minimum

absorption coefficient. Let us start calculation of path length. Attenuation is determined by Beer Lambert law:

$$I = I_0 e^{-\alpha(\nu) pl} \qquad \textbf{equation 6.1}$$

where p is the pressure, l the length, α(υ) is attenuation coefficient as a function of frequency, I_0 is the input intensity and I is the intensity measured after the path.

We make this consideration using a virtual source which is different from the one used for built the database. Absorption coefficients were determined using a different source as well which is not a commercial one, since it was developed by our research team[6,7]. Its main characteristics are reported in the following table:

TEA CO2 laser (tunable on 80 lines)	
Output Energy	500 mJ
Pulse width	100 ns
Beam divergence	0.77 mrad
Spectral range	9÷11μm

Table 6.1: *main characteristic of laser source used for ethylene limit calculation.*

Also the detectors used are different. They are J50 model made by Gentec. Their main characteristics are reported in the following table.

Receiver	
GENTEC J50	
Detector type	piroelectric
Spectral response	1100 nm ÷ 20000 nm
Peak wavelength	1064Nm
Peak response	0.45 A/W
NEP	5 x 10^{-14} W/√Hz
Dark current @ -12 V	0.80 nA
Active area	0.8 mm^2

Table 6.2: *main characteristic of detector used for ethylene absorption coefficient calculation.*

For these reasons absorption coefficients value are different from the one found for the same substance using the other source and the other detectors. The general consideration that follow will otherwise work with minor changing even considering different detectors. The detector used to calculate limit of the system is the same considered in chapter 3 for our

projected Multiwavelenght DIAL. Its main characteristics are again reported in the following figure.

Series KV104: HgCdTe Photodiodes

Series Configurations

Model*	Wavelength (µm) Peak	Cutoff	Size (mm)	Bandwidth (Hz)	D*(60FOV) (Jones,typ)	Responsivity (Amps/Watt)
KV104-1-A-3/11	10.5	>11.5	1 x 1	>20M	3E10	>4
KV104-1-A-3/12	11	>12.3	1 x 1	>20M	3E10	>4
KV104-1-A-3/10	9	>10	1 x 1	>20M	5E10	>4
KV104-0.5-A-3/11	10.5	>11.5	0.5 x 0.5	>50M	3E10	>4
KV104-0.25-A-1/11	10.5	>11.5	0.25x0.25	>100M	3E10	>4
KV104-0.1-1-E/11	10.5	>11.5	0.1 x 0.1	>500M	3E10	>4
KV104-0.5-A-2/8	7.2	>8	0.5 x 0.5	>30M	7E10	>3
KV104-1-A-7/11/TS	10.5	>11.5	1 x 1	>20M	3E10	>4
KV104-1-A-5/11/TS	10.5	>11.5	1 x 1	>20M	3E10	>4

*Key: model-size-package-window/wavelength/options

Options

Various cryogenic packages
- hold times up to 24 hours

Temperature sensor
Windows
ZnSe
ZnSe wedge
Ge

Coatings
10.6 µm
2 µm –13 µm
Cold-filters
Cold stops
- 60°, 45° ,30°

Pixel sizes 2.0 mm to 0.05 mm
Matched amplifiers available

Standard Dewar Configuration

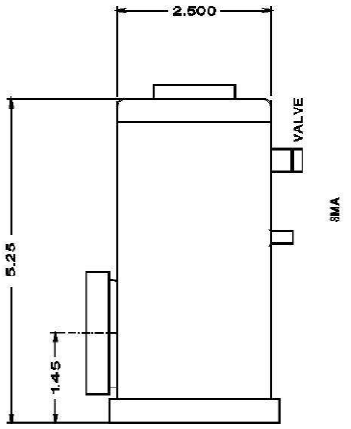

Figure 6.1: *main characteristic of detectors used for ethylene limit calculation.*

Let us start our consideration using a power of 50 mW and absorption coefficient for 10P14, 10P16 lines. The value calculated has to be compared with the Noise Equivalent Power (NEP) that is a good reference for the minimum power measurable from the detector:

$$NEP = \frac{(AB)^{\frac{1}{2}}}{D^*} = 2{,}35 \times 10^{-08}\ W \qquad \textbf{equation 6.2}$$

The sensibility of the detector is high enough to let related electronics be the real limit. Acquisition Card is an Analogic to Digital Converter (ADC) with eight bit. The system could perform measurements with a range from 0.1 mV to 10 V. We are looking for low concentration measurements, so the real problem is due to the capability to distinguish a little change in the Power received by the detector.

We can make an average of n measures so to reduce error of a factor √n, but this method does not change limit level because comparison with Signal to Noise Ratio (SNR) or NEP refers to each single measure not to a statistical sample. So we need to compare measured power (or energy) measured to the minimum measurable. Considering a conversion factor

of 74900 V/W it is impossible to receive 50 mW, corresponding to 3745 W. So we need to limit source power, or the power received by the detector in any case, to a value lower than 0.066 W. So let the range be set to five Volts, corresponding exactly to 0.066 W and consider the 2048 levels with 8 byte. The minimum difference of signal compared to the range is:

$$S_{min} = \frac{Range}{Levels} = \frac{5000}{2048} = 2{,}44\ mV \qquad \textbf{equation 6.3}$$

This signal is equivalent to a difference in power of $3{,}25*10^{-5}$ mW compared to 0.066 mW of maximum range.

Starting from this number we can calculate the path length necessary in order to have a difference in power higher than this number. Let now proceed with analysis necessary to have a correspondence of concentration and partial pressure in standard atmospheric conditions. The conversion factor from units of μg/m^3 to partial pressure is:

$$c = \frac{PM}{V * F.C.} \qquad \textbf{equation 6.4}$$

Where PM is molecular weight, in our case the value is 28.05 g/Mol, V is the volume of one mole of gas, 0.0224 m^3, and F.C. is a conversion factor dependent on the units used, in our case 10^{-6}. This value is used in the formula:

$$c(P) = c\frac{P}{1013} \qquad \textbf{equation 6.5}$$

Where pressure unit is mBar. Finally concentration measured in ppm is linked to the previous one with the following equation:

$$ppm = \frac{R * T}{F * PM} * c(P) \qquad \textbf{equation 6.6}$$

Where R is perfect gas universal constant (0.08314), T is the temperature measured in °K (298 in standard atmosphere) and F is a factor to convert unit from mBar to atmosphere.
Now we use equation 1 and find the length corresponding to the minimum signal calculated in equation 3:

$$l = -\frac{\ln\left(I / I_0\right)}{\alpha(\nu)P} \qquad \textbf{equation 6.7}$$

Now let go back to reality and consider what number can be inserted into formulas. We have different measures. We have also to deal with measures coming from literature.

Absorption coefficients measured and found in literature[8] are reported in the following picture where emission laser lines are provided instead of wavelength in the x axis.

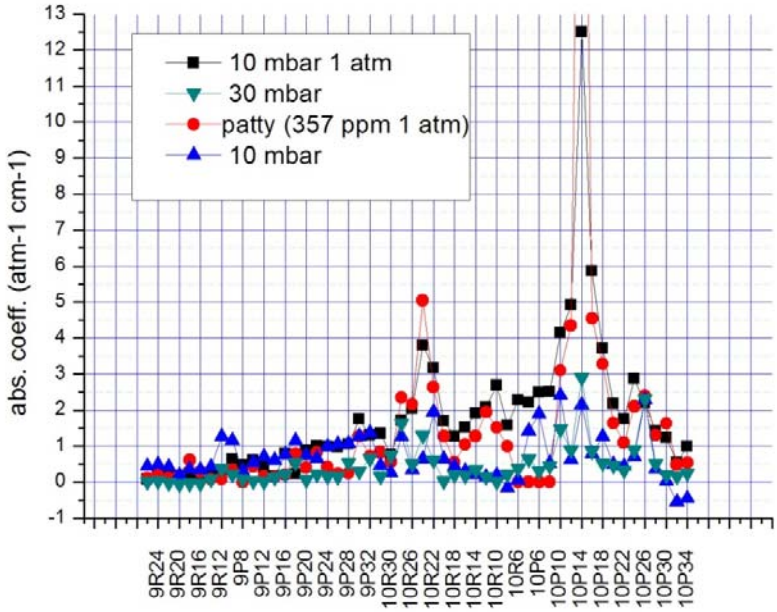

Figure 6.2: *Absorption coefficients as a function of laser emission lines for different measures and one coming from literature data. See text for details.*

Substituting the number in the equation, a minimum path length of 30 m is found for our system if we use the lower absorption coefficient provided for 10P14 CO_2 line, while a minimum Path length of 18 m using the higher one. The longer path length is chosen in order to be sure of being conservative.

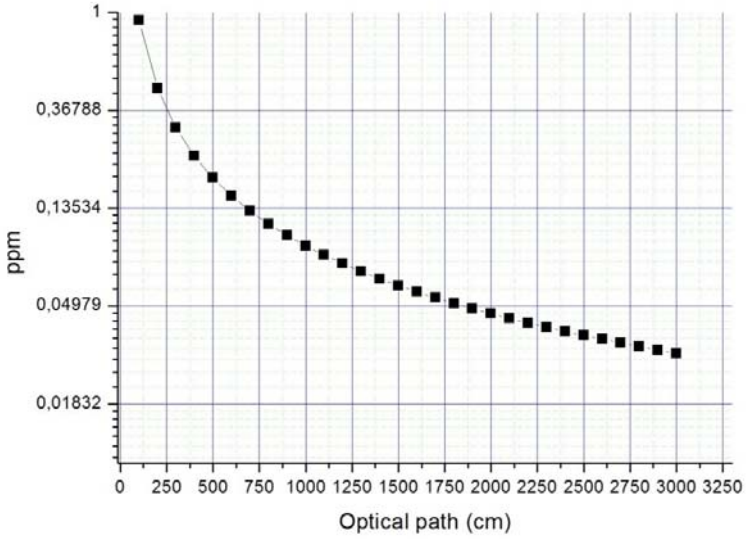

Figure 6.3: *Minimum detectable concentration of ethylene as a function of optical path, when considering the lower absorption coefficient. See text for details.*

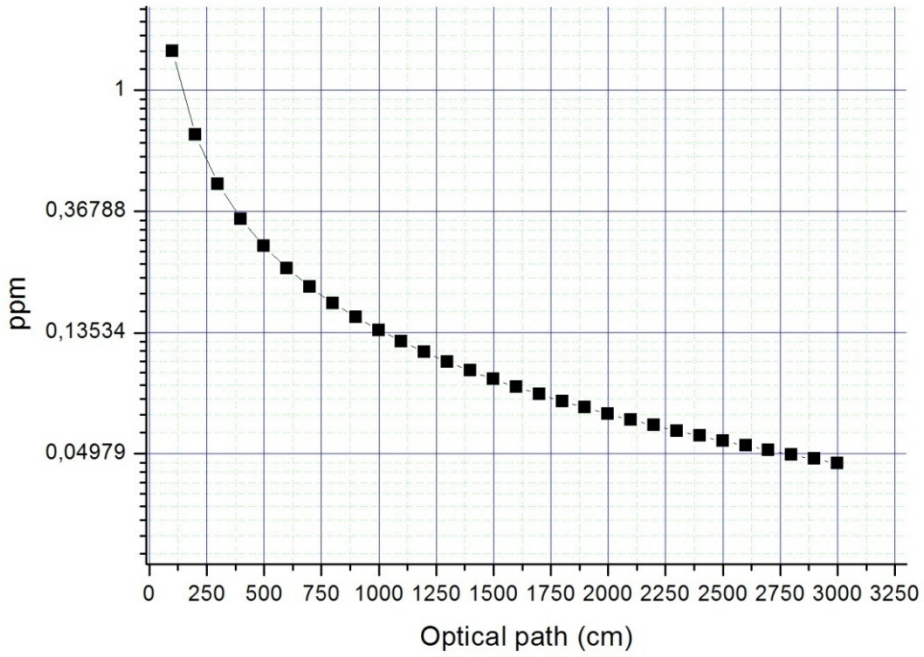

Figure 6.4: *Minimum detectable concentration of ethylene as a function of optical path, when considering the higher absorption coefficient. See text for details.*

1.2. **Concentration measurements limits**

Concentration measurements of ethylene in a sample is based on the well known Beer Lambert law, reported in equation 1. Knowing the energy absorbed by the sample inside a cell of known length and comparing it to that acquired by another sensor before the cell, is possible to calculate concentration of a known compound inside the cell. The principle is to invert equation 1 to find partial pressure, eventually later converted in other unit of measures. Cell length, or optical path in general, and absorption coefficients are known. These last were previously determined for the specific line of the chosen source. So we have:

$$P = -\frac{\ln\left(I / I_0\right)}{\alpha(\nu) l} \qquad \textbf{equation 6.8}$$

Let us know consider the error which affect our partial pressure. For this purpose error propagation has to be applied:

$$\frac{\Delta P}{P} = \frac{\Delta\alpha(\nu)}{\alpha(\nu)} + \frac{\Delta l}{l} + \frac{I_0}{I} * \frac{1}{\ln(\frac{I}{I_0})} * \Delta(\frac{I}{I_0}) \qquad \textbf{equation 6.9}$$

For each variable a priori maximum error, statistical error or square sum of both must be considered. In our case we can use the following assumption:

- Optical path error is one millimeter, so that 0.3 % is relative error using our cell set up. Even if another cell is used, relative error could be considered the same. It is not to be considered comparing its value to the other sources of error.
- Absorption coefficient error is determined experimentally as it was done for our database in chapter 4 and in some way the problem is inverted. For our measurements an error of 10% is generally found. Obviously spectroscopic method could lower relative error down to 10^{-7} but methods and task are completely different[9].
- Error on intensity ratio depends on several factor, among which the scale used and the bit used to read data detector sensitivity is low enough not to consider its value. Generally speaking, relative error could be considered around 0.5 %.

Summing up, the main error is determined by absorption coefficients.
Let us focus our attention on the following bottle neck, just mentioned in the last point of the previous list of error source: the number of bit of our electronic acquisition device. If a standard eight bit is used, the real limit of the system became the mentioned device. Let us suppose a scale of 1 mV minimum and 5 V maximum available. The minimum scale is used in case of big absorption, such that 1 mV is divided by 256 level determine by the 8 bit acquisition device (2^8=256). The minimum voltage difference in this case is 0.004 mV, which means $5.2*10^{-11}$ W of power measurable, so real limit is determined by NEP ($2.35*10^{-8}$ W). The maximum scale is used in case of very low absorption, so that minimum appreciable difference is 5 V divided by 256 levels, that is 19.6 mV. In this case the lower measurable power is $2.6*10^{-7}$ W. The detector NEP is not the limit anymore and the only chance to acquire low absorption signal in this case is to increase optical path. Otherwise, it is possible to increase the bit used. Using a 12 bit acquisition device, the levels number became 4096 and lowest measurable level go down to $1.6*10^{-8}$ W and NEP is the limit again. For this reason a 12 bit acquisition device is as important as a long path multipass cell.

2. PROBLEM RELATED TO PROTOTYPE VALIDATION

Testing the system could be quite difficult because it is needed to insert a very low quantity of material to test lower system sensitivity. There could be different method to handle low quantity of a gas. Let us refer to ethylene and use it as a general example. In our current method, ethylene concentration was measured as partial pressure and so determined by our pressure measure device. Ethylene has to be inserted in gas phase because it reach liquid phase only with pressure higher than 50 bar and temperature lower than 9.5 °C or at 1 bar pressure and temperature of -103 °C. Also in this case volume of liquid material to have 50 ppb in our cell is $1.20*10^{-12}$ c.c., quite a little volume to be handled. In gas phase volume is $1{,}56*10^{-3}$ c.c. in standard condition, while mass is $6.8*10^{-13}$ g. Using our instrumentation, we are able to measure up to 0.02 mbar because, even if device sensibility is 0.001 mbar, pressure is stable only for one minute at the pressure of 0.02 mbar that must be considered the lowest acceptable limit. This value determined a lower sensibility for ethylene concentration of 21 ppm. The only chance to reach ppb accuracy is to use different volume, one much higher than the one used when ethylene is inserted to lower concentration to the requested value. Of course also higher mechanical precision could increase vacuum control and stability.

3. CONCLUSION: A RELIABLE AND CHEAP SYSTEM BASED ON A MULTIPASS CELL IS POSSIBLE

As explained in this chapter, it is possible to built two different systems, one devoted to remote sensing and the other which is essentially a local detector, which share many components and in some way also part of software and methodology. The local detector explained in this chapter is interesting in some way also because it shares technology and is easily implementable if other resources were used to built a multiwavelenght DIAL. It is reliable and has a big sensitivity compared to other multiporpouse local sensor such as electronic nose or spectroscopy not based on a laser source. The reason why it is not commonly used is also shared with the other system: we need fingerprint database related to the system projected and to the source chosen in particular. But it is not a real limit and will be built also considering that it will be useful for different applications.

4. REFERENCES

[1]Baratto C. et al. Monitoring plants health in greenhouse for space missions, Proceedings of the Tenth International Meeting on Chemical Sensors, Sensors and Actuators, B: Chemical Volume 108, Issues 1-2, 278-284 (22 July 2005)

[2] Wisniesky M. E. Wilson C. L., Biological control of post harvest diseases in fruits and vegetables: recent advances, Hortscience, 27 94-98 (1992)

[3] Lai A. et al., Diagnosi precoce e non distruttiva di infezioni fungine in frutti di arancio in post raccolta, Italus Hortus 13 (5) 54 -58 (2006)

[4] Giubileo G. et al. Photoacoustic detection of ethylene traces in biogenic gases, laser physics n° 4 Vol. 12 653-655 (2002)

[5] Giubileo G. et al., Detection of ethylene in smokers breath by laser photoacoustic spectroscopy, SPIE proc. Vol. 5486 280-287 (1994)

[6] C. Bellecci, G. Caputi, F. De Donato, P. Gaudio, M. Valentini, CO_2 Dial for monitoring atmospheric pollutants at the University of Calabria, Il Nuovo Cimento, **18**, 5, 463-472 (1995).

[7] C. Bellecci, P. Aversa, G. Benedetti Michelangeli, G. Caputi, F. De Donato, P. Gaudio, M. Valentini and R. Zoccali, Improvement of Calabria University CO_2 laser DIAL system, Proceeding SPIE, **3104**, 154-157 (1997).

[8] R.R. Patty et al., CO_2 Laser Absorption Coefficients for determining ambient levels of O_3, NH_3, and C_2H_4, Appl. Opt. 13, 2850 (1974)

[9] Demtroder W, Laser Spectroscopy basic concepts and instrumentation 2nd edition, Springer 380-385.

CONCLUSION: AN OVERVIEW OF POSSIBLE SCENARIO AND APPLICATIONS

All the devices described in this work may be considered as part of a global project which allows to monitor a big critical area. Little LIDAR as the one projected and tested, described in chapter two, could be used to give a warning which determines a multiwavelenght-DIAL system, as the one described in chapters three, four and five, to be used for recognition of possible dangerous chemical compounds and concentration measurements. At the same time, a local detector based on multipass cell or long path organized inside a closed space, as a tube station, could give an early warning where the other systems cannot be employed. If all the information are sent to a central room of control and command, for example like the one used to monitor crisis (earthquake, flooding, etc..), a detectors system remotely controlled is able to monitor a big area. An example of this detectors net is shown in the following picture. The glass covered systems are our devices widespread in an urban area.

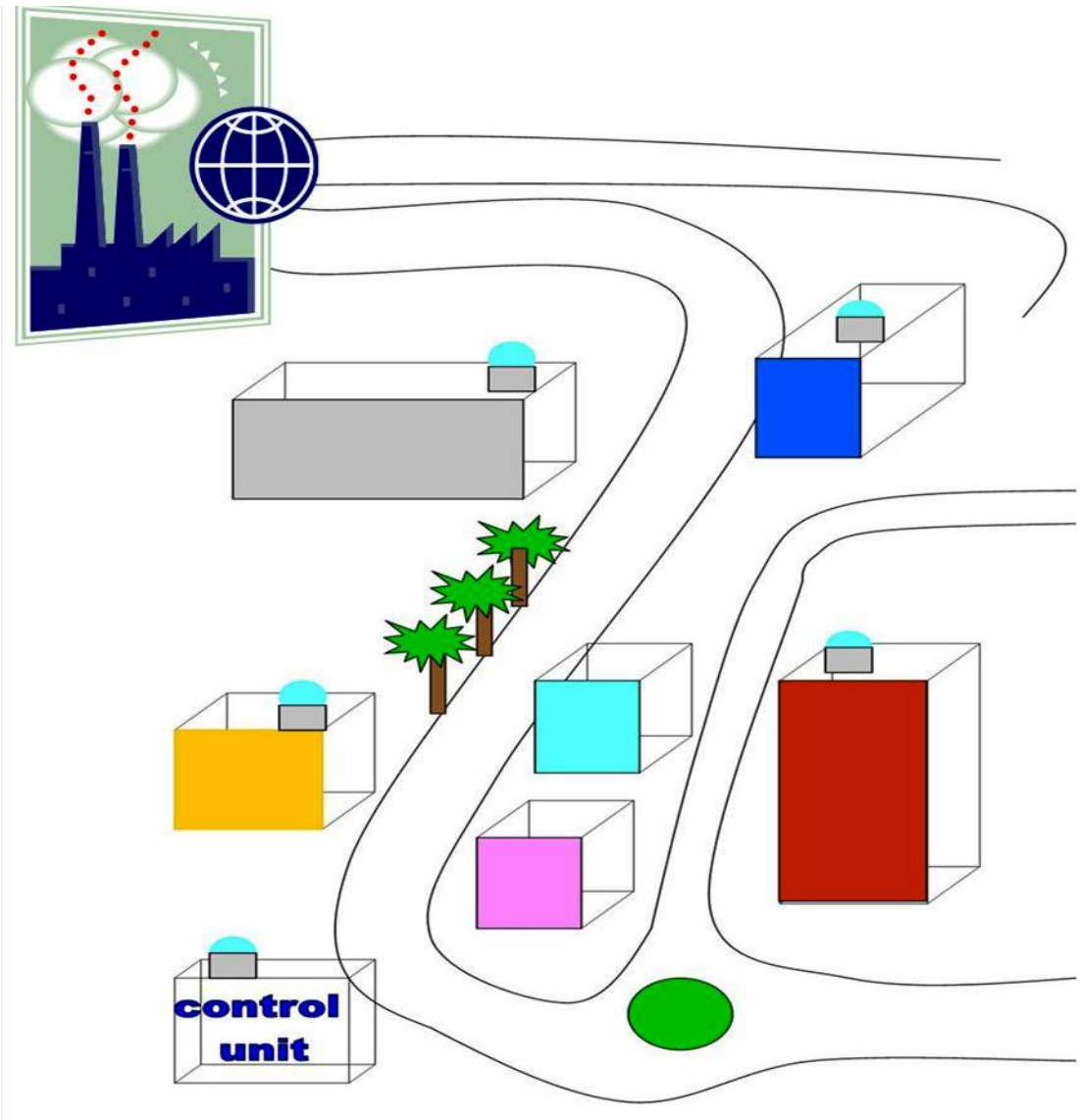

Figure 1: *Schematic representation of possible use of detector described in this work as a net to give an early warning. See text for details.*

Let us sum up our work and try to find out results, projects to be developed and possible new applications.

In chapter one we explored all existing method to identify and measure concentration of dangerous chemical compounds and describe classification and main characteristics of compounds themselves.
In chapter two we presented a mini Lidar able to give a warning that something strange is present in the atmosphere. Device is not still working and the source, the detector or both probably have to be changed. Nevertheless, experience acquired in trying developing a low cost, reliable mini Lidar could represent a first important step in projecting and making a working one. The need of such device is still present, because it is not possible to use a complex and not cheap at all system for monitoring big area. Other devices could be used only after a pre-alarm is provided by a net of low cost widespread detectors.
A new method (there is a patent pending for it[1]) and a new device project for substance identification and concentration measurement was described in chapter 3. It is based on the extension of DIAL method to many wavelengths, method already known in literature as Multiwavelenght DIAL, in this case involving not only concentration measurements but mainly recognition of unknown substances whose fingerprints where previously measured and set in a database. The recognition method is based on the application on Lidar data of multivariate statistical analysis and related methods such as neural network. Both hardware and software components are described. The method seems to be fruitful, but only in field test will demonstrate real ability of substance recognition and discrimination of the method itself. Many modification are probably needed to reach the task of an autonomous working device.
Database making is explained in chapter four. In this chapter experimental set up, including software used for data analysis, and data itself with some typical spectra are described. Problems are also described as well as possible solutions. Database is related to source and it has to be rebuilt when source changes or at least a validation must be performed. Moreover the software for discrimination is strictly connected to database and any variation will determine a modification of the software tools. For this reason database must be frozen in some point during developing to let a software do its job. So new elements in database mean new software as well.
Chapter five is used to describe the specific software used for the analysis and results of data analysis itself. In the second part possible improvements of experimental set up are described and the project of a multipass cell in particular. Many elements of the software are to be developed even considering only the database acquired since now. In particular, the software is not able to give a percentage of identification and, in some way, is not affordable in autonomous classification. The multipass cell is a project, and seems to be a good project. But there is a big difference between the project of a system and the system itself. If resources and time will be available, the affords to realize the project will show if it is as good system as a project.
Chapter six was devoted to describe a possible local detector which have many characteristics in common with the already described Multiwavelenght DIAL. In particular it is possible to use the experimental set up used for database making to make a local detector in which just data analysis is different. Data analysis will use the same database and the main software already developed for the Multiwavelenght DIAL as well. In some way the system already exist since we need just to use data acquired with our experimental set up and use already made database and software for identification. Of course real device needs a lot of engineering work to make our demonstrator a real working and reliable device.
The need of the systems described in the present work is growing every day and the resources needed to reach the task are not enormous. Moreover, also resource needed to realize a commercial device will not be such a big amount, considering the precious service provided. The system will hopefully become “the present big thing in optoelectronics” instead of being, as Lidar and DIAL are usually considered, “the next big thing in optoelectronics”.

[1]Italian Patent request n° RM2010A000211 dated 03/05/2010 “Metodo di analisi di gas in atmosfera mediante una tecnica di tipo DIAL”

ATTACHED A

LABVIEW AND MATLAB PROGRAM USED DURING EXPERIMENTAL ACTIVITY

In the following picture LABVIEW wiring diagram of programs described in chapter 4 are reported:

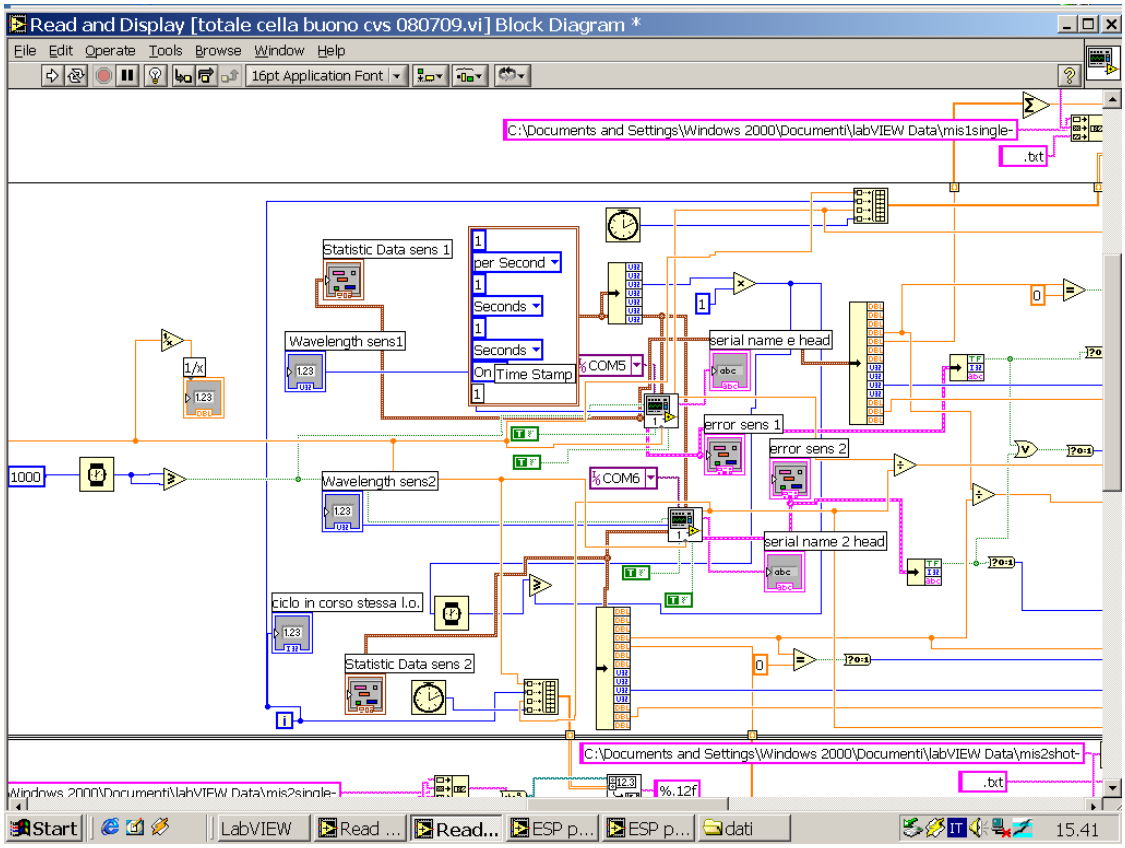

Figure 1: *Wiring diagram of labview program to automatize measures. See figure 4.4.*

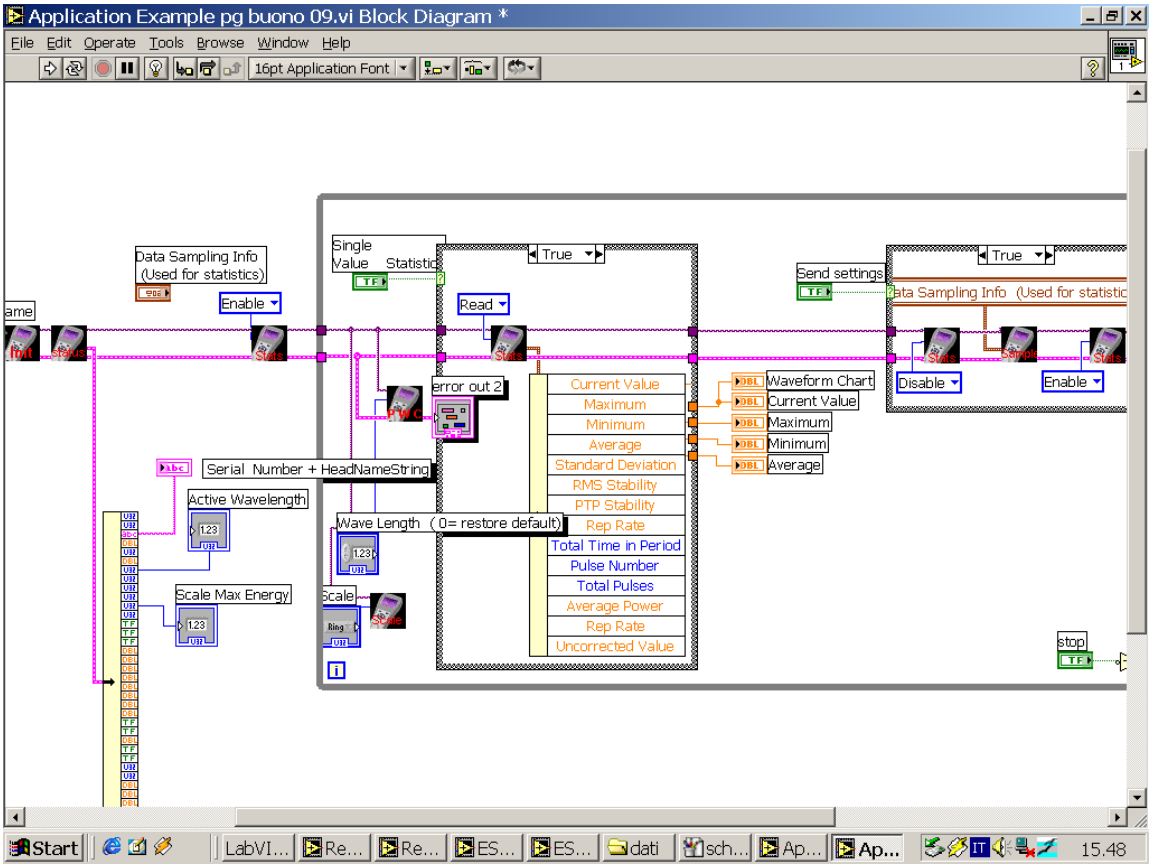

Figure 2: *Front panel and wiring diagram of sensor driver and controller. See figure 4.5.*

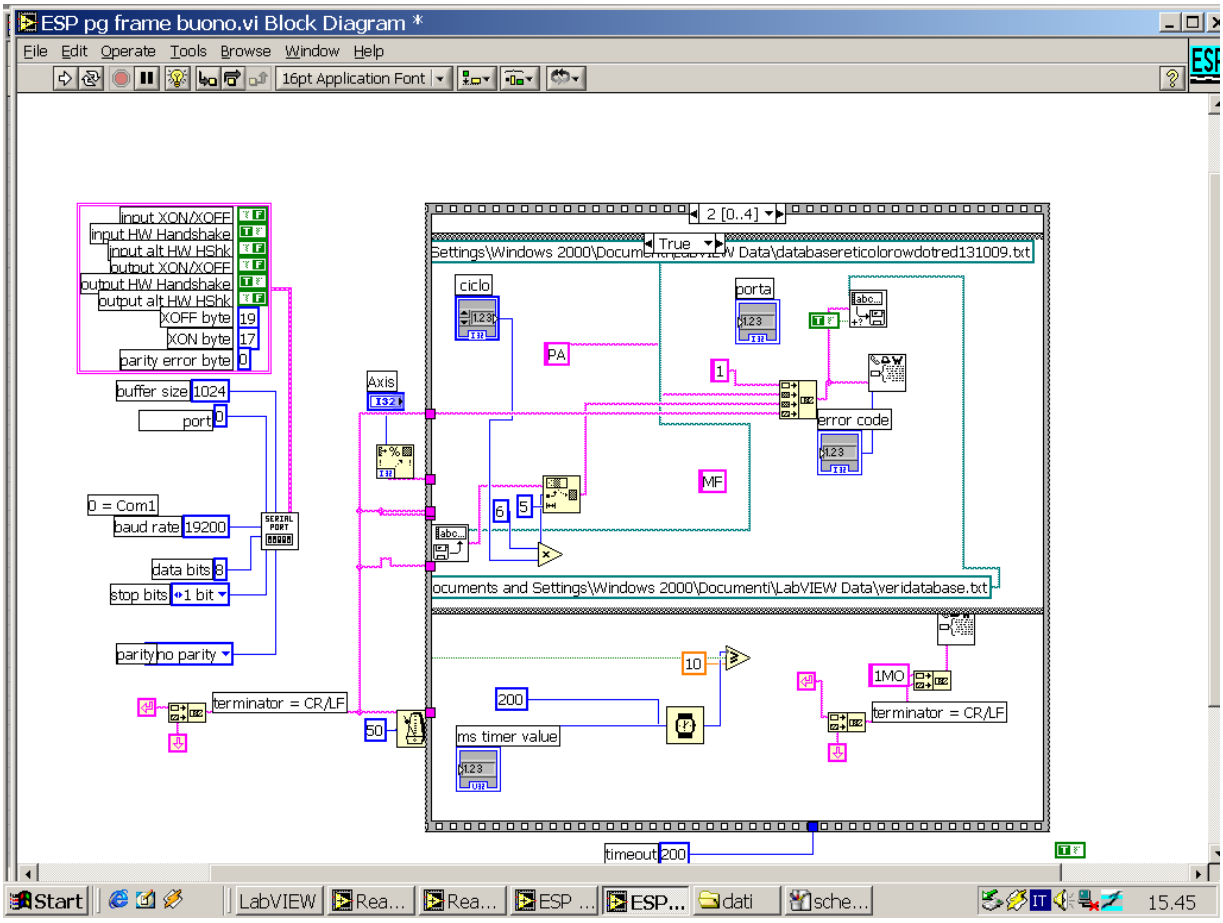

Figure 3: *Wiring diagram of grid controller. See figure 4.6.*

MATLAB PROGRAM TO ELABORATE DATA

List of MATlab command used to filter data and calculate absorption coefficients are reported. List of command are compiled for one of the substance analyzed.

```
%Calcolo del coefficiente di assorbimento di una data sostanza a partire%
% dalla conoscenza dei valori misurati prima e dopo la cella, delle caratteristiche della cella%
%e dei dati ambientali nella cella per i sensori gentec ed il laser a CO2 piccolo%
% %
% %
% %



clc
%disp('*** misurecella.m ***')
%disp('___[01] - Cancellazione variabili...')
clear all
disp('___Ok.')

fprintf('\n')
disp('___Caratteristiche della cella e condizioni ambientali')
fprintf('\n')
%lunghezza della cella in cm
l = 30.00;
errl = 0.1;
%pressione del gas sotto indagine dentro la cella in mm Hg - usualmente la
%tensione di vapore
press = 97.68;
patm=press/760;
pressmb = patm*1013;
pmis =3;
pmisatm = patm/1013;

vol=0.47719125 + 3.14152*(0.5^2)*2*6/1000+3.14152*(0.1^2)*4*1/1000; %volume cella in litri
t = 302; %temperatura
r = 0.0823; %costante dei gas
R = 8.31 % costante dei gas nel S.I.
errp = 0.01; %errore sulla pressione in mbar
errpatm = errp/760; %errore sulla pressione in atmosfere
conv = 0.001; %fattore di conversione
Nav=6.02*10^23; %numero di avogrado

num=20 ; % numero di acquisizioni per lunghezza d'onda; usato solo nel caso non ci sia dato reale
errsens = 15*10^-6;
%I = input('___inserire il valore di lunghezza della cella ');%
%l = input ('_____ valore di lunghezza della cella ')%
%I = input('___inserire il valore dela pressione ');%
%p = input ('_____ valore dela pressione ')%

%carico i file di dati in ingresso

ch1_vuota = load ('C:\Programmi\MATLAB\R2008a\work\civitavecchia\111tricloroetano\mis1single-v260509.dat');
ch2_vuota = load ('C:\Programmi\MATLAB\R2008a\work\civitavecchia\111tricloroetano\mis2single-v260509.dat');
ch12_vuota = load ('C:\Programmi\MATLAB\R2008a\work\civitavecchia\111tricloroetano\mis12single-v260509.dat');
ch1_piena = load ('C:\Programmi\MATLAB\R2008a\work\civitavecchia\111tricloroetano\mis1single-111-tricloroetano.dat');
ch2_piena = load ('C:\Programmi\MATLAB\R2008a\work\civitavecchia\111tricloroetano\mis2single-111-tricloroetano.dat');
ch12_piena = load ('C:\Programmi\MATLAB\R2008a\work\civitavecchia\111tricloroetano\mis12single-111-tricloroetano.dat');

[m,n]=size(ch1_piena);
[p,q]=size(ch12_piena);

volmat = 3;    %volume del materiale introdotto in cella in microlitri
densmat = 1.3376;   %densità del materiale introdotto in cella
massmat = volmat*densmat*10^-6; %massa introdotta in cella
PM = 133.40; %Peso molecolare della sostanza

moli= massmat/PM; %numero di moli

pcalc =moli*R*t/(vol*10^-3)*10^2; %pressione calcolata con la legge dei gas perfetti in mBar

patmcalc =pcalc/1013; %pressione calcolata con la legge dei gas perfetti in atmosfere

errpcalc=((1/t)+(0.05/volmat))*pcalc; %errore sulla pressione in mBar

errpatmcalc = errpcalc/1050;

if (patm>patmcalc)
    patm=patmcalc;
    errpatm = errpatmcalc;
end

if (patm>patmmis+0.01)
    patm=patmmis;
    errpatm=0.5/1013;
end

coeff=(patm*vol)/(r*t*l*vol);

for k=1:m+1;
rapppienacalcparz(k) = 0;
rappvuotocalcparz(k) = 0;
ch1v(k)=0;
ch2v(k)=0;
ch1p(k)=0;
ch2p(k)=0;
end

format long;

for k = 1:m;
    rappvuotocalcparz(k) = ch1_vuota(k,3)./ch2_vuota(k,3); %rapporto tra i canali calcolato da matlab cella vuota
    ch1v(k) = ch1_vuota(k,3); %assegnazione valori canale 1 cella vuota
    ch2v(k) = ch2_vuota(k,3); %assegnazione valori canale 2 cella vuota
    ch1p(k) = ch1_piena(k,3); %assegnazione valori canale 1 cella piena
```

```
    ch2p(k) = ch2_piena(k,3); %assegnazione valori canale 2 cella piena
    rapppienacalcparz(k) = ch1p(k)./ch2p(k); %rapporto tra i canali  calcolato da matlab cella piena
    numvoutini(k) = 0;
    numpoutini(k) =0;


end


%estrazione dei punti corrispondenti a ciascuna lunghezza d'onda per tutte le variabili

for i=1:p;
    for j=20*i-19:20*i;



        subch1p(i,j) = ch1p(j);
        subch2p(i,j) = ch2p(j);
        subch1v(i,j) = ch1v(j);
        subch2v(i,j) = ch2v(j);
        subrappvuotocalc(i,j)=rappvuotocalcparz(j);
        subrapppienacalc(i,j)=rapppienacalcparz(j);

    end
end

%estrazione dei rapporti dalle matrici per lunghezza d'onda e calcolo della
%mediana per la cella vuota

extsubrappvuotocalc1 = subrappvuotocalc(1,20*1-19:20*1);
medianv1 = median(extsubrappvuotocalc1);
extsubrappvuotocalc2 = subrappvuotocalc(2,20*2-19:20*2);
medianv2 = median(extsubrappvuotocalc2);
extsubrappvuotocalc3 = subrappvuotocalc(3,20*3-19:20*3);
medianv3 = median(extsubrappvuotocalc3);
extsubrappvuotocalc4 = subrappvuotocalc(4,20*4-19:20*4);
medianv4 = median(extsubrappvuotocalc4);
extsubrappvuotocalc5 = subrappvuotocalc(5,20*5-19:20*5);
medianv5 = median(extsubrappvuotocalc5);
extsubrappvuotocalc6 = subrappvuotocalc(6,20*6-19:20*6);
medianv6 = median(extsubrappvuotocalc6);
extsubrappvuotocalc7 = subrappvuotocalc(7,20*7-19:20*7);
medianv7 = median(extsubrappvuotocalc7);
extsubrappvuotocalc8 = subrappvuotocalc(8,20*8-19:20*8);
medianv8 = median(extsubrappvuotocalc8);
extsubrappvuotocalc9 = subrappvuotocalc(9,20*9-19:20*9);
medianv9 = median(extsubrappvuotocalc9);
extsubrappvuotocalc10 = subrappvuotocalc(10,20*10-19:20*10);
medianv10 = median(extsubrappvuotocalc10);
extsubrappvuotocalc11 = subrappvuotocalc(11,20*11-19:20*11);
medianv11 = median(extsubrappvuotocalc11);
extsubrappvuotocalc12 = subrappvuotocalc(12,20*12-19:20*12);
medianv12 = median(extsubrappvuotocalc12);
extsubrappvuotocalc13 = subrappvuotocalc(13,20*13-19:20*13);
medianv13 = median(extsubrappvuotocalc13);
extsubrappvuotocalc14 = subrappvuotocalc(14,20*14-19:20*14);
medianv14 = median(extsubrappvuotocalc14);
extsubrappvuotocalc15 = subrappvuotocalc(15,20*15-19:20*15);
medianv15 = median(extsubrappvuotocalc15);
extsubrappvuotocalc16 = subrappvuotocalc(16,20*16-19:20*16);
medianv16 = median(extsubrappvuotocalc16);
extsubrappvuotocalc17 = subrappvuotocalc(17,20*17-19:20*17);
medianv17 = median(extsubrappvuotocalc17);
extsubrappvuotocalc18 = subrappvuotocalc(18,20*18-19:20*18);
medianv18 = median(extsubrappvuotocalc18);
extsubrappvuotocalc19 = subrappvuotocalc(19,20*19-19:20*19);
medianv19 = median(extsubrappvuotocalc19);
extsubrappvuotocalc20 = subrappvuotocalc(20,20*20-19:20*20);
medianv20 = median(extsubrappvuotocalc20);
extsubrappvuotocalc21 = subrappvuotocalc(21,20*21-19:20*21);
medianv21 = median(extsubrappvuotocalc21);
extsubrappvuotocalc22 = subrappvuotocalc(22,20*22-19:20*22);
medianv22 = median(extsubrappvuotocalc22);
extsubrappvuotocalc23 = subrappvuotocalc(23,20*23-19:20*23);
medianv23 = median(extsubrappvuotocalc23);
extsubrappvuotocalc24 = subrappvuotocalc(24,20*24-19:20*24);
medianv24 = median(extsubrappvuotocalc24);
extsubrappvuotocalc25 = subrappvuotocalc(25,20*25-19:20*25);
medianv25 = median(extsubrappvuotocalc25);
extsubrappvuotocalc26 = subrappvuotocalc(26,20*26-19:20*26);
medianv26 = median(extsubrappvuotocalc26);
extsubrappvuotocalc27 = subrappvuotocalc(27,20*27-19:20*27);
medianv27 = median(extsubrappvuotocalc27);
extsubrappvuotocalc28 = subrappvuotocalc(28,20*28-19:20*28);
medianv28 = median(extsubrappvuotocalc28);
extsubrappvuotocalc29 = subrappvuotocalc(29,20*29-19:20*29);
medianv29 = median(extsubrappvuotocalc29);
extsubrappvuotocalc30 = subrappvuotocalc(30,20*30-19:20*30);
medianv30 = median(extsubrappvuotocalc30);
extsubrappvuotocalc31 = subrappvuotocalc(31,20*31-19:20*31);
medianv31 = median(extsubrappvuotocalc31);
extsubrappvuotocalc32 = subrappvuotocalc(32,20*32-19:20*32);
medianv32 = median(extsubrappvuotocalc32);
extsubrappvuotocalc33 = subrappvuotocalc(33,20*33-19:20*33);
medianv33 = median(extsubrappvuotocalc33);
extsubrappvuotocalc34 = subrappvuotocalc(34,20*34-19:20*34);
medianv34 = median(extsubrappvuotocalc34);
extsubrappvuotocalc35 = subrappvuotocalc(35,20*35-19:20*35);
medianv35 = median(extsubrappvuotocalc35);
extsubrappvuotocalc36 = subrappvuotocalc(36,20*36-19:20*36);
medianv36 = median(extsubrappvuotocalc36);
extsubrappvuotocalc37 = subrappvuotocalc(37,20*37-19:20*37);
medianv37 = median(extsubrappvuotocalc37);
extsubrappvuotocalc38 = subrappvuotocalc(38,20*38-19:20*38);
medianv38 = median(extsubrappvuotocalc38);
extsubrappvuotocalc39 = subrappvuotocalc(39,20*39-19:20*39);
medianv39 = median(extsubrappvuotocalc39);
extsubrappvuotocalc40 = subrappvuotocalc(40,20*40-19:20*40);
```

```
medianv40 = median(extsubrappvuotocalc40);
extsubrappvuotocalc41 = subrappvuotocalc(41,20*41-19:20*41);
medianv41 = median(extsubrappvuotocalc41);
extsubrappvuotocalc42 = subrappvuotocalc(42,20*42-19:20*42);
medianv42 = median(extsubrappvuotocalc42);
extsubrappvuotocalc43 = subrappvuotocalc(43,20*43-19:20*43);
medianv43 = median(extsubrappvuotocalc43);
extsubrappvuotocalc44 = subrappvuotocalc(44,20*44-19:20*44);
medianv44 = median(extsubrappvuotocalc44);
extsubrappvuotocalc45 = subrappvuotocalc(45,20*45-19:20*45);
medianv45 = median(extsubrappvuotocalc45);
extsubrappvuotocalc46 = subrappvuotocalc(46,20*46-19:20*46);
medianv46 = median(extsubrappvuotocalc46);
extsubrappvuotocalc47 = subrappvuotocalc(47,20*47-19:20*47);
medianv47 = median(extsubrappvuotocalc47);
extsubrappvuotocalc48 = subrappvuotocalc(48,20*48-19:20*48);
medianv48 = median(extsubrappvuotocalc48);
extsubrappvuotocalc49 = subrappvuotocalc(49,20*49-19:20*49);
medianv49 = median(extsubrappvuotocalc49);
extsubrappvuotocalc50 = subrappvuotocalc(50,20*50-19:20*50);
medianv50 = median(extsubrappvuotocalc50);
extsubrappvuotocalc51 = subrappvuotocalc(51,20*51-19:20*51);
medianv51 = median(extsubrappvuotocalc51);
extsubrappvuotocalc52 = subrappvuotocalc(52,20*52-19:20*52);
medianv52 = median(extsubrappvuotocalc52);
extsubrappvuotocalc53 = subrappvuotocalc(53,20*53-19:20*53);
medianv53 = median(extsubrappvuotocalc53);
extsubrappvuotocalc54 = subrappvuotocalc(54,20*54-19:20*54);
medianv54 = median(extsubrappvuotocalc54);
extsubrappvuotocalc55 = subrappvuotocalc(55,20*55-19:20*55);
medianv55 = median(extsubrappvuotocalc55);
extsubrappvuotocalc56 = subrappvuotocalc(56,20*56-19:20*56);
medianv56 = median(extsubrappvuotocalc56);
extsubrappvuotocalc57 = subrappvuotocalc(57,20*57-19:20*57);
medianv57 = median(extsubrappvuotocalc57);
extsubrappvuotocalc58 = subrappvuotocalc(58,20*58-19:20*58);
medianv58 = median(extsubrappvuotocalc58);
extsubrappvuotocalc59 = subrappvuotocalc(59,20*59-19:20*59);
medianv59 = median(extsubrappvuotocalc59);
extsubrappvuotocalc60 = subrappvuotocalc(60,20*60-19:20*60);
medianv60 = median(extsubrappvuotocalc60);
extsubrappvuotocalc61 = subrappvuotocalc(61,20*61-19:20*61);
medianv61 = median(extsubrappvuotocalc61);
extsubrappvuotocalc62 = subrappvuotocalc(62,20*62-19:20*62);
medianv62 = median(extsubrappvuotocalc62);


%estrazione dei rapporti dalle matrici per lunghezza d'onda e calcolo della
%mediana per la cella piena

extsubrapppienacalc1 = subrapppienacalc(1,20*1-19:20*1);
medianp1 = median(extsubrapppienacalc1);
extsubrapppienacalc2 = subrapppienacalc(2,20*2-19:20*2);
medianp2 = median(extsubrapppienacalc2);
extsubrapppienacalc3 = subrapppienacalc(3,20*3-19:20*3);
medianp3 = median(extsubrapppienacalc3);
extsubrapppienacalc4 = subrapppienacalc(4,20*4-19:20*4);
medianp4 = median(extsubrapppienacalc4);
extsubrapppienacalc5 = subrapppienacalc(5,20*5-19:20*5);
medianp5 = median(extsubrapppienacalc5);
extsubrapppienacalc6 = subrapppienacalc(6,20*6-19:20*6);
medianp6 = median(extsubrapppienacalc6);
extsubrapppienacalc7 = subrapppienacalc(7,20*7-19:20*7);
medianp7 = median(extsubrapppienacalc7);
extsubrapppienacalc8 = subrapppienacalc(8,20*8-19:20*8);
medianp8 = median(extsubrapppienacalc8);
extsubrapppienacalc9 = subrapppienacalc(9,20*9-19:20*9);
medianp9 = median(extsubrapppienacalc9);
extsubrapppienacalc10 = subrapppienacalc(10,20*10-19:20*10);
medianp10 = median(extsubrapppienacalc10);
extsubrapppienacalc11 = subrapppienacalc(11,20*11-19:20*11);
medianp11 = median(extsubrapppienacalc11);
extsubrapppienacalc12 = subrapppienacalc(12,20*12-19:20*12);
medianp12 = median(extsubrapppienacalc12);
extsubrapppienacalc13 = subrapppienacalc(13,20*13-19:20*13);
medianp13 = median(extsubrapppienacalc13);
extsubrapppienacalc14 = subrapppienacalc(14,20*14-19:20*14);
medianp14 = median(extsubrapppienacalc14);
extsubrapppienacalc15 = subrapppienacalc(15,20*15-19:20*15);
medianp15 = median(extsubrapppienacalc15);
extsubrapppienacalc16 = subrapppienacalc(16,20*16-19:20*16);
medianp16 = median(extsubrapppienacalc16);
extsubrapppienacalc17 = subrapppienacalc(17,20*17-19:20*17);
medianp17 = median(extsubrapppienacalc17);
extsubrapppienacalc18 = subrapppienacalc(18,20*18-19:20*18);
medianp18 = median(extsubrapppienacalc18);
extsubrapppienacalc19 = subrapppienacalc(19,20*19-19:20*19);
medianp19 = median(extsubrapppienacalc19);
extsubrapppienacalc20 = subrapppienacalc(20,20*20-19:20*20);
medianp20 = median(extsubrapppienacalc20);
extsubrapppienacalc21 = subrapppienacalc(21,20*21-19:20*21);
medianp21 = median(extsubrapppienacalc21);
extsubrapppienacalc22 = subrapppienacalc(22,20*22-19:20*22);
medianp22 = median(extsubrapppienacalc22);
extsubrapppienacalc23 = subrapppienacalc(23,20*23-19:20*23);
medianp23 = median(extsubrapppienacalc23);
extsubrapppienacalc24 = subrapppienacalc(24,20*24-19:20*24);
medianp24 = median(extsubrapppienacalc24);
extsubrapppienacalc25 = subrapppienacalc(25,20*25-19:20*25);
medianp25 = median(extsubrapppienacalc25);
extsubrapppienacalc26 = subrapppienacalc(26,20*26-19:20*26);
medianp26 = median(extsubrapppienacalc26);
extsubrapppienacalc27 = subrapppienacalc(27,20*27-19:20*27);
medianp27 = median(extsubrapppienacalc27);
extsubrapppienacalc28 = subrapppienacalc(28,20*28-19:20*28);
medianp28 = median(extsubrapppienacalc28);
extsubrapppienacalc29 = subrapppienacalc(29,20*29-19:20*29);
medianp29 = median(extsubrapppienacalc29);
```

```
extsubrapppienacalc30 = subrapppienacalc(30,20*30-19:20*30);
medianp30 = median(extsubrapppienacalc30);
extsubrapppienacalc31 = subrapppienacalc(31,20*31-19:20*31);
medianp31 = median(extsubrapppienacalc31);
extsubrapppienacalc32 = subrapppienacalc(32,20*32-19:20*32);
medianp32 = median(extsubrapppienacalc32);
extsubrapppienacalc33 = subrapppienacalc(33,20*33-19:20*33);
medianp33 = median(extsubrapppienacalc33);
extsubrapppienacalc34 = subrapppienacalc(34,20*34-19:20*34);
medianp34 = median(extsubrapppienacalc34);
extsubrapppienacalc35 = subrapppienacalc(35,20*35-19:20*35);
medianp35 = median(extsubrapppienacalc35);
extsubrapppienacalc36 = subrapppienacalc(36,20*36-19:20*36);
medianp36 = median(extsubrapppienacalc36);
extsubrapppienacalc37 = subrapppienacalc(37,20*37-19:20*37);
medianp37 = median(extsubrapppienacalc37);
extsubrapppienacalc38 = subrapppienacalc(38,20*38-19:20*38);
medianp38 = median(extsubrapppienacalc38);
extsubrapppienacalc39 = subrapppienacalc(39,20*39-19:20*39);
medianp39 = median(extsubrapppienacalc39);
extsubrapppienacalc40 = subrapppienacalc(40,20*40-19:20*40);
medianp40 = median(extsubrapppienacalc40);
extsubrapppienacalc41 = subrapppienacalc(41,20*41-19:20*41);
medianp41 = median(extsubrapppienacalc41);
extsubrapppienacalc42 = subrapppienacalc(42,20*42-19:20*42);
medianp42 = median(extsubrapppienacalc42);
extsubrapppienacalc43 = subrapppienacalc(43,20*43-19:20*43);
medianp43 = median(extsubrapppienacalc43);
extsubrapppienacalc44 = subrapppienacalc(44,20*44-19:20*44);
medianp44 = median(extsubrapppienacalc44);
extsubrapppienacalc45 = subrapppienacalc(45,20*45-19:20*45);
medianp45 = median(extsubrapppienacalc45);
extsubrapppienacalc46 = subrapppienacalc(46,20*46-19:20*46);
medianp46 = median(extsubrapppienacalc46);
extsubrapppienacalc47 = subrapppienacalc(47,20*47-19:20*47);
medianp47 = median(extsubrapppienacalc47);
extsubrapppienacalc48 = subrapppienacalc(48,20*48-19:20*48);
medianp48 = median(extsubrapppienacalc48);
extsubrapppienacalc49 = subrapppienacalc(49,20*49-19:20*49);
medianp49 = median(extsubrapppienacalc49);
extsubrapppienacalc50 = subrapppienacalc(50,20*50-19:20*50);
medianp50 = median(extsubrapppienacalc50);
extsubrapppienacalc51 = subrapppienacalc(51,20*51-19:20*51);
medianp51 = median(extsubrapppienacalc51);
extsubrapppienacalc52 = subrapppienacalc(52,20*52-19:20*52);
medianp52 = median(extsubrapppienacalc52);
extsubrapppienacalc53 = subrapppienacalc(53,20*53-19:20*53);
medianp53 = median(extsubrapppienacalc53);
extsubrapppienacalc54 = subrapppienacalc(54,20*54-19:20*54);
medianp54 = median(extsubrapppienacalc54);
extsubrapppienacalc55 = subrapppienacalc(55,20*55-19:20*55);
medianp55 = median(extsubrapppienacalc55);
extsubrapppienacalc56 = subrapppienacalc(56,20*56-19:20*56);
medianp56 = median(extsubrapppienacalc56);
extsubrapppienacalc57 = subrapppienacalc(57,20*57-19:20*57);
medianp57 = median(extsubrapppienacalc57);
extsubrapppienacalc58 = subrapppienacalc(58,20*58-19:20*58);
medianp58 = median(extsubrapppienacalc58);
extsubrapppienacalc59 = subrapppienacalc(59,20*59-19:20*59);
medianp59 = median(extsubrapppienacalc59);
extsubrapppienacalc60 = subrapppienacalc(60,20*60-19:20*60);
medianp60 = median(extsubrapppienacalc60);
extsubrapppienacalc61 = subrapppienacalc(61,20*61-19:20*61);
medianp61 = median(extsubrapppienacalc61);
extsubrapppienacalc62 = subrapppienacalc(62,20*62-19:20*62);
medianp62 = median(extsubrapppienacalc62);


%trasformazione delle mediane in vettore per i calcoli successivi

medianv = [medianv1 medianv2 medianv3 medianv4 medianv5 medianv6 medianv7 medianv8 medianv9 medianv10 medianv11 medianv12 medianv13
medianv14 medianv15 medianv16 medianv17 medianv18 medianv19 medianv20 medianv21 medianv22 medianv23 medianv24 medianv25 medianv26
medianv27 medianv28 medianv29 medianv30 medianv31 medianv32 medianv33 medianv34 medianv35 medianv36 medianv37 medianv38 medianv39
medianv40 medianv41 medianv42 medianv43 medianv44 medianv45 medianv46 medianv47 medianv48 medianv49 medianv50 medianv51 medianv52
medianv53 medianv54 medianv55 medianv56 medianv57 medianv58 medianv59 medianv60 medianv61 medianv62];
medianp = [medianp1 medianp2 medianp3 medianp4 medianp5 medianp6 medianp7 medianp8 medianp9 medianp10 medianp11 medianp12 medianp13
medianp14 medianp15 medianp16 medianp17 medianp18 medianp19 medianp20 medianp21 medianp22 medianp23 medianp24 medianp25 medianp26
medianp27 medianp28 medianp29 medianp30 medianp31 medianp32 medianp33 medianp34 medianp35 medianp36 medianp37 medianp38 medianp39
medianp40 medianp41 medianp42 medianp43 medianp44 medianp45 medianp46 medianp47 medianp48 medianp49 medianp50 medianp51 medianp52
medianp53 medianp54 medianp55 medianp56 medianp57 medianp58 medianp59 medianp60 medianp61 medianp62];


  %estromissione dei dati non attendibili tramite sostutuzione con la mediana


for i=1:p;
  for j=20*i-19:20*i;
    if ((rappvuotocalcparz(j)>0.3) & (rappvuotocalcparz(j)<2))
       subrappvuotocalc(i,j)=rappvuotocalcparz(j);
    else subrappvuotocalc(i,j)=medianv(i);
        numvoutini(j)=1;
    end

   if ((rapppienacalcparz(j)>0.1) & (rapppienacalcparz(j)<2))
       subrapppienacalc(i,j)=rapppienacalcparz(j);
    else subrapppienacalc(i,j)=medianp(i);
         numpoutini(j)=1;
    end
  end
end

for i=1:p;
  for j=20*i-19:20*i;
      numoutv(i,j)=0;
      numoutp(i,j)=0;
  end
end
```

```
%selezione dei valori che debbono essere sostituiti in base alla distanza
%dalla mediana cambiando il rapporto con il vicino con eventuale
%sostituzione con la mediana
%in caso di permanenza di distanza eccessiva

delta=0.15; %valore che esprime la varianza dei punti rispetto alla mediana tollerata

for i=1:p;
    for j=20*i-18:20*i;
        if ((  subrappvuotocalc(i,j)>medianv(i)-delta) & (subrappvuotocalc(i,j)<medianv(i)+delta))
            subrappvuotocalc(i,j)= subrappvuotocalc(i,j);
        else subrappvuotocalc(i,j) = ch1v(j-1)./ch2v(j);
        end
    end
end
for i=1:p;
    for j=20*i-19:20*i;
      if ((  subrappvuotocalc(i,j)>medianv(i)-delta) & (subrappvuotocalc(i,j)<medianv(i)+delta))
                subrappvuotocalc(i,j)= subrappvuotocalc(i,j);
            else subrappvuotocalc(i,j)= ch1v(j+1)./ch2v(j);
      end
    end
end
for i=1:p;
    for j=20*i-19:20*i;
          if ((  subrappvuotocalc(i,j)>medianv(i)-delta) & (subrappvuotocalc(i,j)<medianv(i)+delta))
                subrappvuotocalc(i,j)= subrappvuotocalc(i,j);
                else subrappvuotocalc(i,j)= medianv(i);
                      numoutv(i,j)=1;
          end
    end
end


 for i=1:p;
    for j=20*i-18:20*i;
        if ((  subrapppienacalc(i,j)>medianp(i)-delta) & (subrapppienacalc(i,j)<medianp(i)+delta))
            subrapppienacalc(i,j)= subrapppienacalc(i,j);
        else subrapppienacalc(i,j) = ch1p(j-1)./ch2p(j);
        end
    end
end
for i=1:p;
    for j=20*i-19:20*i;
      if ((  subrapppienacalc(i,j)>medianp(i)-delta) & (subrapppienacalc(i,j)<medianp(i)+delta))
                subrapppienacalc(i,j)= subrapppienacalc(i,j);
            else subrapppienacalc(i,j)= ch1p(j+1)./ch2p(j);
      end
    end
end
for i=1:p;
    for j=20*i-19:20*i;
          if ((  subrapppienacalc(i,j)>medianp(i)-delta) & (subrapppienacalc(i,j)<medianp(i)+delta))
                subrapppienacalc(i,j)= subrapppienacalc(i,j);
                else subrapppienacalc(i,j)= medianp(i);
                      numoutv(i,j)=1;
          end
    end
end


for i=1:p;
    for j=20*i-19:20*i;

        %estrazione dei punti corrispondenti a ciascuna lunghezza d'onda
        %per i contatori

        subnumoutv(i,j) = numoutv(j);
        subnumoutp(i,j) = numoutp(j);
        subnumvoutini(i,j) = numvoutini(j);
        subnumpoutini(i,j) = numpoutini(j);


    end
end
%trasposizione delle matrici, calcolo delle somme dei canali e delle
%quantita' per il calcolo dei numeri da sottrarre al numero di aquisizioni
subch1pt = subch1p';
subch2pt = subch2p';
subch1vt = subch1v';
subch2vt = subch2v';
subnumvoutinit = subnumvoutini';
subnumpoutinit = subnumpoutini';
subnumoutvt = subnumoutv';
subnumoutpt = subnumoutp';

sumsubch1pt = sum(subch1pt);
sumsubch2pt = sum(subch2pt);
sumsubch1vt = sum(subch1vt);
sumsubch2vt = sum(subch2vt);
sumsubnumvoutinit = sum(subnumvoutinit);
sumsubnumpoutinit = sum(subnumpoutinit);
sumsubnumoutvt = sum(subnumoutvt);
sumsubnumoutpt = sum(subnumoutpt);
subrappvuotocalct = subrappvuotocalc';
subrapppienacalct = subrapppienacalc';
sumsubrappvuotocalct = sum(subrappvuotocalct);
sumsubrapppienacalct = sum(subrapppienacalct);

for i=1:p;
    numoutvtot(i) = sumsubnumoutvt(i) + sumsubnumvoutinit(i);
    numoutptot(i) = sumsubnumoutpt(i) + sumsubnumpoutinit(i);
    if (numoutvtot(i)>10)
        allarmev(i)=1;
    else
        allarmev(i)=0;
    end
     if (numoutptot(i)>10)
```

```
        allarmep(i)=1;
     else
         allarmep(i)=0;
    end
end
%deviazione standard non corretta sulla base delle modifiche


stdsubch1pt = std(subch1pt);
stdsubch2pt = std(subch2pt);
stdsubch1vt = std(subch1vt);
stdsubch2vt = std(subch2vt);

%calcolo dei numeri effettivi per sottrazione, dei rapporti medi a pieno e a
%vuoto

for i=1:p;
    %stdrappvuotocalc(i)=std(subrappvuotocalc(i));
    %stdrapppienacalc(i)=std(subrapppienacalc(i));
    numtotp(i)=num; %-sumsubnumpupt(i)-sumnumoutpt(i);
    numtotv(i)=num; %-sumsubnumvupt(i)-sumsubnumvdownt(i)-sumnumoutvt(i);
end

for i=1:p;
    rappvuotocalc(i)=sumsubrappvuotocalct(i)./num;
    rapppienacalc(i)=sumsubrapppienacalct(i)./num;
end

%calcolo delle deviazioni standard corrette per mezzo delle deviazioni

for i=1:p;
     for j=20*i-19:20*i;
    devrappvuotocalc(i,j) = (rappvuotocalc(i) - subrappvuotocalc(i,j))^2; %deviazione cella vuota
    devrapppienacalc(i,j) = (rapppienacalc(i) - subrapppienacalc(i,j))^2;  %deviazione cella piena
     end
end

devrappvuotocalct = devrappvuotocalc';
devrapppienacalct = devrapppienacalc';

sumdevrappvuotocalct = sum(devrappvuotocalct);
sumdevrapppienacalct = sum(devrapppienacalct);

for i=1:p;
stdrappvuotocalc(i) = (sumdevrappvuotocalct(i)./num)^0.5;  %deviazione standard cella vuota
stdrapppienacalc(i) = (sumdevrapppienacalct(i)./num)^0.5;  %deviazione standard cella piena
end

for i = 1:p;

    lambda(i) = ch12_vuota(i,1); %lunghezze d'onda delle righe impiegate - ripetuta per ogni ciclo

    %misure e calcoli relativi alla cella vuota


    rappvuotomis(i) = ch12_vuota(i,2); %rapporto tra i canali calcolato da labview cella vuota
    std1sensv(i) = 15*10^(-6); %deviazione standard  NEE canale 1 cella vuota
    std2sensv(i) = 15*10^(-6); %deviazione standard  NEE canale 2 cella vuota
    std12(i) = ch12_vuota(i,3); %deviazione standard calcolata da labview per rapporto canali cella vuota
    %std12sensv(i) = ch12_vuota(i,3);  %deviazione standard calcolata da sensore per rapporto canali cella vuota
  %  relstdcalc(i) = std1vsum(i)./ch1v(i) + std2vsum(i)./ch2v(i); %errore relativo per rapporto canali calcolato da labview cella
vuota
    %stdcalcvmat(i) = rappvuotocalc(i)*relstdcalc(i); %errore assoluto rapporto canali calcolato da labview cella vuota
    relstdcalcsens(i) = std1sensv(i)./ch1v(i) + std2sensv(i)./ch2v(i); %errore relativo per rapporto canali calcolato da sensore
cella vuota
    stdcalcsens(i) = rappvuotocalc(i)*relstdcalcsens(i); %errore assoluto rapporto canali calcolato da sensore cella vuota
    stdcalcvmat(i)= stdrappvuotocalc(i);

   % if std12(i)> 2*errsens
    stdcalcv(i)=std12(i);
  %  else stdcalcv(i)=2*errsens;
  %  end



    %misure e calcoli relativi alla cella piena



   std1sensp(i)= (15*10^(-6)); %deviazione standard NEE canale 1 cella piena
   std2sensp(i)= (15*10^(-6)); %deviazione standard NEE canale 2 cella piena
   std12p(i) = ch12_piena(i,3); %deviazione standard calcolata da labview per rapporto canali cella piena
   % std12sensv(i) = ch12_piena(i,4);  %deviazione standard calcolata da sensore per rapporto cella piena
   % rapppienacalc(i) = ch1psum(i)./ch2psum(i); %rapporto tra i canali calcolato da matlab cella piena
   rapppienamis(i) =  ch12_piena(i,2); %rapporto tra i canali calcolato da labview cella piena
  % relstdcalcp(i) = std1psum(i)./ch1p(i) + std2psum(i)./ch2p(i); %errore relativo per rapporto canali calcolato da labview cella
piena
   % stdcalcpmat(i) = rapppienacalc(i)*relstdcalcp(i); %errore assoluto rapporto canali calcolato da labview cella piena
   relstdcalcpsens(i) = std1sensp(i)./ch1p(i) + std2sensp(i)./ch2p(i); %errore relativo per rapporto canali calcolato da sensore
cella piena
   stdcalcpsens(i) = rapppienacalc(i)*relstdcalcpsens(i); %errore assoluto rapporto canali calcolato da sensore cella piena
   stdcalcpmat(i) = stdrapppienacalc(i);

    %if std12p(i)> 2*errsens
   stdcalcp(i)=std12p(i);
    %else stdcalcp(i)=2*errsens;
   % end

    %calcoli relativi al rapporto tra cella piena e vuota ed ai coefficienti di assorbimento

    rapptotcalc(i) = rapppienacalc(i)./rappvuotocalc(i); %rapporto tra i rapporti canali calcolato da matlab
    rapptotmis(i) = rapppienamis(i)./rappvuotomis(i); %rapporto tra i rapporti canali calcolato da labview
    coeffassmat(i) = -(log(rapptotcalc(i)))./(patm*l); %coefficente di assorbimento da matlab in atm-1 cm-1
    coeffasslab(i) = -(log(rapptotmis(i)))./(patm*l); %coefficente di assorbimento con rapporto labview in atm-1 cm-1
    coeffassmol(i) = -(log(rapptotcalc(i)))./coeff; %coeficiente di assorbimento in mol-1 cm-1
    errtotrapprelmat(i) = stdcalcpmat(i)./rapppienacalc(i)+ stdcalcvmat(i)./rappvuotocalc(i); %errore relativo del rapporto dei
rapporti calcolato da matlab
    errtotrappmat(i) = errtotrapprelmat(i)*rapptotcalc(i); %errore relativo del rapporto dei rapporti calcolato da matlab
```

```
    errtotrapprellab(i) = stdcalcp(i)./rapppienamis(i)+ stdcalcv(i)./rappvuotomis(i); %errore totale del rapporto dei rapporti
calcolato da labview
    errtotrapplab(i) = errtotrapprellab(i)*rapptotmis(i); %errore totale del rapporto dei rapporti calcolato da labview
    errtotrappsensonly(i) = 2*errsens; %errore totale del rapporto dei rapporti da sensore
  %  errtotrappsensonlyscaled(i) = 2*errsens./(num); %errore totale del rapporto dei rapporti da sensore scalato
    errpatmmat(i)=errpatm; %errore sulla misura di pressione in cella
    errlmat(i) = errl; %errore sulla lunghezza cella

end

%deviazione standard calcolata con matlab

s_ch1v = std(ch1v);
s_ch2v = std(ch2v);
s_ch1p = std(ch1v);
s_ch2p = std(ch2v);

%calcolo dell'errore in varie versioni

for i=1:p;
    errtotcoeffass(i) = errtotrappmat(i)./rapptotcalc(i)*(1/(patm*l)) + (errpatm./patmcalc^2)*abs(log(rapptotcalc(i)))/l +
(errl./l^2)*abs(log(rapptotcalc(i)))/patm;
    %errore calcolato per propagazione degli errori - matlab
    errtotcoeffassbis(i) = ((errtotrappmat(i)./(rapptotcalc(i)^2)) + errpatm./patmcalc + errl./l)*abs(coeffassmat(i));
    %errore calcolato per propagazione degli errori approssimato - matlab
    errtotcoeffassbismol(i)=errtotcoeffassbis(i)*abs(coeffassmol(i));
    %errore approssimato per coeff ass in moli - matlab
    errtotcoeffassrel(i) = abs(errtotrappmat(i)./(rapptotcalc(i)*log(rapptotcalc(i)))) + errpatmmat(i)/patmcalc + errlmat(i)/l ;
    %errore relativo - matlab
    errtotcoeffassass(i) = errtotcoeffassrel(i)*abs(coeffassmat(i));
    %errore assoluto - matlab
    errtotcoeffasslab(i) = errtotrapplab(i)./rapptotmis(i)*(1/(patmcalc*l)) + (errpatm./patmcalc^2)*abs(log(rapptotcalc(i)))/l +
(errl./l^2)*abs(log(rapptotcalc(i)))/patm;
    %errore calcolato per propagazione degli errori - labview
    errtotcoeffassbislab(i) = ((errtotrapplab(i)./(rapptotmis(i)^2)) + errpatm./patm + errl./l)*abs(coeffasslab(i));
    %erore calcolato per propagazione degli errori approssimato - labview
   % errtotcoeffassassbislab(i) = errtotcoeffassbislab(i)*abs(coeffasslab(i));
    errtotcoeffassbissensonly(i) = ((errtotrappsensonly(i)./(rapptotcalc(i)^2)) + errpatm./patm + errl./l)* abs(coeffassmat(i)) ;
    %erore calcolato per propagazione degli errori approssimato - sensore solo
    %errtotcoeffassbissensonlyass(i) = errtotcoeffassbissensonlyrel(i)*abs(coeffassmat(i));
    %errore assoluto con solo sensore
    errtotcoeffassrellab(i) =abs( errtotrapplab(i)./(rapptotmis(i)*log(rapptotcalc(i)))) + errpatmmat(i)/patm + errlmat(i)/l ;
    %errore relativo - labview
    errtotcoeffassasslab(i) = errtotcoeffassrellab(i)*abs(coeffasslab(i));
    %errore assoluto - labview
end

%calcolo delle matrici trasposte ed altre variabili

lambdat = lambda'; % l.o. trasposta
coeffassmatt =coeffassmat'; %coefficiente assorbimento matlab trasposto
coeffasslabt =coeffasslab'; %coefficiente assorbimento da labview trasposto
coeffassmolt =coeffassmol'; %coefficiente di assorbimento moli trasposto
errtotcoeffassbist = errtotcoeffassbis'; %errore da matlab trasposto
errtotcoeffassbismolt = errtotcoeffassbismol'; % errore in moli da matlab trasposto
errtotcoeffassbislabt = errtotcoeffassbislab';%errore da labview trasposto


for i = 1:p;
    for j = 1:p;
    rappij(i,j) = rapptotmis(j)./rapptotmis(i); %rapporto tra i rapporti dei rapporti riga per riga
    rappcoeffassij(i,j) = coeffassmat(j)./coeffassmat(i); %rapporto tra i coefficienti di assorbimento riga per riga
%    rappcoeffassijlg(i,j) = coeffasslg(j)./coeffasslg(i);
    rappcoeffassmolij(i,j) = coeffassmol(j)./coeffassmol(i);%rapporto tra i coefficienti di assorbimento moli riga per riga
    end
end

for i = 1:p;


   coeffassl = [lambda(i),coeffassmat(i)]; %matrice dei coefficienti di assorbimento con l.o.
   coeffassmoll = [lambda(i),coeffassmol(i)]; %matrice dei coefficienti di assorbimento in moli con l.o.

   %salvataggio di parte dei dati in file .out

    %save 'C:\Documents and Settings\ventura\Documenti\lavoro\FINGERPRINT\DATI SPERIMENTALI\benzexpnew.out' coeffassmat -ASCII -tabs


end

%figure assortite (vedi titolo)

figure(1)
i=1:p;
errorbar(lambda(i),rappvuotocalc(i),stdcalcv(i),'r:.')
title('matlab calculated channel ratio empty cell')
xlabel('wavelenght (micron)')
ylabel('channels ratio')
grid

figure(2)
i=1:p;
errorbar(lambda(i),rappvuotomis(i),std12(i),'r:.')
title('labview calculated channel ratio empty cell')
xlabel('wavelenght (micron)')
ylabel('channels ratio')
grid

figure(5)
i=1:p;
errorbar(lambda(i),rapppienacalc(i),stdcalcp(i),'r:.')
title('matlab calculated channel ratio full cell')
xlabel('wavelenght (micron)')
ylabel('channels ratio')
grid

figure(6)
i=1:p;
```

```
errorbar(lambda(i),rapppienamis(i),std12p(i),'r:.')
title('labview calculated channel ratio  full cell')
xlabel('wavelenght (micron)')
ylabel('channels ratio')
grid

figure(9)
i=1:p;
errorbar(lambda(i),coeffassmat(i),errtotcoeffassbis(i), 'r:.')
title('absorption coefficients with error bar by matlab (atm-1 cm-1)')
xlabel('wavelenght (micron)')
ylabel('absoption coeff. (atm-1 cm-1)')
grid

figure(10)
i=1:p;
plot(lambda(i),coeffassmol(i),'r:.')
title('absorption coefficients (mol-1 cm-1)')
xlabel('wavelenght (micron)')
ylabel('absoption coeff. (mol-1 cm-1)')
grid

figure(11)
i=1:p;
plot(lambda(i),rappcoeffassmolij(i),'r:.')
title(' absorption coefficients ratio (mol-1 cm-1)')
xlabel('wavelenght (micron)')
ylabel(' absoption coeff. ratio')
grid

figure(12)
i=1:p;
errorbar(lambda(i),coeffassmat(i),errtotcoeffassass(i), 'r:.')
title('absorption coefficients with error bar new by matlab (atm-1 cm-1)')
xlabel('wavelenght (micron)')
ylabel('absoption coeff. (atm-1 cm-1)')
grid

figure(13)
i=1:p;
errorbar(lambda(i),coeffasslab(i),errtotcoeffassbislab(i), 'r:.')
title('absorption coefficients with error bar by labview (atm-1 cm-1)')
xlabel('wavelenght (micron)')
ylabel('absoption coeff. (atm-1 cm-1)')
grid

figure(14)
i=1:p;
errorbar(lambda(i),coeffasslab(i),errtotcoeffassasslab(i), 'r:.')
title('absorption coefficients with error bar new by labview (atm-1 cm-1)')
xlabel('wavelenght (micron)')
ylabel('absoption coeff. (atm-1 cm-1)')
grid

figure(15)
i=1:p;
errorbar(lambda(i),coeffassmat(i),errtotcoeffassbissensonly(i), 'r:.')
title('absorption coefficients with error bar by sensor only (atm-1 cm-1)')
xlabel('wavelenght (micron)')
ylabel('absoption coeff. (atm-1 cm-1)')
grid
```

REFERENCES

1. Beil, R. Daum, R. Harig, and G. Matz, Remote sensing of atmospheric pollution by passive FTIR spectrometry, Proc. SPIE Vol. 3493, 32–43, Spectroscopic Environmental Monitoring Techniques (1998).

2. Fiocco G. and L. D. Smullin, Detection of Scattering Layers in the Upper Atmosphere (60 – 140 Km) by Optical Radar, Nature, 199, 1275 – 1276. (1963).

3. C. Bellecci, G. Caputi, F. De Donato, P. Gaudio, M. Valentini, CO_2 Dial for monitoring atmospheric pollutants at the University of Calabria, Il Nuovo Cimento, **18**, 5, 463-472 (1995).

4. Ch. E. Kientz. Chromatography and mass spectrometry of chemical warfare agents, toxins and related compounds: state of the art and future prospects, Journal of Chromatography A, 814, 1-23 (1998).

5. P. D'Agostino and L. R. Provost, Mass spectrometric identification of products formed during degradation of ethyldimethylphosphoramidocyanidate (tabun), Journal of Chromatography, 598, 89-95 (1992).

6. D. K. Rourbaugh, Yu-Chu Yang and J.R. Ward, Identification of degradation products of 2-chloroethylethyl sulfide by gas chromatography-mass spectrometry, Journal of Chromatography, 447, 165-169 (1988).

7. Z. Witkiewicz, M. Mazurek and J. Szulc, Chromatographic analysis of chemical warfare agents, Journal of Chromatography, 503, 293-357 (1990).

8. P. D'Agostino and L. R. Provost, Determination of chemical warfare agents, their hydrolysis products and related compounds in soil, Journal of Chromatography, 589, 287-294 (1992).

9. P. A. D'Agostino, J. R. Hancock, L. R. Provost, Determination of sarin, soman and their hydrolysis products in soil by packed capillary liquid chromatography-electrospray mass spectrometry, Journal of Chromatography A, 912, 291-299 (2001).

10. B.Szostek, J. H. Aldstadt, Determination of organoarsenicals in the environment by solid-phase micro extraction-gas chromatography-mass spectrometry, Journal of Chromatography A, 807, 253-263 (1998).

11. R. M. Black and R. W. Read, Application of liquid chromatography-atmospheric pressure chemical ionization mass spectrometry, and tandem mass spectrometry, to the analysis and identification of degradation products of chemical warfare agents, Journal of Chromatography A, 759 79-92 (1997).

12. R. M. Black and R. W. Read, Analysis of degradation product of organophosphorus chemical warfare agents and related compounds by liquid chromatography-mass spectrometry using electrospray and atmospheric pressure chemical ionization, Journal of Chromatography A, 794 233-244 (1998).

13. Committee on monitoring at chemical agent disposal facilities, Monitoring at chemical agent disposal facilities, National academy of sciences - USA (online: http://www.nap.edu/catalog /11431.html), 2005.

14. Petter Weibring, Hans Edner, and Sune Svanberg, Versatile mobile lidar system for environmental monitoring, Applied Optics vol. 42 n° 18 (20 June 2003).

15. Kent A. Frediksson, DIAL technique for pollution monitoring: improvements and complementary systems, Applied Optics Vol 24 n° 19 (1 October 1985).

16. Z. Wang, S. Zhou, H. Hu et al. Appl. Phys. B 62, 143 (1996).

17. Vladimir A. Kovalev and Michael P. Bristow, Compensational three-wavelenght differential-absorption lidar technique for reducing the influence of differential scattering on ozone-concentration measurements, Applied Optics vol. 35 n° 24 (20 August 1996).

18. P. Rambaldi, M. Douard, J. Wolf, Appl. Phys. B 61, 117 (1995).

19. R. L. Jones, Proc. SPIE 1715, 393 (1992).

20. K. Strong and R.L. Jones, Remote measurement of vertical profiles of atmospheric constituents with a UV-visible ranging spectrometer, Applied Optics vol. 34 n° 27 (20 September 1995).

21. Tetsuo Fukuchi, Takashi Fujii, Naohiko Goto, Koshichi Nemoto, Evaluation of differential absorption lidar (DIAL) measurement error by simultaneous DIAL and null profiling, Opt. Eng. 40(3) 392-397 (March 2001).

22. Takashi Fujii, Tetsuo Fukuchi, Nianwen Cao, Koshichi Nemoto and Nobuo Takeuchi, Trace atmospheric SO_2 measurement by multiwavelenght curve-fitting and wavelength-optimized dual differential absorption lidar, Applied Optics, vol. 43 n°3 (20 January 2002).

23. Fresnel lenses, www.fresneltech.com/pdf/FresnelLenses.pdf

24. Measures R., Laser remote sensing Fundamentals and application, Krieger Publishing Company, Malabar Florida (1992)

25. C. Bellecci, P. Aversa, G. Benedetti Michelangeli, G. Caputi, F. De Donato, P. Gaudio, M. Valentini and R. Zoccali, Improvement of Calabria University CO_2 laser DIAL system, Proceeding SPIE, **3104**, 154-157 (1997).

26. D.K. Killinger and N. Meniuk, Remote probing of the atmosphere using a CO_2 DIAL System, IEEE Journal of quantum electronics, Vol. QE-17, n° 9 september 1981.

27. G.L. Loper, A.R. Calloway, M.A. Stamps and J.A. Gelbwachs, Carbon dioxide laser absorption spectra and low ppb photoacoustic detection of Hydrazine fuels, Applied Optics, Vol. 19, 2726 (1980).

28. Cammann, K., Sens. Actuators B 24-25, 769-772 (1995).

29. Massart, D. L., Vandeginste, B. G. M., Deming, S. N., Michotte, Y., Kaufman, L., Data Handling in Science and Technology 2: Chemometrics: a Textbook; Amsterdam: Eisevier, (1988).

30. Malinowski, E. R., Howery, D. G., Factor Analysis in Chemistry; New York: Wiley, 1980.

31. Rasmussen, G. T., Isenhour, T. L., Lowry, S. R., Ritter, G. L., Anal. Chim. Acta 103, 213-221 (1978).

32. Wold, S., Esbensen, K., Geladi, P., Intell. Lab. Syst. 2, 37 (1987) .

33. Marbach, R., Heise, H. M., Chemometr. Intell. Lab. Syst. 9, 45-63 (1990).

34. Carey, W. P., Beebe, K. R., Sanchez, E., Geladi, P., Kowalski, B. R., Sens. Actuators B 9, 223-234 (1986).

35. Golub, G. H., van Loan, C. F., Matrix Computations; Baltimore: John Hopkins University Press, (1983).

36. Wold, S., Kettaneh-Wold, N., Skagerberg, B., Chemometr. Intell. Lab. Syst. 7, 53-65 (1989).

37. Wold, S., Kettaneh-Wold, N., Chemometr. Intell. Lab. Syst. 14, 71-84 (1992).

38. Rumelhart, D. E., McClelland, J. L., Parallel Distributed Processing: Explorations in the Microstructure of Cognition, Vol. 1: Learning Internal Representations by Error Propagation; Cambridge, MA: MIT Press.

39. Parker, D. B., in: IEEE First International Conference on Neural Networks (San Diego), Caudill, M., Butler, C. (eds.), New York: IEEE, Vol. II, pp. 593-600 (1987).

40. Kohonen, T., Self-Organization and Associative Memory, 3rd edn.; Springer: Berlin, (1989).

41. Hertz, J., Krogh, A., Palmer, R. G., Introduction to the Theory of Neural Computation, Lecture Notes,Vol. 1; New York: Addison-Wesley (1991).

42. Wienke, D., Buydens, L., Trends Anal. Chem. 14, 398-406 (1995).

43. Grossberg, S., Bio/. Cybernet. 23, 121-134 and 187-203 (1976).

44. Weimar, U., Schierbaum, K. D., Göpel, W., Sens. Actuators B 2, 71-78 (1990).

45. Italian Patent request n° RM2010A000211 dated 03/05/2010 “Metodo di analisi di gas in atmosfera mediante una tecnica di tipo DIAL”.

46. www.mathworks.it/products/matlab.

47. www.cfa.harward.edu/hitran.

48. Zhahyang M. and Yuanjun M., An expert system Knowledge Base for the analysis of Infrared Spectra of organophosphorus compounds, Microchemical Journal 53, 371-375 (1996).

49. H. J. P. Smith et al., Fast Atmospheric Signature Code (Spectral Transmittance and Radiance), Air Force Geophysics Laboratory Technical Report AFGL-TR-78-0081, Hanscom AFB, MA (1978).

50. D. K. Killinger and N. Menyuk, Remote probing of the atmosphere using a CO_2 DIAL system, IEEE, Vol. QE-17, NO 9, 1917-1929 (1981).

51. C. Bellecci et al., Database for chemical weapons detection: first results, Optically Based Biological and Chemical Detection for Defence IV, Proceedings of the SPIE, Volume 7116 (2008).

52. www.ni.com/labview

53. NATO - Science for Peace, SfP 982671, http://ppam.inflpr.ro/NATO/Sfp982671.htm.

54. Organization for the Prohibition of Chemical Weapons, IR data adopted by the first session of the conference of the states parties, approved at first and second session – (1997).

55. K. Fukunaga, introduction to statistical pattern recognition, 2nd ed., academic press (1990).

56. www.scintec.it/prodotti/cmp/data_sheet_cmp30.pdf.

57. Zemax Development Corporation, www.zemax.com.

58. Baratto C. et al. Monitoring plants health in greenhouse for space missions, Proceedings of the Tenth International Meeting on Chemical Sensors, Sensors and Actuators, B: Chemical Volume 108, Issues 1-2, 278-284 (22 July 2005).

59. Wisniesky M. E. Wilson C. L., Biological control of post harvest diseases in fruits and vegetables: recent advances, Hortscience, 27 94-98 (1992).

60. Lai A. et al., Diagnosi precoce e non distruttiva di infezioni fungine in frutti di arancio in post raccolta, Italus Hortus 13 (5) 54 -58 (2006).

61. Giubileo G. et al. Photoacoustic detection of ethylene traces in biogenic gases, laser physics n° 4 Vol. 12 653-655 (2002).

62. Giubileo G. et al., Detection of ethylene in smokers breath by laser photoacoustic spectroscopy, SPIE proc. Vol. 5486 280-287 (1994).

63. R.R. Patty et al., CO_2 Laser Absorption Coefficients for determining ambient levels of O_3, NH_3, and C_2H_4, Appl. Opt. 13, 2850 (1974).

64. Demtroder W, Laser Spectroscopy basic concepts and instrumentation 2nd edition, Springer 380-385.

ACKNOWLEDGMENTS

RINGRAZIAMENTI

è dura alla fine di cotanto lavoro
trovar le parole giuste per ognuno
il cui apporto è valso più dell'oro
e non nasconder l'arrosto dietro il fumo.
come avrei fatto senza Pasquale
di cui solo chi lo ha ricevuto
sa ogni apporto quanto vale
ed ogni lavor non è perduto
Come avrei fatto con dubbi e progetti
Senza i consigli del prof. Bellecci
Che a mente e cuor vanno diretti
E talvolta comprende anche i capricci?
Che dire di Arianna
Che con alchimie e prodigi
Supera Merlino di una spanna?
Se gli automatismi al dovere non son ligi
Michela interviene in un baleno
E trova ove è ubicato il freno
Se il dato diviene complicato
Eugenio accorre con i suoi strumenti
E sembra sia intervenuto il fato
Tanto dal veder si resta sgomenti
Ma ciascun dei colleghi ha dato
Chi diceva un consiglio o una parola
Chi rendeva allegro anche un triste fato
Ed a ciascun mio pensier vola.

Ma non posso trascurare la famiglia

Che tanto ha dato con i suoi sacrifici

E a cui i miei studi han creato un parapiglia:

Alla mia fanciulla che capisce i benefici

Un abbraccio lungo quanto il tempo dedicato

Il cui sforzo non verrà dimenticato

Alla mia cucciolina il cui sorriso

Luccicando nel buio della sera

Trasformava la stanchezza in paradiso

Prometto il mio tempo per un'era intera

Alla mamma che mi ha insegnato

A guardar sempre lontano

E che nessun destino è dato

Dichiaro che non ho studiato invano

Al papà i cui consigli più non odo:

non ho dimenticato di badare pure al sodo

Ad Antonio e Rosellina

Che mi hanno un po' adottato:

dovei ringraziarli ogni mattina

per quanto mi hanno coccolato

per correggere il mio incerto inglese

il contributo di Giovanna è certo palese

e per color a cui grazie non ho reso

mi perdonino che non son ricco come Creso